

Protection of eukaryotic cells against pore-forming toxins from pathogenic bacteria

A thesis submitted to Swansea University for the degree of
Doctor of Philosophy

By Thomas James Robert Ormsby B.Sc.

Submitted July 2021

Swansea University Medical School
Ysgol Feddygaeth Prifysgol Abertawe



Swansea University
Prifysgol Abertawe

ABSTRACT

Bacterial infections are a leading cause of mortality and morbidity. Many species of pathogenic bacteria secrete pore-forming toxins to damage eukaryotic cells and facilitate pathogen invasion. Although cells can repair this damage, little is known about the intrinsic protection of cells against these toxins. Side-chain oxysterols and steroids can reduce the severity of bacterial diseases by suppressing immunity. Here we tested the hypothesis that oxysterols and steroids might also enhance the intrinsic protection of eukaryotic cells against pore-forming toxins. We first used the cholesterol-dependent cytolysin pyolysin, which forms pores in bovine endometrial cells. We found that 25-hydroxycholesterol or 27-hydroxycholesterol treatment protected bovine endometrial cells against pyolysin, and that these oxysterols are present in the reproductive tract. The oxysterols reduced pyolysin-induced leakage of potassium and lactate dehydrogenase by $> 65\%$, limited changes to the actin cytoskeleton, and prevented cytolysis. The oxysterols also protected human cervical, lung, and liver epithelial cells against pyolysin damage, and protected cells against *Staphylococcus aureus* α -hemolysin. Mechanistically, oxysterol cytoprotection was partially dependent on activating acetyl-coenzyme A acetyltransferase and liver X receptors. The steroids, progesterone, oestradiol, or hydrocortisone were not protective in bovine endometrial cells. However, hydrocortisone and dexamethasone protected several types of human cells against pyolysin, reducing cytolysis from $> 75\%$ to $< 25\%$, via a glucocorticoid receptor dependent mechanism. Treatment with these glucocorticoids also protected human cells against α -hemolysin and another cholesterol-dependent cytolysin, streptolysin O. However, glucocorticoid cytoprotection was reversibly blocked by the presence of $\geq 4\%$ serum, which led to the discovery that glucocorticoid cytoprotection depended on the rate limiting enzyme of cholesterol biosynthesis, 3-hydroxy-3-methyl-glutaryl-coenzyme A reductase. In conclusion, side-chain oxysterols and glucocorticoids enhance the intrinsic protection of eukaryotic cells against pore-forming toxins. These findings imply that oxysterols and glucocorticoids could help limit the severity of disease caused by pathogens that secrete pore-forming toxins.

DECLARATION

This work has not previously been accepted in substance for any degree and is not concurrently submitted in candidature for any degree.

Signed... (candidate)

Date..... 29/7/2021

STATEMENT 1

This thesis is the result of my own investigations, except where otherwise stated. Where correction services have been used, the extent and nature of the correction is clearly marked in a footnote(s).

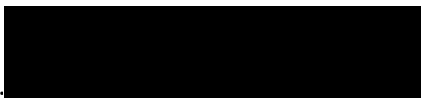
Other sources are acknowledged by footnotes giving explicit references. A bibliography is appended.

Signed... (candidate)

Date..... 29/7/2021

STATEMENT 2

I hereby give consent for my work, if accepted, to be available for photocopying and for photocopying and for inter-library loan, and for the title and summary to be made available to outside organisations.

Signed... (candidate)

Date..... 29/7/2021

TABLE OF CONTENTS

Abstract	i
Declaration	ii
Statement 1	ii
Statement 2	ii
Table of contents	iii
Acknowledgements	viii
List of figures	ix
List of tables	xiii
List of abbreviations	xiv
Publications	xvii
1 Introduction	1
1.1 General introduction	1
1.2 Pore-forming toxins	2
1.3 Cholesterol-dependent cytolysins	5
1.3.1 Plasma membrane cholesterol	5
1.3.2 Pore formation	8
1.3.3 Thiol-activation	9
1.3.4 Pyolysin and <i>Trueperella pyogenes</i>	10
1.3.5 Streptolysin O and <i>Streptococcus pyogenes</i>	11
1.4 <i>Staphylococcus aureus</i> alpha-hemolysin	12
1.5 Consequences of pore formation	13
1.6 Cell repair	15
1.6.1 Membrane remodelling	15
1.6.2 Mitogen-activated protein kinases	17
1.6.3 Inflammasome activation and autophagy	18
1.7 Protection against pore-forming toxin damage	20
1.7.1 Cell tolerance	20
1.7.2 Cell protection	22
1.8 Cholesterol	23
1.8.1 Cholesterol biosynthesis	23
1.8.2 Cholesterol homeostasis	26

1.9	Oxysterols.....	29
1.9.1	Oxysterols and disease	29
1.9.2	Oxysterol structure	29
1.9.3	Oxysterol synthesis	30
1.9.4	Oxysterol membrane organisation	31
1.9.5	Other functions of oxysterols	32
1.10	Steroids	33
1.10.1	Steroids and disease	33
1.10.2	Steroid synthesis	34
1.10.3	Oestrogens.....	36
1.10.4	Progesterone.....	37
1.10.5	Glucocorticoids	37
1.11	Aims and hypotheses	41
2	General materials and methods	43
2.1	General approach to examining cytoprotection.....	43
2.2	Pore-forming toxin preparation	45
2.2.1	Pyolysin.....	45
2.2.2	Streptolysin O	49
2.2.3	<i>Staphylococcus aureus</i> α -hemolysin.....	49
2.3	Cell culture	50
2.3.1	Bovine endometrial cell culture	50
2.3.2	HeLa cell culture	54
2.3.3	A549 cell culture	54
2.3.4	H441 cell culture	55
2.3.5	Hep-G2 cell culture	55
2.3.6	Normal dermal human fibroblasts cell culture.....	55
2.3.7	Passaging cells	55
2.4	Evaluating the consequences of pore formation.....	56
2.4.1	Lactate dehydrogenase assay	56
2.4.2	MTT assay.....	57
2.4.3	CyQUANT assay	58
2.4.4	Potassium leakage	58
2.5	Cell Microscopy	63

2.5.1	Phase contrast microscopy	63
2.5.2	Immunofluorescence	63
2.5.3	Confocal microscopy	64
2.6	Cholesterol measurement	64
2.7	Western blotting	65
2.8	Oxysterol measurement	69
2.8.1	Uterine and ovarian follicular fluid collection	69
2.8.2	Epithelial and stromal cell supernatant sample collection	69
2.8.3	Sample preparation.....	70
2.8.4	Liquid chromatography-mass spectrometry.....	71
2.9	Short interfering RNA design and knockdown	72
2.10	Quantitative polymerase chain reaction	74
2.10.1	Total RNA Extraction	74
2.10.2	Complementary DNA synthesis.....	75
2.10.3	Quantitative PCR	76
2.11	Statistical analysis	78
3	Oxysterols protect bovine endometrial cells against pore-forming toxins from pathogenic bacteria.....	79
3.1	Introduction	79
3.2	Materials and methods.....	82
3.2.1	Cytoprotection experiments	82
3.2.2	Potassium	84
3.2.3	Cholesterol	85
3.2.4	Immunofluorescence	85
3.2.5	Western Blotting	86
3.2.6	Oxysterols	86
3.2.7	Statistical analysis	87
3.3	Results	87
3.3.1	27-hydroxycholesterol protected endometrial cells against pyolysin ..	87
3.3.2	Side-chain oxysterols protect cells against pyolysin.....	97
3.3.3	Cellular cholesterol	101
3.3.4	Liver X receptors have a role in oxysterol cytoprotection.....	108
3.3.5	Side-chain oxysterols protect cells against α -hemolysin	115

3.3.6	Oxysterols are present in the bovine endometrium.....	119
3.4	Discussion	124
4	Side-chain oxysterols protect human epithelial cells against damage from pore-forming toxins	130
4.1	Introduction	130
4.2	Materials and methods.....	132
4.2.1	Cytoprotection experiments	132
4.2.2	Potassium	135
4.2.3	Cholesterol	136
4.2.4	Immunofluorescence	136
4.2.5	Western Blotting	137
4.2.6	Statistical analysis	137
4.3	Results	138
4.3.1	Side-chain oxysterol cytoprotection against pyolysin in HeLa cells .	138
4.3.2	Side-chain oxysterol cytoprotection against pyolysin is generalized	146
4.3.3	Side-chain oxysterols protect cells against α -hemolysin	152
4.3.4	Cellular cholesterol	157
4.3.5	Ion flux does not contribute to oxysterol cytoprotection	162
4.3.6	Liver X receptor agonists protect HeLa cells against pyolysin.....	165
4.4	Discussion	172
5	Glucocorticoids protect human cells against pore-forming toxin damage.....	176
5.1	Introduction	176
5.2	Materials and methods.....	177
5.2.1	Cytoprotection experiments	177
5.2.2	Potassium	180
5.2.3	Cholesterol	180
5.2.4	Immunofluorescence	181
5.2.5	Western blotting	181
5.2.6	Statistical analysis	182
5.3	Results	183
5.3.1	Glucocorticoid cytoprotection against pyolysin in HeLa cells	183
5.3.2	Glucocorticoid cytoprotection is generalized across human cells	190
5.3.3	Cytoprotection is glucocorticoid receptor dependent	199

5.3.4	Cytoprotection is not dependent on changes in cellular cholesterol..	203
5.3.5	Serum impairs glucocorticoid cytoprotection.	208
5.3.6	Ion flux does not contribute to glucocorticoid cytoprotection.....	211
5.3.7	Glucocorticoid cytoprotection is partially dependent on HMGCR ...	215
5.4	Discussion	220
6	General Discussion.....	225
6.1	Side-chain oxysterol cytoprotection	228
6.2	Glucocorticoid cytoprotection	231
6.3	Serum and cytoprotection.....	232
6.4	Cell repair and cytoprotection	234
6.5	Limitations.....	236
6.6	Future applications	238
6.7	Conclusion.....	239
	References	241

ACKNOWLEDGEMENTS

Firstly, I would like to thank Professor Martin Sheldon for giving me my first opportunity in research. His constant guidance has been instrumental to the progress I have made throughout my PhD. I would also like to thank Dr Sian Owens for her assistance with recombinant pyolysin purification and confocal microscopy and Dr James Cronin for demonstrating the art of bovine endometrial cell isolation. Thank you to Professor William Griffiths and Professor Yuqin Wang for allowing me the opportunity to collaborate with their Swansea University Oxysterol Research Group and incorporate mass spectrometry into my research. In addition, I would like to thank Liam Clement and Tom Mills for their support whilst working alongside me during their placement from Bath University.

A special thanks goes out to Anthony Horlock. Having joined the Sheldon group at the same time, we endured the highs and loads of postgraduate study together. Our regular trips to the slaughterhouse provided an entertaining source of discussion and debate.

I would like to thank everyone on the 4th floor of the Institutes of Life Science for creating a wonderful working environment. A particular mention goes out to Sam, Demi, Qiellor, Rhiannon Beadman, and Rhi Gould. We shared many great memories both in and outside the lab and I will always look back on our time together with fondness.

Finally, I would like to thank my partner Anona Davies. Thank you for putting up with me when unsuccessful experiments or a lack of motivation put me in a bad mood, and for tolerating my late-night experiments and writing sessions. You helped me get over the finish line.

LIST OF FIGURES

Figure 1.1 The two major classes of pore-forming toxins	4
Figure 1.2 Structure of the plasma membrane	6
Figure 1.3 Cholesterol-dependent cytolysin membrane insertion.....	9
Figure 1.4 Pyolysin structure and oligomerization	11
Figure 1.5 <i>Staphylococcus aureus</i> α -hemolysin oligomer	13
Figure 1.6 Consequences of pore-forming toxin pore formation.....	14
Figure 1.7 Mechanisms repairing the damage caused by pore-forming toxins	19
Figure 1.8 Mechanisms of achieving resilience to bacterial infection.....	21
Figure 1.9 The mevalonate pathway	25
Figure 1.10 Oxysterol regulation of cholesterol homeostasis.....	28
Figure 1.11 Oxysterol structure	30
Figure 1.12 Endogenous oxysterol synthesis	31
Figure 1.13 Oxysterol membrane organisation.....	32
Figure 1.14 Steroid biosynthesis	35
Figure 2.1 SDS-PAGE analysis of recombinant pyolysin fractions	48
Figure 2.2 Anatomy of the bovine reproductive tract	50
Figure 2.3 The bovine endometrium.....	51
Figure 2.4 Dissection of the bovine endometrium.....	52
Figure 2.5 Epithelial and stromal cell populations.....	54
Figure 2.6 Potassium leaks from cells challenged with α -hemolysin for 15 min	60
Figure 2.7 Control challenge does not cause potassium ion leakage in treated cells.	62
Figure 2.8 Representative whole blot images for the antibodies used in this thesis..	68
Figure 2.9 RNA interference of bovine endometrial and HeLa cells	73
Figure 3.1 Pyolysin damages bovine endometrial cells.....	88
Figure 3.2 Steroids do not protect endometrial epithelial cells against pyolysin.....	90
Figure 3.3 Steroids do not protect endometrial stromal cells against pyolysin	91
Figure 3.4 Dexamethasone does not protect endometrial cells against pyolysin.....	92
Figure 3.5 27-hydroxycholesterol protects endometrial cells against pyolysin.....	93
Figure 3.6 27-hydroxycholesterol consistently protects bovine endometrial cells against pyolysin.....	95
Figure 3.7 27-hydroxycholesterol protection increases with treatment duration.....	95

Figure 3.8 27-hydroxycholesterol protects bovine endometrial cells against pyolysin-induced actin cytoskeletal changes	96
Figure 3.9 25-hydroxycholesterol protects endometrial cells against pyolysin.....	98
Figure 3.10 Side-chain oxysterol protection persists for 24 h	99
Figure 3.11 Oxysterols prevent pyolysin-induced potassium leakage.....	100
Figure 3.12 Oxysterols do not reduce bovine endometrial cell cholesterol.....	102
Figure 3.13 Oxysterols protect bovine endometrial cells against pyolysin in the presence of serum.....	104
Figure 3.14 27-hydroxycholesterol reduces pyolysin binding.....	106
Figure 3.15 27-hydroxycholesterol cytoprotection is partly ACAT dependent.....	107
Figure 3.16 LXR agonists protect bovine endometrial cells against pyolysin.....	109
Figure 3.17 LXR agonists decrease pyolysin-induced potassium leakage in stromal cells	110
Figure 3.18 siRNA targeting <i>NR1H3</i> and <i>NR1H2</i> reduced the abundance of LXR and ABCA1 protein	111
Figure 3.19 27-hydroxycholesterol cytoprotection is partly LXR dependent.....	112
Figure 3.20 T0901317 cytoprotection is LXR dependent.....	113
Figure 3.21 27-hydroxycholesterol and T0901317 increase ABCA1 protein	114
Figure 3.22 27-hydroxycholesterol protects cells against α -hemolysin damage	116
Figure 3.23 27-hydroxycholesterol reduces α -hemolysin-induced potassium leakage in stromal cells	117
Figure 3.24 27-hydroxycholesterol protects bovine endometrial cells against α -hemolysin-induced actin cytoskeletal changes	118
Figure 3.25 Oxysterols are present in bovine uterine and ovarian follicular fluid ..	119
Figure 3.26 Endometrial cells release oxysterols.....	122
Figure 3.27 Pyolysin-induced oxysterol release in stromal and epithelial cells	123
Figure 4.1 Pyolysin causes HeLa cell cytolysis	139
Figure 4.2 Pyolysin induces membrane blebbing and fragments HeLa cells	139
Figure 4.3 Pyolysin damages HeLa cells	140
Figure 4.4 Pyolysin induces HeLa cell plasma membrane blebbing	140
Figure 4.5 Side-chain oxysterols protect HeLa cells against pyolysin damage.....	142
Figure 4.6 Side-chain oxysterols protect HeLa cells against pyolysin-induced actin cytoskeletal changes.....	144
Figure 4.7 Oxysterols protect HeLa cells against pyolysin-induced blebbing.....	145

Figure 4.8 Cytolytic activity of pyolysin in A549, Hep-G2 and NC1-H441 cells...	147
Figure 4.9 Side-chain oxysterols protect A549 cells against pyolysin damage.....	149
Figure 4.10 Oxysterols protect A549 cells against pyolysin-induced actin cytoskeletal changes.....	150
Figure 4.11 27-hydroxycholesterol cytoprotection in Hep-G2 and NC1-H44 cells.	151
Figure 4.12 Cytolytic activity of <i>S. aureus</i> α -hemolysin in HeLa cells.....	152
Figure 4.13 Cytolytic activity of <i>S. aureus</i> α -hemolysin in A549 cells.....	153
Figure 4.14 27-hydroxycholesterol protects HeLa cells against α -hemolysin.....	155
Figure 4.15: 27-hydroxycholesterol protects A549 cells against α -hemolysin.....	156
Figure 4.16 Side-chain oxysterols do not reduce HeLa total cell cholesterol.....	158
Figure 4.17 27-hydroxycholesterol reduces pyolysin binding.....	159
Figure 4.18 27-hydroxycholesterol cytoprotection is partially ACAT-dependent ..	160
Figure 4.19 Sphingomyelinase treatment doesn't prevent 27-hydroxycholesterol cytoprotection.....	161
Figure 4.20 27-hydroxycholesterol and T0901317 reduces pyolysin-induced MAPK phosphorylation.....	163
Figure 4.21 Calcium ion influx and potassium ion efflux does not affect 27-hydroxycholesterol cytoprotection.....	164
Figure 4.22 siRNA reduces the expression of <i>NR1H2</i> and <i>NR1H3</i>	165
Figure 4.23 27-hydroxycholesterol cytoprotection was not LXR dependent	166
Figure 4.24 Liver X receptor agonists protect HeLa cells against pyolysin	167
Figure 4.25 Liver X receptor agonists protect HeLa cells against pyolysin-induced actin cytoskeletal changes	168
Figure 4.26 T0901317 cytoprotection against pyolysin is LXR dependent.....	169
Figure 4.27 Liver X receptor agonists protect A549 cells against pyolysin	170
Figure 4.28 T0901317 protects A549 cells against pyolysin-induced actin cytoskeletal changes.....	171
Figure 5.1 Glucocorticoids protect HeLa cells against pyolysin damage.....	184
Figure 5.2 Dexamethasone protects HeLa cells against a range of pyolysin challenge concentrations	185
Figure 5.3 Glucocorticoid cytoprotection requires > 6 h treatment and persists against longer pyolysin challenge durations	186
Figure 5.4 Glucocorticoids prevent pyolysin-induced HeLa cytoskeletal changes .	187
Figure 5.5 Dexamethasone protects HeLa cells against pyolysin.....	188

Figure 5.6 Glucocorticoids reduce pyolysin-induced HeLa cell blebbing.....	189
Figure 5.7 Glucocorticoids protect A549 cells against pyolysin damage.....	191
Figure 5.8 Glucocorticoids protect A549 cells against pyolysin-induced cytoskeletal changes.....	192
Figure 5.9 Dexamethasone protects A549 cells against a range of pyolysin challenge concentrations	193
Figure 5.10 The cytolytic activity of pyolysin in dermal fibroblasts.....	194
Figure 5.11 Dexamethasone protects multiple cells against pyolysin	194
Figure 5.12 Glucocorticoids protect HeLa and A549 cells against streptolysin O..	196
Figure 5.13 Dexamethasone protects HeLa cells against α -hemolysin damage	197
Figure 5.14 Glucocorticoids do not protect A549 cells against α -hemolysin.....	198
Figure 5.15 Fluticasone protects HeLa and A549 cells against pyolysin damage...	200
Figure 5.16 The glucocorticoid receptor contributes to cytoprotection.....	201
Figure 5.17 Glucocorticoid cytoprotection against pyolysin is <i>NR3C1</i> dependent .	202
Figure 5.18 Glucocorticoids do not reduce HeLa or A549 cell cholesterol.....	204
Figure 5.19 Cholesterol supplementation does not prevent glucocorticoid cytoprotection.....	204
Figure 5.20 Inhibiting ACAT does not prevent glucocorticoid cytoprotection	205
Figure 5.21 Glucocorticoids do not reduce pyolysin binding in HeLa cells.....	206
Figure 5.22 Glucocorticoids reduce pyolysin binding in A549 cells.....	207
Figure 5.23 Serum prevents glucocorticoid cytoprotection in HeLa cells.....	209
Figure 5.24 Serum prevents glucocorticoid cytoprotection in A549 cells.....	210
Figure 5.25 Serum reversibly inhibits glucocorticoid cytoprotection.....	210
Figure 5.26 Glucocorticoids reduce pyolysin-induced MAPK phosphorylation.....	212
Figure 5.27 Potassium ion efflux does not affect dexamethasone cytoprotection...	213
Figure 5.28 Calcium ion influx does not affect glucocorticoid cytoprotection	214
Figure 5.29 Glucocorticoid cytoprotection is dependent on transcription and translation.....	216
Figure 5.30 Glucocorticoid cytoprotection is partially dependent on HMGCR	219
Figure 6.1 Oxysterol cytoprotection in the bovine endometrium	230

LIST OF TABLES

Table 1.1 Classification of pore-forming toxin families.....	4
Table 1.2 Nuclear Receptor Subfamily 3.....	36
Table 2.1 Treatments and inhibitors used throughout this thesis and the vehicles used to reconstitute them.....	44
Table 2.2 Recombinant pyolysin protein concentrations from eluted fractions	47
Table 2.3 Ingredients for SDS-PAGE gel.....	48
Table 2.4 NADH standard curve.....	56
Table 2.5 LDH assay mix stock solutions.....	57
Table 2.6 LDH assay mix recipe.....	57
Table 2.7 Potassium assay buffer recipe	59
Table 2.8 Potassium standard curve	61
Table 2.9 Amplex Red working solution recipe	65
Table 2.10 In-house acrylamide gel recipe (for 1 gel).....	65
Table 2.11 List of antibodies used in this study.....	67
Table 2.12 Short interfering RNA sequences	72
Table 2.13 NanoDrop values for RNA isolated from HeLa cells in this project.....	75
Table 2.14 Complementary DNA synthesis master mix.....	76
Table 2.15 Primer sequences	76
Table 2.16 Reaction set up for quantitative PCR.....	77
Table 2.17 Quantitative PCR plate layout.....	77
Table 2.18 Quantitative PCR cycling conditions.....	77
Table 2.19 Reference gene (<i>RPL19</i>) expression was consistent across treatments ...	78
Table 3.1 Oxysterol concentrations in biological samples.....	120
Table 3.2 Oxysterol concentrations in culture medium	121
Table 4.1 Quantification of HeLa cell morphology after oxysterol treatment and pyolysin challenge.....	146
Table 5.1 Quantification of HeLa cell morphology after glucocorticoid treatment and pyolysin challenge.....	190
Table 5.2 Genes regulated by dexamethasone and serum.....	217
Table 6.1 Summarised cytoprotective findings.....	227

LIST OF ABBREVIATIONS

ABAM	Antibiotic antimycotic
ABCA1	ATP-binding cassette subfamily A member 1
ABCG1	ATP-binding cassette subfamily G member 1
ACAT	Acetyl-coenzyme A acetyltransferase
ADAM10	A disintegrin and metalloprotease 10
AMP	Adenosine monophosphate
ANOVA	Analysis of variance
AP-1	Activating protein-1
APS	Ammonium persulfate
ATCC	American type culture collection
ATP	Adenosine triphosphate
AU	Arbitrary units
BSA	Bovine serum albumin
cDNA	Complementary DNA
CoA	Coenzyme A
COPII	Coat protein II
Cq	Quantification cycle
CYP	Cytochrome P450
DAPI	4,6-diamidino-2-phenylindole
Dexamethasone	1-dehydro-9-fluoro-16-methylhydrocortisone
DMEM	Dulbecco's modified eagle medium
DMSO	Dimethyl sulphoxide
DNA	Deoxyribonucleic acid
DPBS	Dulbecco's phosphate-buffered saline
<i>E. coli</i>	<i>Escherichia coli</i>
ER	Endoplasmic reticulum
ERK1/2	Extracellular signal-regulated kinases 1 and 2
FP	Fluticasone propionate
GPI	Glycosylphosphatidylinositol
HBSS	Hank's balanced salt solution
HGNC	Human Gene Organisation Gene Nomenclature Committee

HMG-CoA	3-hydroxy-3-methyl-glutaryl-coenzyme A
HMGCR	3-hydroxy-3-methyl-glutaryl-coenzyme A reductase
HSD	Hydroxysteroid dehydrogenase
HU	Hemolytic units
Hydrocortisone	11 β , 17 α , 21-Trihydroxypregn-4-ene-3, 20-dione
Idol	Inducible degrader of the LDL receptor
IL	Interleukin
INT	Iodophenyl-3-p-nitrophenyl tetrazolium
JNK	c-Jun (N)-terminal kinase
LB	Luria-Bertani
LBP	Lipopolysaccharide binding protein
LDL	Low-density lipoprotein
LDH	Lactate dehydrogenase
LPS	Lipopolysaccharide
LXR	Liver X receptor
MACPF	Membrane attack complex component/ perforin
MAPK	Mitogen-activated protein kinase
M β CD	Methyl- β -cyclodextrin
mRNA	Messenger RNA
MTT	3-(4,5-dimethylthiazol-2-yl)-2,5-diphenyltetrazolium bromide
NAD ⁺	β -Nicotinamide adenine dinucleotide sodium salt
NADH	β -Nicotinamide adenine dinucleotide sodium salt hydrate
NDHF	Primary normal dermal human fibroblasts
NF- κ B	Nuclear factor κ -light-chain-enhancer of activated B cells
NTC	No template control
Oestradiol	Oestra-1, 3, 5 (10) -triene-3, 17 β -diol
PBS	Phosphate-buffered saline
PCR	Polymerase chain reaction
Progesterone	Pregn-4-ene-3, 20-dione
RNA	Ribonucleic acid
ROR	Retinoic acid receptor-related -related receptor
RPL19	Ribosomal protein L19
RPMI	Roswell park memorial institute

SCAP	SREBP cleavage-activating protein
SDS-PAGE	Sodium dodecyl sulphate polyacrylamide gel electrophoresis
SEM	Standard error of the mean
siRNA	Short interfering RNA
SPE	Solid phase extraction
<i>S. pyogenes</i>	<i>Streptococcus pyogenes</i>
SREBP	Sterol responsive element binding protein
<i>S. aureus</i>	<i>Staphylococcus aureus</i>
SZ58-035	Sandoz 58-035 (3-[Decyldimethylsilyl]-N-[2-(4-methylphenyl)-1-phenethyl]propenamide)
TBST	Tris-buffered saline with 0.1% Tween 20
TEMED	N, N, N', N'-tetramethylethylenediamine
TMH	Transmembrane helices
<i>T. pyogenes</i>	<i>Trueperella pyogenes</i>
Tris	Tris(hydroxymethyl)aminomethane
Tris-HCL	Tris hydrochloride
UPR	Unfolded protein response
25-HC	25-hydroxycholesterol (Cholest-5-ene-3 β ,25-diol)
27-HC	27-hydroxycholesterol ((25R)-Cholest-5-ene-3 β ,26-diol)

PUBLICATIONS

Papers published and issued for peer-review from the findings of this thesis:

Sheldon, I.M., Molinari, P.C., **Ormsby, T.J.R.** and Bromfield, J.J., 2020. Preventing postpartum uterine disease in dairy cattle depends on avoiding, tolerating and resisting pathogenic bacteria. *Theriogenology*. 150, 158-165.

Ormsby, T.J.R., Owens, S.E., Horlock, A.H., Davies, D., Griffiths, W.J., Wang, Y., Cronin, J.G., Bromfield, J.J and Sheldon, I.M., 2021. Oxysterols protect bovine endometrial cells against pore-forming toxins from pathogenic bacteria. *The FASEB Journal*. 35, e21889.

Papers submitted and under peer-review from the findings of this thesis:

Ormsby, T.J.R., Owens, S.E., Cronin, J.G., Bromfield, J.J and Sheldon, I.M., 2021. Glucocorticoids increase tissue cell protection against pore-forming toxins from pathogenic bacteria. *Submitted to Communications Biology*.

1 INTRODUCTION

1.1 GENERAL INTRODUCTION

Pore-forming toxins perforate eukaryotic cell plasma membranes resulting in target cell lysis, the release of molecules that bacteria can use as nutrients, as well as enabling the delivery of additional bacterial virulence factors. In this way, pore-forming toxins promote pathogen growth, facilitate dissemination through host tissues, and cause tissue pathology (Peraro and van der Goot, 2016). The most common family of pore-forming toxins are cholesterol-dependent cytolysins, which bind to cholesterol in the plasma membrane of target cells (Tweten, 2005). These cytolysins form stable pores that cause the leakage of potassium ions within minutes, changes in cell shape and structure, and leakage of cytosolic proteins within 2 h, ultimately resulting in cytolysis (Gonzalez et al., 2011).

Increasing the tolerance of cells to pore-forming toxin damage can limit the severity of disease without decreasing the pathogen burden (Schneider and Ayres, 2008, Medzhitov et al., 2012). Changes in cytosolic molecular concentrations in response to pore formation trigger a variety of secondary reparative responses to improve cell survival, such as mitogen-activated protein kinase (MAPK) activation and cytoskeletal remodelling (Gonzalez et al., 2011, Brito et al., 2019). However, tolerance can also be achieved through damage prevention. Treating cells with certain chemical compounds, such as statins and cyclodextrins, can reduce cellular cholesterol and increase the intrinsic protection of cells against pore-forming toxins in a process termed cytoprotection (Amos et al., 2014, Griffin et al., 2017).

Oxysterols, the ovarian sex steroid hormones, oestradiol (estra-1, 3, 5 (10) -triene-3, 17 β -diol) and progesterone (pregn-4-ene-3, 20-dione), and glucocorticoids are thought to act via their cognate nuclear receptors to modulate the risk of diseases caused by bacteria that secrete pore-forming toxins (Abrams et al., 2020, Reboldi et al., 2014, Lewis, 2003, Stern et al., 2017). Therefore, we wondered whether steroids and oxysterols might alter intrinsic cell protection against pore-forming toxins.

This thesis will focus on intrinsic protection against pyolysin, a cholesterol-dependent cytolysin secreted by *Trueperella pyogenes* that damages the bovine endometrium

contributing to the severity of uterine disease. We will examine the effect of progesterone, oestradiol, glucocorticoid, and oxysterol treatment on the pyolysin-induced cytolysis of bovine endometrial cells. We will then explore the extent of cytoprotection in a range of human cell types and investigate the mechanisms involved. Identifying protective mechanisms can inform strategies to prevent or limit the severity of disease caused by pathogens that secrete pore-forming toxins.

The present chapter will review current literature, commencing with an overview of bacterial pore-forming toxins before focusing on cholesterol-dependent cytolysins and the toxins used throughout this thesis (pyolysin, streptolysin O, and α -hemolysin). Subsequently, we will outline the consequences of membrane pore formation and mechanisms of damage repair. We will then discuss strategies to reduce disease severity by increasing cell tolerance and outline the rationale behind exploring the effect of oxysterols and steroids on cell protection.

1.2 PORE-FORMING TOXINS

Bacterial infections are a leading cause of global mortality and morbidity, particularly impacting the world's most vulnerable populations (Diseases and Injuries, 2020). For example, lower respiratory tract infections accounted for over 2 million deaths in 2016, with > 1 million attributed to *Streptococcus pneumoniae* (Khang and Collaborators, 2018). Additionally, a review in 2005 identified more than 750 million *Streptococcus pyogenes* infections globally per annum, with over 500,000 deaths caused by severe disease (Carapetis et al., 2005). Infection of domesticated animals with bacteria such as *T. pyogenes* and *Staphylococcus aureus* also impacts human well-being through loss of food security, treatment/prevention costs, or sustaining and expanding the prevalence of drug-resistant strains (Ribeiro et al., 2015, Wulf and Voss, 2008).

Pore-forming toxins are proteins with an ability to transform from a water-soluble form to a membrane-inserted form thereby perforating membranes, killing target cells, releasing nutrients, and facilitating the delivery of additional bacterial toxins (Parker and Feil, 2005, Geny and Popoff, 2006). Pore-forming toxins are commonly associated with majorly pathogenic and even drug-resistant bacterial strains (Los et al., 2013). They account for around one third of all toxins released across both Gram-positive and Gram-negative bacteria, making them the most common bacterial virulence factor

(Los et al., 2013). Furthermore, without pore-forming toxins the virulence of many bacterial species is reduced (Kho et al., 2011, Amos et al., 2014, Limbago et al., 2000).

Various host cell receptors have been identified as the target for toxin binding such as glycosylphosphatidylinositol-anchored proteins, a disintegrin and metalloprotease 10 (ADAM10), C-C chemokine receptor type 5, glycans, cholesterol, and other lipids (Wilke and Bubeck Wardenburg, 2010, Alonzo III et al., 2013, Giddings et al., 2003, Shewell et al., 2020). Once bound, pore formation begins with the organisation of proteins into a pre-pore oligomeric structure. Following a complex conformational change, membrane spanning residues insert into the lipid bilayer. The resulting pores range from 0.5 to 100 nm in diameter depending on the toxin (Parker and Feil, 2005).

Pore-forming toxins can be characterised into two large groups; α -pore-forming toxins and β -pore-forming toxins, split according to the secondary structure of their pore-forming domain as demonstrated in Fig 1.1 (Dal Peraro and van der Goot, 2016, Gouaux, 1997). In most α -pore-forming toxins, α -helices are inserted into the membrane during pore formation and the pore-forming domain consists of a hydrophobic helical hairpin buried between two amphipathic layers of α -helices (Cosentino et al., 2016). The α -pore-forming domain typically contain many residues that have a large hydrophobic content. Hydrogen bonds keep the helical structure stable in the membrane. α -pore-forming toxins can permeate membranes in their monomeric form, resulting in pores that are formed in a more dynamic and less defined manner than those formed by β -pore-forming toxins (Cosentino et al., 2016). In β -pore-forming toxins, oligomerization generates a transmembrane β -barrel that lines the pore. Each oligomer subunit comprises of 1 to 2 β -strands that contribute to the overall cylindrical structure in the lipid membrane (Bischofberger et al., 2012). Not all pore-forming toxins can be perfectly classified into α and β subfamilies. The repeats-in-toxin family are not always categorised in this manner due to difficulties in crystallographic analysis (Dal Peraro and van der Goot, 2016). Further characterisation is provided by the Transporter Classification Database, which separates pore forming toxins into over 100 separate subfamilies. The major families and their classification are outlined in Table 1.1. Whilst there are many pore-forming toxins, to study cytoprotection in the present thesis we challenged cells with pyolysin and streptolysin O, members of the large cholesterol-dependent cytolysin family of pore-forming

toxins. We also examined protection against *S. aureus* α -hemolysin, a toxin that does not specifically rely on cholesterol for cytolysis and forms pores of a smaller diameter.

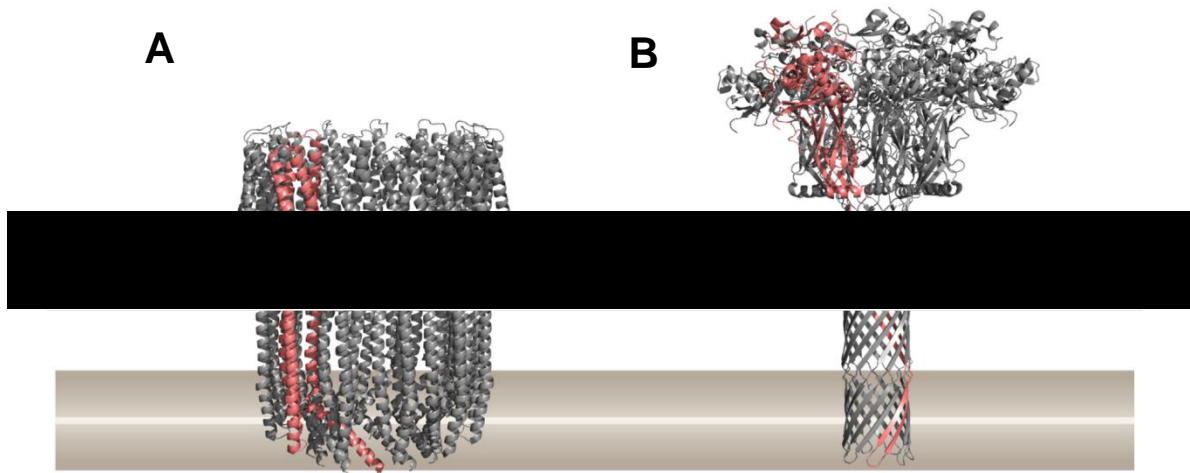


Figure 1.1 The two major classes of pore-forming toxins

(A) α -helical pore-forming toxin oligomer exemplified by the cytolysin A from *Escherichia coli*. (B) β -barrel pore-forming toxin oligomer exemplified by the anthrax toxin protective antigen pore from *Bacillus anthracis* (Omersa et al., 2019).

Table 1.1 Classification of pore-forming toxin families

The major families of pore forming toxins. Toxins used in this project are highlighted in bold (adapted from Dal Peraro and van der Goot (2016)).

Family	Class	Example toxins
Colicins	α	Colicin E1, Colicin A, Colicin N
Actinosporin	α	Equinatoxin II, Sticholysin II, Fragaceatoxin C
Cytolysin A	α	Cytolysin A, Non-haemolytic tripartite enterotoxin, Haemolysin BL
Hemolysin	β	α-hemolysin , γ -hemolysin, leukocidins
Aerolysin	β	Aerolysin, α -toxin, ϵ -toxin, Enterotoxin
Cholesterol-dependent cytolysins	β	Perfringolysin O, Pneumolysin, Streptolysin O, Pyolysin
Membrane attack complex component/ (MACPF)	β	Plu-MACPF, Bth-MACPF
Repeats-in-toxin	?	Bifunctional haemolysin-adenylyl cyclase toxin

1.3 CHOLESTEROL-DEPENDENT CYTOLYSINS

Cholesterol-dependent cytolysins are mainly produced by pathogenic Gram-positive bacteria (Heuck et al., 2010). Over twenty species of the genera *Clostridium*, *Streptococcus*, *Listeria*, *Bacillus* and *Arcanobacterium* (including *T. pyogenes* and *S. pyogenes*) synthesise cholesterol-dependent cytolysins to disrupt target cell plasma membranes and facilitating bacterial invasion via the formation of pores with a diameter of 30 to 50 nm (Tveten, 2005). Like the name suggests, membrane cholesterol is important for cholesterol-dependent cytolysin function, as first reported by Hewitt and Todd (1939), where preincubation of streptolysin O with free cholesterol inhibited hemolytic activity.

1.3.1 Plasma membrane cholesterol

Plasma membrane structure

Eukaryotic cells are encapsulated in a protective plasma membrane that protects the intracellular contents from the surrounding environment (Fig 1.2). To understand how cholesterol-dependent cytolysins interact and perforate the plasma membrane, it is important to understand plasma membrane structure. A bilayer composed of four major phospholipids: phosphatidylcholine, phosphatidylethanolamine, phosphatidylserine, and sphingomyelin provides the structural integrity of the plasma membrane (Cooper, 2000). This bilayer is draped over a cytoskeleton that consists of actin, septin and other microtubule networks and provides a scaffold for various membrane components (Koster and Mayor, 2016, Bezanilla et al., 2015). The external surface of the membrane predominantly consists of phosphatidylcholine and sphingomyelin, whereas the inner layer mainly contains phosphatidylethanolamine and phosphatidylserine (van Meer et al., 2008, Cooper, 2000). The interior of the bilayer contains the hydrophobic fatty acid chains of the phospholipids creating a membrane that is impermeable to water-soluble molecules (van Meer et al., 2008).

The phospholipid bilayer also contains glycolipids and cholesterol. Glycolipids are lipids with a carbohydrate attached by a glycosidic bond found exclusively on the external membrane surface (Curatolo, 1987). They are relatively minor membrane component that contributes to cell stability and recognition (Yamakawa and Nagai,

1978). On the other hand, cholesterol is the most abundant plasma membrane lipid and must be present in the target cell membranes for cholesterol-dependent cytolysin pore-formation (Giddings et al., 2003). Cholesterol orientates in the biological membrane perpendicular to the lipid bilayer. The hydroxyl group at the 3 β position of the cholesterol molecule is positioned where water meets the membrane and the cholesterol side chain points towards the hydrophobic interior of the bilayer (Yeagle, 1985).

Plasma membrane lipids are organised into a variety of different sub compartments, as specific lipids interact preferentially with one another (Singer and Nicolson, 1972, Simons and Vaz, 2004, Sezgin et al., 2017). For example, cholesterol preferentially associates with saturated lipids, such as sphingomyelin (Slotte, 1999, Barenholz and Thompson, 1980). These cholesterol and sphingomyelin-enriched nanodomains range from 10 to 200 nm in diameter and are termed lipid rafts (Pike, 2006, Sezgin et al., 2017).

Whilst lipids provide the structural integrity of the eukaryotic cell plasma membrane, proteins are bedded within the phospholipid bilayer to carry out specific cellular functions. Transmembrane proteins span the membrane, typically functioning as a transport gateway. Additionally, a different variety of proteins are anchored to the plasma membrane via covalently attached lipids (Ray et al., 2017). These attachments range from simple fatty acids to complex glycosylphosphatidylinositol (GPI) anchors. The lipid modifications control a diverse range of critical cell functions including membrane signalling and trafficking (Resh, 2006).

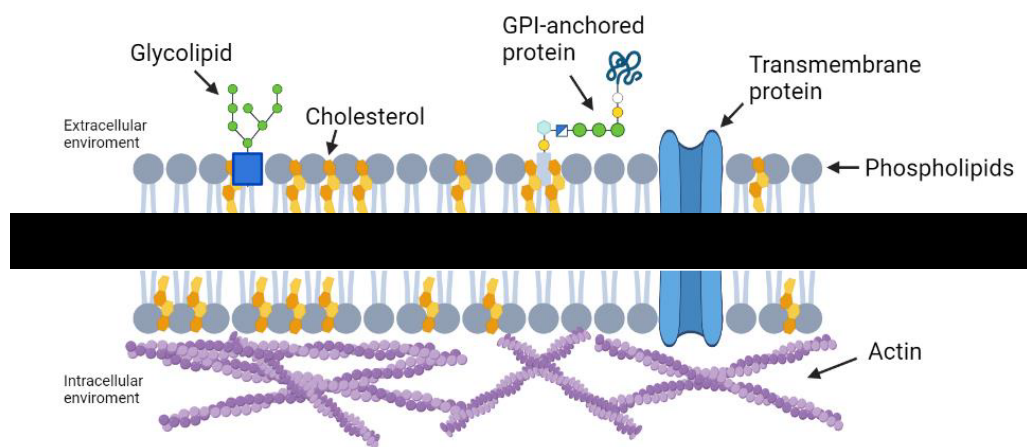


Figure 1.2 Structure of the plasma membrane

Diagram of a eukaryotic cell plasma membrane displaying key structures of interest. Created with BioRender.com.

Interaction between cholesterol-dependent cytolysins and membrane cholesterol

The 3 β -hydroxy group, the stereochemistry of the sterol ring system, and the side-chain stemming from carbon 17 are thought to be the key features of the cholesterol molecule that interact with cholesterol-dependent cytolysins (Prigent and Alouf, 1976). However, the 3 β -hydroxy group is small relative to the head groups of phospholipids, remaining relatively hidden and complexed in the membrane in the presence of excess phospholipids. When the concentration of cholesterol exceeds 35 mol% (molar percentage) of total membrane lipids there is increased surface exposure of the cholesterol molecule, permitting cholesterol-dependent cytolysin binding (Das et al., 2013). Conversely, depleting cellular cholesterol reduces the accessibility of plasma membrane cholesterol to cholesterol-dependent cytolysins.

Using a mutant version of perfringolysin O labelled with ¹²⁵I, that binds but does not form pores in mammalian cells, Das et al. (2014) identified three separate ‘pools’ of plasma membrane cholesterol. The cholesterol that accumulates in the presence of excess cholesterol, allowing cholesterol-dependent cytolysin binding was termed the ‘labile pool’ and is referred to as accessible cholesterol throughout the present thesis. The cholesterol in-accessible to the mutant perfringolysin O was then split into two further ‘pools’. The first of these ‘pools’, termed the ‘sphingomyelin-sequestered pool’, refers to the cholesterol that is typically sequestered in complexes with sphingomyelin and only became available for cholesterol-dependent cytolysin binding after sphingomyelin was destroyed by sphingomyelinase (Das et al., 2014, Endapally et al., 2019, McConnell and Radhakrishnan, 2003). Finally, a ‘residual pool’ of cholesterol was not available for cholesterol-dependent cytolysin binding even after sphingomyelinase treatment. The ‘residual pool’ of cholesterol is vital for membrane stability and depleting it compromises cell morphology and viability (Das et al., 2013).

Although the importance of membrane cholesterol in cholesterol-dependent cytolysin function is clear, there are indications that additional cellular receptors may exist. Intermedilysin, a cholesterol-dependent cytolysin secreted by *Streptococcus intermedius*, uses cluster of differentiation 59 as a binding receptor (Dowd et al., 2012). When cholesterol-depleted human red blood cells were exposed to intermedilysin, the initial membrane interaction and pre-pore assembly could occur without the presence of cholesterol, though cholesterol is required for pore insertion (Hughes et al., 2009). Additionally, a recent study by Shewell et al. (2020)

demonstrates that cholesterol-dependent cytolysins also use glycans such as glycolipids, glycoproteins and GPI-anchored glycoproteins as cellular receptors in an independent mechanism to cholesterol. All the cholesterol-dependent cytolysins screened bound to glycans, although with varying specificity. For example, lectinolysin bound to a single structure, whereas streptolysin O and perfringolysin O interacted with a broad range of glycans (Shewell et al., 2020).

1.3.2 Pore formation

The cholesterol-dependent cytolysin molecule typically consists of four distinct domains (Fig 1.3A). Domain 4 consists of two four-stranded beta-sheets that are interconnected into four loops: three short loops and a longer highly conserved tryptophan-rich undecapeptide loop. These loops insert into the membrane upon binding and are responsible for cholesterol-toxin interaction that stimulates pore formation (Ramachandran et al., 2002, Farrand et al., 2010). A recent study by Shewell et al. (2020) has proposed that domain 4 initially interacts with glycoconjugate receptors to direct and accumulate the toxin monomers on the target cell surface. A pre-pore oligomer is developed via the lateral diffusion and association of cholesterol-dependent cytolysin monomers linked by hydrogen bonding (Soltani et al., 2007). The entire cholesterol-dependent cytolysin oligomer assembly takes place in the pre-pore state, with oligomerization halted before pore insertion (Leung et al., 2014, Hotze and Tweten, 2012). Once the pre-pore oligomer is formed, there is a disengagement with the glycoconjugate receptors (Shewell et al., 2020), and the vertical collapse of domain 1 and the buckling of domain 2 support the insertion of both transmembrane helices in domain 3 into the plasma membrane (Hotze and Tweten, 2012).

Individual toxin monomers contribute to the overall β -barrel that inserts into the lipid bilayer (Rosado et al., 2008). However, a fully enclosed β -barrel is not necessary for the insertion of the transmembrane helices, and arcs formed from the incomplete oligomerization of cholesterol-dependent cytolysin monomers can still perforate the plasma membrane (Leung et al., 2014, Sonnen et al., 2014).

Regardless of the extent of oligomerization, the inserted transmembrane helices compromise the integrity of the plasma membrane. The hydrophilic inner surface of the β -barrel destabilizes the lipid membrane encapsulated by the cholesterol-dependent cytolysin oligomer (Leung et al., 2014). As a result, lipids are expelled generating a

pore in the lipid bilayer (Leung et al., 2014). The consequences of this pore formation will be discussed in section 1.5.

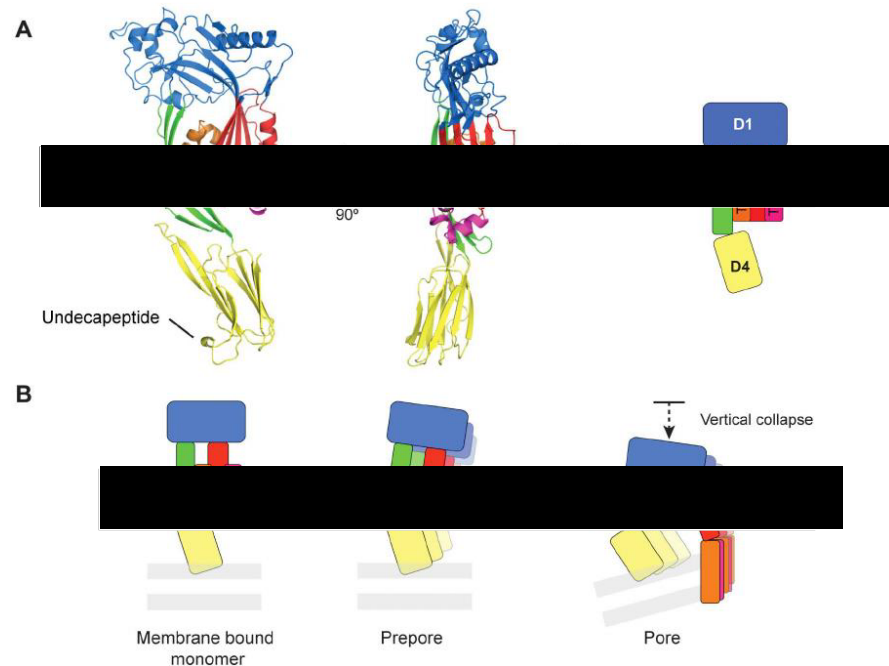


Figure 1.3 Cholesterol-dependent cytolysin membrane insertion

(A) A crystal structure of perfringolysin O (B) Schematic representation of cholesterol-dependent cytolysin pore formation. Binding is carried out through the tip of domain (D) 4. This initiates a conformational change of domain 2 that facilitates the insertion of the transmembrane helices (TMH) (Reboul et al., 2014).

1.3.3 Thiol-activation

Most crude cholesterol-dependent cytolysins are only active in a chemically reduced state. Activity is reversibly lost by oxidation (Billington et al., 2000). To restore activity, a thiol group (or other reducing agent) can be added (hence the term thiol activation). A thiol is an organosulfur compound that contains a carbon-bonded sulfhydryl (R-SH) group (R represents an organic substitute such as an alkyl). The necessity to become thiol activated is derived from a cysteine residue that is located within the conserved undecapeptide sequence (location shown in Fig 1.3). It is the oxidation of this residue that leads to the reduced activity, possibly by impairing of other crucial amino acids such as the three tryptophan residues that are found in the same location (Iwamoto et al., 1987).

The need to be thiol-activated is not a characteristic of all cholesterol-dependent cytolysins. Pyolysin does not show any requirement for thiol activation and is not susceptible to any thiol blocking agents (Billington et al., 1997). It is clearly still a

cholesterol-dependent cytolysin though as it exhibits the same amino acid homology as other cholesterol-dependent cytolysins. However, in the afore mentioned undecapeptide sequence Alanine is substituted for the typical cysteine residue (Billington et al., 2000).

1.3.4 Pyolysin and *Trueperella pyogenes*

Pyolysin is a useful toxin for examining cholesterol-dependent cytolysins that forms pores in many types of mammalian cells. As thiol activation is not required, pyolysin is spontaneously active *in vitro*, easing experimental use. Pyolysin is secreted by *Trueperella pyogenes*; a Gram-positive, nonmotile, anaerobic species of bacteria that commonly resides in the urogenital, gastrointestinal, and upper respiratory tracts of cattle, goats, horses, musk deer, pigs, and sheep (Ribeiro et al., 2015). *Trueperella pyogenes* is an opportunistic pathogen that causes mastitis, abscesses, pneumonia, and endometritis (Jost and Billington, 2005). For example, *T. pyogenes* contributes to uterine disease in cattle. Reduced milk yield and infertility are resulting complications and cost the United States and European dairy industries a combined \$2 billion annually (Sheldon et al., 2009).

Parturition disrupts the protective endometrial epithelium of the bovine reproductive tract, exposing the underlying sensitive stromal cells (Amos et al., 2014). There is an upsurge in bacteria in the uterine lumen surrounding birth, with *T. pyogenes*, *E. coli*, and *S. aureus* commonly isolated from diseased animals (Bonnett et al., 1991, Sheldon et al., 2002). However, of all the bacteria located within the uterus following parturition, *T. pyogenes* is most associated with the severity of pathology (Bonnett et al., 1991, Westermann et al., 2010).

Trueperella pyogenes secretes several virulence factors including neuraminidases, fimbriae, and collagen-binding proteins (Jost and Billington, 2005). However, most of the pathology and tissue damage surrounding uterine disease is associated with the secretion of pyolysin (Ribeiro et al., 2015). Indeed, it has been shown that a pyolysin-deleted *T. pyogenes* mutant does not trigger bovine endometrial cell cytolysis (Amos et al., 2014). The biological significance of the interaction between pyolysin and the bovine endometrium in uterine disease informed the decision to use this as a model system to explore cell protection.

Pyolysin is a 55 kDa protein encoded by a gene that consists of 1,605 base pairs (Billington et al., 1997). A sequence based structural model demonstrates that pyolysin also consists of the typical four domains demonstrated by cholesterol-dependent cytolysins (Fig 1.4A), showing clear similarity with the structure of perfringolysin O (Fig 1.3A), the archetypal cholesterol-dependent cytolysin (Pokrajac et al., 2012). The isolated domain 4 of pyolysin binds to target cell membranes but also forms oligomers with itself (Pokrajac et al., 2013). Electron micrographs demonstrate that oligomerized pyolysin monomers form typical ring-shaped structures (Fig 1.4B).

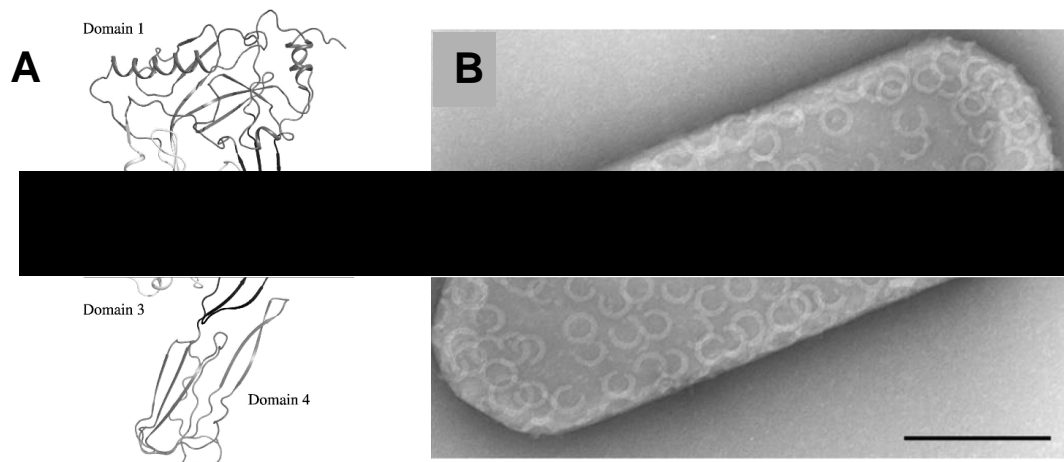


Figure 1.4 Pyolysin structure and oligomerization

(A) Structural model of pyolysin based on the crystal structure of perfringolysin O. (B) Electron microscopy of pyolysin oligomers on cholesterol crystals; scale bar = 100 nm (Pokrajac et al., 2013).

1.3.5 Streptolysin O and *Streptococcus pyogenes*

Streptococcus pyogenes is a Gram-positive bacterium that commonly colonises the skin and throat, causing a wide range of disease that significantly contributes to global morbidity and mortality (Wannamaker, 1970). Pathology takes the form of cellulitis, impetigo, scarlet fever, bacterial pharyngitis, and pneumonia, with severe invasive infections progressing to necrotizing fasciitis and streptococcal toxic shock syndrome (Cunningham, 2000).

Streptolysin O is one of over twenty proteins secreted by *Streptococcus pyogenes* to enhance virulence (Alouf, 1980, Sierig et al., 2003, Bhakdi et al., 1985). Streptolysin O is a typical thiol-activated cholesterol-dependent cytolysin that interacts with cholesterol and multiple glycans in target bilayers (Shewell et al., 2020), and is regularly utilised to investigate cholesterol-dependent cytolysins (Babiychuk et al.,

2009, Turner et al., 2020). Purified streptolysin O is lethal to mice and rabbits within minutes when injected intravenously (Barnard and Todd, 1940, Howard and Wallace, 1953). Furthermore, mice infected with a mutant streptolysin O deleted *Streptococcus pyogenes* had a significantly higher survival rate than those infected with wild-type bacteria (Limbago et al., 2000).

1.4 STAPHYLOCOCCUS AUREUS ALPHA-HEMOLYSIN

Staphylococcus aureus is an opportunistic pathogen that is one of the leading causes of human bacterial infection, infecting the skin and soft tissues, the bloodstream and the respiratory tract (Lowy, 1998). Production of α -hemolysin (the archetypal toxin of a distinct family of pore-forming toxins; see Table 1.1) is key to the pathogenesis of sepsis, pneumonia, and severe skin infections (Bubeck Wardenburg and Schneewind, 2008, Kennedy et al., 2010). Expression of α -hemolysin contributes directly to *S. aureus* virulence (Patel et al., 1987).

A disintegrin and metalloprotease 10 is required for the cytolytic activity of α -hemolysin, as the toxin interacts directly with ADAM10 in plasma membrane lipid rafts (Wilke and Bubeck Wardenburg, 2010). Seven α -hemolysin monomers oligomerize on the membrane surface to form a mushroom shaped complex as shown in Fig 1.5 (Song et al., 1996). The stem of the complex is initially folded and located within the cap, but is then dynamically inserted into the cell forming a transmembrane pore (Menestrina et al., 2001). Pores vary in diameter from 1.4 to 2.8 nm throughout various points of the 'stem', and are selectively permeable for monovalent ions, excluding calcium (Song et al., 1996). Deoxyribonucleic acid (DNA) fragmentation and apoptosis are induced as a result (Bantel et al., 2001). However, at high concentrations, the toxin will bind non-specifically to the lipid bilayer of most eukaryotic cells (Hildebrand et al., 1991), forming larger pores that permit calcium ion influx in some cell types (Walev et al., 1993).

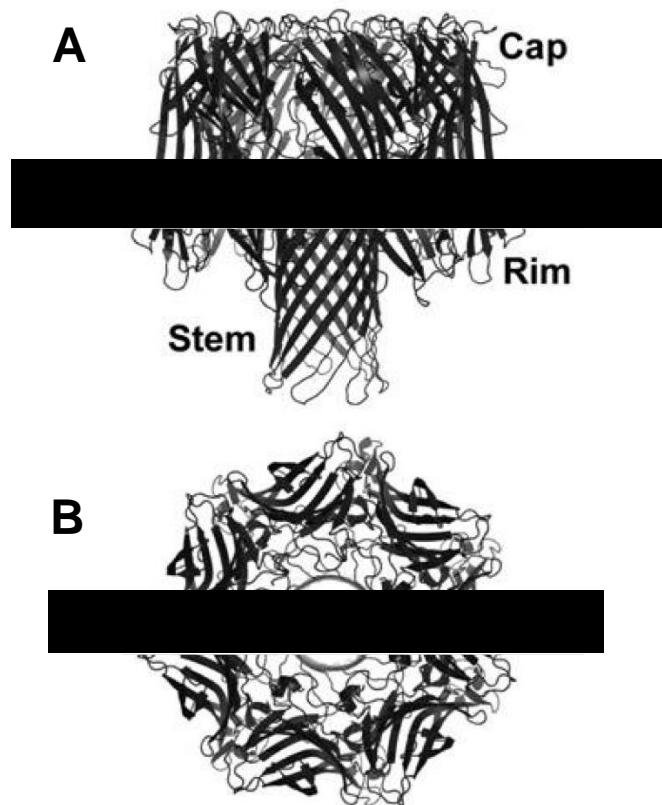


Figure 1.5 *Staphylococcus aureus* α -hemolysin oligomer

(A) Side and (B) top views of the crystal structure of *S. aureus* α -hemolysin (Song et al., 1996, Berube and Bubeck Wardenburg, 2013).

1.5 CONSEQUENCES OF PORE FORMATION

Perforation of the plasma membrane by pore-forming toxins leads to an increase in membrane permeability, allowing the leakage of cytosolic content (Fig 1.6). The primary consequence of compromised membrane integrity is a change in cytoplasmic ion composition and a loss of membrane potential (Bischofberger et al., 2009). However, different pore-forming toxins form pores of varying sizes, triggering different responses in target cells (Bischofberger et al., 2012). The large pores formed by cholesterol-dependent cytolysins permit rapid calcium ion entry and potassium efflux as well as the leakage of molecules such as lactate dehydrogenase (LDH) and adenosine triphosphate (ATP) within 2 h (Hotze and Tweten, 2012, Gonzalez et al., 2011, Bonfini and Buchon, 2016). Several secondary consequences are triggered by the changes in cytosolic molecular concentrations, promoting recovery and cell survival, and these will be described in detail in the next section (Gonzalez et al., 2011).

Plasma membrane damage by pore-forming toxins can also trigger changes in cell shape within 15 min, such as the formation of large blebs (Keyel et al., 2011). As cellular structure declines, the internal hydrostatic pressure causes the actin cytoskeleton to decouple from the plasma membrane and individual bulges of the intracellular matrix protrude from the cell (Fackler and Grosse, 2008).

Ultimately, a major consequence of pore-forming toxins is target cell cytolysis. Excessive pore formation leads to necrosis, partly due to the decreased intracellular ATP and potassium deregulating mitochondrial activity (Kennedy et al., 2009, Knapp et al., 2010). Lower toxin concentrations can activate a range of programmed cell death pathways such as apoptosis, pyroptosis (both caspase dependent), and necroptosis (caspase independent) (Lin et al., 2010).

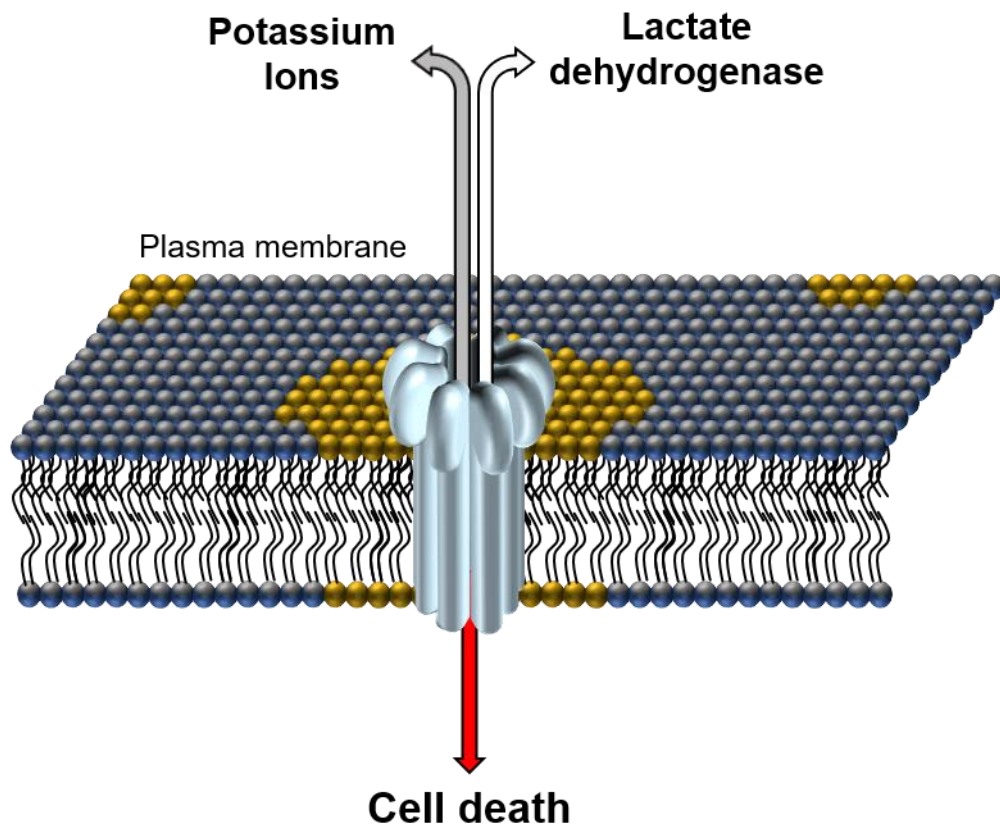


Figure 1.6 Consequences of pore-forming toxin pore formation

A visual representation of the consequences of eukaryotic cell membrane perforation by bacterial pore-forming toxins.

1.6 CELL REPAIR

Although high concentrations of pore-forming toxins can cause rapid cell cytolysis, throughout infection many cells are exposed to sublytic concentrations that initiate pro-survival responses in response to the changes in cytosolic molecular concentrations (Gonzalez et al., 2011, Bischofberger et al., 2012). Though several of these processes are described below and summarised in Fig 1.7, it is likely that more remain to be characterised.

1.6.1 Membrane remodelling

The influx of extracellular calcium ions following cholesterol-dependent cytolysin pore-formation activates cytoskeletal remodelling to reduce tension, facilitate vesicle recruitment, and promote membrane repair (McNeil and Steinhardt, 1997, Jimenez and Perez, 2017). Sustained cytosolic calcium concentrations activate various cytoskeleton-modulating enzymes, such as Ras-related C3 botulinum toxin substrate 1, Ras homolog family member A and calpains, to break down actomyosin structures (Iliev et al., 2007, Ono and Sorimachi, 2012). Activated calpains break down interactions between actin and actin-binding proteins, separating the cytoskeleton from the plasma membrane (Redpath et al., 2014). Rab3 promotes continued actin remodelling, assisting lysosomes to bind and fuse to the plasma membrane (Encarnacao et al., 2016). Endoplasmic reticulum (ER) proteins translocate to the plasma membrane. The ER chaperone Gp96 interacts with the actin motor protein non-muscle myosin II and the actin adaptor filament A regulating non-muscle myosin IIA cortical bundles and stabilizing the remodelling (Mesquita et al., 2017).

Prolonged elevation of intracellular calcium can be toxic. Activated intracellular proteinases and phospholipases cause irreversible damage to the phospholipid bilayer and cytoskeleton (Geeraerts et al., 1991). Therefore, mediating calcium ion influx appears crucial to determining cell fate and repairing the compromised membrane allows cells to recover from the disruption triggered by pore formation (McNeil and Kirchhausen, 2005). Indeed, streptolysin O permeabilization of THP-1 monocytes was shown to be reversible, with membrane resealing dependent on the presence of calcium; recovering cells remained viable for several days after the challenge and maintained their ability to proliferate (Walev et al., 2001). Several mechanisms

coalesce to regulate calcium-dependent plasma membrane repair, in response to pore-forming toxin damage and these are described below (Andrews and Corrotte, 2018).

Calcium influx depolarises cortical actin and recruits components such as annexin A1 to stabilize and repair damaged and blebbing membranes (McNeil et al., 2006). Annexin A1 links membrane either side of protruding blebs, generating a 'plug' or 'patch repair'. In this way, the compromised, pore containing membrane is separated from the rest of the cytoplasm, preventing further efflux of cytosolic content (Romero et al., 2017, Babiychuk et al., 2011). Blebbing cells appear more likely to recover from streptolysin O damage and inhibiting plasma membrane blebbing with blebbistatin increased the likelihood of cell lysis (Babiychuk et al., 2011, Keyel et al., 2011). Repaired blebs isolate surplus intracellular calcium and might be removed from the plasma membrane to spare the rest of the cell from further damage, though this is disputed (Babiychuk et al., 2009, Babiychuk et al., 2011). Andrews and Corrotte (2018) suggest that these large blebs do not detach from the membrane and simply reflect actin cytoskeleton disassembly. Much smaller vesicles (around 50 nm) can be shed in the process of membrane repair, but these are generated by the endosomal sorting complexes required for transport (ESCRT) pathway (Jimenez et al., 2014, Andrews and Corrotte, 2018, Wolfmeier et al., 2016).

Endocytosis is another calcium-dependent reparative mechanism (Idone et al., 2008). Calcium sensors such as synaptotagmin VII, dysferlin, and N-ethylmaleimide-sensitive factor attachment protein receptors trigger lysosomal exocytosis in response to pore formation (Rodriguez et al., 1997, Chakrabarti et al., 2003, Defour et al., 2014). Lysosomes release enzymes, such as acid sphingomyelinase. Sphingomyelin tends to cluster near cholesterol and so is likely to be adjacent to pore-forming toxin (specifically cholesterol-dependent cytolysin) pores (Truman et al., 2011). Acid sphingomyelinase hydrolyses sphingomyelin, forming ceramide rich plasma membrane invaginations termed caveolae (Corrotte et al., 2013). These caveolae promote pore-removal via endocytosis (Corrotte et al., 2012). Pore-containing endosomes undergo ubiquitination and interact with components of the ESCRT pathway as they enter the lumen of multivesicular bodies and are degraded (Corrotte et al., 2012).

Following the shedding or internalisation of pores, cells can return to original cytoskeletal organisation and establish normal cytosolic calcium concentrations.

1.6.2 Mitogen-activated protein kinases

The MAPK family, comprised of over 50 different proteins in mammals are involved in intracellular regulation in response to extracellular signals (Porta et al., 2011). They largely respond to stress, coordinating host cell survival, metabolism and proliferation (Cargnello and Roux, 2011). Activation of the MAPK pathways is augmented by the potassium efflux caused by pore-formation, triggering membrane repair and cell survival mechanisms (Porta et al., 2011, Kloft et al., 2009). Activated MAPKs can translocate to the nucleus and function as an enzyme, phosphorylating and activating transcription factors (McCain, 2013). Phosphorylation of p38 occurs imminently in response to a range of toxins including *S. aureus* α -hemolysin, streptolysin O, and pneumolysin, and wanes after several hours (Ratner et al., 2006, Husmann et al., 2006). Phosphorylation of the extracellular signal-regulated kinases 1 and 2 (ERK1/2) and c-Jun (N)-terminal kinase (JNK) are also commonly identified (Stassen et al., 2003, Aguilar et al., 2009). Pyolysin challenge induces the phosphorylation of all three of these MAPKs in both bovine endometrial stromal and HeLa cervical cells (Preta et al., 2015, Pospiech et al., 2021). Thus, the phosphorylation of p38, ERK1/2, and JNK will be examined in the present thesis.

Activated p38 facilitates the recovery of original potassium ion concentrations following proaerolysin or listeriolysin O challenge, promoting cell survival (Gonzalez et al., 2011). Additionally, p38 up-regulates genes involved in the activation of the unfolded protein response (UPR) and the expression of cation efflux proteins (Bischof et al., 2008). Activation of the UPR by listeriolysin O stimulates lipid synthesis, potentially enhancing membrane repair and increasing the movement of vesicles between the ER and the Golgi (Cassidy and O'Riordan, 2013).

The JNK pathway has been viewed as a key regulator of cellular defence to pore-forming toxins, up-regulating innate immune signalling and p38 specific pathways via the activating protein-1 (AP-1) transcription factor (Kao et al., 2011). Loss of either the p38 or JNK pathway can lead to a hypersensitivity to pore-forming toxins (Huffman et al., 2004).

Activation of ERK1/2 in response to insult by pore formation also contributes to cell survival by inducing the shedding of cell adhesion and intracellular-contact molecules, potentially assisting in the shedding of pores (Brito et al., 2019). Additionally, ERK activation contributes to the recovery of cellular ion homeostasis (Gonzalez et al., 2011).

1.6.3 Inflammasome activation and autophagy

The decrease in intracellular potassium caused by a multitude of pore-forming toxins such as aerolysin, pneumolysin and *S. aureus* α -hemolysin can also trigger inflammasome assembly (Gurcel et al., 2006, McNeela et al., 2010, Soong et al., 2012, Witzenrath et al., 2011). Specifically, the Ipaf and Nalp3 inflammasomes are assembled in response to aerolysin pore formation and proceed to activate caspase-1 and the sterol responsive element binding proteins (SREBPs) (Gurcel et al., 2006). The caspase-1 dependent SREBP activation results in an increase in cellular cholesterol that may improve cell survival (Gurcel et al., 2006). Downstream targets of caspase-1 also include interleukin (IL)-1 β and IL-18, pro inflammatory cytokines that play essential roles in innate and adaptive immunity (Dinarello, 1998), and both are secreted from cells in response to pore-forming toxin challenge (Walev et al., 1995, Meixenberger et al., 2010, Dunne et al., 2010).

Autophagy is another defence mechanism against pore-formation, triggered by a drop in the cytosolic ATP / adenosine monophosphate (AMP) ratio that prompts AMP-activated protein kinase phosphorylation. Phosphorylated AMP-activated protein kinase then initiates autophagy by inhibiting the target of rapamycin receptor complex 1 (Stanfel et al., 2009), triggering the formation of autophagosomes (Gutierrez et al., 2007). These autophagosomes interact with the endocytic pathway, forming autophagolysosomes by fusing with lysosomes, and degrade bacterial toxins promoting cell survival (Saka et al., 2007). Cells that cannot generate autophagic vacuoles in response to pore-forming toxins demonstrate a poorer prognosis, confirming a link between autophagy and cell survival (Gutierrez et al., 2007). Additionally, autophagy contributes to ER remodelling and helps remove and detect organelles damaged by pore-formation (Brito et al., 2019).

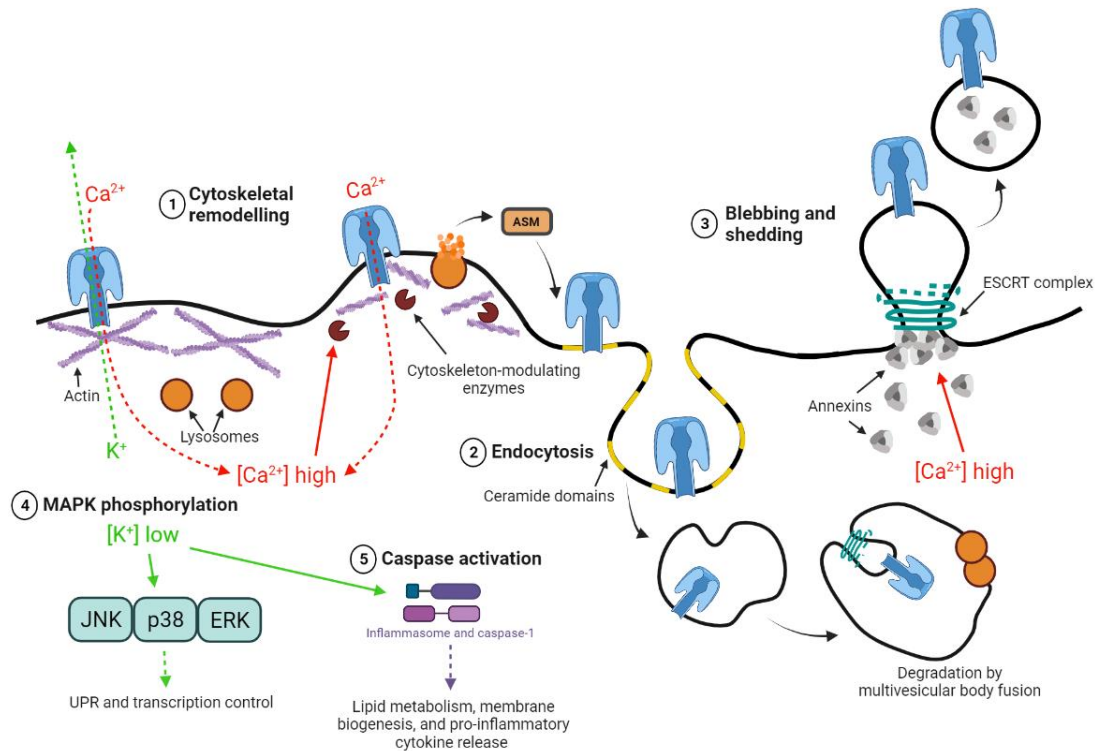


Figure 1.7 Mechanisms repairing the damage caused by pore-forming toxins

Changes in cytosolic ion concentrations trigger a variety of pro-survival responses. **(1)** Calcium influx triggers cytoskeletal remodelling to reduce plasma membrane tension by activating cytoskeleton-modulating enzymes and triggering lysosome secretion. **(2)** Acid sphingomyelinase (ASM) released from lysosomes hydrolyses sphingomyelin to form ceramide-rich domains which facilitate the endocytosis of pores. Toxins are then trafficked to multivesicular bodies and degraded by lysosomes. **(3)** Increased calcium ion concentrations recruit annexins to damage sites clogging pores. The recruitment of ESCRT subunits facilitates the budding and release of pore-forming toxin containing vesicles. **(4)** Potassium ion efflux activates MAPK signalling, which controls the UPR and other protective responses. **(5)** Decreased cytosolic potassium concentrations also trigger inflammasome assembly and caspase-1 activation. Downstream effects of caspase-1 include SREBP activation the secretion of IL-1 β and IL-18. Created with BioRender.com.

1.7 PROTECTION AGAINST PORE-FORMING TOXIN DAMAGE

The reparative processes discussed in section 1.7 can react to pore-formation and mediate cell damage, however, increasing toxin concentrations ultimately results in cell cytolysis. Alternatively, increasing intrinsic cell protection in advance of toxin challenge might reduce the severity of disease caused by pathogens that secrete pore-forming toxins.

1.7.1 Cell tolerance

It is commonly assumed that resilience to infection is achieved by combatting invading pathogens directly (Medzhitov et al., 2012). Activation of the innate and adaptive immune response kills invading microbes and limits the number of pathogenic bacteria, though these pathways, termed resistance mechanism (McCarville and Ayres, 2018). The innate immune response provides an immediate defence to pathogens that does not depend on prior exposure (Takeuchi and Akira, 2010). Cells use pattern recognition receptors to recognise pathogen-associated molecular patterns and trigger the secretion of inflammatory mediators that induce vasodilation, attract and activate immune cells, and induce the production of acute phase proteins and reactive oxygen species (Medzhitov and Janeway Jr, 2000). Adaptive immunity relies on prior exposure of T and B cells to specific antigens. Antigen presenting cells process pathogenic antigens and present them to T-cells triggering T cell activation. Subsequently, T cells detect and destroy infected cells, secrete cytokines, and activate B cells to commence antibody production (Bonilla and Oettgen, 2010). However, an immune response can be energetically expensive, requiring a 15% to 30% increase in resting metabolic rate (Lochmiller and Deerenberg, 2000).

Avoidance mechanisms limit pathogen exposure with minimal metabolic cost and include intrinsic behaviours to maintain hygiene and avert diseased animals, possibly by identifying the odour of pathogens or infection (Curtis, 2007, Curtis, 2014). However, the effectiveness of avoidance mechanisms can depend on pathogen transmissibility and population density.

Alternatively, survival can be achieved by limiting the consequential effects of an invasive microorganism. Cell tolerance (not immunological tolerance) is the ability to restrict the damage caused by pathogenic invasion without decreasing the pathogen burden (Schneider and Ayres, 2008, Read et al., 2008, Medzhitov et al., 2012). While

there is extensive knowledge about resistance mechanisms, research in the field of tolerance is still developing. Examples of tolerance mechanisms against bacterial pathogens include damage repair (including the pathways described in section 1.6) to help restore the integrity of compromised tissues and reprogramming cellular responses to help generate energy and substrates for tissue repair (Sheldon et al., 2020, Escoll and Buchrieser, 2018). Additionally, protecting cells against bacterial toxins is a mechanism of improving tissue tolerance that increases resilience. Protection implies defending or guarding against attack, injury, or damage. Protective mechanisms include physical barriers such as epithelial and mucus layers and neutralising toxins with antimicrobial peptides, acute phase proteins, and mucosal glycoproteins (Hein et al., 2002, Gruys et al., 2005, Epanand and Vogel, 1999, Linden et al., 2008).

Collectively these resistance, avoidance, and tolerance mechanisms combine to increase the resilience to bacterial infection and prevent or restrict the severity of disease (Fig 1.8) (Schneider and Ayres, 2008, Read et al., 2008).

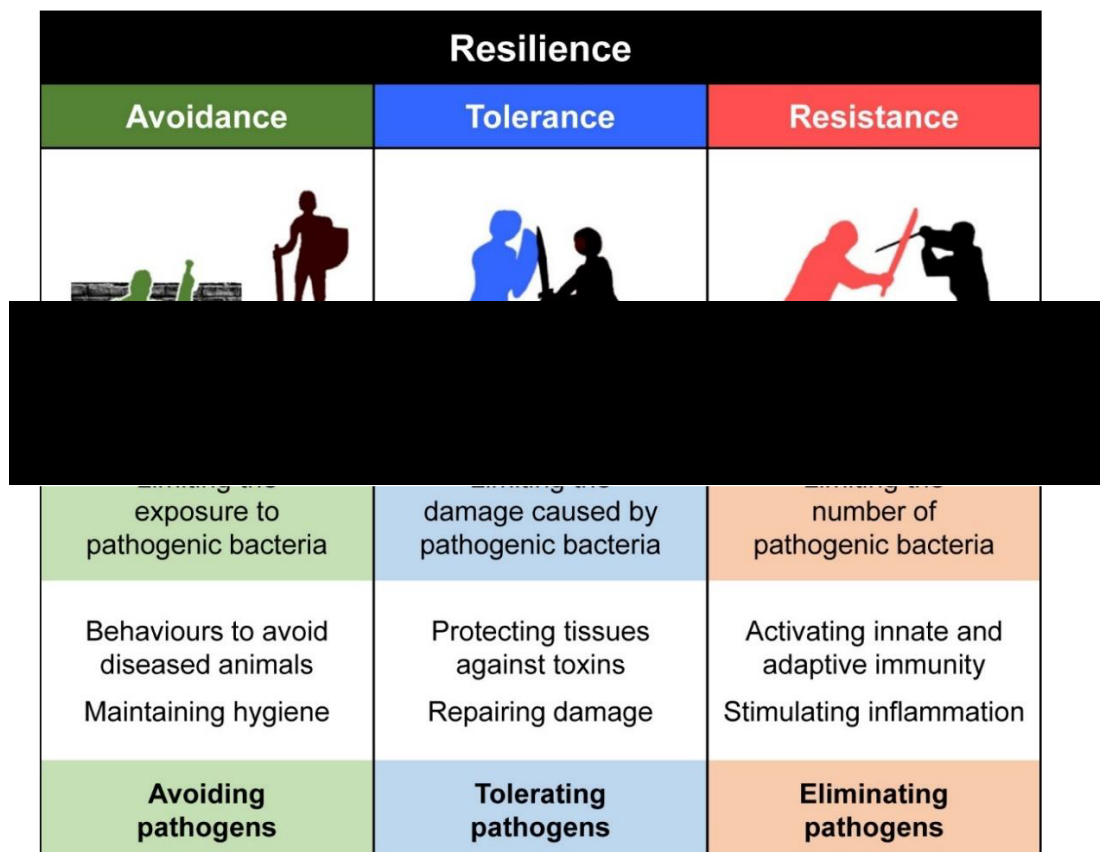


Figure 1.8 Mechanisms of achieving resilience to bacterial infection

Resilience to infection is a product of the complementary strategies of avoidance, tolerance, and resistance. This cartoon displays the concept for each strategy (Sheldon et al., 2020).

1.7.2 Cell protection

As mentioned above, protecting cells against pore-forming toxin damage is a potential method of increasing tissue tolerance to bacterial infection and reducing disease severity, though there is currently limited research in this field.

Protection can be achieved by impairing pore-forming toxin function. Small molecules can bind to specific regions of toxin monomers, preventing pore-formation. For example, amentoflavone and verbascoside can bind between domains 3 and 4 on pneumolysin monomers inhibiting oligomerization (Zhao et al., 2017, Zhao et al., 2016). Additionally, editing the availability of toxin binding receptors can prevent membrane interaction. Indeed, inhibiting ADAM10 (required for *S. aureus* α -haemolysin binding) with GI254023X improves pathology (Kennedy et al., 2010).

Pore-forming toxins can be neutralized by molecules with a high affinity to them; examples include β -sitosterol (a cholesterol mimic) and allicin (Li et al., 2015, Arzanlou and Bohlooli, 2010). Synthetic plasma membranes (termed liposomes) have been developed to draw cholesterol-dependent cytolysins away from their cellular targets, however, they suffer from a variety of drawbacks such as *in vivo* stability, immune clearance, and the need to alter their composition depending on the toxin (Henry et al., 2015). Stealth coatings have been used to disguise liposomes from immune cell clearance, however, these can result in off target immune effects (Immordino et al., 2006).

Finally, protection can be achieved by treating cells with chemical compounds that increase intrinsic cell protection against pore-forming toxin damage, thereby improving tissue tolerance. This process is termed cytoprotection. Current research screening for cytoprotective agents has focused on reducing cellular cholesterol, as cholesterol is essential for cholesterol-dependent cytolysin pore-formation and most of the other molecules that act as pore-forming toxin binding receptors are located in cholesterol-rich lipid rafts (Fivaz et al., 2000, Fivaz et al., 1999). Treating cells with cyclodextrins depletes total cellular cholesterol, decreasing cholesterol-dependent cytolysin binding and pore formation (Giddings et al., 2003). For example, a 24 h treatment with > 0.1 mM methyl- β -cyclodextrin (M β CD) protected bovine endometrial cells against the cytolytic activity of pyolysin (Amos et al., 2014).

Statins also provide cytoprotection against cholesterol-dependent cytolysin damage by decreasing cholesterol synthesis through the inhibition of 3-hydroxy 3-methylglutaryl coenzyme A reductase (HMGCR) (Maron et al., 2000). Specifically, simvastatin confers bronchial and alveolar epithelial cells with resistance to pneumolysin damage and atorvastatin protected bovine endometrial stromal cells against pyolysin challenge (Statt et al., 2015, Griffin et al., 2017, Griffin et al., 2018). Additionally, inhibiting farnesyl diphosphate farnesyltransferase 1 (also known as squalene synthase) with zaragozic acid or bisphosphonates and treating cells with the isoprenoids farnesyl and geranylgeranyl pyrophosphate reduces cell cholesterol and provides protection against pyolysin damage (Griffin et al., 2017, Griffin et al., 2018, Pospiech et al., 2021).

1.8 CHOLESTEROL

As described above, cholesterol is an important focus of cell protection against pore-forming toxins (particularly cholesterol-dependent cytolysins). The abundance of cellular cholesterol partially depends on cholesterol biosynthesis via the mevalonate pathway (Bloch, 1992). Exogenous cholesterol can also be obtained through the LDL receptor mediated endocytosis of circulating plasma lipoproteins. These lipoproteins are then hydrolysed by endosomal lysosomes to provide free cholesterol (Brown and Goldstein, 1976, Brown and Goldstein, 1986). Finally, cholesterol can be obtained from the cholesterol esters stored in lipid droplets via cholesterol ester hydrolase (Brown and Goldstein, 1976, Goldstein and Brown, 1990, Hu et al., 2010). Intracellular cholesterol is tightly controlled by feedback mechanisms involving SREBPs, the liver X receptors, and the enzyme acetyl-coenzyme A acetyltransferase (ACAT) (Brown and Goldstein, 1997, Edwards et al., 2002, Gill et al., 2008).

1.8.1 Cholesterol biosynthesis

The mevalonate pathway incorporates a series of enzymes that regulate cellular cholesterol biosynthesis (Goldstein and Brown, 1990, Bloch, 1965). Initially acetoacetyl-coenzyme A (CoA) is formed by condensing two acetyl-CoA molecules (synthesized from cytosolic acetate), and then converted to 3-hydroxy-3-methylglutaryl-CoA (HMG-CoA) by HMG-CoA synthase (Fig 1.9). Mevalonate is then produced by HMGCR in the rate limiting step of cholesterol biosynthesis, before it is metabolised to isopentenyl pyrophosphate and subsequently dimethylallyl pyrophosphate. Farnesyl pyrophosphate is formed by a series of condensation

reactions catalysed by farnesyl pyrophosphate synthase (Miziorko, 2011). Specifically, dimethylallyl pyrophosphate and isopentenyl pyrophosphate condense to form geranyl pyrophosphate, which reacts with an additional unit of isopentenyl pyrophosphate yielding farnesyl pyrophosphate. This is a branch point of the pathway with subsequent reactions leading to the production of various end products. For example, geranylgeranyl pyrophosphate synthase converts farnesyl pyrophosphate to geranylgeranyl pyrophosphate, leading to the production of prenylated proteins. However, in the first specific step in cholesterol biosynthesis, squalene synthase converts farnesyl pyrophosphate to squalene, and subsequently lanosterol is produced by lanosterol synthase. A further series of reactions convert lanosterol to 7-dehydrocholesterol, which is then reduced to form cholesterol (Bloch, 1965). Newly synthesised cholesterol and its precursors contribute to many biological pathways. Significantly, cholesterol is a precursor for vital metabolites such as bile acids, steroids, fat soluble vitamins, and oxysterols.

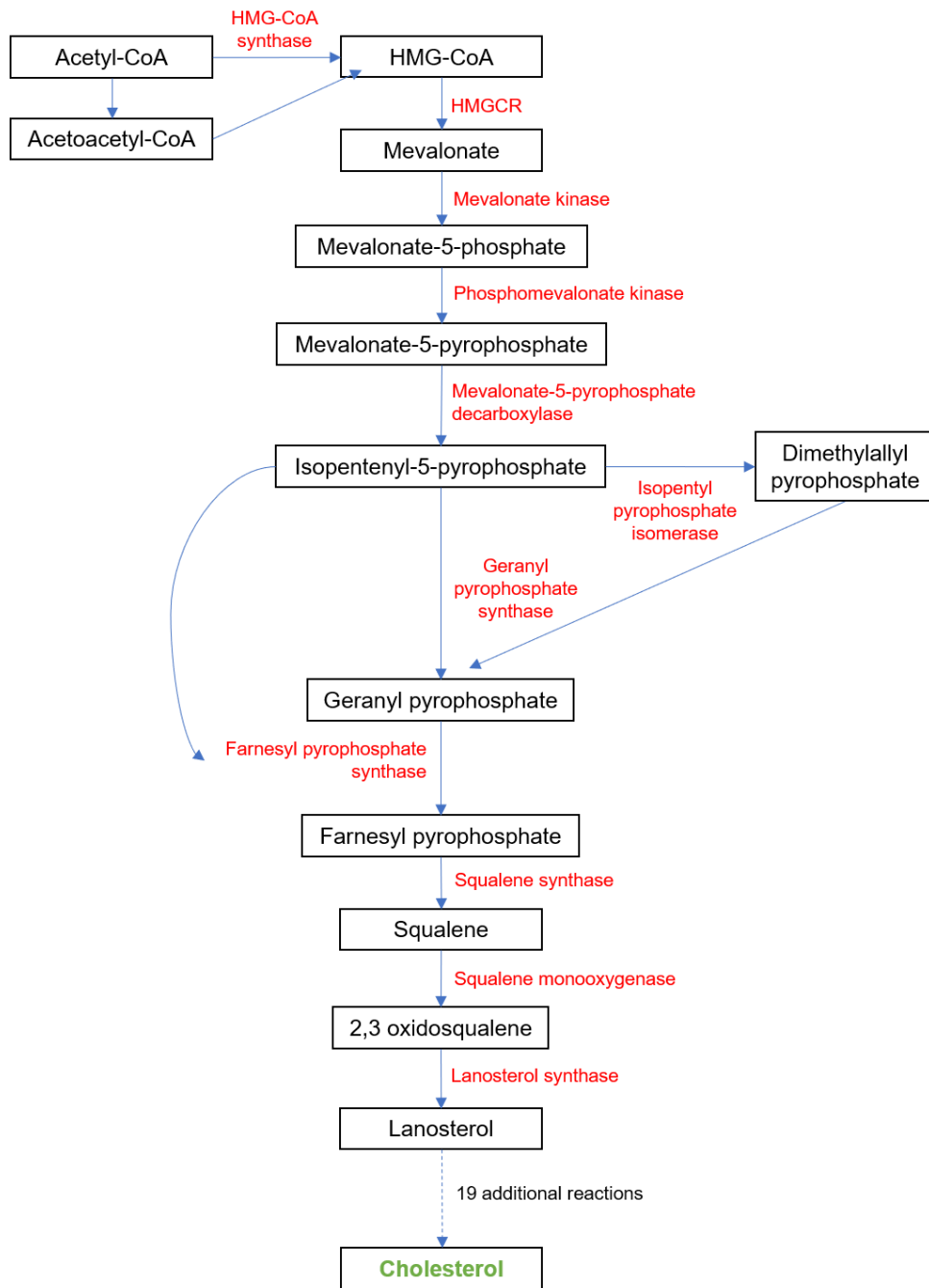


Figure 1.9 The mevalonate pathway

A stepwise illustration of cholesterol synthesis from acetyl-CoA via the mevalonate pathway. The enzymes involved are labelled in red.

1.8.2 Cholesterol homeostasis

Cells must avoid an excess accumulation of cholesterol as it can form toxic crystals and trigger apoptotic signalling pathways (Tabas, 2002). Although cholesterol itself plays the pivotal role, oxysterols feedback as auxiliary regulators functioning to maintain appropriate cellular cholesterol concentrations through several pathways (Fig 1.10) (Gill et al., 2008).

Intracellular cholesterol concentrations can be transcriptionally regulated by the ER-bound SREBPs (Brown and Goldstein, 1997). There are three known isoforms of SREBP: SREBP-1a, SREBP-1c (are involved in fatty acid metabolism) and SREBP-2 (involved in cholesterol and lipid synthesis). Initially residing in the ER, SREBPs are escorted to the Golgi apparatus by the SREBP cleavage-activating protein (SCAP) (Goldstein et al., 2006). The SREBP cleavage-activating protein contains a binding site for coat protein II (COPII) proteins which cluster the SCAP-SREBP complex into COPII coated vesicles that bud from the ER and fuse with the Golgi. In the Golgi, SREBPs undergo sequential proteolysis by the transmembrane enzymes Site-1 and Site-2 protease, yielding active fragments that enter the nucleus (Goldstein et al., 2006, Brown and Goldstein, 1999). Activated SREBPs control HMGCR along with the majority of the downstream mevalonate pathway enzymes (Sakakura et al., 2001). Additionally, SREBPs can increase LDL receptor transcription boosting exogenous cholesterol uptake (Brown 1990). The LDL receptor activity is inversely proportional to cellular cholesterol and so its synthesis is suppressed as sterols over accumulate (Brown and Goldstein, 1986). Cholesterol and oxysterols inhibit cholesterol synthesis by blocking SREBP activation. Cholesterol binds to SCAP, promoting the binding of SCAP to the ER anchor protein Insig (Radhakrishnan et al., 2004). Oxysterols bind to Insig-2 (Fig 1.10, 1), inducing Insig-SCAP binding (Radhakrishnan et al., 2007). As a result of Insig binding, the COPII proteins can no longer bind to SCAP and the SCAP-SREBP complex can no longer move to the Golgi.

The liver X receptors (LXRs) also contribute to maintaining cholesterol homeostasis and are activated by oxysterols to initiate cholesterol clearance (Fig 1.10, 2) (Willy et al., 1995). The two liver X receptor isoforms, LXR α (*NR1H3*) and LXR β (*NR1H2*) share a 77% identity at the amino acid level and differ primarily on expression (Farnegardh et al., 2003). While LXR α is predominantly expressed in the liver, there are also high levels in the ovary and uterus; LXR β is ubiquitously expressed (Mouzat

et al., 2013). The liver X receptors bind to oxysterols, form heterodimers with retinoid X receptor α , and bind to direct repeat-4 elements in target genes to control expression (Janowski et al., 1996). Target genes include the ATP-binding cassette transporter super-family (such as ATP binding cassette subfamily A member 1 (ABCA1) and ATP binding cassette subfamily G member 1 (ABCG1)), that facilitate cholesterol efflux (Edwards et al., 2002). Additionally, LXRs increase fatty acid synthesis by enhancing SREBP-1c transcription (Schultz et al., 2000), and promote the inducible degrader of the LDL receptor (Idol), reducing exogenous cholesterol uptake by restricting the endocytosis of LDL (Zelcer et al., 2009).

Newly synthesised cholesterol leaves the ER. It is transported to the plasma membrane via non-vesicular mechanisms, to other sites such as endosomes (Baumann et al., 2005), or can be converted to cholesterol esters for storage as cytosolic lipid droplets by ACAT (Chang et al., 2009). Oxysterols can increase ACAT-dependent cholesterol esterification within minutes (Fig 1.10, 3) (Lange et al., 1999). Resulting cholesterol esters are stored as neutral lipid droplets, decreasing the amount of free cholesterol in the plasma membrane (Du et al., 2004). Oxysterols also promote the movement of membrane cholesterol to the endoplasmic reticulum for storage in a pool accessible to ACAT (Lange and Steck, 1997).

Finally, oxysterols can rapidly control cell cholesterol by regulating HMGCR (Fig 1.10, 4) (Lange et al., 2008, Song et al., 2005). Oxysterols such as 25-hydroxycholesterol (Cholest-5-ene-3 β ,25-diol) and 27-hydroxycholesterol ((25R)-Cholest-5-ene-3 β ,26-diol) promote the binding of HMGCR to Insig, triggering ubiquitination and proteasome-dependent degradation. This decreases the half-life of HMGCR from ~12 h to less than 1 h, reducing the synthesis of mevalonate from HMG-CoA (Jo and Debose-Boyd, 2010).

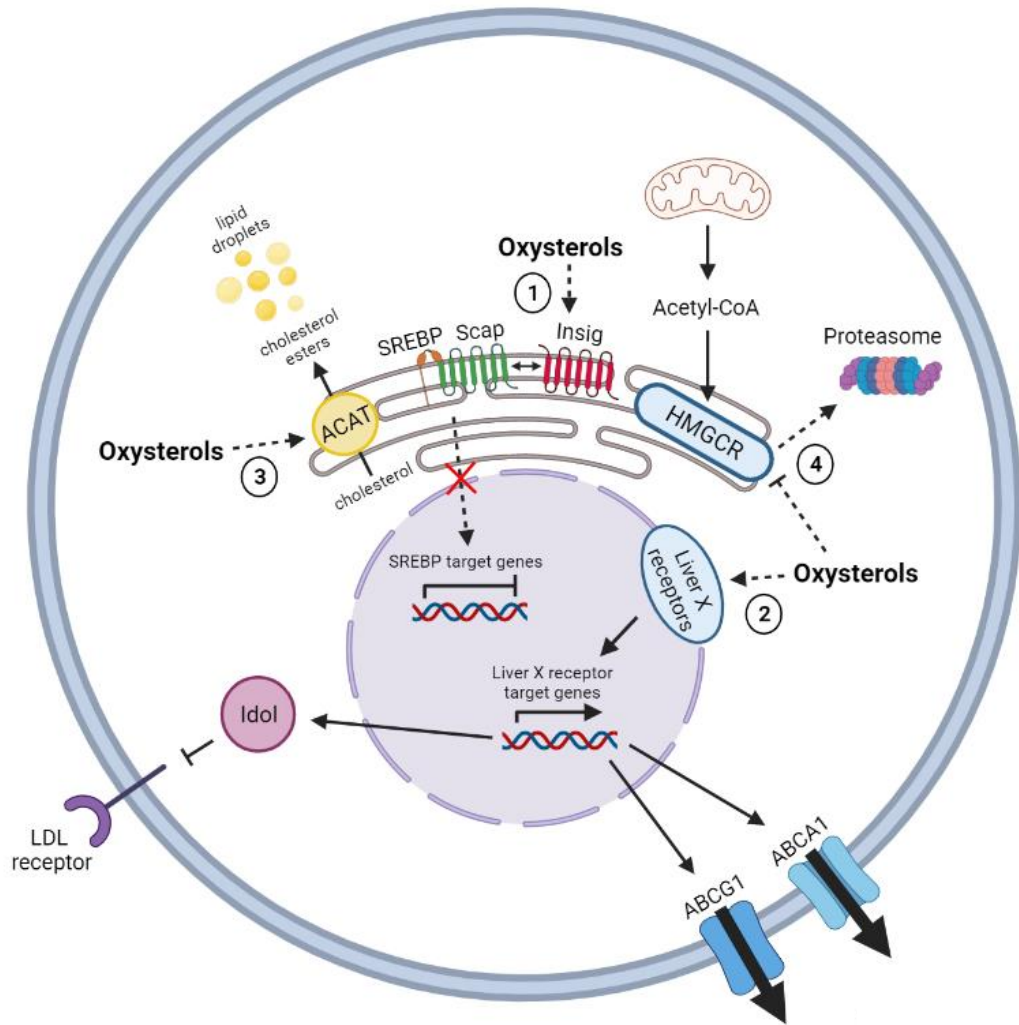


Figure 1.10 Oxysterol regulation of cholesterol homeostasis

Certain oxysterols modulate cholesterol homeostasis through several molecular mechanisms including (1) suppression of SREBP activation, (2) liver X receptor activation, (3) increased storage of cholesterol as esters, (4) accelerated degradation of HMGCR. Created with BioRender.com.

1.9 OXYSTEROLS

1.9.1 Oxysterols and disease

As well as controlling cholesterol homeostasis, oxysterols also regulate immunity and suppress the inflammation caused by bacterial infection (Joseph et al., 2003, Cyster et al., 2014, Bauman et al., 2009, Reboldi et al., 2014, Ito et al., 2015). Liver X receptor activation by oxysterols can suppress the inflammatory response by promoting the synthesis of anti-inflammatory polyunsaturated fatty acids and suppressing genes under the control of pro-inflammatory transcription factors such as nuclear factor κ -light-chain-enhancer of activated B cells (NF- κ B), AP-1, nitric oxide synthase and cyclooxygenase (Spann and Glass, 2013, Joseph et al., 2003). Lipopolysaccharide (LPS) from *E. coli* (an endotoxin derived from the outer bacterial membrane) induces cholesterol 25-hydroxylase (CH25H) to produce 25-hydroxycholesterol in macrophages, negatively regulating the adaptive immune response by suppressing B cell proliferation and class switching to immunoglobulin A (Bauman et al., 2009, Reboldi et al., 2014). Macrophages unable to produce this oxysterol overproduce the interleukin 1 family of inflammatory cytokines (Reboldi et al., 2014). Additionally, the interferon stimulated production of 25-hydroxycholesterol provides immunity to several bacterial species such as *Listeria monocytogenes* and *Shigella flexneri* infection by mobilising plasma membrane cholesterol (Abrams et al., 2020).

1.9.2 Oxysterol structure

Oxysterols are 27-carbon oxidised forms of cholesterol, formed enzymatically or via cholesterol autoxidation, and are commonly produced as intermediates in pathways converting cholesterol to steroid hormones or bile acids (Schroepfer, 2000). The addition of extra oxygen substitutes, such as hydroxyl, carbonyl, epoxy, hydroperoxyl or carboxyl groups, form molecules with diverse biological effects (Olkkonen and Hynynen, 2009). Oxysterols can be classified according to the location of the additional oxygen group (Fig 1.11). Oxidation of the cholesterol at various points on the side-chain forms ligands that regulate cholesterol homeostasis through LXR binding, inhibiting the processing of SREBP-2 and cholesterol esterification through ACAT (Lehmann et al., 1997, Radhakrishnan et al., 2007, Du et al., 2004). Ring-modified oxysterols have markedly different functions; demonstrating little activity with the LXRs and with several ligands, such as 7-ketocholesterol and 7 β -

hydroxycholesterol possessing potent cytotoxic and pro-apoptotic properties, therefore, this thesis has focused on side-chain oxysterols (Lordan et al., 2009).

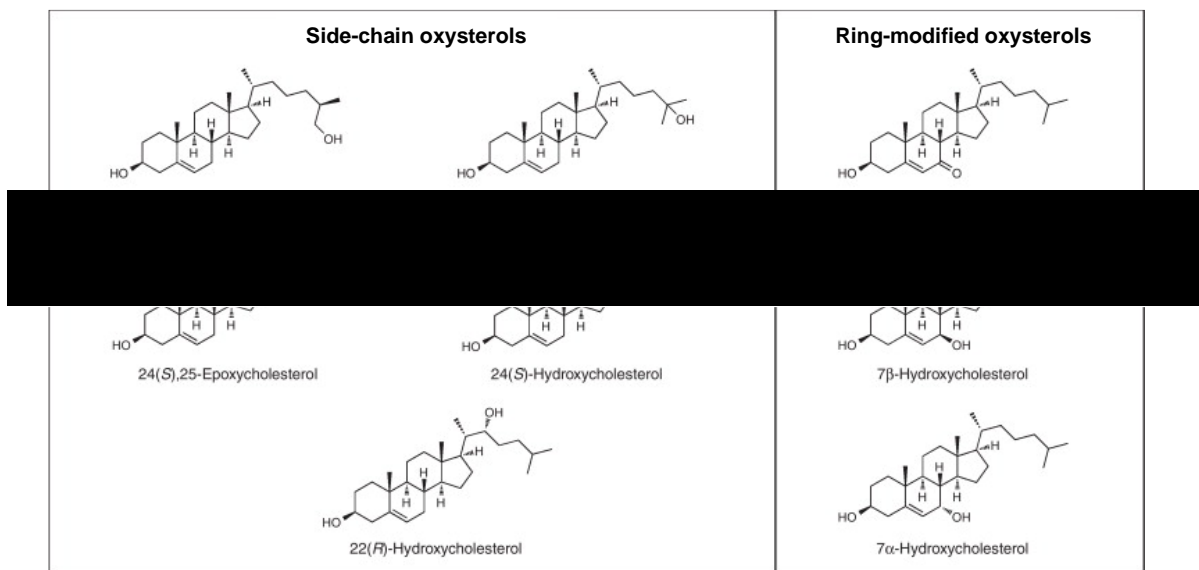


Figure 1.11 Oxysterol structure

The structures of commonly occurring side-chain and ring-modified oxysterols (Bielska et al., 2012).

1.9.3 Oxysterol synthesis

Many oxysterols are produced from cholesterol in the mitochondria or endoplasmic reticulum by cholesterol hydroxylases that belong to the cytochrome P450 (CYP) family (Russell, 2000). The oxysterols 27-, 24(s)-, 7 α -, and 4 β -hydroxycholesterol are the physiologically important products of this pathway most abundant in human serum (Fig 1.11). The enzymes CYP7A1 and CYP27A1 produce 7 α - and 27-hydroxycholesterol respectively as the first step of classic and alternative bile acid synthesis (Bjorkhem and Eggertsen, 2001). Excess cholesterol is eliminated from the brain across the blood brain barrier by the production of the more polar 24(S)-hydroxycholesterol catalysed by CYP46A1 (Bjorkhem et al., 2019), and 4 β -hydroxycholesterol is the product of CYP3A4, an enzyme involved in xenobiotic and steroid hormone metabolism (Bodin et al., 2002). Additionally, 25-hydroxycholesterol is produced by CH25H, a microsomal enzyme not in the P450 family (Lund et al., 1998). Cholesterol autoxidation occurs through non-enzymatical reactions initiated by free radical species or reactive oxygen species attack (Fig 1.12), producing endogenous oxysterols commonly modified at the 7-carbon position (Zerbinati and Iuliano, 2017).

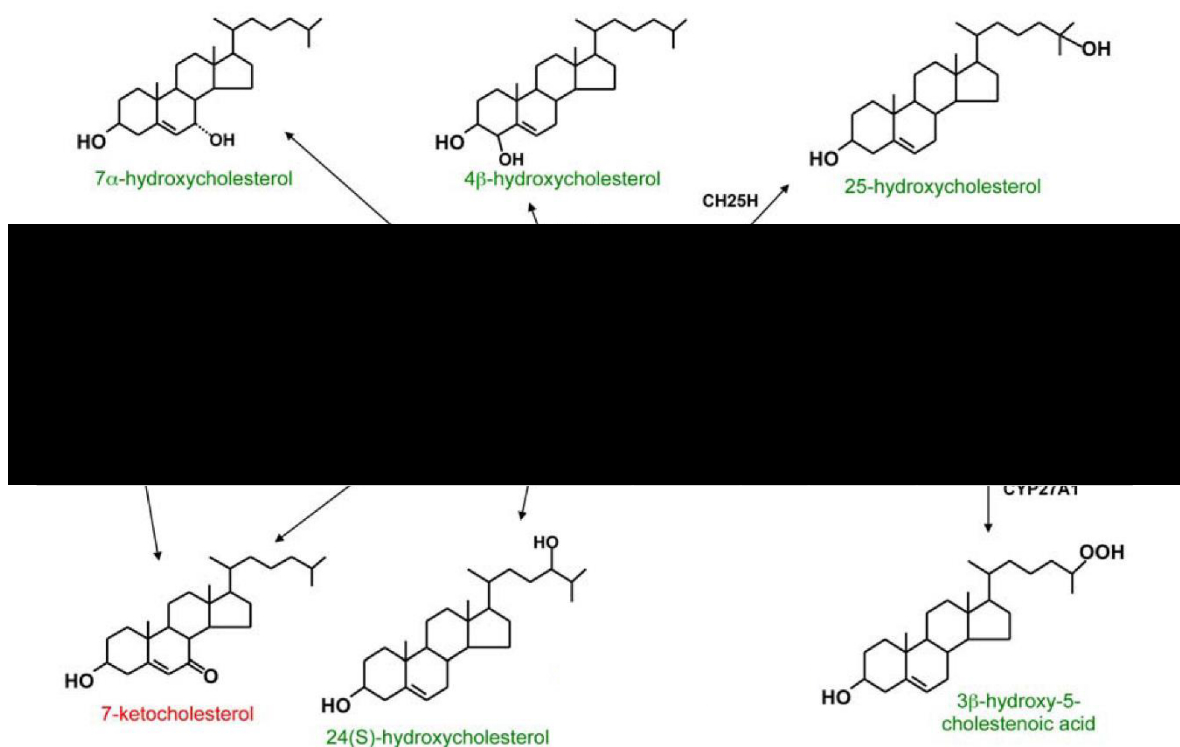


Figure 1.12 Endogenous oxysterol synthesis

The synthetic pathway of commonly occurring endogenous oxysterols. The names of enzymatically derived molecules are presented in green and the cholesterol autoxidation products are in red (Olkkonen et al., 2012).

1.9.4 Oxysterol membrane organisation

The structural modifications to cholesterol make oxysterol molecules more hydrophilic and alter lipid packing properties, enabling several products to transfer through membranes at a much faster rate than cholesterol itself (Olkkonen and Hynynen, 2009). The orientation of oxysterols in membranes is often studied in model monolayers and differs significantly from cholesterol (Fig 1.13). Side chain oxysterols have polar groups at each end of the molecule and favour a horizontal orientation in the membrane, only positioning perpendicularly under high surface pressure. Ring modified oxysterols are angled in the membrane under low pressure, positioning both polar groups close to the bilayer exterior (Kauffman et al., 2000). The additional oxygen groups mean that oxysterols do not condense in the membrane as effectively as cholesterol, and can increase membrane permeability (Theunissen et al., 1986). Decreased membrane integrity is thought to be a causative factor in the underlying cytotoxic effects of some oxysterols (O'Callaghan et al., 2001).

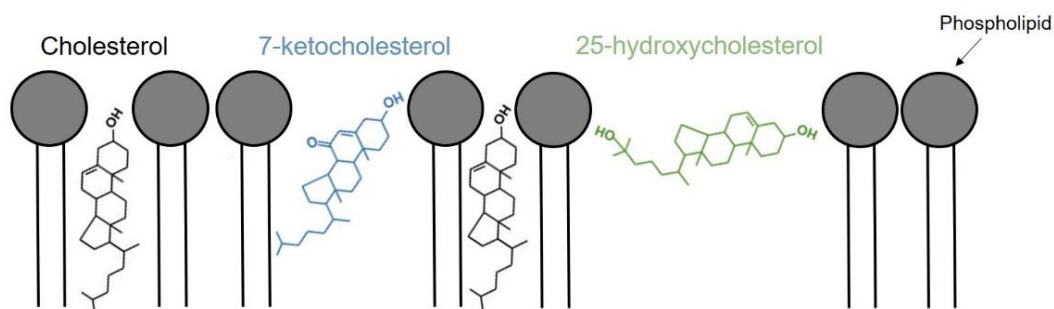


Figure 1.13 Oxysterol membrane organisation

Schematic representation of the organisation of cholesterol (black) and the oxysterols 7-ketocholesterol (blue) and 25-hydroxycholesterol (green) in a model phospholipid monolayer; adapted from (Olkkonen and Hynynen, 2009).

1.9.5 Other functions of oxysterols

Oxysterols also bind to the retinoic acid receptor-related receptor (ROR) family, that includes three subtypes $ROR\alpha$, $ROR\beta$, and $ROR\gamma$ (Ma and Nelson, 2019). Several oxysterols including 22R-hydroxycholesterol, 24S-hydroxycholesterol, 25-hydroxycholesterol and 27-hydroxycholesterol are ligands for both $ROR\alpha$ and $ROR\gamma$ (Mutemberezi et al., 2016), acting as agonists or inverse agonists to either activate or repress transcription respectively (Wang et al., 2010). For example, 20S-hydroxycholesterol, 22R-hydroxycholesterol, and 25-hydroxycholesterol have been shown to activate $ROR\gamma$ promoting the recruitment of co-activators, whereas 24S-hydroxycholesterol suppresses the constitutive activity of both $ROR\alpha$ and $ROR\gamma$ (Jin et al., 2010, Wang et al., 2010). As of yet, no oxysterols have demonstrated binding with $ROR\beta$ (Mutemberezi et al., 2016). Activated RORs contribute to cholesterol metabolism. For example, *CYP7B1* (the gene coding for oxysterol 7 α -hydroxylase) is a downstream target of $ROR\alpha$ and regulates the metabolism of 25-hydroxycholesterol and 27-hydroxycholesterol to bile acids (Wada et al., 2008). Additionally, $ROR\gamma$ plays a key role in Th17 cell differentiation (Soroosh et al., 2014).

Oxysterols also have some oestrogenic activity. Several oxysterols demonstrate oestrogen receptor α activation in transfected HeLa cells (Sato et al., 2004), and oxysterols including 22R-hydroxycholesterol, 24S-hydroxycholesterol, 25-hydroxycholesterol and 27-hydroxycholesterol inhibit the oestradiol activation of oestrogen receptor α and β (Umetani et al., 2007). In particular, 27-hydroxycholesterol has been described as a selective oestrogen receptor modulator (DuSell et al., 2008), promoting the proliferation of oestrogen receptor positive breast cancer cells (Nelson

et al., 2013, Wu et al., 2013), and inhibiting the oestrogen-dependent production of nitric oxide by vascular cells, reducing oestrogen-induced vasorelaxation (Umetani et al., 2007).

1.10 STEROIDS

1.10.1 Steroids and disease

Like oxysterols, cholesterol-derived steroids also modulate immunity and the risk of disease caused by bacterial infection. Glucocorticoid treatment suppresses the inflammation and immunopathology associated with bacterial infection, and concentrations of the ovarian sex steroids progesterone and oestradiol affect the susceptibility of the bovine endometrium to bacterial infection.

Ovarian sex steroids and disease

The ovarian cycle can affect the risk of bacterial infection in the bovine endometrium. To prepare for pregnancy, significant physical changes occur in response to the ovarian sex steroids progesterone and oestradiol (Wira et al., 2005, Lewis, 2003). In the follicular phase of the oestrus cycle, oestradiol concentrations are elevated, and the endometrium is more resistant to infection. On the contrary, the high progesterone concentrations experienced during the luteal phase can predispose the endometrium to infection (Lewis, 2003, Lewis, 2004, Rowson et al., 1953). Although the ovarian cycle has demonstrated clear effects on uterine disease progression, the role of oestradiol and progesterone remains unclear. Cells collected from the bovine uterine lumen at different points of the oestrous cycle secrete differing amounts of cytokines and chemokines (Fischer et al., 2010). However, treating endometrial cells with oestradiol or progesterone, or inhibiting their cognate nuclear receptors, did not alter the secretion of IL-1 β , IL6 or IL8, and the gene expression of *IL1 β* , *IL6*, *CXCL8* and *CCL5* (Saut et al., 2014). As ovarian steroids do not appear to modulate disease severity by manipulating the innate immune response, then perhaps they alter the intrinsic protection of cells to bacterial pathogens.

Glucocorticoids and disease

Glucocorticoids can be included in the effective treatment of a variety of infections caused by bacteria that secrete pore-forming toxins, such as sore throats, pneumonia,

tuberculosis, meningitis, and septic shock (Marik et al., 2008, Hayward et al., 2012, Meijvis et al., 2011). Host tissues secrete cytokines and other inflammatory mediators as a mechanism of eliminating invading pathogens. Excessive cytokine release can be harmful and glucocorticoids function to regulate the inflammatory response (Rhen and Cidlowski, 2005). However, glucocorticoid therapy poses potentially harmful side-effects including immunosuppression, hypertension, osteoporosis, weight gain and Cushing's syndrome (Yasir et al., 2018). The potentially therapeutic benefits of glucocorticoid treatment must be weighed against the side-effects they might cause. To ensure that the benefits outweigh the consequences, trials commonly investigate patient outcomes. For example, in a review examining 17 randomised control trials comprising 2,264 participants, glucocorticoid therapy reduced the mortality and morbidity of adults with severe community acquired pneumonia (Stern et al., 2017). Furthermore, glucocorticoid treatment can improve the outcome of patients with acute bacterial meningitis (de Gans et al., 2002, van de Beek, 2009). The benefits of glucocorticoid therapy are typically attributed to mediation of the inflammatory response. However, we wondered if it is possible that glucocorticoids increase the intrinsic protection of cells to invading bacterial pathogens, thereby preventing damage.

In a study by Jamieson et al. (2010), influenza infection triggered a generalized stress response in mice elevating serum glucocorticoid concentrations and suppressing the immune response. The virus-induced glucocorticoid production was necessary to reduce the mortality of a secondary bacterial infection with *Listeria monocytogenes* (Jamieson et al., 2010). As mentioned above, benefits were attributed to the mediation of the inflammatory response and the effects of glucocorticoids on the intrinsic protection of cells to invading bacterial pathogens were not considered. Additionally, in red-winged blackbirds, higher endogenous glucocorticoid concentrations were associated with a greater resilience to infection (Schoenle et al., 2018). Though in a subsequent study by the same group, supplying exogenous glucocorticoids was associated with reduced tolerance and resistance to infection (Schoenle et al., 2019).

1.10.2 Steroid synthesis

Steroids are biologically active organic compounds, typically comprised of 17 carbon atoms fused into four ring structures with varying functional groups stemming from

the fourth core ring. Steroidogenic cells do not typically store steroid hormones, instead they are synthesized as required in a pathway consisting of a series of cytochrome P450 enzymes, hydroxysteroid hydrogenases and steroid reductases (Miller, 1988, Parker and Schimmer, 1995). The cholesterol side-chain cleavage enzyme (CYP11A) commences steroid synthesis by catalysing the conversion of cholesterol to pregnenolone (Hanukoglu, 1992). The cholesterol side-chain cleavage enzyme is located on the inner mitochondrial membrane and is found in all steroidogenic tissues (Miller, 1988). Pregnenolone is then converted to progesterone by 3 β -hydroxysteroid dehydrogenase. Progesterone and pregnenolone form the precursors for all other steroid hormones (Fig 1.14). Steroid hormones can be further classified by their target nuclear receptor, outlined in Table 1.2. Secreted steroids pass through target cell membranes, exerting genomic and non-genomic effects through receptor binding.

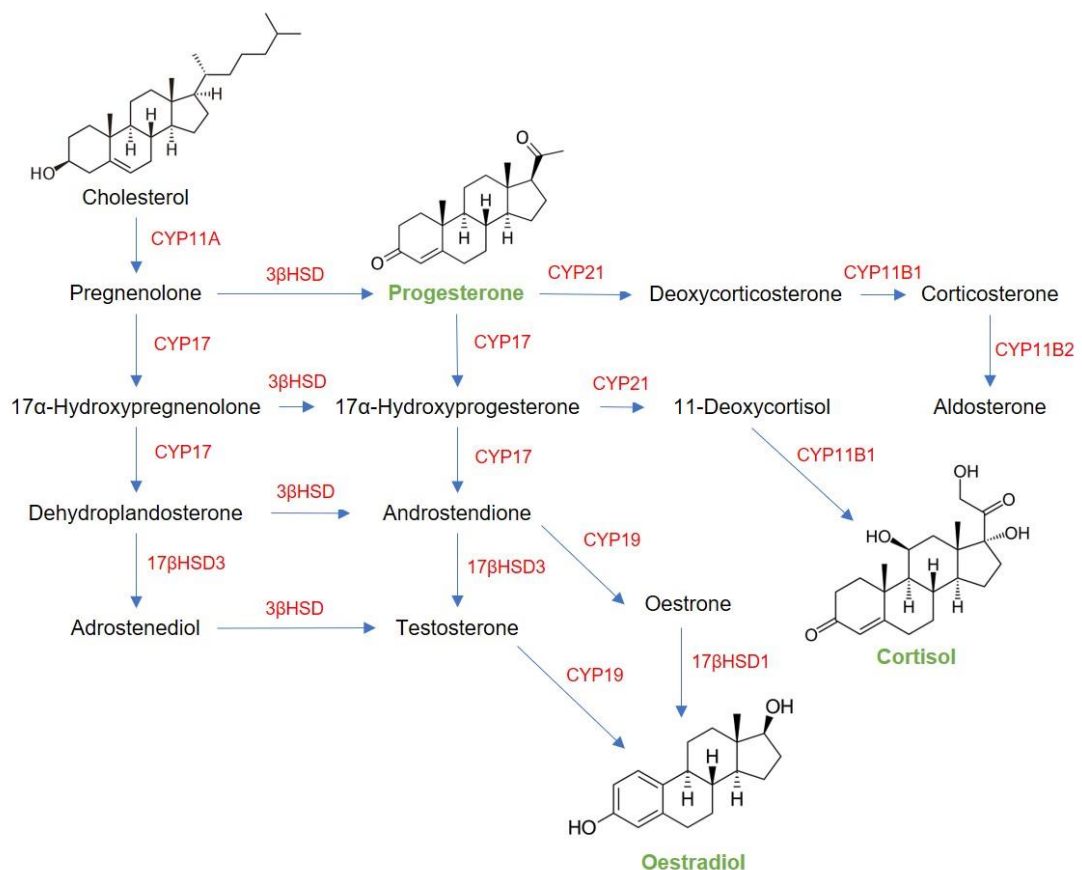


Figure 1.14 Steroid biosynthesis

The synthesis of the three endogenous steroids examined in this thesis (highlighted in green). The hydroxysteroid dehydrogenase (HSD) and the cytochrome P450 (CYP) enzymes involved are labelled in red.

Table 1.2 Nuclear Receptor Subfamily 3

Receptor	Gene	Target hormone (Ligand)
Group A: Oestrogen Receptors		
Oestrogen Receptor- α	<i>NR3A1</i>	Oestradiol
Oestrogen Receptor- β	<i>NR3A2</i>	Oestradiol
Group B: 3-Ketosteroid Receptors		
Glucocorticoid Receptor	<i>NR3C1</i>	Cortisol
Mineralocorticoid Receptor	<i>NR3C2</i>	Aldosterone
Progesterone Receptor	<i>NR3C3</i>	Progesterone
Androgen Receptor	<i>NR3C4</i>	Testosterone

1.10.3 Oestrogens

Oestrogens are the primary female sex hormones and are responsible for the development and regulation of the female reproductive system and secondary sex characteristics. Genomic effects are exerted through the two forms of the oestrogen receptor, α and β , located on the sixth and fourteenth chromosome (6q25.1 and 14q23.2) respectively (Giguere et al., 1998). The receptors interact with oestrogen response elements in the promoters of target genes and recruit various co-activators to mediate transcriptional regulation (McDonnell and Norris, 2002). Oestrone, oestradiol and oestriol are three endogenous oestrogens found in women. Oestetrol is a fourth major oestrogen found exclusively in pregnant women. Oestradiol is the major oestrogen in fertile women, demonstrating higher serum concentrations and superior oestrogenic activity. Oestradiol is around eighty times more potent than oestriol and 12 times more potent than oestrone (Thomas and Potter, 2013). It is responsible for the development of female reproductive characteristics along with the regulation of the menstrual and oestrous reproductive cycles (Hall et al., 2001). Production mainly occurs within the ovarian follicles, but small amounts are also formed in the testicles, the adrenal glands, fat, the liver, the breasts, and the brain (Findlay et al., 2010).

1.10.4 Progesterone

Progesterone, along with 17α -hydroxyprogesterone and 17α -hydroxypregnenolone, is a precursor for the synthesis of other endogenous steroids, and so it is produced by a variety of tissues including the adrenal glands, testes, and ovaries (Taraborrelli, 2015). Progesterone functions through the progesterone receptor and is essential for the reproductive process, aiding fetal growth through many pathways (Di Renzo et al., 2016). For example, progesterone in the myometrium counteracts the stimulatory activity of prostaglandins and oxytocin to reduce uterine contractility and decrease the risk of premature labour (Fanchin et al., 2000). Progesterone modulates the maternal immune response suppressing inflammation and permitting fetal acceptance (Schwartz et al., 2009). Additionally, progesterone prevents lactation during pregnancy, with milk production occurring when progesterone concentrations fall after parturition (Spencer and Bazer, 2002).

Overall, it is generally accepted that progesterone and oestradiol exert opposing effects on steroid nuclear receptors with menstruation and ovulation controlled by the rhythmic regulation of ovarian hormone concentration. Specifically, in the bovine uterus, high follicular oestrogen increased the abundance of oestradiol and progesterone receptors. In turn, progesterone and oestrogen receptor levels were low at cycle stages associated with higher progesterone concentrations (Kimmins and MacLaren, 2001).

1.10.5 Glucocorticoids

Cortisol

Cortisol (11β , 17α , 21-Trihydroxypregn-4-ene-3, 20-dione) is the principal endogenous glucocorticoid hormone (referred to as hydrocortisone when supplied as a medication) and is primarily produced by the zona fasciculata of the adrenal cortex (Chrousos, 2009). The release and production of cortisol is regulated by the hypothalamus-pituitary axis (Kadmiel and Cidlowski, 2013). Cortisol and other glucocorticoids modulate genomic effects through glucocorticoid receptor binding. Secreted cortisol affects most organ systems because the glucocorticoid receptor is expressed in almost every tissue in the human body and contributes significantly to the metabolic, cardiovascular, and immunological systems (Kadmiel and Cidlowski, 2013).

Physiological stress such as burns and in extreme cases septic shock, are well associated with activating the hypothalamic-pituitary-adrenal axis, leading to an increase in cortisol that helps with the maintenance of vascular tone, endothelial integrity, cardiac contractility, and potential catecholamine actions (Arafah, 2006, Munck et al., 1984). Septic shock can elevate basal cortisol to an average of 880 nmol/litre compared with a control level of 352 nmol/litre (Ho et al., 2006). However, in general the reported range of cortisol in stress varies and the optimum concentrations are not known (Sam et al., 2004). This variation in cortisol affects vulnerability to further infection.

In dairy cattle transportation and hot conditions induce stress. Complications include decreased milk production, reduced fertility, and increased susceptibility to disease (Buffington et al., 1983, Chirase et al., 2004, Crowe and Williams, 2012, Kadzere et al., 2002). Both heat and transport induced stress can trigger a short-term increase in plasma cortisol concentrations (Alvarez and Johnson, 1973, Christison and Johnson, 1972, Nanda et al., 1990). As a stress hormone, cortisol suppresses immune function by down-regulating key inflammatory transcription factors, increases blood sugar concentrations through gluconeogenesis and assists in fat, protein, and carbohydrate metabolism (Heck et al., 1997, Jonat et al., 1990), though its impact on intrinsic cell protection is unknown.

Dexamethasone

The anti-inflammatory properties of glucocorticoids are the basis for the pharmaceutical development of drugs, such as dexamethasone, that are used in the treatment of many inflammatory disorders, such as rheumatic problems, skin diseases, asthma, chronic obstructive pulmonary disorder and brain swelling (Rhen and Cidlowski, 2005). Dexamethasone (1-dehydro-9-fluoro-16-methylhydrocortisone) is a synthetic pregnane (a C21 steroid derivative with carbons present at positions 1 through 21) and derivative of cortisol. The binding affinity of dexamethasone to the glucocorticoid receptor was found to be four times greater than that of cortisol (Kontula et al., 1983).

The glucocorticoid receptor

Glucocorticoids exert effects through binding to the widely expressed glucocorticoid receptor (Hollenberg et al., 1985). The human glucocorticoid receptor is derived from

a single gene, *NR3C1*, that contains nine exons. Alternative splicing at exon 9 generates two main glucocorticoid receptor isoforms (α and β) (Bamberger et al., 1995). Glucocorticoid receptor α is ubiquitously expressed and mediates the classic glucocorticoid effects, whereas the β isoform has a more selective distribution, is typically found at lower concentrations than glucocorticoid receptor α , and does not bind to glucocorticoid agonists due to its altered binding domain (Oakley et al., 1996). Several other glucocorticoid receptor isoforms have been detected in tissues and certain cancer cells (Krett et al., 1995, Beger et al., 2003). Differing abundance of the individual glucocorticoid receptor isoforms regulating independent sets of genes might partly explain the cell and tissue-specific response to glucocorticoid treatment (Kadmiel and Cidlowski, 2013, Oakley and Cidlowski, 2011).

Glucocorticoids readily cross cell membranes to combine with the glucocorticoid receptor in designated tissues. Unbound glucocorticoid receptor, located in the cytosol of cells, are attached to chaperone proteins such as the heat shock proteins 90, 70 and 40 (Dittmar and Pratt, 1997, Schneikert et al., 1999). When a ligand/hormone binds to the glucocorticoid receptor, the connected heat shock protein releases, and the receptor translocates into the nucleus (Isohashi and Okamoto, 1993). The liganded glucocorticoid receptor dimers then slot into the glucocorticoid response elements in the DNA helix, leading to the enhancement and/or repression of gene transcription, typically within a few hours (Duma et al., 2006, Ratman et al., 2013, Wang et al., 2004). However, global glucocorticoid recruitment assays indicate that only a small portion of glucocorticoid response elements are occupied by the receptor and these sites vary in cell-specific manner due to differences in the chromatin landscape that alters response element exposure (John et al., 2011). Alternatively, the glucocorticoid receptor can also regulate transcription by physically interacting with other transcription factors without tethering directly to DNA; examples include the Jun subunit of AP-1 and the p65 subunit of the nuclear factor κ -light-chain-enhancer of activated B cells (NF- κ B) (Nissen and Yamamoto, 2000, Yang-Yen et al., 1990). Reported membrane bound glucocorticoid receptors potentially allow cortisol to trigger alternative fast acting non-genomic actions on target cells (Strehl et al., 2011).

Glucocorticoid receptor genomic effects regulate the transcription of a variety of genes controlling development, signal transduction, transport, metabolism, and immune response (Wang et al., 2004). Most of the glucocorticoid receptor anti-inflammatory

effects stem from interactions with NF- κ B and AP-1. Repression of the NF- κ B pathway reduces the expression of pro-inflammatory cytokines (i.e.: IL-1 α and tumour necrosis factor α) and genes that contribute to T-cell developmental pathways, mediated by the glucocorticoid-induced leucine zipper (Beaulieu and Morand, 2011, Ayroldi and Riccardi, 2009). Glucocorticoids suppress a variety of AP-1 driven genes involved in inflammation and immune dysregulation such as IL-6, and also suppress proliferative genes such as c-Jun (Wei et al., 1998). Additionally, glucocorticoids upregulate genes such as the dual specificity protein phosphatase (decreasing MAPK phosphorylation) and the IL-1 receptor protein kinase 3, repressing Toll-like receptor and IL-1 receptor signalling (Ayroldi et al., 2012).

There is not total specificity between steroid hormones and their target receptors, and many steroid hormones can bind to several different nuclear receptors. Oestradiol, aldosterone, and progesterone, alongside cortisol, are all chemically similar molecules that can still fit into the glucocorticoid receptor binding site (Kontula et al., 1983). However, structural differences prevent necessary contacts, and could suggest an explanation for the selectivity of the glucocorticoid receptor for the endogenous ligand cortisol (von Langen et al., 2005).

Side-effects of glucocorticoid treatment

Although glucocorticoids can have substantial therapeutic benefits, prolonged use, particularly at high concentrations, can have severe adverse effects (Schacke et al., 2002). Metabolic disorders include the development of Cushingoid features, hyperglycaemia, adrenal suppression (Barnes and Adcock, 2009, Hoes et al., 2011). Skin atrophy stems from reduced keratinocyte and dermal fibroblast proliferation (Oikarinen and Autio, 1991, Oikarinen et al., 1998). Glucocorticoid-induced osteoporosis increases the risk of fractures and long-term treatment in children can impair growth and delay puberty (Dykman et al., 1985, Reid, 2000, Skoner et al., 2000).

Another complication of glucocorticoid therapy is the reduced sensitivity or even resistance that can develop in patients treated for chronic diseases (Ramamoorthy and Cidlowski, 2013). This increases the vulnerability of patients to exaggerated inflammatory responses (Rodriguez et al., 2016).

1.11 AIMS AND HYPOTHESES

Protecting cells against damage can increase the tolerance of tissues to bacterial pathogens. The present thesis aimed to explore methods of increasing the intrinsic protection of eukaryotic cells against the damage caused by pore-forming toxins. Side-chain oxysterols, the ovarian sex steroids oestradiol and progesterone, and glucocorticoids are thought to modulate the risk of disease caused by bacteria that secrete pore forming toxins (Abrams et al., 2020, Lewis, 2003, Stern et al., 2017). With this in mind, the present thesis tests the hypothesis that side-chain oxysterols and steroids alter the intrinsic protection of eukaryotic cells against pore-forming toxins.

We used pyolysin as a model toxin to study cytoprotection because it does not require thiol activation and forms pores in many types of mammalian cells (Jost and Billington, 2005, Amos et al., 2014). In the first experimental chapter of this thesis (*Chapter 3*) we focused on cells from the bovine endometrium, a target tissue of pyolysin. There we tested the hypothesis that progesterone, oestradiol, glucocorticoids, and side-chain oxysterols, alter bovine endometrial cell protection against pore-forming toxins. The first objective was to determine whether treatment of primary bovine endometrial cells with the steroids or oxysterols reduced the damage caused by a subsequent challenge with pyolysin. Cytoprotection was assessed by measuring the leakage of potassium ions and LDH into cell supernatants, by evaluating toxin-induced changes to the actin cytoskeleton, and by assessing cell viability. The second objective was to determine whether oxysterol cytoprotection extended beyond pyolysin to protection against α -hemolysin from another endometrial pathogen, *S. aureus* (Sheldon et al., 2002). The third objective was to examine the mechanisms of side-chain oxysterol cytoprotection in bovine endometrial cells. We examined whether cellular cholesterol abundance, ACAT activity, and LXR expression contributed to side-chain oxysterol cytoprotection. The final objective was to explore the type and abundance of oxysterols in the ovary and uterus using mass spectrometry.

Having examined the protection of bovine endometrial cells against pore-forming toxins, we then aimed to explore the protection of human tissue cells. In *Chapter 4* we tested the hypothesis that treatment with side-chain oxysterols would protect human epithelial cells against pore-forming toxin damage. The first objective was to determine whether side-chain oxysterol treatment protected several types of human epithelial cells against pyolysin or *S. aureus* α -hemolysin. Again, cytoprotection was

assessed by measuring the leakage of potassium ions and LDH into cell supernatants, and changes in cell viability and the cytoskeleton. The subsequent objective was to examine the protective mechanisms involved in side-chain oxysterol cytoprotection and we investigated ion flux, MAPK activation, liver X receptor expression and ACAT activity.

Chapter 5 challenged the hypothesis that glucocorticoids increase the intrinsic protection of human cells against pore-forming toxins. The first objective was to establish whether glucocorticoid treatment would protect human tissue cells against pyolysin, streptolysin O, or *S. aureus* α -hemolysin. Cytoprotection was assessed as in *Chapters 3* and *4*. The second objective was to determine the role of the glucocorticoid receptor in cytoprotection. The final objective was to examine potential mechanisms for glucocorticoid cytoprotection. We investigated the involvement of MAPKs, ion flux, cellular cholesterol, and specific gene activation.

2 GENERAL MATERIALS AND METHODS

2.1 GENERAL APPROACH TO EXAMINING CYTOPROTECTION

The present thesis used a consistent approach to examine the cytoprotective properties of oxysterols and steroids. We first challenged cells with a range of concentrations of pyolysin to determine a suitable challenge for use in experiments exploring cytoprotection. We evaluated the consequences of pore formation by measuring the leakage of lactate dehydrogenase (LDH), the leakage of potassium, and cell cytolysis. Cells were then treated with a range of concentration of steroids or oxysterols to investigate their effect on cell protection to determine effective treatment concentrations. The treatments and vehicles used throughout the present thesis are listed in Table 2.1. Cytoprotection was attributed to treatments that reduced the toxin-induced leakage of LDH, leakage of potassium, cell cytolysis and cytoskeletal changes. We examined the extent of cytoprotection, by repeating experiments in multiple cell lines and with several toxins. Finally, we investigated cytoprotective mechanisms. We explored the effect of treatment on cellular cholesterol, as manipulating cholesterol homeostasis is an effective method of protecting cells against cholesterol-dependent cytolysins (Amos et al., 2014, Statt et al., 2015). Additionally, we used synthetic agonists, short interfering ribonucleic acid (siRNA) and inhibitors to target genes or receptors that might be involved in cytoprotection (Table 2.1).

Table 2.1 Treatments and inhibitors used throughout this thesis and the vehicles used to reconstitute them

Compound	Use in thesis	Product code and supplier	Vehicle
Progesterone	Treatment	#P8783; Merck, Gillingham, UK	Ethanol
Oestradiol	Treatment	#E2758; Merck	Ethanol
Hydrocortisone	Treatment	#H0888; Merck	Ethanol/ dimethyl sulfoxide (DMSO, #6768-51; Merck)
Dexamethasone	Treatment	#D4902; Merck	DMSO
25-hydroxycholesterol	Treatment	#700019P; Avanti Polar Lipids, Alabama, United States	Methanol
27-hydroxycholesterol	Treatment	#LM4114; Avanti Polar Lipids	Methanol
Methyl- β -cyclodextrin (M β CD)	Treatment	#C4555, Merck	Phosphate-buffered saline (PBS, #10010023; Thermo Fisher Scientific).
Sphingomyelinase	Treatment	#S8633, Merck	Buffered aqueous glycerol solution
Cholesterol	Treatment	#C3045, Merck	Ethanol
T0901317	Synthetic agonist	#2373; Tocris, Abingdon, UK	DMSO
GW3965	Synthetic agonist	#2474; Tocris	DMSO
Fluticasone propionate	Synthetic agonist	#2007; Tocris	DMSO
SZ58-035	Inhibitor	#S9318; Merck	DMSO
RU486	Inhibitor	#M8046; Merck	DMSO
Cycloheximide	Inhibitor	#01810; Merck	DMSO
Actinomycin D	Inhibitor	#A9415; Merck	DMSO

2.2 PORE-FORMING TOXIN PREPARATION

2.2.1 Pyolysin

Pyolysin was selected as the model cholesterol-dependent cytolysin to explore the cytoprotective properties of oxysterols and steroids as it is spontaneously active *in vitro* and has successfully been utilised to explore protection against cholesterol-dependent cytolysins in the past (Billington et al., 1997, Amos et al., 2014, Griffin et al., 2018). *Trueperella pyogenes* secretes pyolysin, damaging endometrial cells and contributing to the progression of uterine disease in cattle (Billington et al., 1997, Sheldon et al., 2006), therefore we used a model system of bovine endometrial cells challenged with pyolysin to explore cytoprotection.

Protein expression

Recombinant pyolysin was generated from a plasmid (pGS59) containing 6xHis-linked pyolysin, generously provided by Prof B.H. Jost (University of Arizona). For this project, pyolysin was purified from a 1 g *Escherichia coli* pellet provided by Dr S. Owens that was generated as previously described (Billington et al., 1997). Briefly, 5 µl plasmid deoxyribonucleic acid (DNA) was added to 50 µl BL21 (DE3) *E. coli* (#BIO-85032; Bionline, London, UK) in 17 x 100 mm polypropylene tubes (#2059; Thermo Fisher Scientific, Paisley, UK), mixed by swirling, and placed on ice for 30 min. The tube was incubated in a water bath at 42°C for 45 s and returned to ice for 2 min, thereby triggering heat-shock driven plasmid DNA internalisation. The plasmid *E. coli* mixture was then transferred to a 1 ml reaction tube containing 950 µl Luria-Bertani (LB) broth (#L3022; Merck). The tube was placed horizontally in a shaking incubator set at 180 rpm and incubated at 37°C for 1 h. Warm 1.5% LB agar plates containing 100 µg/ml ampicillin (#A0166; Merck) were prepared and 100 µl plasmid *E. coli* mixture was added after the incubation period was complete. The remaining 900 µl was centrifuged at 6,000 x g for 5 min. After centrifugation, the supernatant was discarded, and the pellet was resuspended in 100 µl fresh LB broth and plated on a separate LB agar ampicillin plate. Plates were incubated at 37°C overnight.

The next day, a single colony was selected from the transformation plates, inoculated into 10 ml LB broth (100 µl/ml ampicillin), and incubated at 37°C overnight again. The following morning, 5 ml of this culture was incubated in 500 ml LB broth (100 µl/ml ampicillin) at 37°C and shaken at 180 rpm until the OD₆₀₀ reached 0.6. Protein

expression was induced by adding 1 mM isopropyl- β -D-thiogalactopyranoside (#BP1755-10; Thermo Fisher Scientific) for 3 h. Incubation temperature was then reduced to 25°C and agitation to 150 rpm overnight. The following morning, cultures were centrifuged at 5,000 x g for 10 min (4°C). The supernatant was then discarded, and the pellet was divided into 1 g portions ready for protein purification.

Protein purification

Pyolysin protein purification was carried out in a cold room at 4°C. A 1 g *E. coli* cell pellet was resuspended in 20 ml of HisTALON xTractor buffer (#635651; Clontech, California, US), with 10 μ l benzonase (#E8263-5KU; Merck). The solution was centrifuged at 10,000 x g for 20 min and clarified supernatant was collected and stored on ice (10 μ l of the supernatant, later referred to as the soluble fraction, was aliquoted for sodium dodecyl sulphate polyacrylamide gel electrophoresis (SDS-PAGE) analysis). Equilibration and elution buffer (#635651; Clontech) were filtered through a 0.22 μ m vacuum filter (#99250; TPP, Trasadingen, Switzerland), then 8 ml of equilibration buffer was ran through a 1 ml cobalt resin FPLC cartridge for His-tagged protein purification (#635655; Clontech). We ran clarified supernatant through the column and the 6xHis tag on the recombinant protein bound to the cobalt ions in the column resin bed. The column was washed with 8 ml of equilibration buffer then 7 ml of wash buffer (0.66 ml elution buffer added to 9.34 ml equilibration buffer). The recombinant pyolysin was eluted by running 8 ml of elution buffer through the column and 1 ml fractions were collected in 1.5 ml reaction tubes (#616201; Greiner Bio-One, Gloucester, UK). The elution buffer displaced the His-tagged recombinant protein as the 150 nM imidazole competitively binds to the cobalt ions in the column allowing it to flow through the column and be collected. The concentration and abundance of pyolysin was determined using a DC assay and SDS-PAGE analysis.

DC assay

A Bio-Rad DC protein assay (#5000111; Bio-Rad, Hercules, California, United States) is a colorimetric assay used to distinguish the concentration of protein via the solubilisation of a detergent. The protein interacts with an alkaline copper tartrate solution, reducing the fiolin reagent and giving rise to characteristic colour changes. A protein standard curve was attained by using 0.5, 1.0, 1.5, 2.0 and 2.5 mg/ml concentrations of bovine serum albumin (BSA, #A7906; Merck). Five μ l of standard

or sample were added in duplicate into the wells of a clear flat bottom 96 well plate (#437958; Thermo Fisher Scientific). The assay was performed using the reagents provided by the Bio-Rad DC protein assay kit (reagent A, B and S). Working reagent was prepared by combining 60 μ l reagent S and 3 ml reagent A. To start the reaction, 25 μ l working reagent and 200 μ l reagent B were added to each well. The plate was incubated at room temperature on a shaker for 15 min. Absorbance was read at 750 nm using a POLARstar Omega microplate reader (POLARstar Omega; BMG Labtech, Aylesbury, UK). The inter- and intra-assay coefficients of variation for the DC assay were < 6% and < 5% respectively. The protein concentrations from the first 4 eluted fractions are shown below (Table 2.2). As expected, fraction 2 contained the majority of protein.

Griffin et al. (2017) determined that the activity of pyolysin was 628,338 hemolytic units (HU)/mg protein by using a hemolysis assay carried out with horse red blood cells. Therefore, the concentration of pyolysin used in the experiments in the present thesis is reported in HU.

Table 2.2 Recombinant pyolysin protein concentrations from eluted fractions

Fraction	1	2	3	4
Protein concentration mg/ml	0.09	3.87	0.62	0.01

SDS-PAGE

We used SDS-PAGE analysis to confirm that fraction 2 contained the majority of the recombinant pyolysin protein. A 12% acrylamide running gel and the stacking gel were prepared as shown in Table 2.3. Eluted fractions 1 to 5 and the soluble fraction were combined with 2X Laemmli sample buffer (#161-0737; Bio-Rad) and boiled at 95°C for 10 min to prepare for SDS-page analysis. Five μ l of each sample were loaded onto the gel. Electrophoresis was carried out at room temperature and ran for 40 min at 200 volts. Gels were stained overnight in Coomassie stain (50% distilled water, 40% methanol, 10% acetic acid and 0.5% Coomassie blue R250 (#1610436; Bio-Rad), and destained with destain solution (50% dH₂O, 40% methanol and 10% acetic acid) until clear. Figure 2.1 confirms that the majority of the recombinant pyolysin eluted in fraction 2, and therefore this fraction was used for the experiments throughout the present thesis.

Table 2.3 Ingredients for SDS-PAGE gel

Reagent	Product code and supplier	12% Running gel	Stacking gel
Distilled water	N/A	3.5 ml	1.75 ml
Separating buffer 4x Solution	#7732-18-5; Melford Laboratories, Ipswich, UK	2.5 ml	0.75 ml
30 % Acrylamide	#A374; Merk	4 ml	0.5 ml
Ammonium persulfate (APS; 10% solution)	#A3678; Merck	100 μ l	50 μ l
TEMED (N, N, N', N'-tetramethylethylenediamine)	#161-0800; Bio-Rad	10 μ l	3 μ l

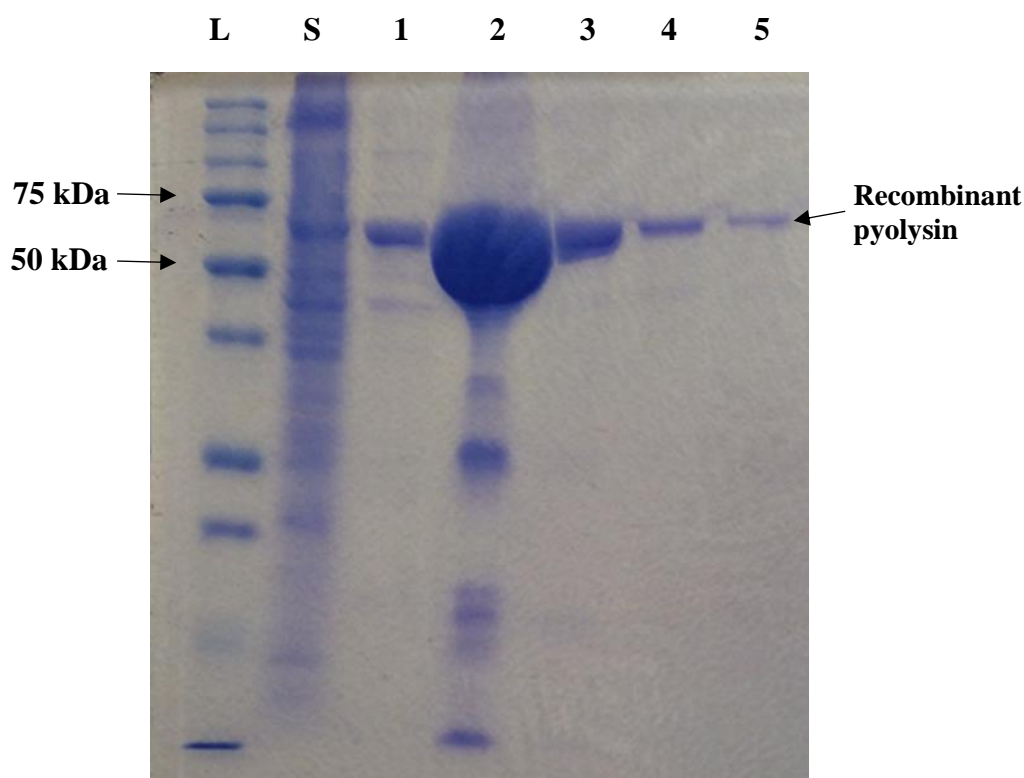


Figure 2.1 SDS-PAGE analysis of recombinant pyolysin fractions

L = All protein blue standard. S = soluble fraction: (BL21 (DE3) *E. coli* cell lysate with over-expressed recombinant pyolysin, 1 to 5 refer to the 1 ml eluted protein fractions. Most of the protein was eluted in fraction 2. Smaller bands possibly reflect breakdown products of pyolysin or histidine rich *E. coli* proteins.

2.2.2 Streptolysin O

Streptolysin O was purchased from Merck (#S5265) and stored according to the manufacturer's instructions. A storage buffer consisting of 10 ml Dulbecco's phosphate-buffered saline (DPBS, #14190250; Thermo Fisher Scientific), 10 mg BSA, and 15.4 g (10 mM) dithiothreitol was prepared in a 20 ml universal tube (#201170; Greiner Bio-One) and gently rotated for 10 min. The streptolysin O was reconstituted in the storage buffer (1 mg/ml) by gently rotating at room temperature for 1 h. After reconstitution, 200 μ l aliquots were stored at -20°C. Prior to use, aliquots were incubated at 37 °C for 30 min.

2.2.3 *Staphylococcus aureus* α -hemolysin

Staphylococcus aureus α -hemolysin (#H9395; Merck) was reconstituted, according to the manufacturer's instructions, in deionized water to yield a 0.5 mg/ml solution that was stored at 4°C.

2.3 CELL CULTURE

2.3.1 Bovine endometrial cell culture

Anatomy of the bovine uterus

The bovine uterus consists of a body and two horns suspended in the pelvic cavity. An ovary resides at the end of each horn and produces a single ovum per oestrus cycle (Fig 2.2). The walls of the uterus are comprised of the perimetrium, myometrium and the endometrium.

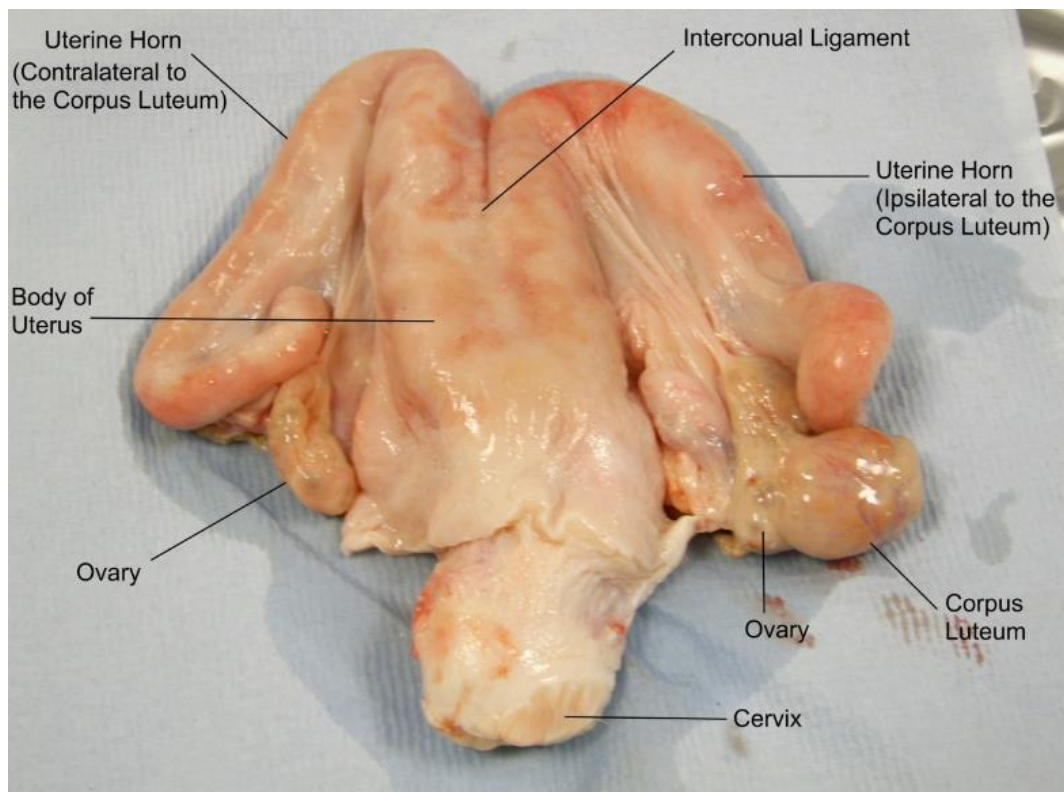


Figure 2.2 Anatomy of the bovine reproductive tract

The bovine female genital tract as received from the St Merryn Abattoir (Cronin et al., 2014).

The endometrium lines the inside of the uterus and consists of a single layer of columnar epithelial cells covering underlying stromal cells (Fig 2.3). Blood vessels are located between the endometrium and myometrium, and monocytes migrate into the stromal cell layers maturing into macrophages. The endometrial surface has protruding caruncles, that interact with the fetal placenta during pregnancy, and is covered in a protective layer of mucus.

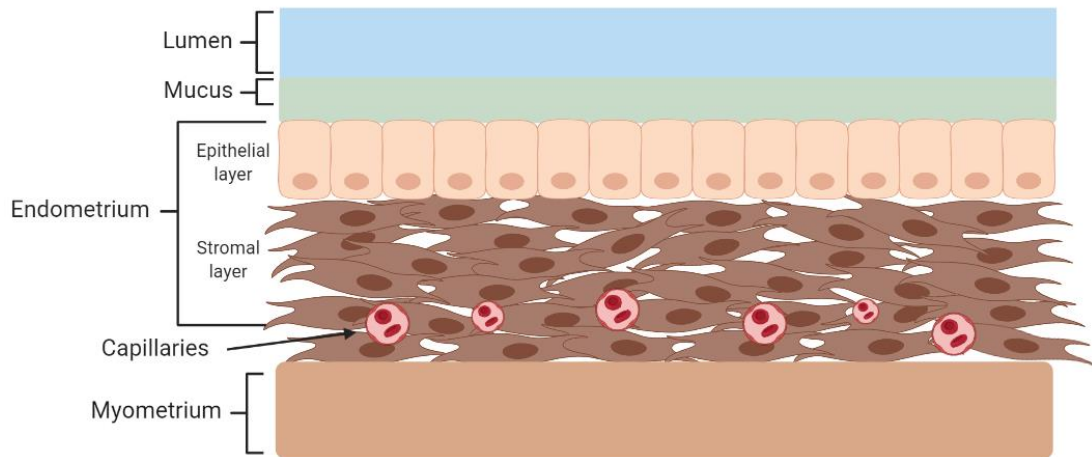


Figure 2.3 The bovine endometrium

A cross section of the bovine endometrium, displaying the individual layers from the uterine lumen to the myometrium. Created with BioRender.com.

Tissue collection

Bovine endometrial epithelial and stromal cells were isolated from uteri as described previously (Cronin et al., 2012, Turner et al., 2014). Bovine female genital tracts were collected from post-pubertal, non-pregnant, mixed breed beef cattle that demonstrated no sign of infection or disease. The cattle were slaughtered as part of the daily work at the St Merryn Abattoir, Merthyr Tydfil. Approval was granted by the United Kingdom Department for Environment, Food and Rural Affairs under the animal by-products registration (EC) No. 1069/2009 (registration number U1268379/ABP/OTHER). Immediately following collection, uteri were individually bagged and placed in a cool box filled with ice ready for transport.

Tissue processing

In preparation for dissection, all work surfaces were cleaned with 70% ethanol and covered in aluminium foil. The uteri were rinsed with 70% ethanol. An incomplete transverse incision was made across the ipsilateral horn just above the interconual ligament (Fig 2.2). The endometrium was then opened by cutting vertically towards the ovary. Endometrial wash solution comprising DPBS and 1% antibiotic antimycotic (ABAM, #A5955; Merck) was used to thoroughly wash the endometrium. The endometrium was then separated from the myometrium in thin strips (Fig 2.4) and placed directly into 60 ml pots (#219270; Greiner Bio-one) containing 25 ml Hank's balanced salt solution (HBSS, #14175095; Thermo Fisher Scientific) with 1% ABAM. The tissue was washed by swirling, transferred to a second pot containing 25 ml HBSS,

and gently swirled again. The tissue was dissected into 5 mm² pieces, placed in a 50 ml tube (#210261; Greiner Bio-One) containing 25 ml HBSS, and then incubated at 37°C for 10 min.

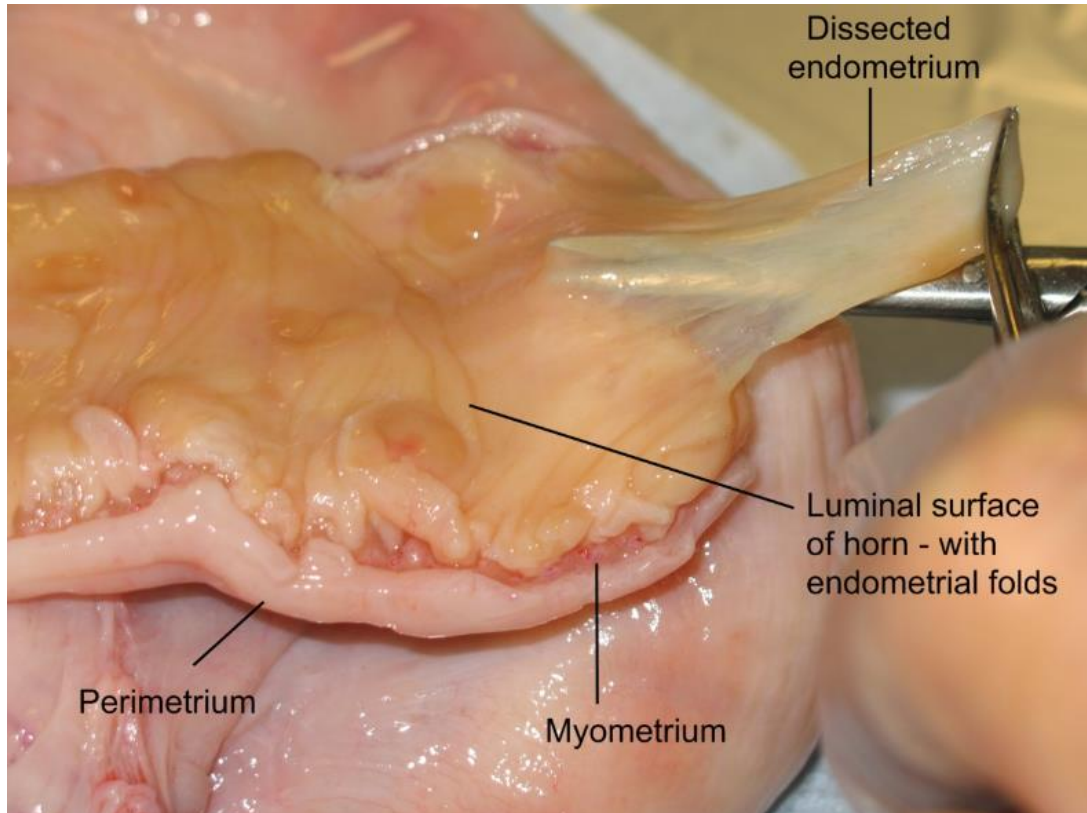


Figure 2.4 Dissection of the bovine endometrium

Visual representation of the endometrium being separated from the myometrium in thin strips using sterile forceps and scissors (Cronin et al., 2014).

Tissue digestion

A sterile digestive solution was freshly prepared consisting of 250 ml HBSS, 125 mg Collagenase II (#C6885; Merck), 250 mg BSA (#A9418; Merck), 600 µl 4% DNase I (#DN25; Merck) and 600 BAEE units' trypsin ethylenediaminetetraacetic acid (#T4049; Merck). After incubation, the supernatant was decanted from the tissue and the digestive solution was added to reach a total volume of 40 ml. Tubes containing digestive solution were incubated in a shaking water bath for 1 h. Digested supernatant was sieved through a 70-µm mesh cell strainer to remove debris, and then through a 40-µm mesh cell strainer (pluriStrainer®, Cambridge Bioscience, Cambridge, UK) into 5 ml of warm stop solution comprising of HBSS with 10% fetal bovine serum (FBS, #FB-1550/506; Biosera, East Sussex, UK).

Media preparation

Cells were cultured in complete medium comprising Roswell Park Memorial Institute (RPMI)-1640 medium (#31870-025; Thermo Fisher Scientific), 10% FBS, 1% ABAM, and 1% L-glutamine (#25030-024; Thermo Fisher Scientific).

Epithelial cell culture

The larger epithelial cells were collected by back-flushing the 40- μ m mesh cell strainers with complete culture medium. The resulting cell suspension was transferred to 25 cm² flasks (#391-3143; VWR, Lutterworth, UK) and incubated at 37°C in humidified air with 5% CO₂ for at least 48 h to allow time for the epithelial cells to adhere. Contaminating stromal cells were removed thanks to their selective attachment properties (Fortier et al., 1988). Medium was discarded and cells were washed with 5 ml sterile warm (37°C) PBS (#10010023; Thermo Fisher Scientific). The PBS was discarded, and cells were incubated with 2 ml warm accutase for 2 to 5 min whilst the stromal cells detached from the culture surface. Progress was closely monitored through a microscope to determine when the stromal cells had detached. Accutase containing detached stromal cells was discarded and replaced with fresh culture medium. Flasks were incubated under humidified air containing 5% CO₂ at 37°C. Medium was replenished every 48 h and once confluency was achieved, cells were maintained in 75 cm² flasks (#734-2705; VWR). Microscopy was used to determine that cell populations were > 95% pure (Fig 2.5) (Fortier et al., 1988). For experiments cells were used from passage 1 and 2.

Stromal cell culture

To isolate stromal cells, the digestive filtrate collected in the stop solution was centrifuged at 700 x g for 7 mins. The supernatant was discarded, 5 ml of sterile water was added to the pellet, and the suspension was vortexed to lyse contaminating red blood cells. Fresh warm (37°C) stop solution (45 ml) was added, and the suspension was centrifuged at 700 x g for a further 7 mins. The supernatant was decanted, the cell pellet was resuspended in 15 ml complete culture medium, and the suspension was then transferred to 75 cm² flasks. Stromal cells adhered to culture flasks within 18 h, at which time the culture supernatant containing contaminating epithelial cells was discarded, stromal cells were washed with 5 ml warm PBS, and fresh culture medium was added. Flasks were incubated under humidified air containing 5% CO₂ at 37°C with medium was replenished every 48 h. (Greiner Bio-One). Microscopy was used to

determine that cell populations were > 95% pure (Fig 2.5) (Fortier et al., 1988). Alternatively, cells can be distinguished by prostaglandin production, with epithelial cells producing significantly more than stroma cells (Fortier et al., 1988). For experiments cells were used from passage 1 and 2.

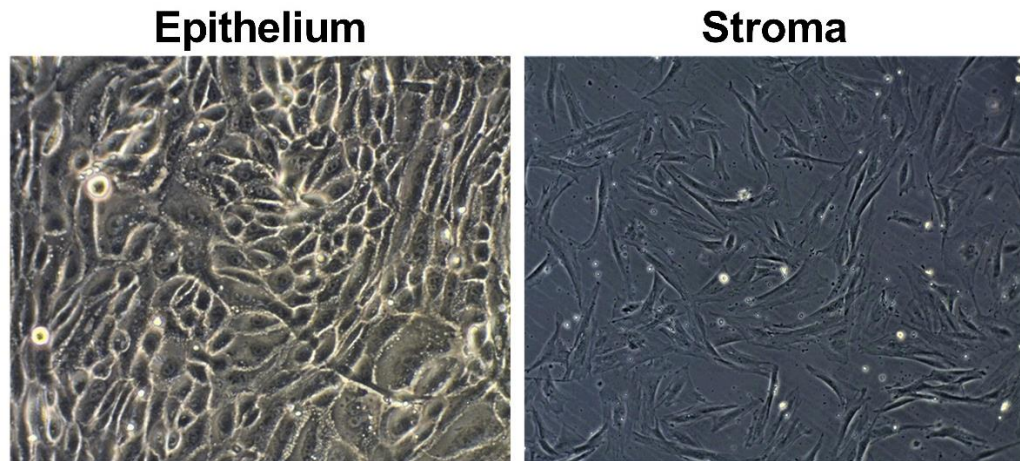


Figure 2.5 Epithelial and stromal cell populations

Representative phase contrast microscopy images of purified bovine endometrial epithelial and stromal cell populations.

2.3.2 HeLa cell culture

Immortal HeLa cervical cells (#CCL-2) were purchased for this thesis (#93021013; Public Health England, Salisbury, UK) and cultured in complete medium comprising Dulbecco's Modified Eagle Medium (DMEM, #41965039; Thermo Fisher Scientific), 10% FBS and 1% ABAM. Cells were maintained in 75 cm² flasks and cultured under humidified air containing 5% CO₂ at 37°C. Medium was replenished every 48 to 72 h. For experiments, cells were used from passage 5 to 30 and seeded in 1 ml/well complete media at a density of 4×10^4 cells/well using 24-well tissue culture plates unless otherwise stated.

2.3.3 A549 cell culture

A549 alveolar epithelial cells were purchased from American Type Culture Collection (#CCL-185; ATCC, Manassas, Virginia, United States) were cultured in complete medium comprising RPMI-1640, 10% FBS, 1% ABAM and 1% L-Glutamine. Cells were incubated in 75 cm² flasks at 37°C under humidified air containing 5% CO₂ and medium was replenished every 48 to 72 h. For experiments, cells were used from

passage 8 to 35 and seeded in 1 ml/well complete media at a density of 4×10^4 cells/well using 24-well tissue culture plates unless otherwise stated.

2.3.4 H441 cell culture

NCI-H441 lung cells (#HTB-174; ATCC) were cultured in complete medium comprising RPMI-1640, 10% FBS, 1% ABAM and 1% L-glutamine. Cells were incubated in 75 cm² flasks at 37°C under humidified air containing 5% CO₂ and medium was replenished every 48 to 72 h. For experiments, cells were used from passage 20 to 30 and seeded in 1 ml/well complete media at a density of 4×10^4 cells/well using 24-well tissue culture plates.

2.3.5 Hep-G2 cell culture

Hep-G2 liver cells (#HB-8065; ATCC) were cultured in complete medium comprising DMEM, 10% FBS and 1% ABAM. Cells were incubated in 75 cm² flasks at 37°C under humidified air containing 5% CO₂ and medium was replenished every 48 to 72 h. For experiments, cells were used from passage 15 to 30 and seeded in 1 ml/well complete media at a density of 4×10^4 cells/well using 24-well tissue culture plates.

2.3.6 Normal dermal human fibroblasts cell culture

Primary normal dermal human fibroblasts (NDHF) primary cells were purchased from Promocell (#C-12302; Heidelberg Germany). Cells were cultured in Fibroblast Growth Medium 2 with Supplement Mix (#C23020; Promocell) and incubated in 75 cm² flasks under humidified air containing 5% CO₂. Cells were grown to 95% confluence and were passaged every 2 to 3 days up to 10 passages. For experiments, cells were seeded in 1 ml/well complete media at a density of 1.4×10^4 cells/well using 24-well tissue culture plates.

2.3.7 Passaging cells

The passaging of cells was carried out in a sterile class 2 hood. Spent medium was discarded from flask, and cells were washed with 5 ml sterile warm (37°C) PBS. The PBS was discarded, and flasks were incubated with 2 ml accutase (#A6964; Merck) at 37°C for at least 5 min. Once a single cell suspension had been achieved, 8 ml of complete culture medium (as specified above) was used to deactivate the accutase. Prior to experiments, a Z1 Coulter Particle Counter (Beckman Coulter, High

Wycombe, UK) was used to count the number of cells per ml in the suspension according to the manufacturer's instructions.

2.4 EVALUATING THE CONSEQUENCES OF PORE FORMATION

2.4.1 Lactate dehydrogenase assay

The release of LDH into cell supernatants was quantified by the LDH-dependent conversion of lactate to pyruvate via the reduction of β -Nicotinamide adenine dinucleotide sodium salt (NAD⁺) to β -Nicotinamide adenine dinucleotide sodium salt hydrate (NADH), which is detected by the NADH-dependent reduction of a tetrazolium salt to red formazan (Decker and Lohmann-Matthes, 1988). A 1.25 mM NADH standard stock solution was prepared in serum-free medium and used to generate a 0 to 20 nmol NADH standard curve (Table 2.4). Then 20 μ l of standard curve or cell supernatant and 30 μ l Tris(hydroxymethyl)aminomethane (Tris) hydrochloride (Tris-HCL) buffer pH 8.2 (Merck) were added in duplicate to a half-area 96-well plate (#675061; Greiner Bio-One).

Table 2.4 NADH standard curve

NADH (nmol)	Standard stock solution (μ l)	Media (μ l)
0	0	20
5	4	16
7.5	6	14
10	8	12
12.5	12	8
15	14	6
17.5	16	4
20	20	0

An assay mix consisting of 54 mM sodium L-lactate (#L7022; Merck), 0.66 mM 2-p-iodophenyl-3-p-nitrophenyl tetrazolium (INT, #I8377; Merck), 0.28 mM phenazine methosulfate (#P9625; Merck) and 1.3 mM NAD⁺ (#N0632; Merck) was prepared in Tris-HCL buffer pH 8.2 (from the stock solutions shown in Table 2.5) as shown in Table 2.6, and 50 μ l was added to each well of the 96-well plate.

Table 2.5 LDH assay mix stock solutions

Solution	Concentration	Mass (mg)	Dissolved in:
Lactate	54 mM (10X stock)	605	10 ml assay buffer
INT	0.66 mM (100X stock)	33.3	1 ml DMSO
Phenazine	0.28 mM (100X stock)	8.5	1 ml PBS
NAD ⁺	1.3 mM (10X stock)	89	10 ml assay buffer

Table 2.6 LDH assay mix recipe

Solution	Volume (ml)
Lactate	1
INT	0.1
Phenazine	0.1
NAD ⁺	1
LDH assay buffer	7.8

Optical density (OD₅₇₀) was measured using a POLARstar Omega micro plate reader before and after a 30 min incubation at 37.5°C. The difference in optical density represented the amount of NADH generated in each supernatant. Lactate dehydrogenase activity is defined as the amount of enzyme that catalyzes the conversion of lactate to pyruvate with the generation of 1 μmole of NADH per minute at 37.5°C and so the amount of LDH in each supernatant was calculated through the following equation: LDH Activity [nmole/min/ml] = (NADH × dilution factor) / (reaction time × volume of sample added to well [ml]). The inter- and intra-assay coefficients of variation for the LDH assay were < 2% and < 4% respectively.

2.4.2 MTT assay

A 3-(4,5-dimethylthiazol-2-yl)-2,5-diphenyltetrazolium bromide (MTT, #M2128; Merck) assay was used to assess viable cells after pore-forming toxin challenge as validated previously for the use of bovine endometrial cells challenged with pyolysin (Amos et al., 2014). The assay measured the reduction of MTT into an insoluble formazan product by the mitochondria of viable cells (Mosmann, 1983). At the end of each experiment medium was discarded and replaced with 250 μl cell specific serum-free medium containing 1 mg/ml MTT and incubated in the dark for 2 h at 37°C. After 2 h, the MTT solution was discarded, and formazan crystals were dissolved in 300 μl

DMSO in a shaker in the dark. The resulting solution was transferred to a clear flat bottom 96-well plate (#437958; Thermo Fisher Scientific), with 100 μ l samples added in duplicate. Absorbance was read at 570 nm using a POLARstar Omega micro plate reader.

2.4.3 CyQUANT assay

The CyQUANT® Cell Proliferation Assay Kit (#C7026; Thermo Fisher Scientific) was used to quantify DNA as a measure of viable NDHF cells following pore-forming toxin challenge according to the manufacturer's instructions. An MTT assay was not used because of the low metabolic activity of NDHF cells. Immediately following the conclusion experiments, cell supernatants were removed, and cells were frozen at -80°C overnight. The CyQUANT GR dye/cell lysis buffer was prepared by diluting the concentrated cell-lysis buffer stock 20-fold in distilled water, and then diluting the CyQUANT GR stock solution 400-fold in diluted cell lysis buffer. Plates were thawed to room temperature and 250 μ l of CyQUANT GR dye/cell lysis buffer solution was added to individual wells and incubated in the dark at room temperature for 5 min. Samples (100 μ l) were added in duplicate to black 96-well half area clear bottom plates (#734-4155; VWR). Fluorescence was measured with a POLARstar Omega micro plate reader using 480 nm excitation and 520 nm emission.

2.4.4 Potassium leakage

The leakage of potassium from cells was measured by flame photometry as described previously (Turner et al., 2020). A potassium-free choline buffer was prepared by adding the ingredients shown in Table 2.7 to 500 ml distilled water and adjusted to pH 7.4 with 2 M NaOH.

Table 2.7 Potassium assay buffer recipe

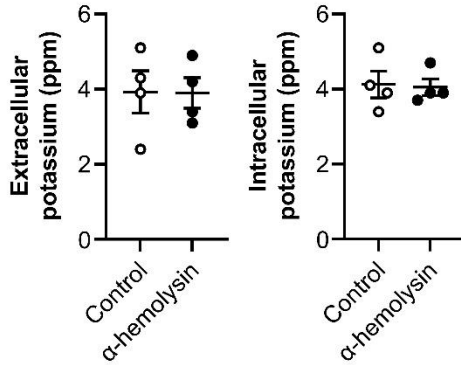
Ingredient	Product code and supplier	Mass (mg)	Concentration (mM)
Ammonium chloride	#213330; Merck	267.5	10
Calcium chloride	#10043-52-4; Thermo Fisher Scientific	83.3	1.5
Choline chloride	#C1879; Merck	9000	129
Citric acid	#C0759; Merck	480.3	5
D-(+)-glucose	#G5767; Merck	500	5.6
Magnesium chloride	#M8266; Merck	38	0.8
Phosphoric acid	#79622; Merck	245	5

In preparation for experiments, cells were seeded for 24 to 48 h in complete medium at 1.5×10^5 cells per well in 6-well culture plates (#92006T; TPP) and treated in serum-free medium for a further 24 h. Supernatants were discarded, and cells were washed three times with the potassium assay buffer. Cells were challenged with control medium or pyolysin for 5 min, or α -hemolysin for 15 min at 37°C. A 15 min α -hemolysin challenge was selected as no potassium leakage was detected from bovine endometrial stromal cells or HeLa cells after a 5 min challenge period (Fig 2.6). Supernatants were collected after the challenge period. Cells were then washed three times in ice-cold potassium assay buffer and lysed with 0.5% Triton X-100 (#T9284; Merck) in dH₂O for 20 min on a rocker at room temperature. All samples were centrifuged at 11,000 x g for 5 min to separate cell debris. Potassium was measured in supernatants and lysates using a Jenway PFP7 flame photometer (Cole-Parmer, Stone, Staffordshire, UK) according to the manufacturer's instructions. Distilled water was aspirated through the flame photometer for 15 min to reach operating temperature, before the readout was set to zero. A 500 ppm potassium stock solution was prepared by dissolving 95.4 mg potassium chloride (KCL; equating to 50 mg/ potassium) in 100 ml distilled water. A 0 to 25 ppm potassium standard curve was prepared by diluting the KCL stock solution as shown in Table 2.8.

Bovine endometrial stromal cells

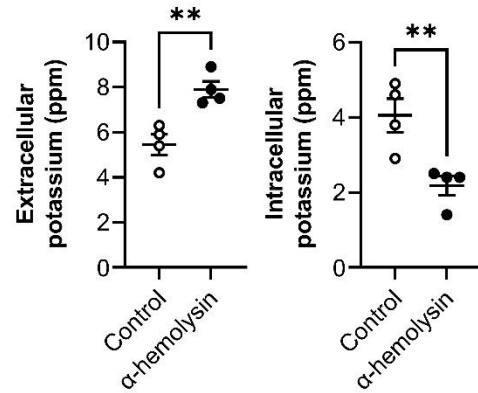
A 5 min α -hemolysin challenge

○ Control ● α -hemolysin



B 15 min α -hemolysin challenge

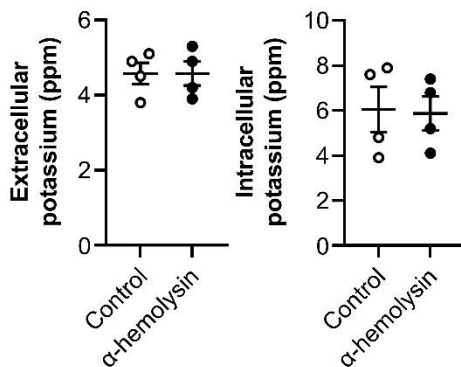
○ Control ● α -hemolysin



HeLa cervical cells

C 5 min α -hemolysin challenge

○ Control ● α -hemolysin



D 15 min α -hemolysin challenge

○ Control ● α -hemolysin

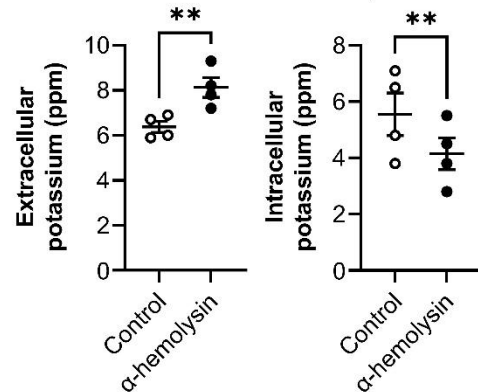


Figure 2.6 Potassium leaks from cells challenged with α -hemolysin for 15 min

Extracellular and intracellular potassium from (A, B) bovine endometrial stromal and (C, D) HeLa cervical challenged for 5 min or 15 min with control medium or 8 μ g α -hemolysin. Dots represent the values from 4 independent experiments; data were analysed by t-test, **P < 0.01.

Table 2.8 Potassium standard curve

Potassium (ppm)	KCL stock (ml)	Distilled water (ml)
25	2.5	47.5
20	2	48
15	1.5	48.5
10	1	49
5	0.5	49.5

A 25 ppm potassium standard was aspirated, and the fuel settings were adjusted to obtain a peak reading. Once a peak reading was reached, the readout was set to 25. The other standards were read without adjusting the readout value and a standard curve was plotted. Samples were then aspirated, and readouts were recorded. Distilled water was continually aspirated between samples and the top standard (25 ppm) was periodically checked to ensure the readout remained consistently at 25 ppm. The standard curve was then used to adjust the readout values to ppm. The inter- and intra-assay coefficients of variation were < 4%.

Although supernatants and lysates were measured to obtain extracellular and intracellular potassium readouts for each sample, only data for extracellular potassium is reported in *Results* as the pyolysin-induced potassium leakage was represented equally by both data sets (Fig 2.7). Additionally, as the control challenge did not cause potassium leakage in cells treated with side-chain oxysterols (Fig 2.7A), LXR agonists (Fig 2.7B), or glucocorticoids (Fig 2.7C), only pyolysin challenge data is reported for treatments in *Results*.

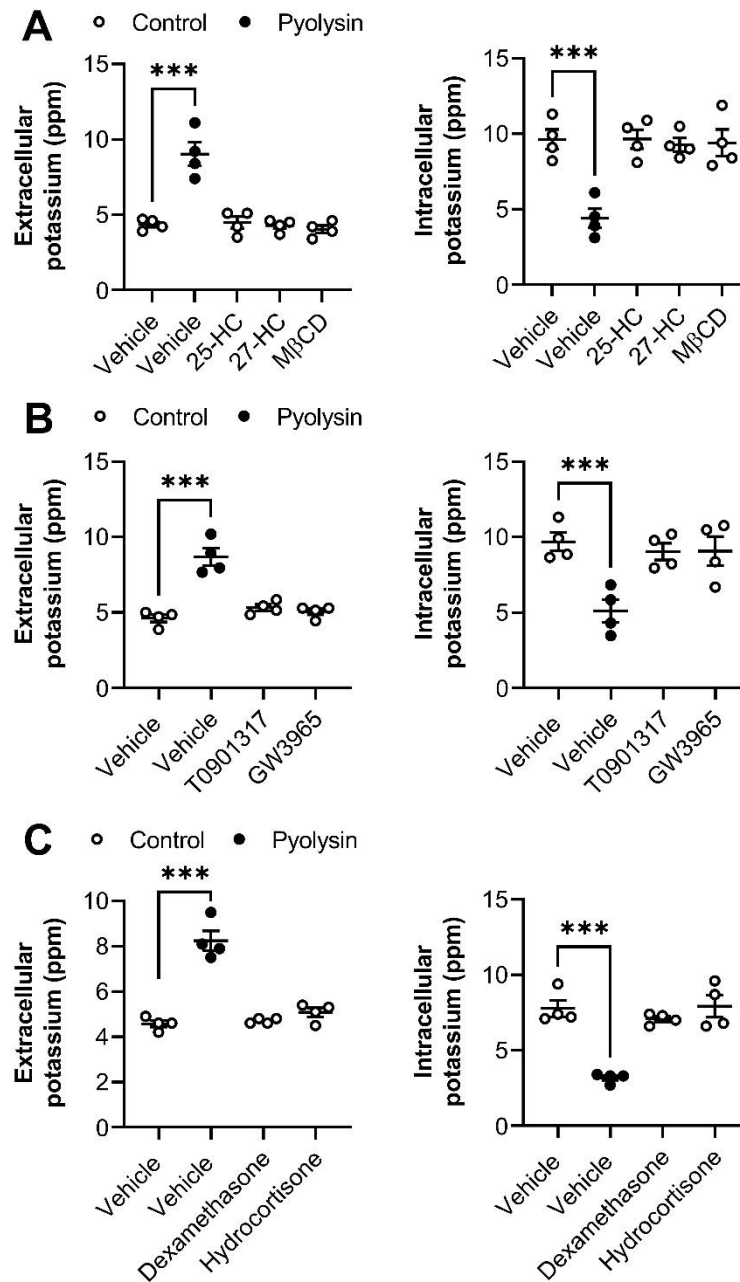


Figure 2.7 Control challenge does not cause potassium ion leakage in treated cells
 Extracellular and intracellular potassium from HeLa cells treated for 24 h with vehicle, (A) 10 ng/ml 25-hydroxycholesterol (25-HC), 10 ng/ml 27-hydroxycholesterol (27-HC), 1 mM M β CD, (B) 25 nM T0901317, 125 nM GW3965, (C) 10 μ M dexamethasone, or 10 μ M hydrocortisone and then challenged for 5 min with control medium or 100 HU pyolysin. Dots represent individual values from 4 independent experiments; statistical significance was determined using one-way ANOVA with Dunnett's post hoc test; pyolysin challenge effects cellular potassium, ***P < 0.001.

2.5 CELL MICROSCOPY

2.5.1 Phase contrast microscopy

To visually quantify the damage caused by pore forming toxins transmitted light micrographs of cells were captured as described previously (Turner et al., 2020). Cells were cultured in 24-well plates (#92024, TPP) and after the specified duration of toxin challenge, an Axiovert 40C inverted microscope and AxioCam ERc5s microscope camera (Zeiss, Jena, Germany) were used to capture images.

2.5.2 Immunofluorescence

To examine the cytoskeleton, cells were stained with the actin dye phalloidin as described previously (Turner et al., 2020, Pospiech et al., 2021). Cells were seeded in complete medium on glass cover slips (#631-0150; VWR) in 24-well culture plates for 24 to 48 h. Relevant treatments were applied for 24 h in serum-free medium, and cells were challenged with control medium or medium containing pyolysin for 2 h, or α -hemolysin for 24 h. At the end of the challenge period, cells were washed with 500 μ l PBS, fixed with 200 μ l PBS containing 4% paraformaldehyde (#158127; Merck), washed twice again with PBS, and then permeabilized for 10 min in 250 μ l PBS containing 0.2% Triton X-100. The cells were blocked for 30 min in 250 μ l PBS containing 0.5% BSA and 0.1% Triton X-100 and then incubated for 1 h with 200 μ l Alexa Fluor 555-conjugated phalloidin (1:1000 dilution in PBS, #A34055; Thermo Fisher Scientific). Cells were washed with 0.1% Triton X-100 in PBS three times, and then mounted onto microscope slides using Vectashield with 4,6-diamidino-2-phenylindole (DAPI, #H-1200-10; Vector Laboratories Inc., Burlington, CA, USA) to visualize cell nuclei. The cells were examined using an Axio Imager M1 fluorescence microscope and images were captured using an AxioCamMR3 (Zeiss).

Cells were stained with CellMask Deep Red plasma membrane stain (#C10046; Thermo Fisher Scientific) to investigate cell shape following pyolysin challenge according to the manufacturer's instructions. Cells were cultured on glass cover slips in 24-well culture plates in complete medium for 24 h, treated for 24 h in serum-free media and challenged for 2 h with control medium or medium containing pyolysin. At the end of the challenge period, cells were washed twice with 500 μ l PBS, incubated with 250 μ l CellMask Deep Red (diluted 1:2000 in PBS) for 10 min at 37°C, washed again with PBS, and fixed with 200 μ l PBS containing 4% paraformaldehyde.

Coverslips were mounted onto microscope slides using Vectashield with DAPI to visualize cell nuclei, and the cells were examined using an Axio Imager M1 fluorescence microscope and images captured using an AxioCamMR3.

2.5.3 Confocal microscopy

To visualize changes in cellular cholesterol content, cells were stained with the cholesterol dye filipin III, as described previously (Turner et al., 2020). Cells were seeded at a density of, 5×10^4 cells/well in complete medium on glass cover slips in 24-well culture plates for 24 h then treated in serum-free medium for 24 h. Coverslips were washed with 500 μ l PBS, fixed with 200 μ l PBS containing 4% paraformaldehyde, and washed twice again with PBS. Cells were stained with 50 μ g/ml filipin III from *Streptomyces filipinensis* (stock diluted 1:160 in 200 μ l PBS #F4767; Merck) for 45 min at room temperature before a final three PBS washes. Cover slips were mounted using polyvinyl alcohol mounting medium with 1,4-diazabicyclo-(2,2,2)-octane (#10981; Merck). A LSM710 confocal microscope (Zeiss) with the Zeiss Zen 2010 software was used to examine cellular cholesterol and images captured using a 40 \times oil objective and a 410 to 476 nm channel range. All coverslips were subjected to identical exposure times and conditions.

2.6 CHOLESTEROL MEASUREMENT

Cellular cholesterol was quantified from cells seeded at 1.5×10^5 cells/well in 6-well plates using the Amplex Red Cholesterol Assay Kit, according to the manufacturer's instructions (#A12216; Thermo Fisher Scientific). At the end of the treatment period, cells were washed twice with 500 μ l DPBS and then collected in 250 μ l 1X Reaction Buffer and stored at -20°C . Samples were defrosted at room temperature and sonicated for 10 min, ensuring the absence of a pellet. The assay was carried out on a black 96-well half-area plate (#734-1626; VWR). A standard curve was created by diluting the 5.17 mM cholesterol reference standard provided in 1X Reaction Buffer to give concentrations from 0 to 20 μ M and 25 μ l was added in duplicate to the 96-well plate. Samples were diluted appropriately in 1X Reaction Buffer and 25 μ l was added in duplicate to the plate. An assay mix was prepared as shown in Table 2.9 and 25 μ l was added to each well that contained standard or sample. The plate was incubated in the dark at 37°C for 30 min before fluorescence was measured by a POLARstar Omega micro plate reader using excitation in the range of 530 nm and emission 590 nm. The

inter- and intra-assay coefficients of variation for the cholesterol assay were < 5%. Protein abundance was also measured in the samples using a DC protein assay and cholesterol concentrations were normalized to protein (Nicholson and Ferreira, 2009).

Table 2.9 Amplex Red working solution recipe

Material	Volume required for 100 assays (µl)
Amplex® Red reagent stock solution	37.5
Horseradish peroxidase	25
Cholesterol oxidase, from <i>Streptomyces</i>	25
Cholesterol esterase, from <i>Pseudomonas</i>	2.5
1X Reaction Buffer	2.41

2.7 WESTERN BLOTTING

Protein isolation and Western blotting was performed as described previously, with minor modifications (Bromfield and Sheldon, 2011, Griffin et al., 2018). To extract protein for Western blotting, cells were washed with 500 µl of ice-cold PBS and lysed with 100 µl of PhosphoSafe extraction reagent (#71296; Merck). Protein concentration was quantified using a DC assay as described in section 2.2.1. Acrylamide gels were constructed as shown in Table 2.10, left to polymerize for 30 min, and 10 µg of protein or 10 µl Precision Plus All Blue Protein Standard (#1610373; Bio-Rad) were added to individual lanes. Proteins were separated in a mini trans-blot PROTEAN electrophoresis cell (Bio-Rad) for 40 min at 180 V (PowerPac Basic, Bio-Rad).

Table 2.10 In-house acrylamide gel recipe (for 1 gel)

Reagent	7.5 % Gel	10 % Gel	12 % Gel	Stacking Gel
Water	5 ml	4.2 ml	3.5 ml	1.75 ml
4 x Tris & SDS (Separating buffer)	2.5 ml	2.5 ml	2.5 ml	0.75 ml (stacking buffer)
30 % Acrylamide	2.5 ml	3.3 ml	4 ml	0.5 ml
APS (10% solution)	100 µl	100 µl	100 µl	50 µl
TEMED	10 µl	10 µl	10 µl	3 µl

Proteins were transferred onto polyvinylidene difluoride membranes (GE Healthcare, Chalfont, St Giles, UK) by semi-dry transfer for 25 V for 30 min in a Trans-Blot Turbo Transfer System (Bio-Rad). Membranes were then blocked with a 1 h room temperature incubation in Tris-buffered saline containing 0.1% Tween 20 (TBST, #P7949; Merck) with 5% BSA, before being probed overnight at 4°C with the relevant antibody of interest (Table 2.11).

After incubation, membranes were washed five times for 5 min in TBST before secondary antibodies were added in TBST with 5% BSA for an hour at room temperature. Membranes were then washed a further five times with TBST. Protein reactivity was visualized using enhanced chemiluminescence (Clarity Western enhanced chemiluminescence substrate, #1705061; Bio-Rad) and captured with a ChemiDoc XRS System (Bio-Rad) using Quantity One software (Bio-Rad). After imaging, membranes were stripped for 7 min with Restore Western Blot Stripping Buffer (#21059; Thermo Fisher Scientific) and reprobed to detect another primary antibody, or with α -tubulin or β -actin to normalize protein loading. A representative whole blot image for each of the antibodies used in the present thesis is displayed in Fig 2.8. The average peak density of bands was quantified using Fiji and target proteins were normalized to α -tubulin or β -actin; phosphorylated proteins were normalized to their cognate total protein (Schindelin et al., 2012).

Table 2.11 List of antibodies used in this study

Antibody target	Species raised in and clonality	Predicted molecular weight (kDa)	Supplier	Product code	RRID
Primary antibodies					
LXR α	Rabbit monoclonal	50	Abcam	ab176323	AB_2877144
LXR β	Rabbit polyclonal	51	Abcam	ab28479	AB_776097
ABCA1	Mouse monoclonal	254	Abcam	ab18180	AB_444302
diphosphorylated ERK1/2	Mouse monoclonal	44/42	Merck	M8159	AB_477245
ERK1/2	Rabbit polyclonal	44/42	Abcam	ab17942	AB_2297336
phospho-p38	Rabbit monoclonal	43	Cell Signaling	4511	AB_2139682
p38	Rabbit monoclonal	40	Cell Signaling	8690	AB_10999090
phospho-JNK	Rabbit polyclonal	54/46	Cell Signaling	9251	AB_331659
JNK	Rabbit polyclonal	54/46	Cell Signaling	9252	AB_2250373
HMGCR	Rabbit monoclonal	97	Abcam	ab174830	AB_2749818
Glucocorticoid receptor	Rabbit monoclonal	94/91	Cell Signaling	12041	AB_2631286
α tubulin	Rabbit monoclonal	52	Cell Signaling	2144	AB_2210548
β actin	Mouse monoclonal	42	Abcam	ab8226	AB_306371
α -His-pyolysin antibody	Rabbit polyclonal	55	Generously gifted by Prof. B.H. Jost, University of Arizona	N/A	N/A
Secondary antibodies					
Anti-rabbit IgG	Goat polyclonal	N/A	Cell Signaling	7074	AB_2099233
Anti-mouse IgG	Horse polyclonal	N/A	Cell Signaling	7076	AB_330924

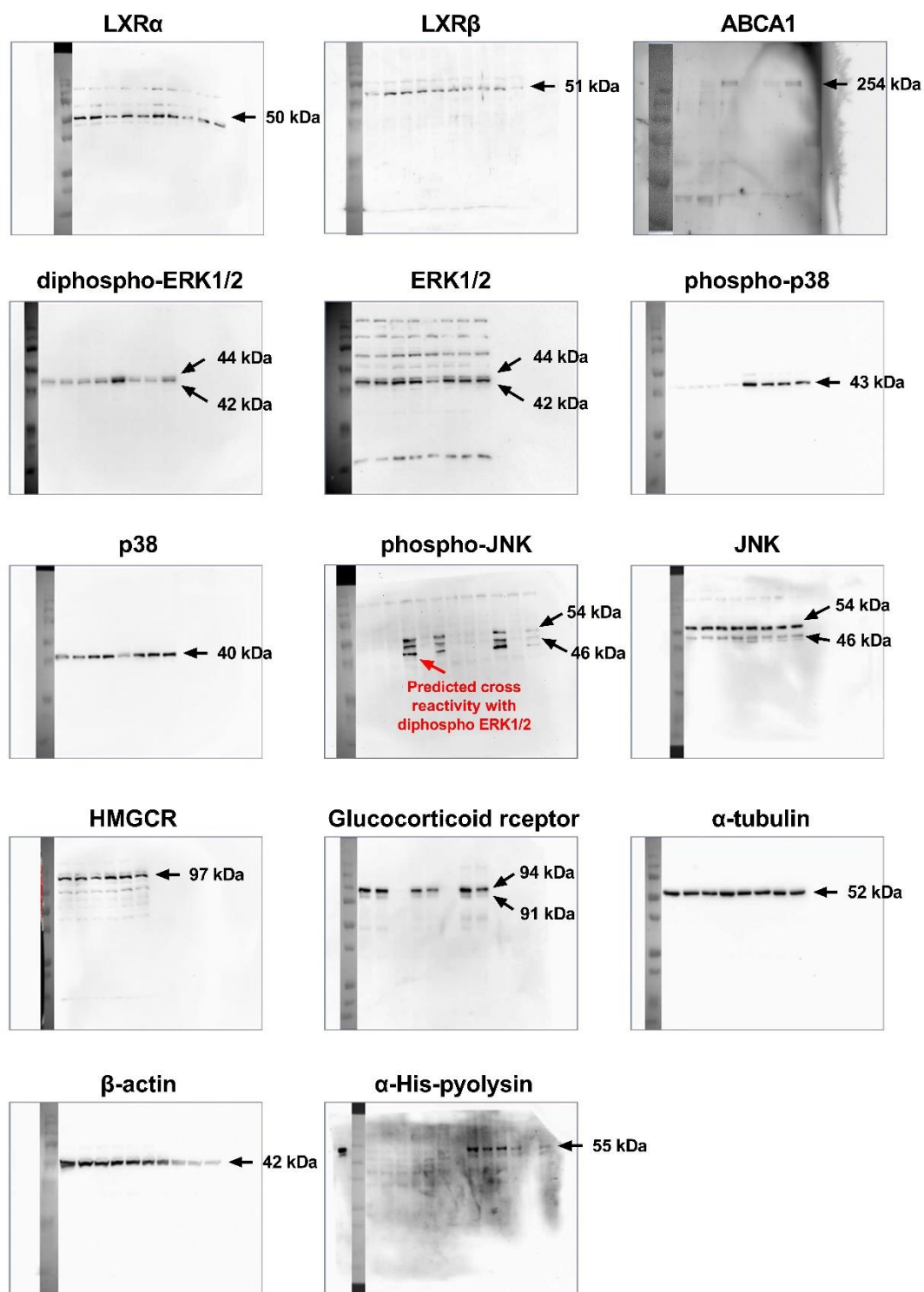


Figure 2.8 Representative whole blot images for the antibodies used in this thesis
 Representative Western blot images, captured with a ChemiDoc XRS System, for each of the antibodies used in the present thesis. Protein was collected from bovine endometrial stromal cells for the LXR α and ABCA1 blots, from bovine endometrial epithelial cells for the LXR β blot, and from HeLa cervical cells for the remaining targets.

2.8 OXYSTEROL MEASUREMENT

2.8.1 Uterine and ovarian follicular fluid collection

Oxysterols were quantified in the ovary and uterus, from bovine female genital tracts collected from healthy, post-pubertal, mixed breed cattle slaughtered as part of the daily work at the St Merryn Abattoir, Merthyr Tydfil. Immediately following collection, the uteri were individually bagged and placed in a cool box filled with ice ready for transport. At the laboratory, the uteri were rinsed with sterile PBS and the surface of the endometrium was exposed by a longitudinal cut in each uterine horn. Fluid was aspirated from the surface of the endometrium using sterile 20-gauge needle and 2 ml endotoxin-free syringe (BD Medical, Oxford, U.K.).

Ovaries were separated from the reproductive tract within 15 min of slaughter and stored in a thermos containing medium comprising Medium 199 (#31150030; Thermo Fisher Scientific), 1 % ABAM and 0.1% BSA, that was heated to 37.5°C. On returning to the laboratory, the ovaries were rinsed with sterile PBS before a sterile 20-gauge needle and 2 ml endotoxin-free syringe was used to aspirate follicular fluid from dominant (> 8 mm external diameter) and emerged (4 to 8 mm external diameter) ovarian follicles. The presence of a corpus luteum indicated that the selected animals were cyclic, and only healthy follicles with clear fluid were selected for aspiration.

2.8.2 Epithelial and stromal cell supernatant sample collection

Oxysterols were quantified in the supernatants of bovine endometrial stromal and epithelial cells following a lipopolysaccharide (LPS) or pyolysin challenge; two major virulence factors of uterine pathogens (Sheldon et al., 2002, Amos et al., 2014, Bonnett et al., 1991, Sheldon et al., 2010).

Ultrapure LPS from *E. coli* 0111:B4 (#tlrl-3pelps; Invivogen, Toulouse, France) was reconstituted to 5 mg/ml in ultrapure, endotoxin-free water (provided by Invivogen alongside the LPS) and vortexed for 10 min. For storage, the LPS was further diluted to 1 mg/ml in the ultrapure, endotoxin-free water, and stored at -20°C in 2 ml salinized glass vials (#27029; Merck). Prior to use, LPS was defrosted at room temperature, sonicated for 5 min in a sonicating water bath, and vortexed for 1 min prior to diluting to required challenge concentration (1 µg/ml) in control serum-free medium (RPMI-1640). The diluted LPS solution was the vortexed for an additional 1 min before use.

For experiments, epithelial and stromal cells were seeded at 1.5×10^5 cells per well in complete medium in 6-well culture plates for 24 h and 48 h, respectively, then incubated for 24 h in serum-free medium. Cells were then challenged for 24 h with control serum-free medium, or medium containing a sub-lytic concentration of 5 HU pyolysin or 1 $\mu\text{g/ml}$ LPS. Collected supernatants were stored at -80°C ready for extraction.

2.8.3 Sample preparation

To examine the oxysterol content of bovine endometrial uterine and ovarian fluid and endometrial cell supernatants, samples were prepared for liquid chromatography-mass spectrometry as described by Abdel-Khalik et al. (2017). For biological fluid samples, 100 μl was added dropwise to 1 ml ethanol containing 2 ng of $[25,26,26,26,27,27,27\text{-}^2\text{H}_6]$ 24R/S-hydroxycholesterol, 2 ng of $[25,26,26,26,27,27,27\text{-}^2\text{H}_7]$ 22R-hydroxycholesterol-4-en-3-one, and 400 ng of $[25,26,26,26,27,27,27\text{-}^2\text{H}_7]$ cholesterol (Avanti Polar Lipids) whilst under sonication in an ultrasonic bath for 5 min. The solution was then adjusted to 70% ethanol and sonicated for a further 5 min. For cell supernatants, 1 ml was added to 2.3 ml ethanol using the same standards under sonication. Solutions were then centrifuged at $17,000 \times g$ for 30 min at 4°C and any debris were separated ready for oxysterol extraction. Then, 200-mg Certified Sep-Pak C18 columns (Waters, Elstree, Herts, U.K.) were used to separate oxysterols and steroid acids from cholesterol. Columns were conditioned, before samples were run through at a rate of 1 to 2 drops per second. A further 5.5 ml 70% ethanol was added to the column to give the oxysterol containing fraction: solid phase extraction (SPE)1 fraction 1. Samples were divided into equal volumes, labelled A and B, and dried overnight in a vacuum.

Once dried, SPE1-Fraction 1 samples were dissolved in 100 μl isopropanol and 1 ml of 50 mM phosphate buffer (pH7). To samples labelled "A", 3 μl of cholesterol oxidase from *Streptomyces* (2 mg/ml in H_2O , 44 units/mg protein; Merck) was added, "B" samples were left untreated. Both A and B were incubated in a water bath for 1 h at 37.5°C before the addition of 2 ml absolute methanol and 150 μl glacial acetic acid. Finally, 150 mg of $[^2\text{H}_0]$ Girard P reagent (#1126-58-5; Tokyo Chemical Industry, Oxford, UK) was added to all samples and vortexed. The derivatization reaction was then allowed to occur overnight, in the dark, at room temperature. To remove excess

derivatization reagent, we used 60-mg Oasis HLB (Waters) columns. Samples were ran through the columns three times and were diluted to 35% and 17.5% methanol for the second and third time respectively. The flow through was discarded and sterols were eluted from the columns with 3 x 1 ml 100% methanol (to give SPE2 fraction 1 to 3) and 1 ml absolute ethanol (to give SPE2 fraction 4). All SPE2 fractions were stored at -20°C ready for analysis.

2.8.4 Liquid chromatography-mass spectrometry

Samples were analyzed on an Orbitrap Elite (Thermo Fisher Scientific) equipped with an electrospray probe, and a Dionex Ultimate 3000 LC system (Thermo Fisher Scientific) (Griffiths et al., 2013, Crick et al., 2015). Two injections were carried out per sample with three or more scan events per injection. One event was a high-resolution (120,000, full width at half maximum height, at m/z 400) MS scan event in the Orbitrap analyzer and the rest were multi-stage fragmentation (MS_n) scan events in the linear ion trap. Quantification was performed with Xcalibur 3.0 (Thermo Fisher Scientific) by stable isotope dilution using 24 R/S-[25,26,26,26,27,27,27-²H₆]hydroxycholesterol as the internal standard. Where authentic standards were unavailable, oxysterols were identified by retention time, mass and by second generation product ion (MS³). Peak areas were used to calculate concentrations (Crick et al., 2015).

2.9 SHORT INTERFERING RNA DESIGN AND KNOCKDOWN

Previously validated siRNA (designed in the siDESIGN Centre package from Dharmacon GE healthcare) was used to target the genes *NRIH2*, *NRIH3* and *HMGCR* (Table 2.12) (Griffin et al., 2017, Griffin et al., 2018) . A SMARTPool of siRNA targeting *NR3C1* was purchased from Horizon Discovery (#003424-00-0005; Horizon Discovery, Cambridge, UK).

Table 2.12 Short interfering RNA sequences

Gene	Species	Direction	Sequence (5'-3')
<i>NRIH2</i>	Human	Sense	G.A.A.G.A.A.G.A.A.G.A.U.U.C.G.G.A.A.A.U.U
		Antisense	U.U.U.C.C.G.A.A.U.C.U.U.C.U.U.C.U.U.C
	Bovine	Sense	A.G.G.U.G.A.A.G.G.U.G.U.C.C.A.G.U.U.A.U.U
		Antisense	U.A.A.C.U.G.G.A.C.A.C.C.U.U.C.A.C.C.U
<i>NRIH3</i>	Human	Sense	C.C.U.C.A.A.G.G.A.U.U.U.C.A.G.U.U.A.U.U.U
		Antisense	A.U.A.A.C.U.G.A.A.A.U.C.C.U.U.G.A.G.G
	Bovine	Sense	G.C.U.A.A.A.U.G.A.U.G.C.U.G.A.G.U.U.U.U.U
		Antisense	A.A.A.C.U.C.A.G.C.A.U.C.A.U.U.U.A.G.C
<i>HMGCR</i>	Human	Sense	G.G.A.U.A.A.A.C.C.G.A.G.A.A.A.G.A.A.A.U.U
		Antisense	U.U.U.C.U.U.U.C.U.C.G.G.U.U.U.A.U.C.C

ON-TARGETplus non-targeting control pool scramble siRNA (#001810-10-05; Horizon Discovery) or target siRNA was dissolved in siRNA buffer (#B-002000-UB-100; Horizon Discovery) to a final concentration of 20 μ M. The scramble or target siRNA was then diluted in the required volume of OptiMEM medium (#11058021; Thermo Fisher Scientific) with 15 μ l Lipofectamine RNA-iMax (#13778150; Thermo Fisher Scientific) added per ml OptiMEM in sterile 2 ml reaction tubes. The siRNA was vortexed for 30 s and then left to incubate for 15 min at room temperature to allow siRNA complex formation. The siRNA complex solution was then added to tissue culture plates before the cell type of interest was added in antibiotic-free culture medium. Specific volumes and concentrations are described in detail where relevant in each research chapter. Cells were incubated with siRNA for 48 h before treatments were added as previously described (Griffin et al., 2018, Griffin et al., 2017, Kadiyala et al., 2016). The effect of RNA interference on pyolysin challenge is displayed in Fig 2.9.

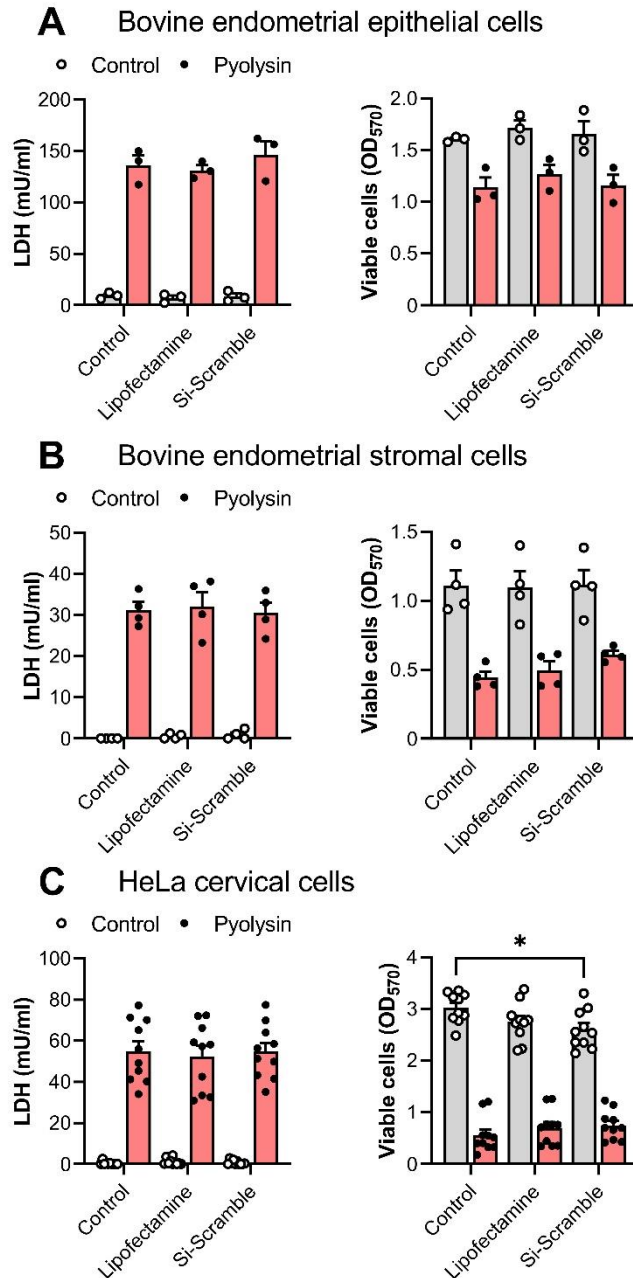


Figure 2.9 RNA interference of bovine endometrial and HeLa cells

Leakage of LDH and viability of (A) bovine endometrial epithelial, (B) stromal cells and (C) HeLa cervical cells treated for 48 h with control medium, or medium containing lipofectamine, or transfected for 48 h with scramble siRNA. Cells were then cultured for 24 h in serum-free medium and challenged for 2 h with control medium or pyolysin (epithelium 200 HU, stroma 25 HU, HeLa 100 HU). Data are presented as mean (SEM); statistical significance was determined using two-way ANOVA and Dunnett's post hoc test; *P < 0.05.

2.10 QUANTITATIVE POLYMERASE CHAIN REACTION

Quantitative polymerase chain reaction (PCR) was used to assess the effectiveness of siRNA targeting *NRIH2* and *NRIH3* in HeLa cervical cells.

2.10.1 Total RNA Extraction

Total RNA was isolated from HeLa cells in preparation for quantitative PCR using the RNeasy Mini Kit (#74104; Qiagen, Crawley, UK), according to the manufacturer's instructions. Cells were lysed by the addition of with 350 μ l RLT lysis buffer and thorough scraping. Lysates were transferred to 1.5 ml reaction tubes, and 350 μ l 70% ethanol was added (mixed by gentle pipetting). Lysates were loaded into RNeasy mini spin columns and were centrifuged at 8,500 x g for 15 secs and the flow through was discarded. Then 700 μ l RW1 buffer was added to the spin column and centrifuged again at 8,500 x g for 15 s and the flow through was discarded. The process repeated with 500 μ l RPE buffer. An additional 500 μ l of RPE buffer was added and the column was centrifuged at 8,500 x g for 2 min. Flow through was discarded and spin columns were transferred to new 2 ml collection tubes and centrifuged at 13,000 x g for 1 min to dry the membranes. Spin columns were then transferred to new 1.5 ml collection tubes and 30 μ l RNase-free water was pipetted directly on to the spin column membrane. Spin columns were centrifuged at 8,500 x g for 1 min. Eluted RNA was ran through columns again to achieve a maximum yield.

Quantification of eluted RNA was carried out using the NanoDrop spectrometer (ND-100 Spectrometer, Labtech International, Uckfield UK). All samples were assumed to be free from contamination as the ratios obtained at 260/280 nm and 260/230 nm were between 1.8 and 2.2 (as shown in Table 2.13). Samples were then stored at -80°C until use.

Table 2.13 NanoDrop values for RNA isolated from HeLa cells in this project

Replicate	Sample	RNA (ng/ μ l)	260/280 nm	260/230 nm
1	Control	365.8	2.09	2.16
	siScramble	355.8	2.12	1.87
	siNRIH2	348.1	2.11	1.88
	siNRIH3	370.1	2.1	2.06
	siNRIH2+3	355.6	2.09	2.02
2	Control	517.7	2.08	2
	siScramble	523.4	2.07	2.1
	siNRIH2	523.8	2.07	2.11
	siNRIH3	494.6	2.06	2.07
	siNRIH2+3	535.1	2.07	1.87
3	Control	398.9	2.15	1.86
	siScramble	429.1	2.14	2.03
	siNRIH2	432.6	2.14	2.1
	siNRIH3	405.8	2.15	2.08
	siNRIH2+3	384.9	2.15	1.8

2.10.2 Complementary DNA synthesis

In preparation for quantitative polymerase chain reaction (PCR), complementary DNA (cDNA) was synthesised from 1000 ng extracted RNA using the QuantiTect Reverse Transcription kit (#205311; Qiagen), according to the manufacturer's instructions. Total RNA was defrosted on ice and 1000 ng was added to 2 μ l genomic DNA wipeout buffer in a 200 μ l PCR tube. Ice cold RNase-free water was added to reach a total volume of 14 μ l. Samples were vortexed for 30 s, briefly centrifuged, then incubated at 42°C for 2 min in a T100™ Thermal Cycler (Bio-Rad). A reverse transcription master mix was prepared as shown in Table 2.14 and 6 μ l was added to each sample. Samples were briefly vortexed and centrifuged and then incubated in a thermal cycler at 42°C for 15 mins for cDNA synthesis, then at 95°C for 3 min to inactivate the reverse transcription enzyme. Samples were then kept on ice ready for quantitative PCR.

Table 2.14 Complementary DNA synthesis master mix

Reagent	Volume (µl)
Quantiscript® Reverse Transcriptase	1
Quantiscript RT Buffer	4
RT Primer mix	1

2.10.3 Quantitative PCR

For quantitative PCR we used previously validated primers (designed using the NCBI primer design tool) against the human genes *NR1H2* and *NR1H3*, with ribosome-like protein 19 (*RPL19*) used as a reference (sequences are shown in Table 2.15) (Griffin et al., 2018).

Table 2.15 Primer sequences

Gene	Direction	Sequence (5' – 3')
<i>RPL19</i>	Forward	GCGAGCTCTTTCCTTTCGCT
	Reverse	TGCTGACGGGAGTTGGCATT
<i>NR1H2</i>	Forward	CAGACTGGGGCGTCCTTTC
	Reverse	GACTGCGACTGTGACTGTGA
<i>NR1H3</i>	Forward	GGAGGTACAACCCTGGGAGT
	Reverse	AGCAATGAGCAAGGCAAACCT

Primers were reconstituted to 10 µM in RNase-free water. The total reaction volume used for quantitative PCR was 25 µl and was prepared as shown in Table 2.16 with 1.5 µl RNase-free water used as a no template control (NTC). The reaction was performed in triplicate on white low-profile plates (#MLL9651; Bio-Rad) using a plate set up as shown in Table 2.17. Standard curves were generated from mRNA extracted from untreated HeLa cell lysates using a 10-fold serial dilution from neat to 1×10^{-4} in nuclease-free water.

Table 2.16 Reaction set up for quantitative PCR

Component	Volume (µl)
2x QuantiFast SYBR Green PCR Master Mix (#204054, Qiagen)	12.5
Forward Primer	0.25
Reverse Primer	0.25
RNase-free water	10.5
cDNA	1.5
Total volume	25

Table 2.17 Quantitative PCR plate layout

	1	2	3	4	5	6	7	8	9	10	11	12
A	<i>RPL19</i> standard curve			<i>NR1H2</i> standard curve			<i>siNR1H3: NR1H3</i>			NTC <i>RPL19</i>	NTC <i>NR1H3</i>	NTC <i>NR1H2</i>
B							<i>siNR1H3: NR1H2</i>					
C							<i>siNR1H2: RPL19</i>					
D							<i>siNR1H2: NR1H3</i>					
E	<i>NR1H3</i> standard curve			Scramble: <i>RPL19</i>			<i>siNR1H2: NR1H2</i>					
F				Scramble: <i>NR1H3</i>			<i>siNR1H2+3: RPL19</i>					
G				Scramble: <i>NR1H2</i>			<i>siNR1H2+3: NR1H3</i>					
H				<i>siNR1H3: RPL19</i>			<i>siNR1H2+3: NR1H2</i>					

Once wells were loaded, the plate was centrifuged at 500 x g for 1 min. Quantitative PCR was then carried out on the CFX Connect Real-time thermal cycler (Bio-Rad) using the SYBR green protocol and the cycling conditions described in Table 2.18.

Table 2.18 Quantitative PCR cycling conditions

Step	Time	Temperature (°C)	Cycles
Initial activation	5 min	95	1
Denaturation	10 s	95	40
Annealing	30 s	60	
Hold	Infinite	4	1

Sample target and reference gene abundance was determined using the quantification cycle (Cq) values from the appropriate standard curve and changes in mRNA abundance were then determined from the ratio of target gene Cq to reference gene Cq, using Bio-Rad CFX manager software version 2.1. We used *RPL19* as the reference gene and Cq values remained consistent regardless of treatments as shown in Table 2.19. Data presented in *Results* for target gene expression is normalized to the expression of *RPL19*.

Table 2.19 Reference gene (*RPL19*) expression was consistent across treatments

Treatment	Cq value
Scramble	17.35 - 18.32
si <i>NR1H2</i>	17.53 - 18.27
si <i>NR1H3</i>	17.36 - 18.34
si <i>NR1H2+NR1H3</i>	17.47 - 18.19

2.11 STATISTICAL ANALYSIS

All graphs were prepared using GraphPad Prism 9.0.1 (GraphPad Software, San Diego, California, USA). The statistical unit was the animal used to isolate cells or to collect fluid from, or each independent experiment with the relevant cell line. Statistical analysis was performed using GraphPad Prism 9.0.1 with significance attributed when $P < 0.05$, and data reported as arithmetic mean \pm the standard error of the mean (SEM). Data was analyzed for normality using the Shapiro-Wilks test, with data assumed to be normally distributed when $P > 0.05$. Comparisons between treatments or challenges were made using one-way or two-way analysis of variance (ANOVA) followed by a Dunnett, Bonferroni or Tukey post hoc test for multiple comparisons, or unpaired two-tailed Student's t-test, as appropriate for the experimental data and as specified in *Results* and figure legends. In experiments using a range of treatment concentrations, P-values are reported for the ANOVA, presenting the effect of treatment on pore-forming toxin challenge. Significant differences between independent treatments or toxin challenges are presented as follows; * $P < 0.05$, ** $P < 0.01$ and *** $P < 0.001$. Numerical values are reported where the differences between treatments and vehicle control were $0.05 \leq P \leq 0.2$. In experiments investigating the effect of 27-hydroxycholesterol treatment duration on cytoprotection, correlation was evaluated using Pearson's correlation coefficient.

3 OXYSTEROLS PROTECT BOVINE ENDOMETRIAL CELLS AGAINST PORE-FORMING TOXINS FROM PATHOGENIC BACTERIA

3.1 INTRODUCTION

Parturition in mammals is often followed by infection of the uterus with multiple pathogenic bacteria, and disruption of the protective epithelium of the endometrium to expose the underlying stroma. This is a particular problem in *Bos taurus* dairy cattle, where pathogenic bacteria cause postpartum uterine disease and infertility in up to 40% of animals (Sheldon et al., 2019, Ribeiro et al., 2016). Many of these pathogenic bacteria secrete toxins that form pores in cell membranes leading to cell damage. The occurrence and severity of disease depends on how effectively the immune system kills and removes pathogens, and how well tissues limit damage and tolerate the presence of pathogens (Medzhitov et al., 2012, Read et al., 2008, Sheldon et al., 2019, Sheldon et al., 2020). The immune system is regulated, at least in part, by steroid hormones and oxysterols (Wira et al., 2015, Spann and Glass, 2013, Ogawa et al., 2005, Cain and Cidlowski, 2017). However, it is not known whether steroid hormones or oxysterols can also affect the ability to tolerate pathogens by protecting cells against the damage caused by pore-forming toxins.

Uterine pathogens such as *Trueperella pyogenes*, *Escherichia coli*, and *Staphylococcus aureus* secrete pore-forming toxins that can damage the bovine endometrium (Sheldon et al., 2002, Amos et al., 2014, Griffin et al., 1974, Bonnett et al., 1991). *Trueperella pyogenes* secretes pyolysin, which is a member of the cholesterol-dependent cytolysin family of pore-forming toxins (Amos et al., 2014, Peraro and van der Goot, 2016, Billington et al., 1997). These cytolysins specifically bind cholesterol, and not other sterol or oxysterol molecules, and/or require cholesterol-rich areas in the plasma membrane for pore formation (Bielska et al., 2014, Peraro and van der Goot, 2016, Flanagan et al., 2009, Tweten, 2005, Griffin et al., 2018, Billington et al., 1997). There are three pools of cholesterol in plasma membranes: an essential pool, a sphingomyelin-bound pool, and a pool of labile cholesterol (Das et al., 2013, Das et al., 2014). It is thought that cholesterol-dependent

cytolysins bind to the accessible labile pool of cholesterol in plasma membranes, typically when the content of cholesterol exceeds 35 mol% (molar percentage) of plasma membrane lipids (Das et al., 2013). Pyolysin is secreted as a 55 kDa monomer and 30 to 50 molecules of pyolysin oligomerize to form a β -barrel transmembrane pore in the plasma membrane with an 18 nm internal diameter (Billington et al., 1997, Preta et al., 2016, Amos et al., 2014). These pores lead to leakage of potassium ions from cells within minutes, leakage of cytosolic proteins, such as lactate dehydrogenase (LDH) within an hour, changes in the cytoskeleton, and ultimately cytolysis (Tveten, 2005, Gonzalez et al., 2011, Turner et al., 2020, Peraro and van der Goot, 2016). *Staphylococcus aureus* secretes α -hemolysin, which binds to the plasma membrane where 7 molecules oligomerize to form β -barrel transmembrane pores with a 1.6 nm internal diameter, which also leads to leakage of cytosolic molecules and causes cytolysis (Song et al., 1996, Berube and Bubeck Wardenburg, 2013). Although innate immunity and cellular repair mechanisms are well characterized (Gurcel et al., 2006, Amos et al., 2014, Gonzalez et al., 2011, Bromfield et al., 2015, Wira et al., 2005, Andrews and Corrotte, 2018), less is known about intrinsic protection of cells against damage caused by pore-forming toxins.

Steroid hormones and oxysterols are derivatives of cholesterol that act through nuclear receptors to control important physiological functions associated with reproduction and metabolism. However, steroid hormones and oxysterols also modulate immunity and the risk of disease (Wira et al., 2015, Ogawa et al., 2005, Cain and Cidlowski, 2017, Dang et al., 2017). For example, in the follicular phase of the oestrus cycle, oestradiol concentrations are elevated, and the endometrium is more resistant to infection, whilst the high concentrations of progesterone experienced during the luteal phase can predispose to infection (Lewis, 2003, Lewis, 2004, Wira et al., 2005).

The trauma of parturition can invoke a stress response, thereby increasing plasma cortisol concentrations (Hudson et al., 1976). Primiparous cows experience stressful events such as regular pen movements, calving and milking for the first time and demonstrate increased plasma cortisol concentrations compared to multiparous cows (Galvão et al., 2010). Furthermore, primiparous cows also have higher incidence of metritis compared to multiparous cows, and this could be partially attributed to the greater cortisol plasma concentrations in primiparous cattle (Galvão et al., 2010). Glucocorticoids such as cortisol reduce inflammation through multiple pathways,

including inhibiting the intracellular signaling pathways associated with innate immunity, but they may also effect the tolerance of cells to bacterial toxins (Cain and Cidlowski, 2017).

Side-chain oxysterols, such as 25-hydroxycholesterol and 27-hydroxycholesterol, also suppressing innate immunity, reducing inflammation (Dang et al., 2017, Joseph et al., 2003, Cunningham, 2000). Side-chain oxysterols are formed in cells that synthesize steroid hormones or bile acids, or during cholesterol catabolism, and they have a physiological role in cholesterol homeostasis. Side-chain oxysterols act, via transcription factors such as the liver X receptors (LXR) LXR α (encoded by *NR1H3*) and LXR β (*NR1H2*), which are both expressed in the ovary and uterus (Janowski et al., 1996, Wang and Tontonoz, 2018, Mouzat et al., 2013), and by activating acetyl-coenzyme A acetyltransferase (ACAT) to catalyze cholesterol esterification (Du et al., 2004). Furthermore, the interferon stimulated production of 25-hydroxycholesterol activates ACAT, mobilizing plasma membrane cholesterol to provide immunity against several bacterial species such as *Listeria monocytogenes* and *Shigella flexneri* infection. Therefore, we wondered whether steroids or side-chain oxysterols, in addition to modulating immunity, might alter cell-intrinsic protection against the damage caused by pore-forming toxins in the endometrium.

In the present chapter, we tested the hypothesis that progesterone, oestradiol, glucocorticoids, or side-chain oxysterols, alter bovine endometrial cell protection against pore-forming toxins. To test this hypothesis, we treated bovine endometrial epithelial and stromal cells with steroids or oxysterols, then challenged the cells with pore-forming toxins to screen for protective compounds. We used pyolysin because *T. pyogenes* is a major pathogen of the endometrium and pyolysin causes endometrial cell damage (Bonnett et al., 1991, Amos et al., 2014). Cytoprotection was initially assessed by measuring the pyolysin induced leakage of the cytosolic protein LDH and by evaluating cell viability. Promising compounds were then explored further by measuring changes to cytoskeleton, potassium ion leakage and cytoprotection against *S. aureus* α -hemolysin. We also explored the role of LXRs in cytoprotection and examined the presence of oxysterols in the endometrium.

3.2 MATERIALS AND METHODS

3.2.1 Cytoprotection experiments

For experiments exploring cytoprotection, epithelial and stromal cells (isolated as described in *Chapter 2*) were seeded in 1 ml/well complete medium at a density of 5×10^4 /ml using 24-well tissue culture plates (unless otherwise specified), with stromal cells incubated for 24 h and epithelial cells for 48 h to establish 70% confluency. To select an appropriate concentration of pyolysin (generated and purified as described in *Chapter 2*) to challenge cells, stromal and epithelial cells were cultured for 24 h in 1 ml/well serum-free medium and then challenged for 2 h with control serum-free medium (comprising 200 μ l Dulbecco's phosphate-buffered saline (DPBS) for 15 min, then supplemented with 400 μ l serum-free medium up to 2 h) or medium containing a range of concentrations of pyolysin, as specified in *Results*. Serum-free medium was used because the 1.12 ± 0.05 mM cholesterol present in the FBS used in the present study (quantified from 2 independent aliquots of FBS and analysed by Anthony Horlock with the cholesterol oxidase-enzymatic endpoint method using the Randox Daytona Plus, Randox Laboratories Ltd., Crumlin, UK) might confound the results by binding to pyolysin. A 2 h challenge was used because we established previously that 2 h was sufficient to cause cytolysis (Griffin et al., 2018, Amos et al., 2014); and, we aimed to examine cytoprotection against pore-forming toxins, whereas a longer challenge might also reflect cell repair and replication. At the end of the challenge period, supernatants were collected to measure the leakage of LDH, and cell viability was measured using a 3-(4,5-dimethylthiazol-2-yl)-2,5-diphenyltetrazolium bromide (MTT) assay as described in *Chapter 2*.

To examine whether steroids, side-chain oxysterols or synthetic LXR agonists protected cells against damage by pyolysin, stromal and epithelial cells were treated in 1 ml/well serum-free medium with vehicle or the range of treatment concentrations specified in *Results* of progesterone, oestradiol, hydrocortisone, dexamethasone 25-hydroxycholesterol, 27-hydroxycholesterol, according to the manufacturers' instructions. Progesterone, oestradiol, and hydrocortisone concentrations were selected spanning and exceeding physiological plasma concentrations in cattle, which are ~30 nM, ~10 pM, and ~20 nM respectively (Sheldon et al., 2002, Galvão et al., 2010, Savio et al., 1993). Oxysterol concentrations were selected, in the absence of

data in cattle, based on concentrations in human plasma of 2 ± 3 ng/ml 25-hydroxycholesterol and 154 ± 43 ng/ml 27-hydroxycholesterol, with the latter selected for initial experiments because it is the most abundant (Dzeletovic et al., 1995). The synthetic LXR agonists T0901317 (N-(2,2,2-trifluoro-ethyl)-N-[4-(2,2,2-trifluoro-1-hydroxy-1-trifluoro-methyl-ethyl)-phenyl]-benzenesulfonamide) and GW3965 (3-(3-(2-chloro-3-trifluoromethylbenzyl-2,2-diphenylethylamino)propoxy)phenylacetic acid) were used as described previously (Schultz et al., 2000, Oliver et al., 2001). Treatments were applied for 24 h based on previous studies of cytoprotection (Statt et al., 2015, Griffin et al., 2018), except for experiments exploring the duration of 27-hydroxycholesterol required to protect cells against pyolysin, where cells were for a range of times up to 24 h, as specified in *Results*. After the treatment period, the supernatants were discarded, and then the cells were challenged for 2 h, except where specified in *Results*, with control serum-free medium or medium containing the selected concentrations of pyolysin that caused cell damage (stroma, 25 HU; epithelium, 200 HU), without further treatment.

To examine the role of LXR α and LXR β in oxysterol cytoprotection against pyolysin, we used short interfering ribonucleic acid (siRNA) to target *NR1H3* and *NR1H2*, respectively, as validated previously in bovine endometrial cells by a > 90% reduction in expression of *NR1H3* and *NR1H2* messenger RNA (mRNA) (Griffin et al., 2018). Cells were transfected with scrambled siRNA (ON-TARGETplus Non-targeting Control Pool; Horizon discovery) or siRNA designed using Dharmacon siDESIGN Centre to target *NR1H3* or *NR1H2* (described in *Chapter 2*). A mixture of 20 pmol siRNA, 1.5 μ l Lipofectamine RNAiMAX Reagent and 100 μ l Opti-MEM 1 medium was added to each well of a 24-well plate and incubated for 20 min at room temperature. Bovine endometrial stromal and epithelial cells were then seeded with 5×10^4 cells in 900 μ l RPMI-1640 medium with 10% FBS for 48 h. Cells were then treated with vehicle, 25 ng/ml 27-hydroxycholesterol or 25 nM T0901317 for 24 h in serum-free medium prior to a 2 h challenge with control medium or medium containing pyolysin (stroma, 25 HU; epithelium, 200 HU). At the end of the challenge period, supernatants were collected to measure the leakage of LDH, and cell viability was measured using an MTT assay.

To examine the role of ACAT in oxysterol cytoprotection we used the selective ACAT inhibitor Sandoz 58-035 (SZ58-035) (Ross et al., 1984) Bovine endometrial stromal

and epithelial cells were washed twice with phosphate-buffered saline (PBS) then treated with vehicle or 10 μ M SZ58-035 in serum-free medium for 16 h as previously described (Abrams et al., 2020). The cells were then washed twice with PBS then incubated for 24 h in serum-free culture medium containing 25 ng/ml 27-hydroxycholesterol or 25 nM T0901317 in combination with vehicle or 10 μ M SZ58-035. Cells were challenged for 2 h with control medium or medium containing pyolysin (stroma, 25 HU; epithelium, 200 HU). At the end of the challenge period, supernatants were collected to measure the leakage of LDH, and cell viability was measured using an MTT assay.

To determine if cytoprotection extended beyond cholesterol-dependent cytolysins, after a 24 h treatment in serum-free medium containing vehicle or 25 ng/ml 27-hydroxycholesterol, the cells were challenged for 24 h with 8 μ g/ 5×10^4 cells α -hemolysin (added in 200 μ l Dulbecco's phosphate-buffered saline (DPBS) for 15 min, then supplemented with 400 μ l serum-free medium up to 24 h) from *Staphylococcus aureus*. The concentration of α -hemolysin and duration of challenge was based on previous work (Mestre et al., 2010); and, on preliminary experiments in HeLa cervical and A549 cells (data shown in *Chapter 4*; Fig 4.12, 4.13) where shorter challenge periods did not cause sufficient cytolysis to explore cytoprotection. At the end of the challenge period, supernatants were collected to measure the leakage of LDH, and cell viability was measured using an MTT assay.

3.2.2 Potassium

The leakage of potassium from cells was measured to further evaluate cytoprotection against cytolysin-induced membrane pores, as described previously (Turner et al., 2020), and in *Chapter 2*. Cells were seeded at a density of 1.5×10^5 cells/well in 3 ml/well complete medium using 6-well culture plates. Stromal cells were incubated for 24 h and epithelial cells for 48 h, before treatment in 3 ml/well serum-free medium containing vehicle, 5 ng/ml 25-hydroxycholesterol, 25 ng/ml 27-hydroxycholesterol, 25 nM T0901317, 125 nM GW3965, or 0.5 mM M β CD as a positive control to deplete cellular cholesterol (Griffin et al., 2018, Amos et al., 2014). The supernatants were discarded, the cells were washed three times with potassium-free choline buffer (129 mM choline-Cl, 0.8 mM MgCl₂, 1.5 mM CaCl₂, 5 mM citric acid, 5.6 mM glucose, 10 mM NH₄Cl, 5 mM H₃PO₄, pH 7.4; all Merck), and then incubated in potassium-free

choline buffer with control medium or pyolysin for 5 min (epithelium, 200 HU; stroma, 25 HU), or α -hemolysin for 15 min (no potassium leakage was visible from stromal cells after 5 min of α -hemolysin challenge). Supernatants were then collected, and potassium was measured using a Jenway PFP7 flame photometer as described in *Chapter 2*.

3.2.3 Cholesterol

To quantify cellular cholesterol, epithelial and stromal cells (1.5×10^5 cells/well) were cultured for 24 h and 48 h respectively in 3 ml/well complete medium using 6-well culture plates. Cells were then treated for 24 h in 3 ml/well serum-free medium containing vehicle, 5 ng/ml 25-hydroxycholesterol, 25 ng/ml 27-hydroxycholesterol or 0.5 mM M β CD. At the end of the treatment period, cells were washed twice with DPBS and collected in 250 μ l cholesterol assay 1X Reaction Buffer and stored at -20°C. Cellular cholesterol was measured using the Amplex Red Cholesterol Assay Kit as described in *Chapter 2*. Protein abundance was measured in samples using a DC protein assay, and cholesterol concentrations were normalized to protein concentrations (Nicholson and Ferreira, 2009).

3.2.4 Immunofluorescence

To examine the cytoskeleton, cells were stained with the actin dye phalloidin, as described previously (Turner et al., 2020), and in *Chapter 2*. Briefly, 5×10^4 epithelial or stromal cells were cultured on glass cover slips in 24-well culture plates in complete medium for 24 h or 48 h, respectively, before treatment for 24 h in serum-free medium containing vehicle, 25 ng/ml 27-hydroxycholesterol or 25 nM T0901317. The supernatants were discarded, and the cells challenged with control medium or medium containing pyolysin for 2 h, or α -hemolysin for 24 h. At the end of the challenge period cells were stained with Alexa Fluor 555-conjugated phalloidin and 4,6-diamidino-2-phenylindole (DAPI) then imaged as described in *Chapter 2*. The proportion of cells that had cytoskeletal changes (cytoskeletal contraction, disrupted shape, or loss of actin fibre definition) were counted using > 45 stromal or > 150 epithelial cells per treatment, across 3 independent images per replicate.

Filipin III from *Streptomyces filipinensis* was used to stain cholesterol, using stromal cells because of their higher cholesterol content than epithelial cells (Amos et al., 2014). Briefly, 5×10^4 epithelial or stromal cells/well were seeded in complete

medium on glass cover slips in 24-well culture plates for 24 h or 48 h, respectively before treatment for 24 h in serum-free medium with vehicle, 25 ng/ml 27-hydroxycholesterol, 5 ng/ml 25-hydroxycholesterol, or 0.5 mM M β CD. Staining and imaging was carried out as described in *Chapter 2*. Three independent images were captured per treatment replicate, and total cell fluorescence was calculated from 3 cells per image using Fiji (Schindelin et al., 2012).

3.2.5 Western Blotting

Binding of pyolysin to plasma membranes was quantified as described previously with minor modifications (Billington et al., 1997, Amos et al., 2014). Stromal cells were seeded at a density of 1.5×10^5 cells/well in 3 ml/well complete medium using 6-well culture plates for 24 h, and then treated for 24 h in 3 ml/well serum-free medium containing vehicle, 50 nM progesterone, 0.1 nM oestradiol, 10 μ M hydrocortisone, 25 ng/ml 27-hydroxycholesterol or 0.5 mM M β CD, before a 2 h challenge with control serum-free medium or 25 HU pyolysin. The medium was then discarded, and the cells were washed with 300 μ l ice-cold PBS and lysed with 100 μ l PhosphoSafe Extraction Reagent. Protein was extracted and quantified using a DC assay, and 10 μ g/lane protein separated using 10% (vol/vol) SDS-polyacrylamide gel electrophoresis as described in *Chapter 2*. The average peak density of bands was quantified and normalized to α -tubulin using Fiji (Schindelin et al., 2012).

To validate the effectiveness of siRNA targeting *NR1H2* and *NR1H3*, cell lysates were stored in PhosphoSafe Extraction Reagent for Western blot quantification of LXR α , and LXR β , and adenosine triphosphate binding cassette subfamily A member 1 (ABCA1), which is an LXR-induced protein (Ito et al., 2015). Protein was separated using 10% (LXR α and LXR β) and 7.5% (ABCA1) SDS-polyacrylamide gel electrophoresis as described in *Chapter 2*. Average peak band density was quantified and normalized to α -tubulin or β -actin using Fiji as described in *Results* (Schindelin et al., 2012).

3.2.6 Oxysterols

To quantify oxysterols in the ovary and uterus of freshly slaughtered cattle using liquid chromatography-mass spectrometry as described in *Chapter 2*, fluid was collected from dominant (> 8 mm external diameter) and emerged (4 to 8 mm external diameter) ovarian follicles and uterine fluid aspirated from the surface of the endometrium. In

addition, we explored whether oxysterols were secreted into endometrial epithelial or stromal cell supernatants in response to lipopolysaccharide (LPS) or pyolysin as described in *Chapter 2*. The LPS acted as a positive control, as LPS stimulates the release of 25-hydroxycholesterol from murine macrophages (Reboldi et al., 2014).

3.2.7 Statistical analysis

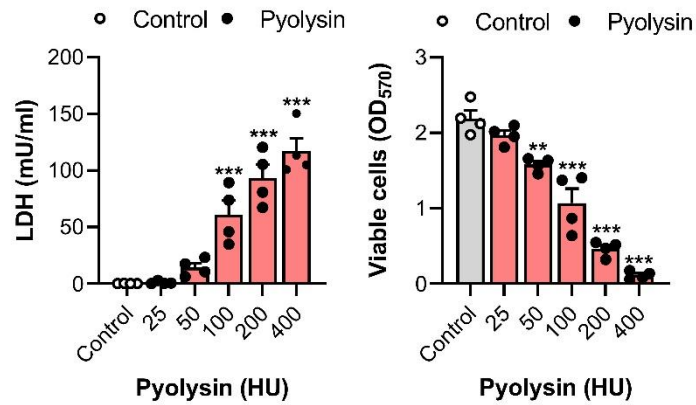
The statistical unit was the animal used to isolate cells or to collect fluid samples from. Statistical analysis was performed using GraphPad Prism 9.0.1. Data are reported as arithmetic mean (SEM), and significance attributed when $P < 0.05$. Comparisons between treatments or challenges were made using analysis of variance (ANOVA) followed by Dunnett, Bonferroni or Tukey post hoc test for multiple comparison, or unpaired two-tailed Student's t-test as specified in *Results*. Correlation was evaluated using Pearson's correlation coefficient.

3.3 RESULTS

3.3.1 27-hydroxycholesterol protected endometrial cells against pyolysin

To first determine concentrations of pyolysin to test cytoprotection we challenged endometrial epithelial and stromal cells for 2 h with a range of concentrations of pyolysin. Pyolysin-induced pore formation was determined by the leakage of LDH into cell supernatants, and cytolysis was evaluated by measuring cell viability. In both epithelial and stromal cells, pyolysin caused a concentration-dependent leakage of LDH and a reduction in cell viability (Fig 3.1). For subsequent cytoprotection experiments, we selected $200 \text{ HU}/5 \times 10^4$ cells pyolysin to challenge epithelial cells and $25 \text{ HU}/5 \times 10^4$ cells pyolysin to challenge stromal cells as these concentrations increase LDH leakage ($P < 0.001$, ANOVA and Dunnett's post hoc test, $n=4$) and caused cytolysis, significantly reducing cell viability ($P < 0.001$, ANOVA and Dunnett's post hoc test, $n=4$).

A Epithelium



B Stroma

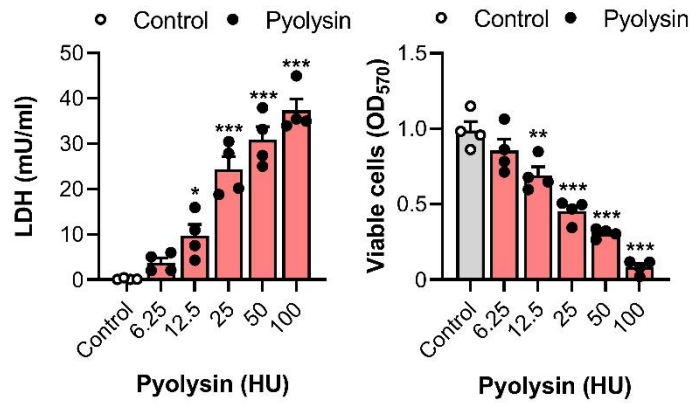


Figure 3.1 Pyolysin damages bovine endometrial cells

Leakage of LDH into supernatants, and cell viability determined by MTT assay for bovine endometrial (A) epithelial and (B) stromal cells challenged for 2 h with control medium or the indicated concentrations of pyolysin. Data are presented as mean (SEM) using values from 4 independent animals; statistical significance was determined using one-way ANOVA and Dunnett's post hoc test; *P < 0.05, **P < 0.01, ***P < 0.001.

To screen for cytoprotective treatments, epithelial and stromal cells were treated for 24 h with a range of concentrations of progesterone, oestradiol, hydrocortisone, dexamethasone, or 27-hydroxycholesterol, and then challenged for 2 h with control medium or pyolysin. As before, pyolysin increased the leakage of LDH into cell supernatants ($P < 0.001$, Fig 3.2, 3.3) and caused cytolysis as determined by reduced cell viability ($P < 0.001$, Fig 3.2, 3.3). Compared with vehicle, treatment with progesterone, oestradiol or hydrocortisone had little effect on the pyolysin-induced leakage of LDH or cytolysis (Fig 3.2, 3.3). There was a trend for reduced cytolysis in epithelial cells treated with the synthetic glucocorticoid dexamethasone, though there was no reduction in LDH leakage, and it did not protect stromal cells (Fig 3.4). However, 27-hydroxycholesterol reduced pyolysin-induced leakage of LDH and protected against cytolysis in both cell types (Fig 3.5). Specifically, 25 ng/ml 27-hydroxycholesterol reduced pyolysin-induced leakage of LDH from epithelial and stromal cells by 56% and 82% ($P < 0.001$, two-way ANOVA and Dunnett's post hoc test) respectively; and reduced pyolysin-induced cytolysis in epithelial and stromal cells from $> 60\%$ to $< 5\%$ and $< 15\%$ ($P < 0.05$) respectively. The use of a control challenge demonstrated that 27-hydroxycholesterol did not affect the leakage of LDH ($P > 0.99$) or cell viability ($P > 0.63$) of endometrial cells.

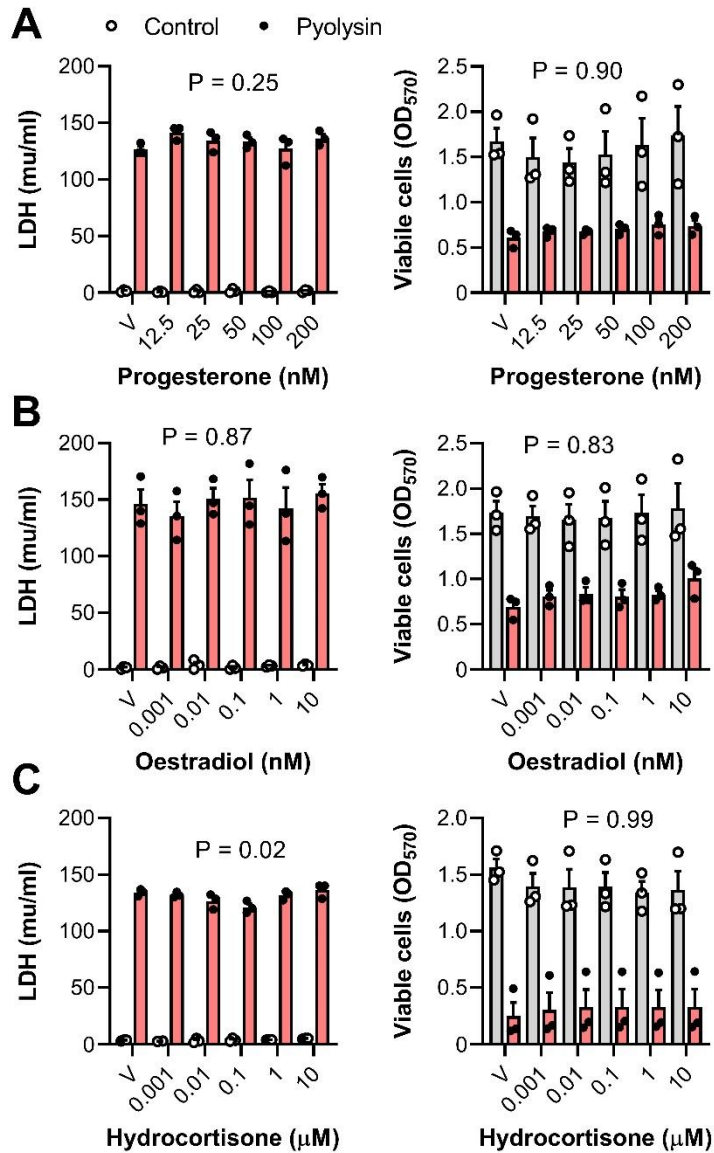


Figure 3.2 Steroids do not protect endometrial epithelial cells against pyolysin

Leakage of LDH and viability of bovine endometrial epithelial cells treated for 24 h in serum-free medium containing vehicle (V) or the indicated concentrations of progesterone, oestradiol, or hydrocortisone and then challenged for 2 h with control medium or 200 HU pyolysin. Data are presented as mean (SEM) using cells from 3 independent animals; statistical significance determined by two-way ANOVA and P-values reported for the effect of each treatment on pyolysin challenge.

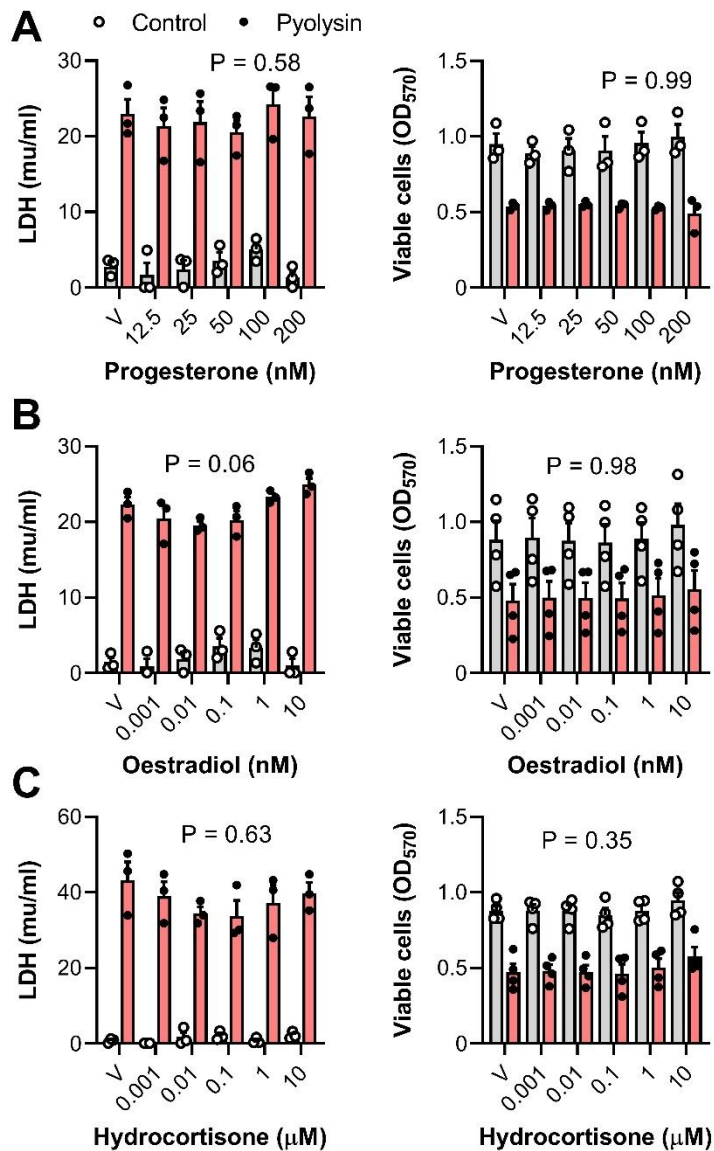


Figure 3.3 Steroids do not protect endometrial stromal cells against pyolysin

Leakage of LDH and viability of bovine endometrial stromal cells treated for 24 h in serum-free medium containing vehicle (V) or the indicated concentrations of (A) progesterone, (B) oestradiol, or (C) hydrocortisone and then challenged for 2 h with control medium or 25 HU pyolysin. Data are presented as mean (SEM) using cells from ≥ 3 independent animals; statistical significance determined by two-way ANOVA and P-values reported for the effect of each treatment on pyolysin challenge.

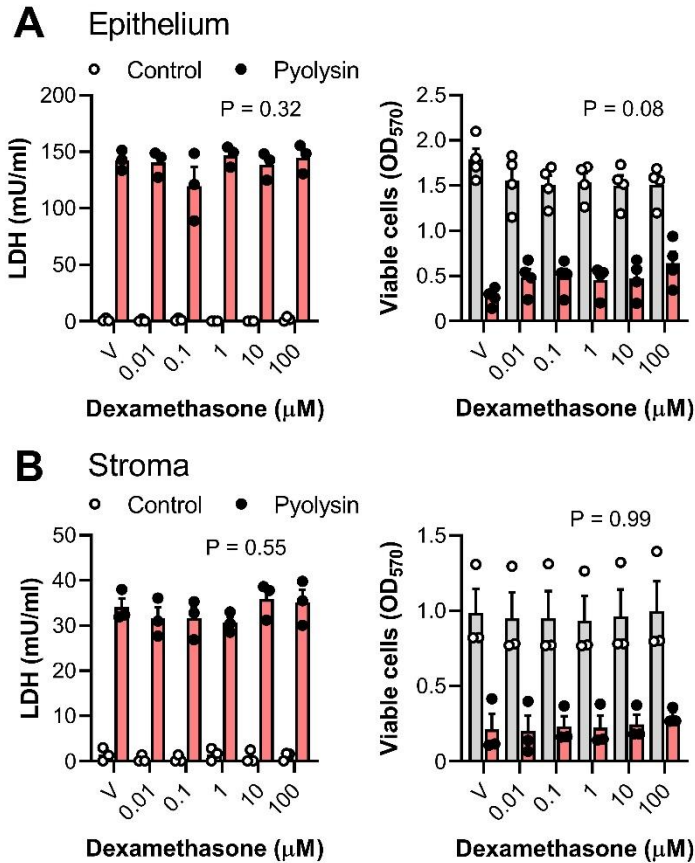


Figure 3.4 Dexamethasone does not protect endometrial cells against pyolysin

Leakage of LDH and viability of (A) epithelial or (B) stromal cells treated for 24 h in serum-free medium containing vehicle (V) or the indicated concentrations of dexamethasone and then challenged for 2 h with control medium or pyolysin (epithelium 200 HU, stroma 25 HU). Data are presented as mean (SEM) using cells from ≥ 3 independent animals; statistical significance determined by two-way ANOVA and P-values reported for the effect of treatment on pyolysin challenge.

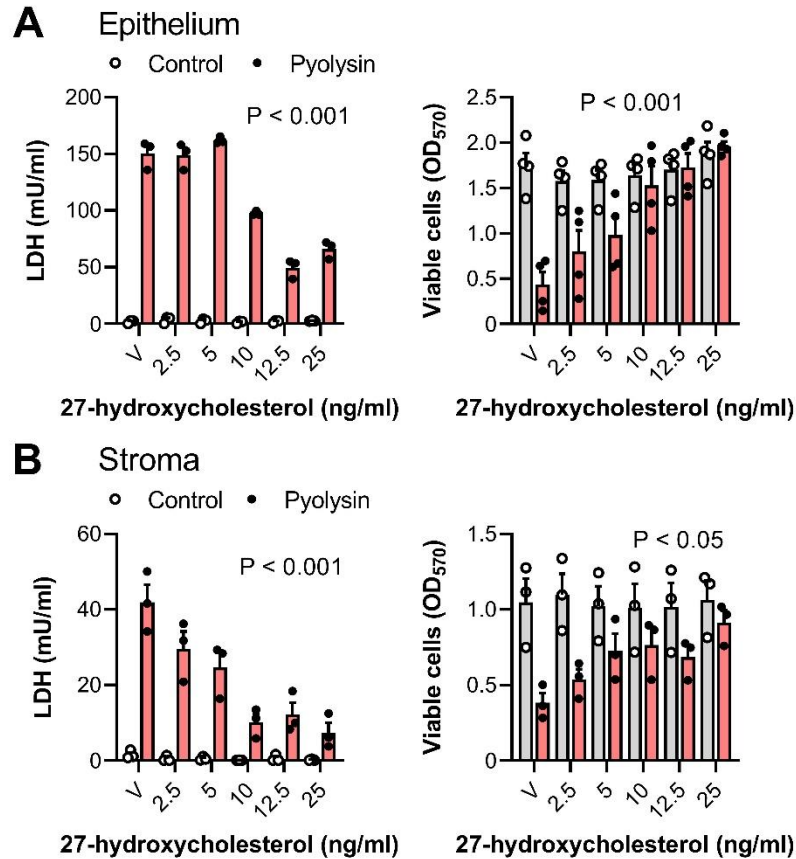


Figure 3.5 27-hydroxycholesterol protects endometrial cells against pyolysin

Leakage of LDH and viability of (A) epithelial or (B) stromal cells treated for 24 h in serum-free medium containing vehicle (V) or the indicated concentrations of 27-hydroxycholesterol and then challenged for 2 h with control medium or pyolysin (epithelium 200 HU, stroma 25 HU). Data are presented as mean (SEM) using cells from ≥ 3 independent animals; statistical significance determined by two-way ANOVA and P-values reported for the effect of treatment on pyolysin challenge.

Treatment with 25 ng/ml 27-hydroxycholesterol consistently reduced pyolysin-induced cytolysis of epithelial cells from a further 6 animals (Fig 3.6A), and stromal cells from a further 9 animals (Fig 3.6B), in experiments carried out to assess whether biological variation between animals might influence our observations. Furthermore, the level of cytoprotection was correlated with the duration of 27-hydroxycholesterol treatment (from 0 to 24 h) in epithelial (Pearson's correlation coefficient, $r^2 = 0.94$, $P < 0.001$; Fig 3.7A) and stromal (Pearson's correlation coefficient, $r^2 = 0.94$, $P < 0.001$; Fig 3.7B) cells, with protection evident after > 8 h treatment ($P < 0.001$, ANOVA and Dunnett's post hoc test).

To examine whether 27-hydroxycholesterol also protected cells against changes in the actin cytoskeleton and cell shape, cells were stained with phalloidin (Turner et al., 2020). Challenging epithelial and stromal cells for 2 h with pyolysin reduced the definition of actin fibers, altered cell shape, and in some cells the cytoskeleton collapsed (Fig 3.8). However, 24 h treatment with 27-hydroxycholesterol protected against pyolysin-induced cytoskeletal changes in epithelial cells (22 ± 2 vs $99 \pm 1\%$ cells damaged, t-test, $P < 0.01$, $n = 3$, Fig 3.8A) and stromal cells (30 ± 9 vs $77 \pm 8\%$ cells damaged, t-test, $P < 0.01$, $n = 4$, Fig 3.8B).

Together these results provided evidence that 27-hydroxycholesterol, protected bovine endometrial epithelial and stromal cells against pyolysin. As the concentrations of progesterone, oestradiol and glucocorticoids screened in our model system did not significantly protect endometrial cells against pyolysin, further experiments in the present chapter focused on side-chain oxysterols.

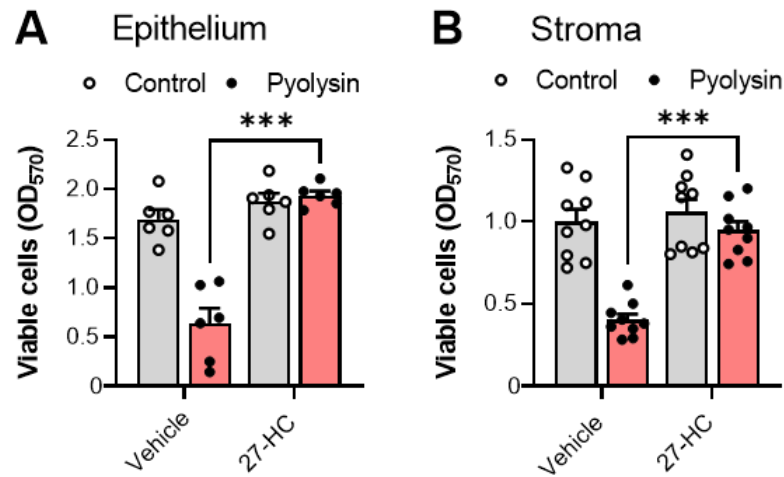


Figure 3.6 27-hydroxycholesterol consistently protects bovine endometrial cells against pyolysin

Viability of (A) epithelial or (B) stromal cells treated for 24 h in serum-free medium containing vehicle or 25 ng/ml 27-hydroxycholesterol (27-HC) then challenged for 2 h with control medium or pyolysin (epithelium 200 HU, stroma 25 HU). Data are presented as mean (SEM) using cells from 6 independent animals for epithelial cells and 9 animals for stromal cells; statistical significance determined by two-way ANOVA and Bonferroni's post hoc test; *** $P < 0.001$.

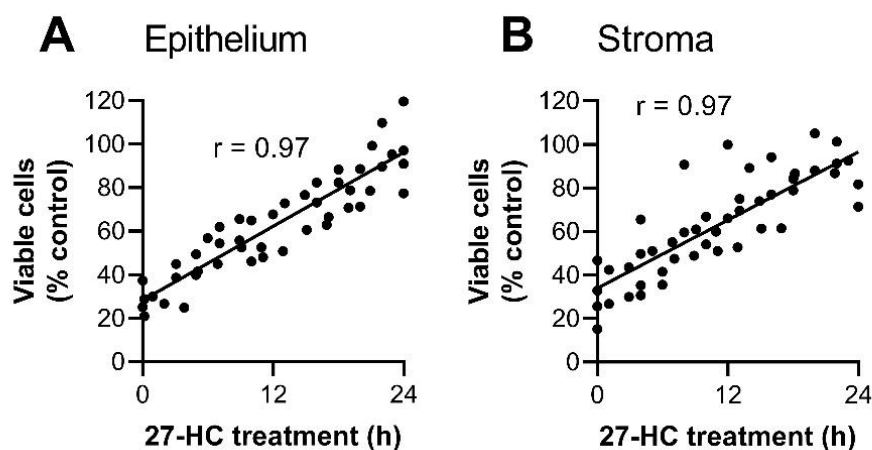


Figure 3.7 27-hydroxycholesterol protection increases with treatment duration

Viable cells expressed as a percentage of control challenge for (A) epithelial and (B) stromal cells treated for the indicated time periods with 25 ng/ml 27-hydroxycholesterol (27-HC), and then challenged for 2 h with control medium or pyolysin (epithelium 200 HU, stroma 25 HU). Dots represent individual values from 4 independent animals, and Pearson correlation coefficients are reported (r). Line of best fit is displayed.

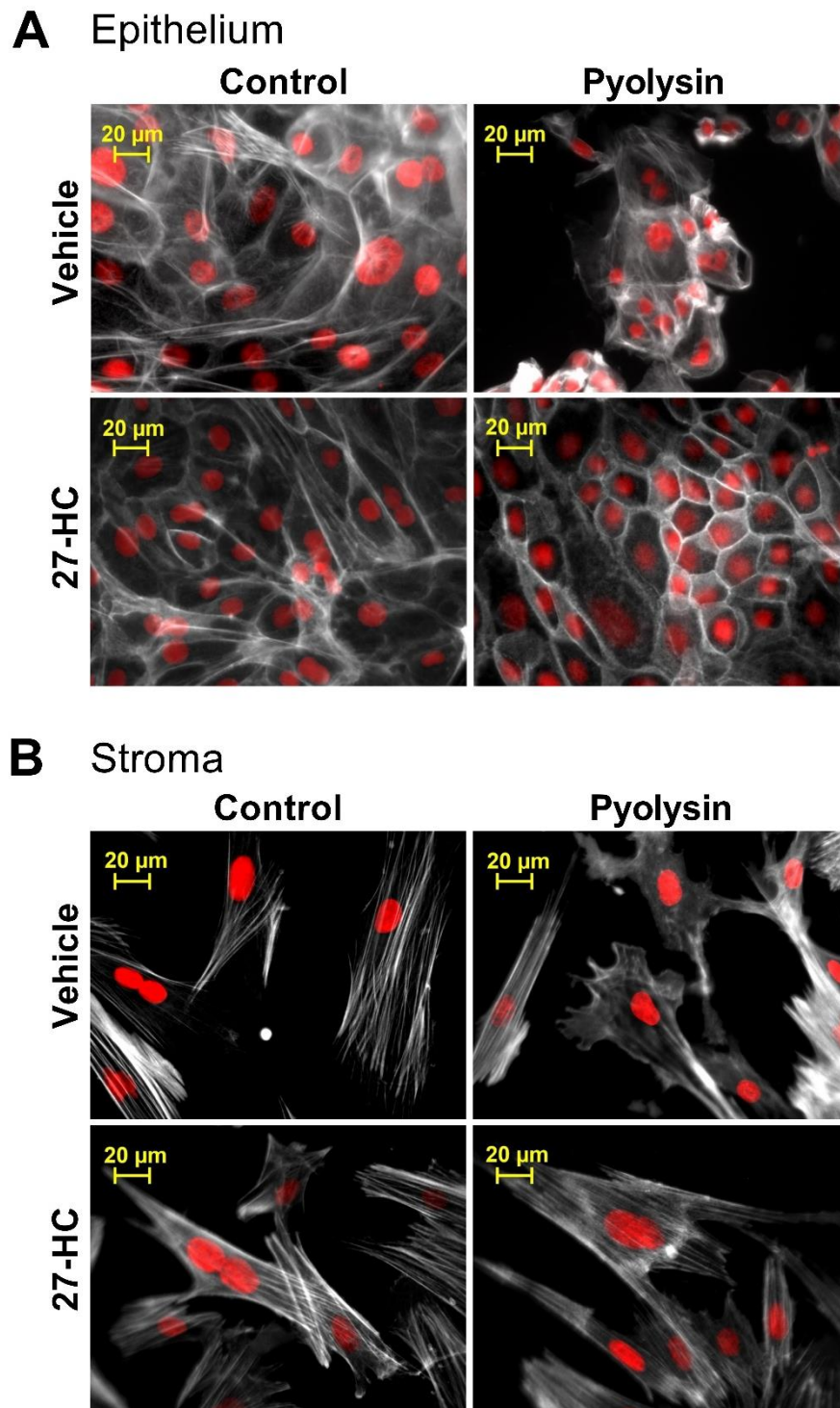


Figure 3.8 27-hydroxycholesterol protects bovine endometrial cells against pyolysin-induced actin cytoskeletal changes

Fluorescent microscope images of (A) epithelial and (B) stromal cells treated for 24 h with vehicle or 25 ng/ml 27-hydroxycholesterol (27-HC), then challenged for 2 h with control medium or pyolysin (epithelium 200 HU, stroma 25 HU), and stained with fluorescent phalloidin (white) and DAPI (red); images are representative of 4 independent experiments. Quantification of cytoskeletal changes are reported in text.

3.3.2 Side-chain oxysterols protect cells against pyolysin

To explore whether cytoprotection against pyolysin was limited to 27-hydroxycholesterol, we treated endometrial cells for 24 h with another oxysterol, 25-hydroxycholesterol, prior to the 2 h challenge with pyolysin (Fig 3.9). Treatment with 50 ng/ml 25-hydroxycholesterol reduced stromal cell viability by 37% ($P < 0.001$, Fig 3.10B, grey bars), though lower concentrations did not significantly alter cell viability ($P = 0.91$). Significantly, 25-hydroxycholesterol reduced the pyolysin-induced leakage of LDH from both epithelial and stromal cells and protected against cytolysis. Specifically, 5 ng/ml 25-hydroxycholesterol reduced pyolysin-induced leakage of LDH from epithelial and stromal cells by 84% and 79% ($P < 0.001$, two-way ANOVA and Dunnett's post hoc test), respectively, and reduced pyolysin-induced cytolysis from $> 60\%$ to $> 5\%$ and 25% respectively ($P < 0.01$).

To test whether oxysterol cytoprotection against pyolysin persisted beyond the 2 h challenge period, we treated endometrial cells with vehicle, 5 ng/ml 25-hydroxycholesterol, or 25 ng/ml 27-hydroxycholesterol for 24 h, but then challenged the cells for 24 h with pyolysin without further treatments. Both 25-hydroxycholesterol and 27-hydroxycholesterol prevented the pyolysin-induced leakage of LDH and cytolysis in both epithelial and stromal cells (Fig 3.10).

To evaluate whether oxysterols protected against the initial formation of pyolysin pores, we measured the leakage of potassium into cell supernatants 5 min after a pyolysin challenge (Gonzalez et al., 2011, Turner et al., 2020). Epithelial and stromal cells were treated for 24 h with vehicle, 5 ng/ml 25-hydroxycholesterol or 25 ng/ml 27-hydroxycholesterol. We used 0.5 mM M β CD used as a control because it depletes cholesterol from plasma membranes (Das et al., 2013, Amos et al., 2014). Vehicle treated epithelial and stromal cells leaked potassium within 5 min of pyolysin challenge, and M β CD reduced pyolysin-induced leakage of potassium from stromal but not epithelial cells (Fig 3.11). However, treatment with 25-hydroxycholesterol or 27-hydroxycholesterol prevented pyolysin-induced leakage of potassium in both epithelial ($P < 0.05$, Fig 3.11A) and stromal ($P < 0.001$, Fig 3.11B) cells. Collectively, the data in Fig 3.2 to 3.11 provide evidence that 25-hydroxycholesterol and 27-hydroxycholesterol protect endometrial cells against pyolysin.

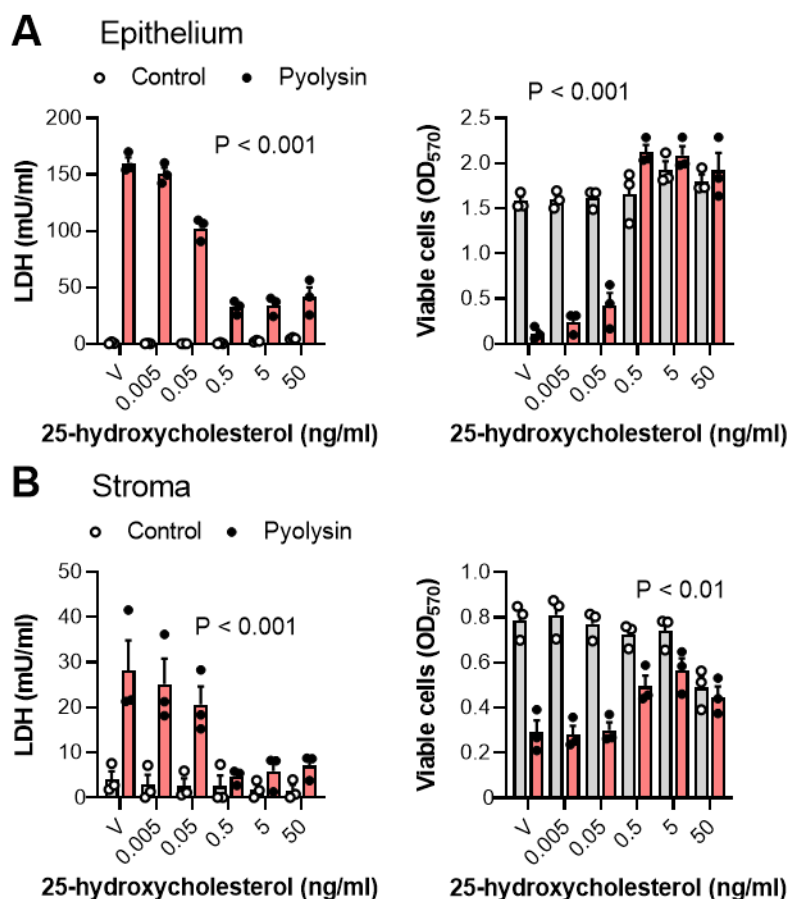


Figure 3.9 25-hydroxycholesterol protects endometrial cells against pyolysin

Leakage of LDH and viability of (A) epithelial and (B) stromal cells treated for 24 h in serum-free medium containing vehicle (V) or the indicated concentrations of 25-hydroxycholesterol and then challenged for 2 h with control medium or pyolysin (epithelium 200 HU, stroma 25 HU). Data are presented as mean (SEM) using cells from ≥ 3 independent animals; statistical significance determined by two-way ANOVA and P-values reported for the effect of treatment on pyolysin challenge.

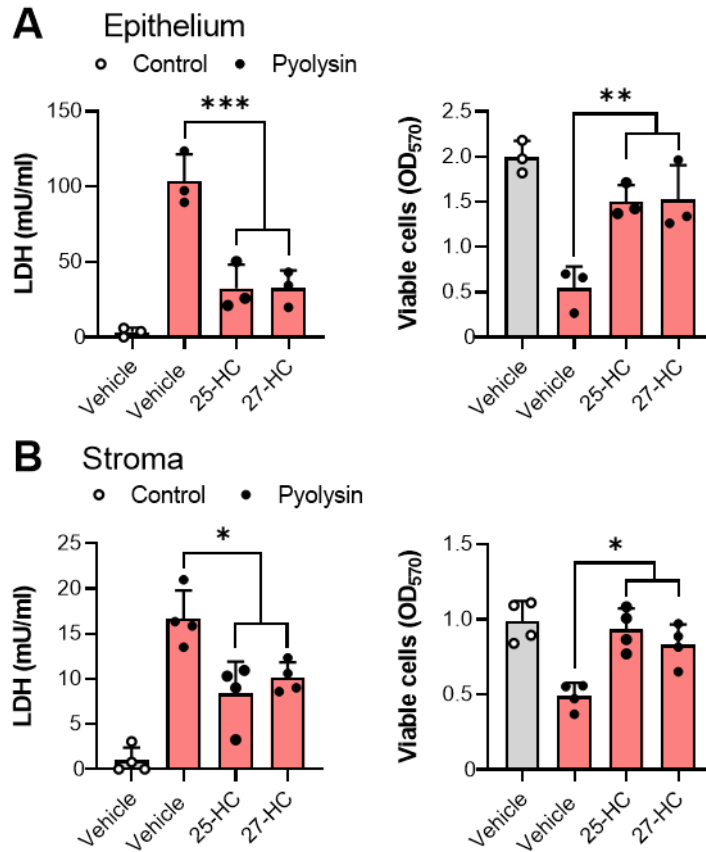


Figure 3.10 Side-chain oxysterol protection persists for 24 h

Leakage of LDH and viability of (A) epithelial and (B) stromal cells treated for 24 h in serum-free medium containing vehicle, 5 ng/ml 25-hydroxycholesterol (25-HC), or 25 ng/ml 27-hydroxycholesterol (27-HC) and then challenged for 2 h with control medium or pyolysin (epithelium 200 HU, stroma 25 HU). Data are presented as mean (SEM) using cells from ≥ 3 independent animals; statistical significance determined by one-way ANOVA and Dunnett's post hoc test; * $P < 0.05$, ** $P < 0.01$, *** $P < 0.001$.

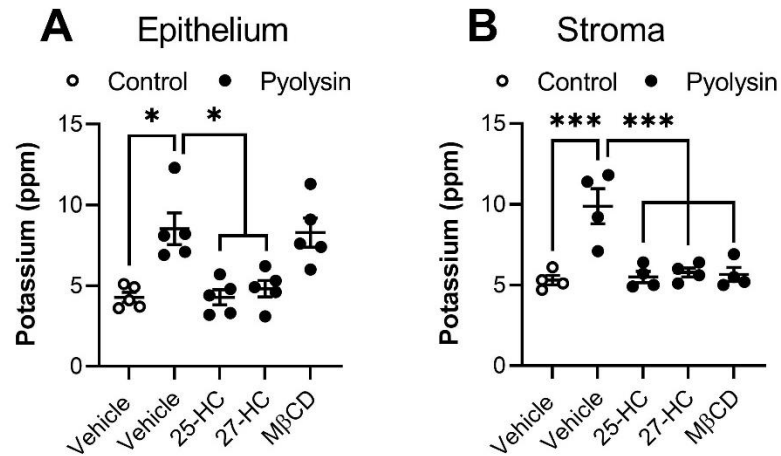


Figure 3.11 Oxysterols prevent pyolysin-induced potassium leakage

Leakage of potassium from (A) epithelial and (B) stromal cells treated for 24 h with vehicle, 5 ng/ml 25-hydroxycholesterol (25-HC), 25 ng/ml 27-hydroxycholesterol (27-HC), or 1 mM MβCD, and then challenged for 5 min with control medium or pyolysin (epithelium 200 HU, stroma 25 HU). Dots represent the values from ≥ 4 independent animals; statistical significance was determined using one-way ANOVA with Dunnett's post hoc test; * $P < 0.05$, *** $P < 0.001$.

3.3.3 Cellular cholesterol

We next considered potential mechanisms for side-chain oxysterol cytoprotection. Cholesterol-dependent cytolyticins bind cholesterol in plasma membranes and reducing cellular cholesterol using M β CD or statins can protect against cytotoxicity (Statt et al., 2015, Amos et al., 2014). We found that treatment with 0.5 mM M β CD for 24 h reduced bovine endometrial epithelial cell cholesterol by 26% compared with vehicle (Fig 3.12A), and stromal cell cholesterol by 43% (Fig 3.12B). However, 25-hydroxycholesterol and 27-hydroxycholesterol did not significantly alter the abundance of cholesterol in epithelial ($P = 0.81$ and $p = 0.37$, respectively, Fig 3.12A), or stromal cells ($P = 0.93$ and $P = 0.89$, respectively, Fig 3.12B).

To further examine cellular cholesterol, we stained stromal cells with filipin III, which binds to unesterified cholesterol (Maxfield and Wustner, 2012). Methyl- β -cyclodextrin reduced filipin III binding, with a 44% reduction in fluorescence compared with the vehicle control (Fig 3.12C, D). However, there was no significant effect of 25-hydroxycholesterol ($P = 0.39$) or 27-hydroxycholesterol ($P = 0.98$) on filipin III binding, although there appeared to be increased staining surrounding the nucleus.

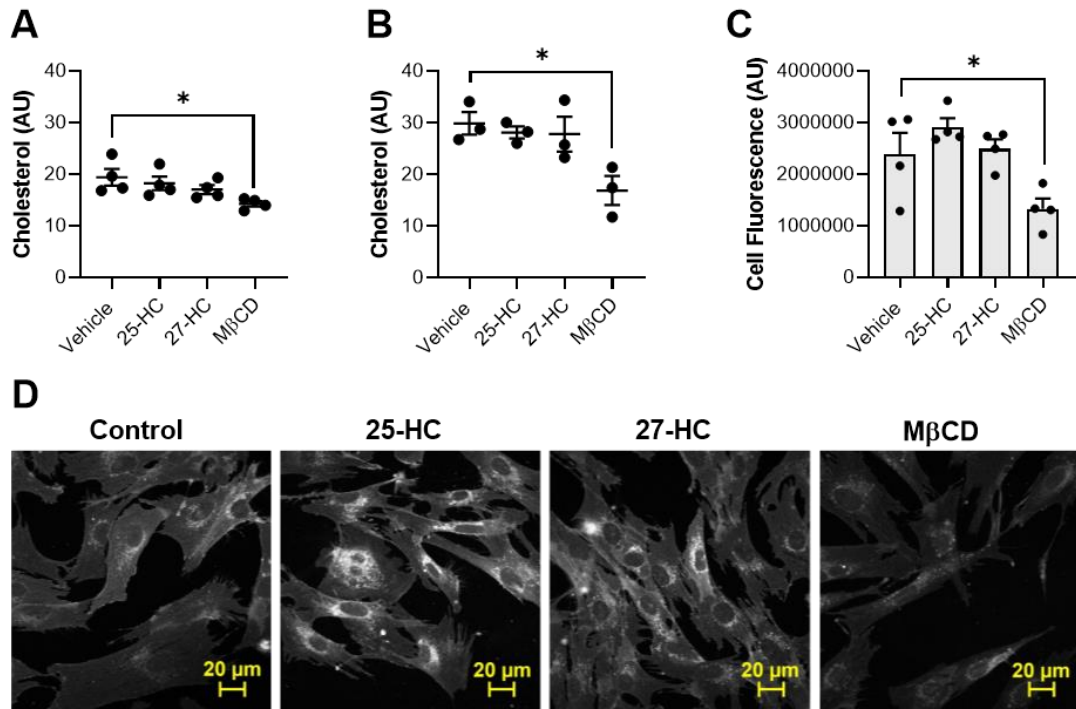


Figure 3.12 Oxysterols do not reduce bovine endometrial cell cholesterol

Cellular cholesterol in (A) epithelial and (B) stromal cells treated for 24 h with vehicle, 5 ng/ml 25-hydroxycholesterol (25-HC), 25 ng/ml 27-hydroxycholesterol (27-HC), or 0.5 mM MβCD. Data are presented as mean (SEM) from ≥ 3 independent animals; statistical significance was determined using one-way ANOVA with Dunnett's post hoc test; treatment effects cholesterol, * $P < 0.05$. Additionally, total cell fluorescence was quantified (C) from confocal microscope images (D) of cells stained using filipin III to visualize cholesterol (white, scale bars are 20 μm). Data are presented as mean (SEM) using cells from 4 independent animals; statistical significance was determined using one-way ANOVA and Dunnett's post hoc test; * $P < 0.05$.

Serum-free medium was used for experiments exploring cytoprotection. However, cells can take up cholesterol from the lipoproteins in serum (Brown and Goldstein, 1986). To investigate whether this might alter side-chain oxysterol cytoprotection, we treated epithelial and stromal cells for 24 h with 27-hydroxycholesterol or 25-hydroxycholesterol in culture medium containing 10% fetal calf serum, prior to the 2 h pyolysin challenge. As serum contains LDH, it was not possible to evaluate the leakage of LDH. Treatment with 27-hydroxycholesterol or 25-hydroxycholesterol in the presence of serum protected both epithelial cells (Fig 3.13A) and stromal cells (Fig 3.13B) against pyolysin-induced cytolysis.

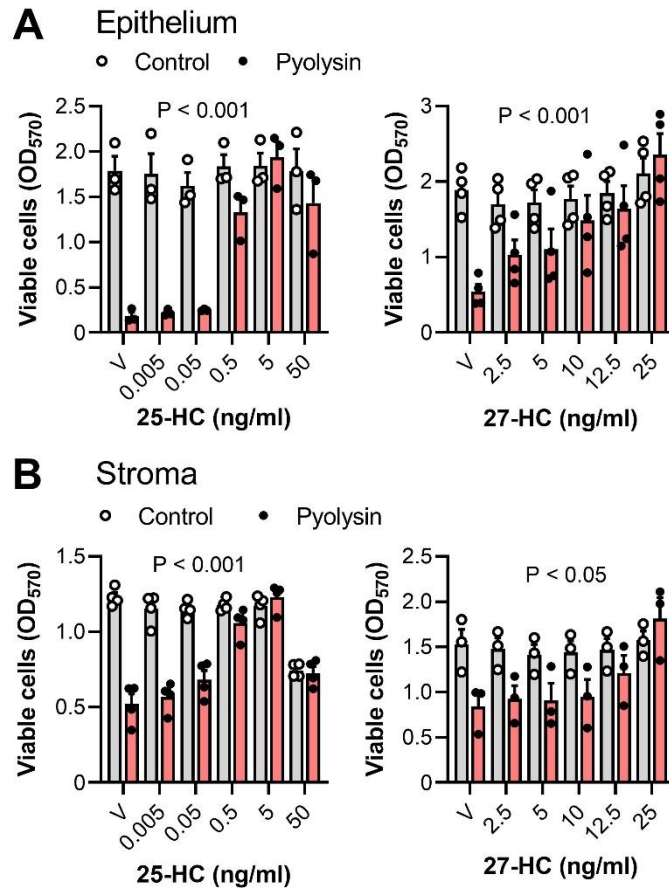


Figure 3.13 Oxysterols protect bovine endometrial cells against pyolysin in the presence of serum

Viability of (A) epithelial and (B) stromal cells treated for 24 h with vehicle, or the indicated concentrations of 25-hydroxycholesterol (25-HC) or 27-hydroxycholesterol (27-HC) in complete medium containing 10% serum, and then challenged for 2 h with control serum-free medium or pyolysin (epithelium 200 HU, stroma 25 HU). Data are presented as mean (SEM) from ≥ 3 independent animals; statistical significance was determined using two-way ANOVA and P-values reported for the effect of treatment on pyolysin challenge.

As cholesterol-dependent cytolysins bind accessible cholesterol in plasma membranes (Das et al., 2013), we also examined the binding of pyolysin to cells. Stromal cells were used because they contain more cholesterol than epithelial cells. Treatment with M β CD reduced pyolysin binding by 85%, compared with vehicle, and treatment with 27-hydroxycholesterol reduced pyolysin binding by 65% (Fig 3.14).

Accessible cholesterol in plasma membranes can be depleted with little effect on total cellular cholesterol, by activating ACAT esterification of cholesterol by side-chain oxysterols but not LXR agonists (Du et al., 2004, Abrams et al., 2020). To examine whether ACAT contributed to cytoprotection against pyolysin damage, we treated endometrial cells with the ACAT inhibitor SZ58-035 for 16 h, followed by treatment with vehicle, 27-hydroxycholesterol, or the LXR agonist T0901317 for a further 24 h in the continued presence of SZ58-035 for a further 24 h. Treatment with SZ58-035 impaired 27-hydroxycholesterol, but not T0901317 cytoprotection against pyolysin challenge in epithelial (Fig 3.15A) and stromal (Fig 3.15B) cells. Collectively, these data provide evidence to suggest the side-chain oxysterol cytoprotection is partly dependent on reducing accessible membrane cholesterol.

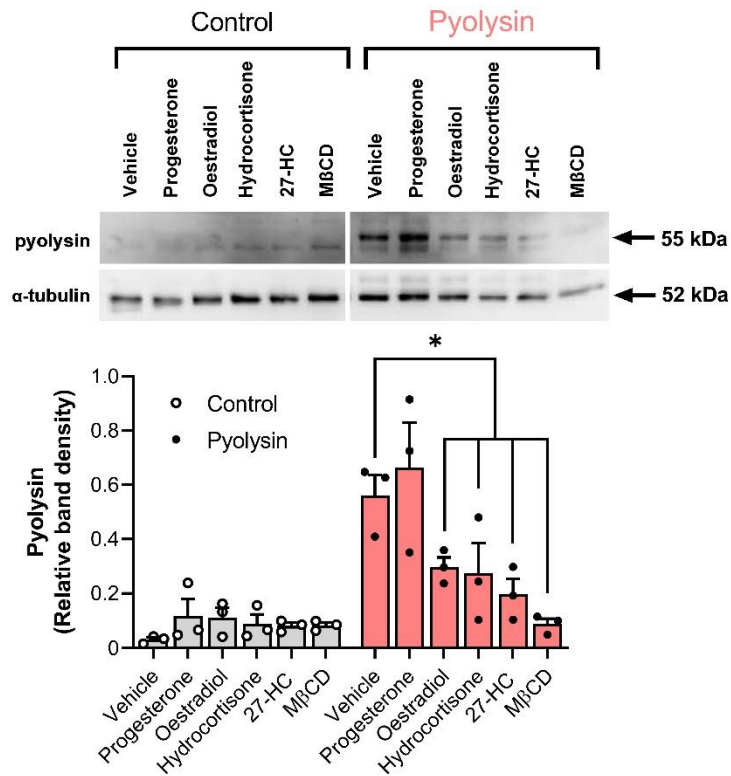


Figure 3.14 27-hydroxycholesterol reduces pyolysin binding

Representative Western blot of pyolysin binding and α -tubulin for stromal cells treated for 24 h with vehicle, 50 nM progesterone, 0.1 nM oestradiol, 10 μ M hydrocortisone, 25 ng/ml 27-hydroxycholesterol (27-HC), or 0.5 mM M β CD and then challenged for 2 h with control medium or 25 HU pyolysin. Densitometry data were normalized to α -tubulin and presented as mean (SEM) from 3 experiments; statistical significance was determined using ANOVA with Dunnett’s post hoc test; *P < 0.05.

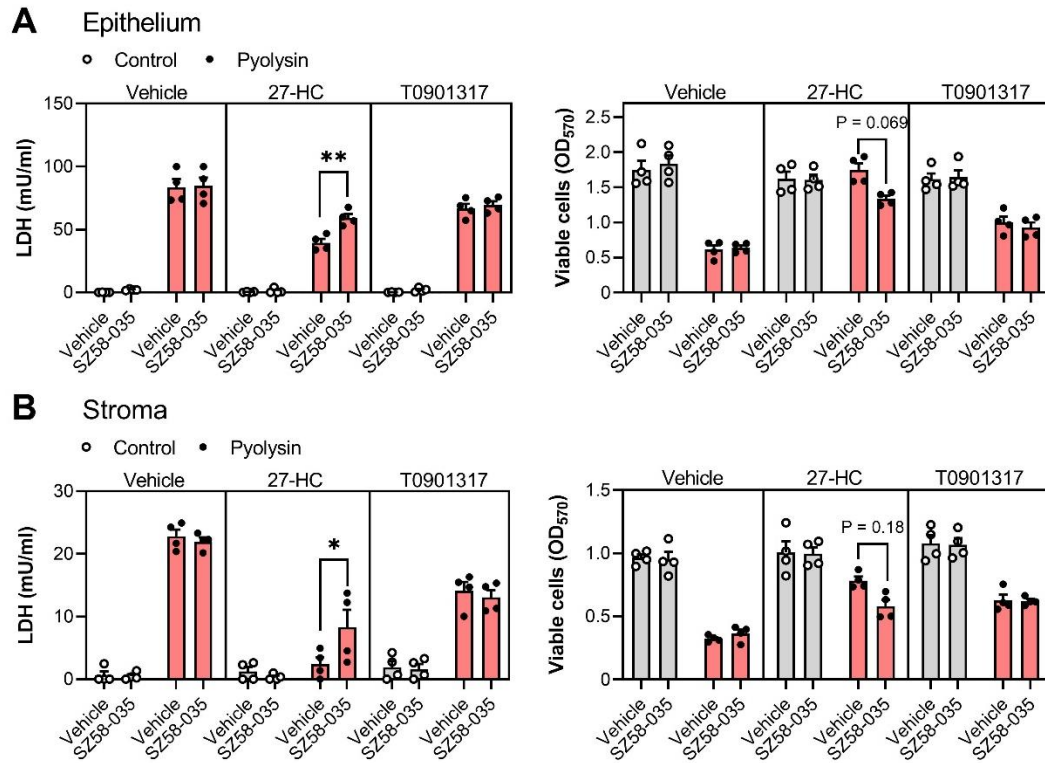


Figure 3.15 27-hydroxycholesterol cytoprotection is partly ACAT dependent

Leakage of LDH and viability of (A) epithelial and (B) stromal cells cultured for 16 h with vehicle or 10 μ M SZ5-035, then treated for 24 h with vehicle, 25 ng/ml 27-hydroxycholesterol (27-HC), or 25 nM T0901317, in the continuing presence of vehicle or SZ5-035, and then challenged for 2 h with control medium or pyolysin (epithelium 200 HU, stroma 25 HU). Data are presented as mean (SEM) from 4 independent experiments; statistical significance was determined using two-way ANOVA and Tukey's post hoc test; * $P < 0.05$, ** $P < 0.01$.

3.3.4 Liver X receptors have a role in oxysterol cytoprotection

We next examined the role of LXRs in cytoprotection against pyolysin because oxysterols are ligands for LXR α and LXR β (Wang and Tontonoz, 2018). Our first approach was to use T0901317 and GW3965, which are synthetic ligands for both LXR α and LXR β , but structurally unrelated to oxysterols (Schultz et al., 2000, Oliver et al., 2001, Wang and Tontonoz, 2018). Endometrial cells were treated for 24 h with a range of concentrations of T0901317 or GW3965, followed by a 2 h challenge with pyolysin. Treatment with T0901317 or GW3965 reduced the pyolysin-induced LDH leakage from epithelial cells by up to 25% ($P < 0.01$, Fig 3.16A) and 33% ($P < 0.05$, Fig 3.17B) respectively, but did not significantly prevent cytolysis. In stromal cells, both T0901317 ($P < 0.001$, Fig 3.16C) and GW3965 ($P < 0.001$, Fig 3.16D) reduced pyolysin-induced leakage of LDH and cytolysis. Specifically, 50 nM T0901317 and 250 nM GW3965 reduced pyolysin-induced LDH leakage from stromal cells by 70% and 75%, respectively. Treatment with T0901317 or GW3965, did not reduce the pyolysin-induced leakage of potassium from epithelial cells (Fig 3.17A), however, they tended to reduce potassium leakage from stromal cells ($P = 0.07$, Fig 3.17B).

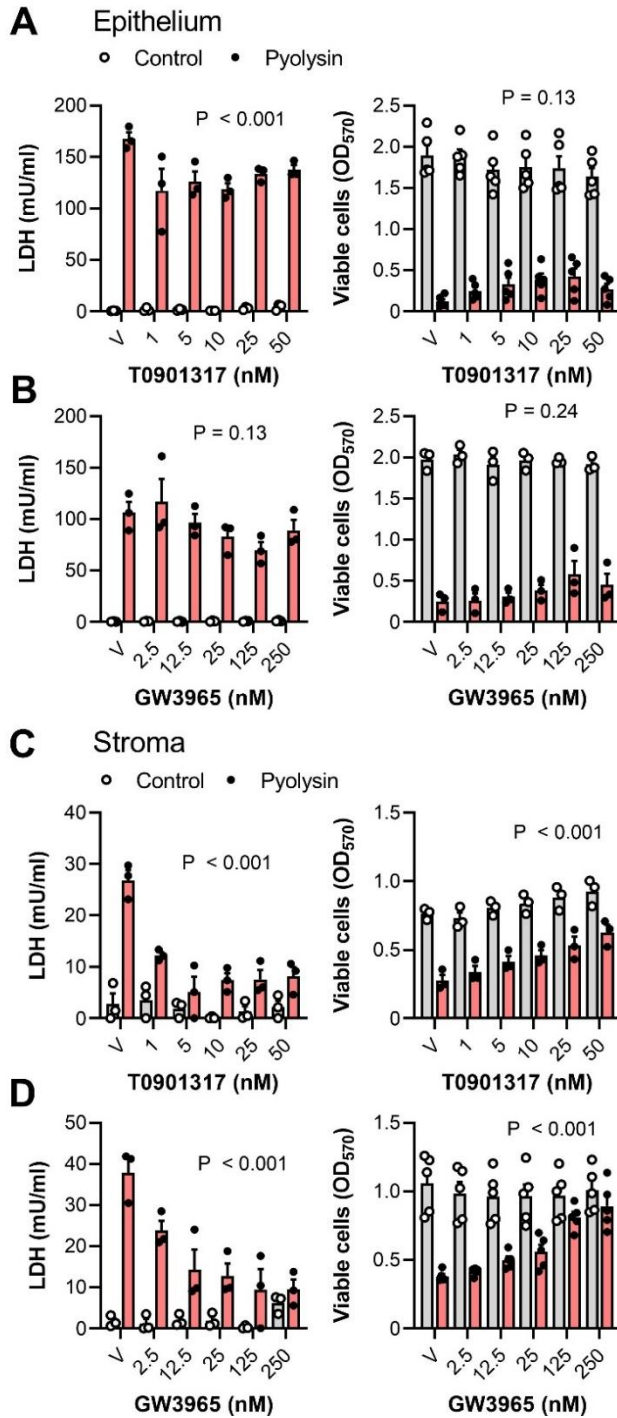


Figure 3.16 LXR agonists protect bovine endometrial cells against pyolysin

Leakage of LDH and viability of (A, B) epithelial and (C, D) stromal cells cultured for 24 h in serum-free medium containing vehicle (V) or the indicated concentrations of (A, C) T0901317, or (B, D) GW3965 and then challenged for 2 h with control medium or pyolysin (epithelium 200 HU, stroma 25 HU). Data are presented as mean (SEM) using cells from ≥ 3 independent animals; statistical significance determined by two-way ANOVA and P-values reported for the effect of treatment on pyolysin challenge.

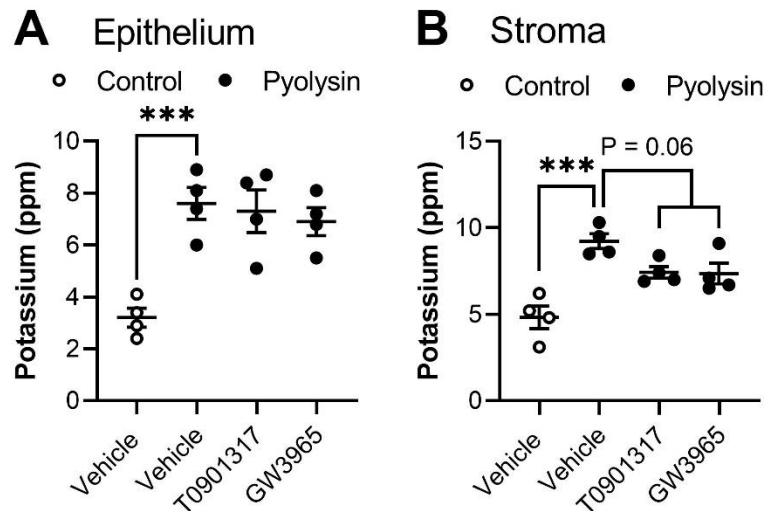


Figure 3.17 LXR agonists decrease pyolysin-induced potassium leakage in stromal cells

Leakage of potassium from (A) epithelial and (B) stromal cells treated for 24 h with vehicle, 25 nM T0901317, 125 nM GW3965, and then challenged for 5 min with control medium or pyolysin (epithelium 200 HU, stroma 25 HU). Dots represent the values from 4 independent animals; statistical significance was determined using one-way ANOVA with Dunnett's post hoc test; *** $P < 0.01$.

Our second approach was to reduce the expression of LXR α and LXR β using siRNA to target *NR1H3* and *NR1H2*, respectively, as previously validated at the mRNA and protein level (Griffin et al., 2018). Additional validation in this study demonstrated that siRNA targeting *NR1H3* and *NR1H2* reduced LXR α and LXR β protein abundance, and the abundance of the LXR-induced protein ABCA1 (Fig 3.18) (Ito et al., 2015). Epithelial and stromal cells were transfected with siRNA targeting *NR1H3* and *NR1H2* independently and in combination, before 24 h treatment with 27-hydroxycholesterol or T0901317, and then a 2 h challenge with pyolysin. Targeting both *NR1H3* and *NR1H2*, limited the protective effect of 27-hydroxycholesterol on pyolysin-induced LDH leakage and cytolysis in epithelial cells (scramble vs. double knockdown, 68% vs. 56% reduction in LDH leakage, 2% vs 21% cytolysis, Fig 3.19A) and stromal cells (94% vs. 70% reduction in LDH leakage, 23% vs. 31% cytolysis, Fig 3.19B). Targeting both *NR1H3* and *NR1H2* also diminished T0901317 cytoprotection in both epithelial and stromal cells (Fig 3.20).

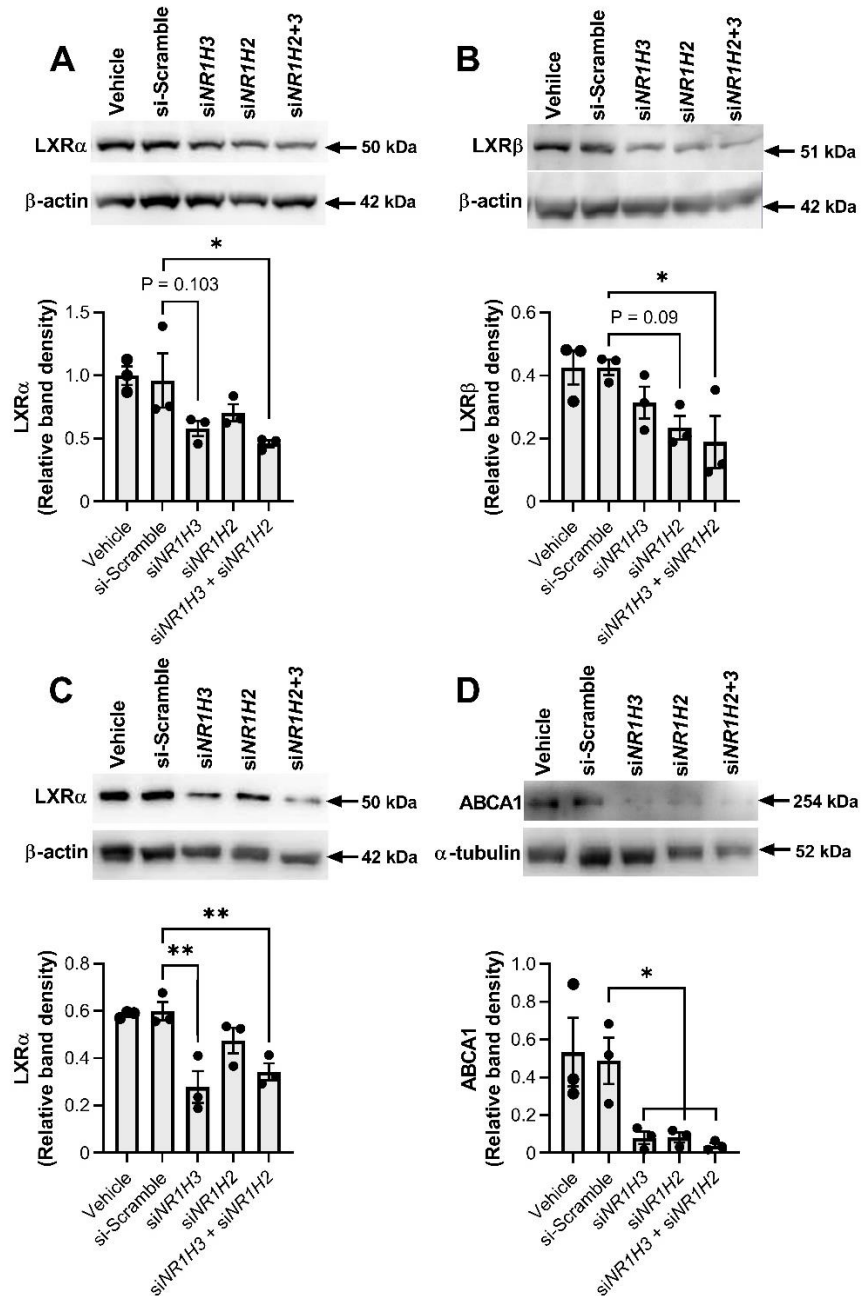


Figure 3.18 siRNA targeting *NR1H3* and *NR1H2* reduced the abundance of LXR and ABCA1 protein

Representative Western blots of LXR α , LXR β , and ABCA1 in (A,B) epithelial and (C,D) stromal cells (Western blots for LXR β in stromal cells had staining that precluded analysis) transfected with scrambled siRNA or siRNA targeting *NR1H3* or *NR1H2*. β and-actin and α -tubulin were used as loading controls. Image representative from 4 independent experiments. Densitometry data were normalized to the loading control and presented as mean (SEM); statistical significance was determined using one-way ANOVA and P-values are reported for Dunnett's post hoc test; *P < 0.05, **P < 0.01.

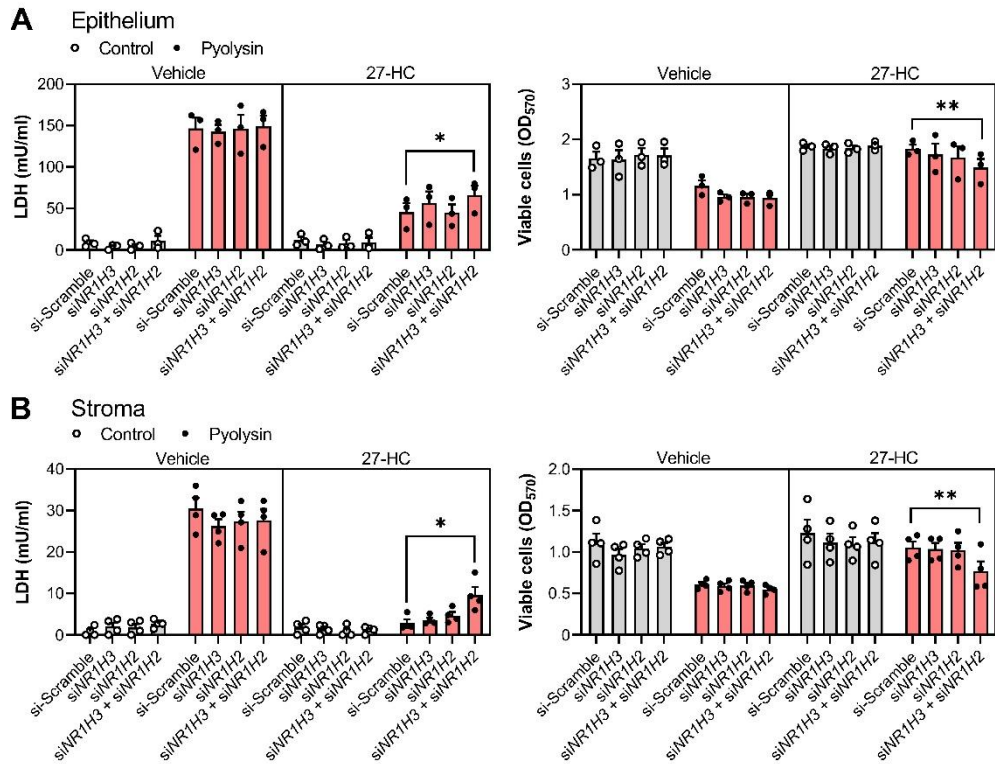
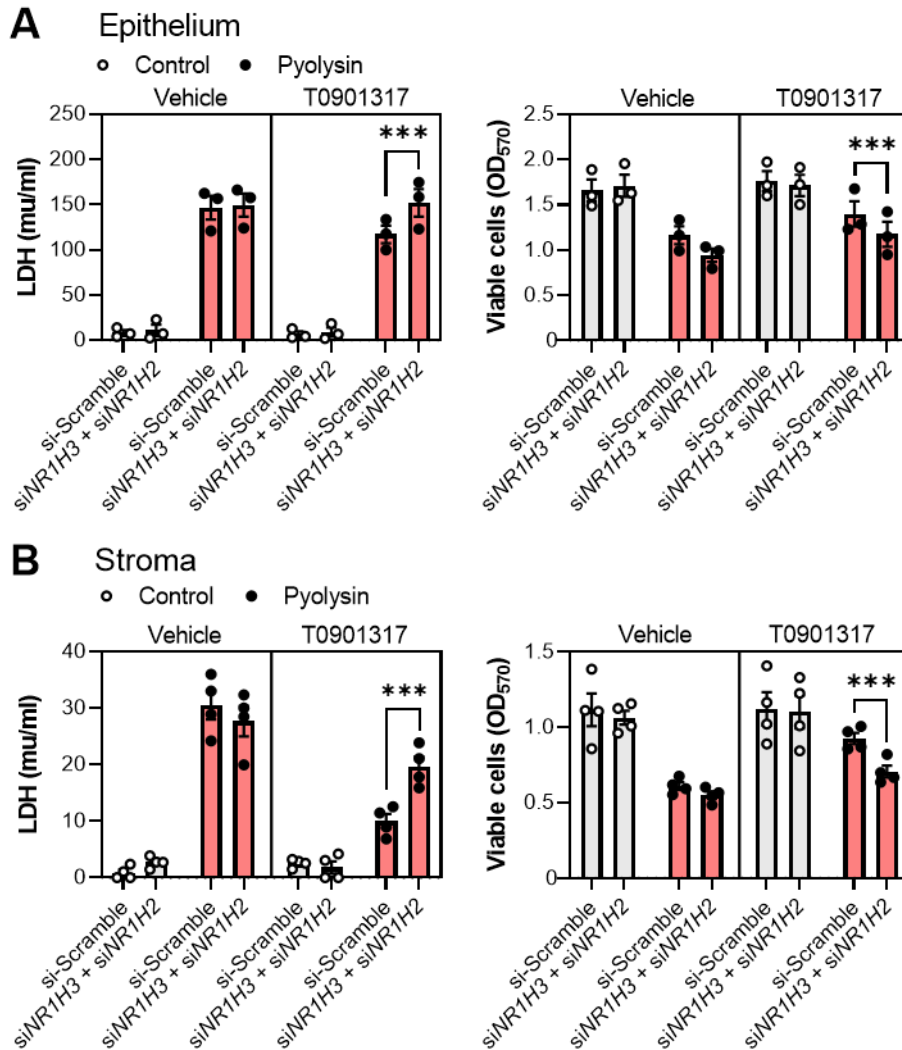


Figure 3.19 27-hydroxycholesterol cytoprotection is partly LXR dependent

Leakage of LDH and viability of (A) epithelial and (B) stromal cells transfected for 48 h with scramble siRNA or siRNA targeting *NR1H2* and *NR1H3*, treated for 24 h with vehicle or 25 ng/ml 27-hydroxycholesterol (27-HC), and then challenged for 2 h with control medium or pyolysin (epithelium 200 HU, stroma 25 HU). Data are presented as mean (SEM) from 4 independent animals; statistical significance was determined using two-way ANOVA and Tukey's post hoc test; * $P < 0.05$, ** $P < 0.01$.



To provide verification that 27-hydroxycholesterol and T0901317 induced target gene expression at the concentrations used in this study, we examined the treatment effect on ABCA1 abundance (Fig 3.21). T0901317 increased ABCA1 protein abundance in both epithelial and stromal cells. Additionally, 27-hydroxycholesterol increased ABCA1 abundance in epithelial cells and there was a trend for an increase in stroma cells. Taken together, these data provide evidence that cytoprotection against pyolysin is at least partially dependent on both LXR α and LXR β .

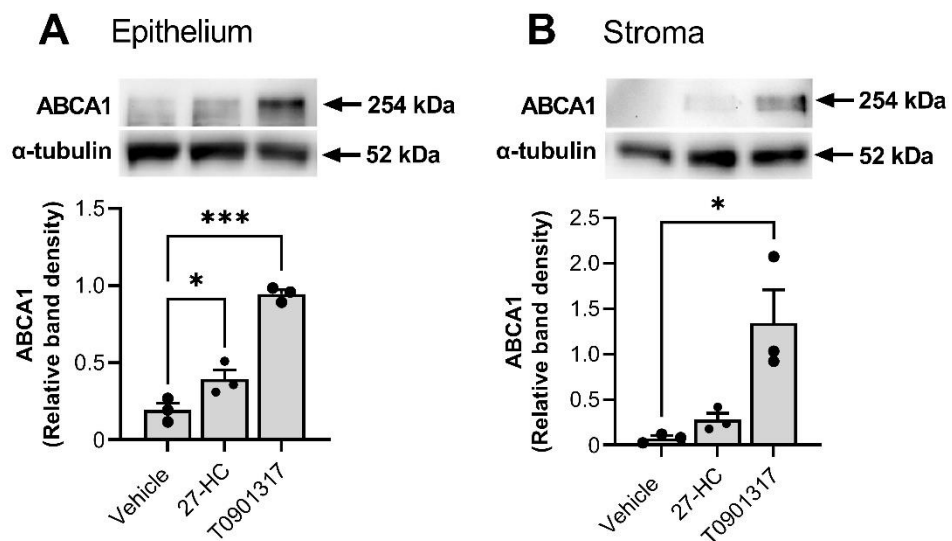


Figure 3.21 27-hydroxycholesterol and T0901317 increase ABCA1 protein

Representative Western blots of ABCA1 in (A) epithelial and (B) stromal cells treated for 24 h with vehicle, 25 ng/ml 27-hydroxycholesterol (27-HC), or 25 nM T0901317. α -tubulin was used as a loading control. Image representative from 3 independent experiments. Densitometry data for ABCA1 were normalized to α -tubulin and presented as mean (SEM); statistical significance was determined using one-way ANOVA and P-values are reported for Dunnett's post hoc test; *P < 0.05, ***P < 0.001.

3.3.5 Side-chain oxysterols protect cells against α -hemolysin

To determine whether oxysterol cytoprotection extended beyond pyolysin, we treated cells for 24 h with vehicle, 25 ng/ml 27-hydroxycholesterol, or 25 nM T0901317, and then challenged the cells with *S. aureus* α -hemolysin for 24 h in the absence of further treatments (Fig 3.22). The α -hemolysin challenge induced the leakage of LDH, reduced the viability of stromal cells (Fig 3.22B) and there was a trend for reduced epithelial cell viability ($P = 0.1$, Fig 3.22A). 27-hydroxycholesterol treatment reduced LDH leakage and cytolysis in both cell types, although T0901317 had no significant affect. A 15 min α -hemolysin challenge did not cause potassium leakage from epithelial cells ($P = 0.99$, Fig 3.23A), however, 27-hydroxycholesterol, but not T0901317, reduced the leakage of potassium from stromal cells (Fig 3.23B).

Treatment with 27-hydroxycholesterol also protected against α -hemolysin-induced changes in the cytoskeletal of epithelial cells (44 ± 3 vs $90 \pm 3\%$ cells damaged, t-test, $P < 0.01$, $n = 3$, Fig 3.24A) and stromal cells (9 ± 1 vs $62 \pm 6\%$ cells damaged, t-test, $P < 0.01$, $n = 3$, Fig 3.24B). Together these data provide evidence for 27-hydroxycholesterol cytoprotection of endometrial epithelial and stromal cells against an α -hemolysin.

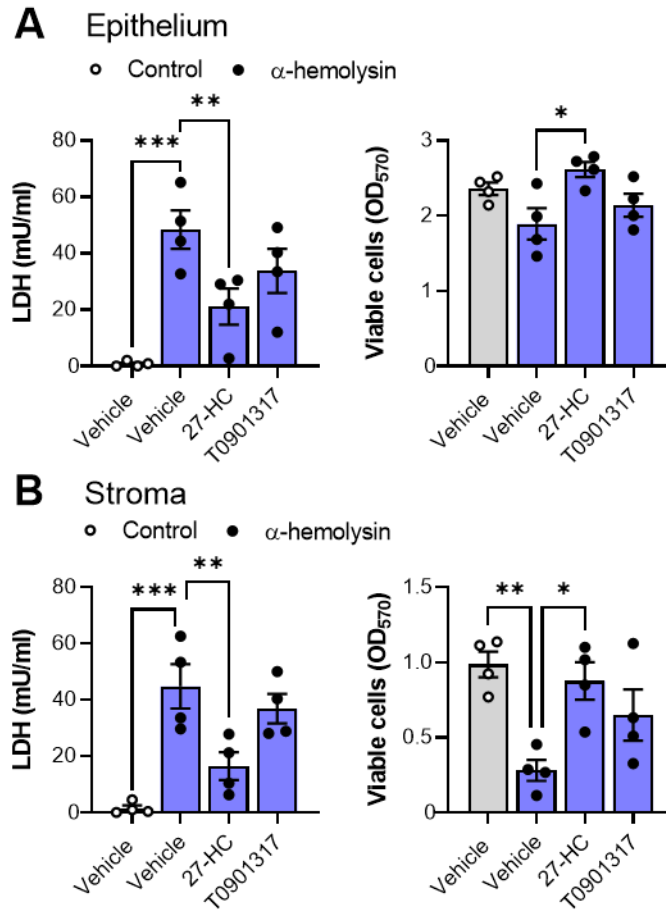


Figure 3.22 27-hydroxycholesterol protects cells against α -hemolysin damage

Leakage of LDH and viability of (A) epithelial and (B) stromal cells cultured for 24 h in serum-free medium containing vehicle, 25 ng/ml 27-hydroxycholesterol (27-HC), or 25 nM T0901317 and then challenged for 24 h with control medium or 8 μ g α -hemolysin. Data are presented as mean (SEM) using cells from 4 independent animals; statistical significance determined by one-way ANOVA and Dunnett's post hoc test; *P < 0.05, **P < 0.01, ***P < 0.001.

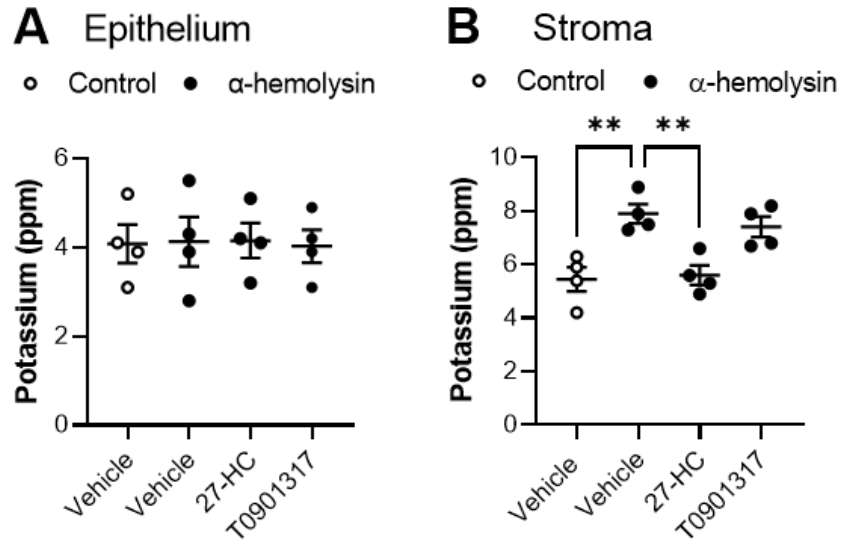


Figure 3.23 27-hydroxycholesterol reduces α -hemolysin-induced potassium leakage in stromal cells

Leakage of potassium from (A) epithelial and (B) stromal cells treated for 24 h with vehicle, 25 ng/ml 27-hydroxycholesterol (27-HC), 25 nM T0901317, and then challenged for 15 min with control medium or 8 μ g α -hemolysin. Dots represent the values from 4 independent animals; statistical significance was determined using one-way ANOVA with Dunnett's post hoc test; **P < 0.01.

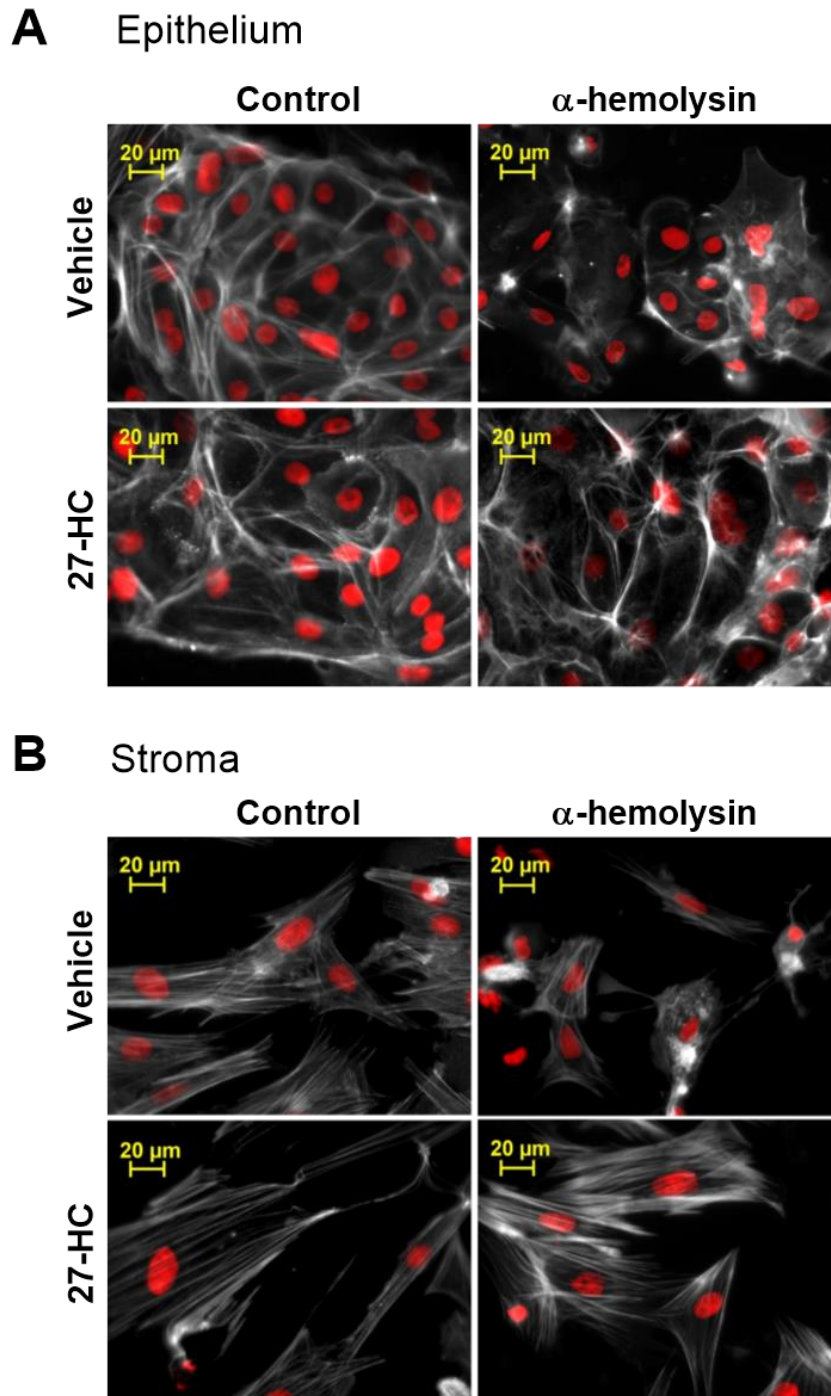


Figure 3.24 27-hydroxycholesterol protects bovine endometrial cells against α -hemolysin-induced actin cytoskeletal changes

Fluorescent microscope images of (A) epithelial and (B) stromal cells treated for 24 h with vehicle or 25 ng/ml 27-hydroxycholesterol (27-HC), then challenged for 2 h with control medium or 8 μ g α -hemolysin and stained with fluorescent phalloidin (white) and DAPI (red); images are representative from 3 independent experiments. Quantification of cytoskeletal changes are reported in text.

3.3.6 Oxysterols are present in the bovine endometrium

We used mass spectrometry to understand the biological relevance of oxysterols in the bovine reproductive tract. We detected a range of oxysterols in uterine and ovarian follicular fluid, with the abundance greater in the latter (Fig 3.25, Table 3.1). Notably, 25-hydroxycholesterol and 27-hydroxycholesterol were detected in the uterine fluid as well as 7 α -25-hydroxycholesterol, a 25-hydroxycholesterol metabolite.

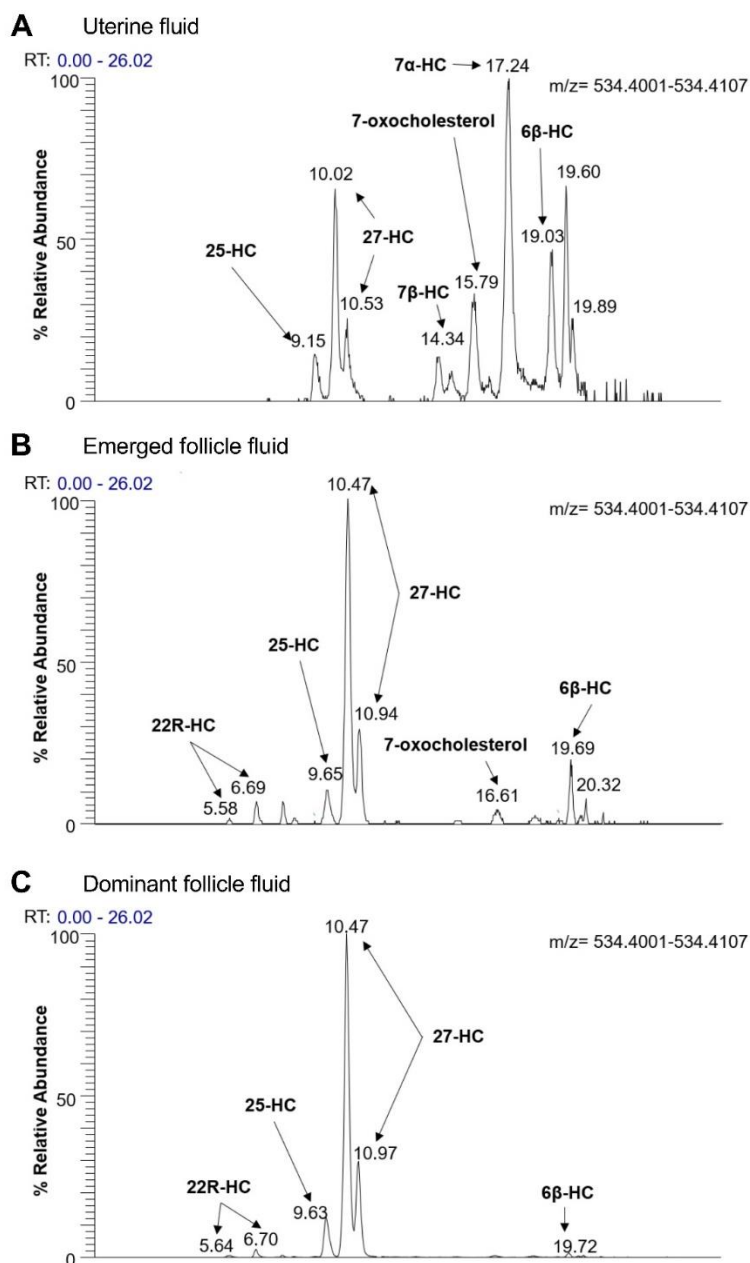


Figure 3.25 Oxysterols are present in bovine uterine and ovarian follicular fluid
Chromatographic separation (m/z 534.4054 \pm 5 ppm) of indicated oxysterols from (A) uterine fluid and (B) emerged and (C) dominant ovarian follicular fluid sample derivatized with [$^2\text{H}_0$] Girard P reagent.

Table 3.1 Oxysterol concentrations in biological samples

Concentrations of oxysterols in samples of uterine or follicular fluid from emerged (4-8 mm diameter) or dominant (> 8 mm diameter) ovarian follicles (data are reported as mean \pm SEM, n= 3 per sample). * Dehydration products of cholestane-3 β ,5 α ,6 β -triol.

Oxysterol	Uterine fluid (ng/ml)	Emerged follicle fluid (ng/ml)	Dominant follicle fluid (ng/ml)
22R-hydroxycholesterol	0.2 \pm 0.2	2.3 \pm 0.8	2.4 \pm 1.5
24S-hydroxycholesterol	0.2 \pm 0.2	0.2 \pm 0.1	0.5 \pm 0.1
25-hydroxycholesterol	3.9 \pm 0.6	13.4 \pm 10.5	26.8 \pm 11.4
25-hydroxycholest-4-en-3-one	0.0 \pm 0.0	0.1 \pm 0.1	2.1 \pm 1.8
27-hydroxycholesterol	19.9 \pm 4.9	104.3 \pm 69.7	244.6 \pm 99.5
27-hydroxycholest-4-en-3-one	0.0 \pm 0.0	0.5 \pm 0.2	6.8 \pm 5.2
7 β -hydroxycholesterol	0.8 \pm 0.8	0.4 \pm 0.2	0.4 \pm 0.2
7 α -hydroxycholesterol	8.3 \pm 4.9	0.9 \pm 0.6	1.1 \pm 0.0
7 α -hydroxycholest-4-en-3-one	17.0 \pm 8.4	0.2 \pm 0.1	1.3 \pm 1.1
6 β -hydroxycholesterol*	7.1 \pm 0.9	2.3 \pm 0.6	2.2 \pm 0.2
6 β -hydroxycholest-4-en-3-one*	0.8 \pm 0.5	0.2 \pm 0.1	0.9 \pm 0.6
7-oxocholesterol	13.2 \pm 1.5	2.8 \pm 1.0	6.8 \pm 5.1
24,25-epoxycholesterol	0.6 \pm 0.6	7.5 \pm 4.9	9.3 \pm 7.3
24,25-epoxycholest-4-en-3-one	0.0 \pm 0.0	0.3 \pm 0.2	6.6 \pm 5.3
24,27-dihydroxycholesterol	0.5 \pm 0.5	5.8 \pm 3.0	4.8 \pm 3.0
24,27-dihydroxycholest-4-en-3-one	0.0 \pm 0.0	0.3 \pm 0.2	2.6 \pm 2.3
7 α ,25-dihydroxycholesterol	1.3 \pm 0.7	0.7 \pm 0.4	2.0 \pm 1.5
7 α ,25-dihydroxycholest-4-en-3-one	1.5 \pm 0.4	1.5 \pm 0.5	16.7 \pm 12.6
7 α ,27-dihydroxycholesterol	0.0 \pm 0.0	0.2 \pm 0.2	0.0 \pm 0.0
7 α ,27-dihydroxycholest-4-en-3-one	2.3 \pm 0.7	1.3 \pm 0.2	13.8 \pm 6.4
3 β ,7 β -dihydroxycholest-5-en-26-oic acid	0.0 \pm 0.0	2.3 \pm 0.2	2.0 \pm 1.0
7 β -hydroxy-3-oxocholest-4-en-26-oic acid	0.0 \pm 0.0	0.3 \pm 0.17	0.5 \pm 0.2
3 β ,7 α -dihydroxycholest-5-en-26-oic acid	4.9 \pm 2.5	13.2 \pm 6.9	6.5 \pm 4.2
7 α -hydroxy-3-oxocholest-4-en-26-oic acid	81.3 \pm 20.0	76.8 \pm 21.0	258.9 \pm 136.8
3 β ,22R-dihydroxycholest-5-en-26-oic acid	0.0 \pm 0.0	23.5 \pm 14.7	23.9 \pm 13.5
22R-hydroxy-3-oxocholest-4-en-26-oic acid	0.0 \pm 0.0	3.0 \pm 1.6	11.1 \pm 4.7
20R,22R,25-trihydroxycholesterol	0.9 \pm 0.9	10.7 \pm 5.5	2.4 \pm 1.8
20R,22R,25-trihydroxycholest-4-en-3-one	1.1 \pm 0.8	2.4 \pm 0.7	39.5 \pm 21.3
7 α ,24,25-trihydroxycholest-4-en-3-one	4.8 \pm 2.5	4.3 \pm 1.3	20.5 \pm 13.2
3 β -hydroxycholest-5-enoic acid	12.7 \pm 6.8	283.3 \pm 249.4	295.8 \pm 118.4
3-oxocholest-4-enoic acid	4.4 \pm 3.1	20.8 \pm 12.9	11.1 \pm 4.7
3 β ,7 α ,24-trihydroxycholest-5-en-26-oic acid	0.0 \pm 0.0	0.57 \pm 0.57	0.0 \pm 0.0
7 α ,24-dihydroxy-3-oxocholest-4-en-26-oic acid	3.6 \pm 1.8	5.1 \pm 0.2	16.4 \pm 6.8
3 β ,7 α ,25-trihydroxycholest-5-en-26-oic acid	0.0 \pm 0.0	0.8 \pm 0.6	1.5 \pm 0.9
7 α ,25-dihydroxy-3-oxocholest-4-en-26-oic acid	2.5 \pm 1.4	3.1 \pm 1.1	12.3 \pm 6.3

As Gram-negative bacteria and *T. pyogenes* are common endometrial pathogens, we next considered whether endometrial cells might secrete oxysterols in response to their major virulence factors, LPS and pyolysin (Sheldon et al., 2010, Sheldon et al., 2002, Griffin et al., 1974, Bonnett et al., 1991, Amos et al., 2014). We also used LPS as a control because it stimulates the release of 25-hydroxycholesterol from murine macrophages (Reboldi et al., 2014). Epithelial and stromal cells were challenged with 1 μ g/ml LPS or a 5 HU sub-lytic concentration of pyolysin for 24 h, and the supernatants collected for mass spectrometry. Few oxysterols were collected in serum-free culture medium (Table 3.2); however, epithelial cell supernatants contained several oxysterols, notably including 25-hydroxycholesterol (Fig 3.26, 3.27A). The concentration of 25-hydroxycholesterol increased by 97% following LPS challenge and by 220% following pyolysin challenge. However, 27-hydroxycholesterol was not detected in stromal or epithelial cell supernatants, and 25-hydroxycholesterol was barely detectable in the supernatant of stromal cells (Fig 3.26, 3.27B). Together these data provide evidence for oxysterols in the reproductive tract, and the release of 25-hydroxycholesterol from epithelial cells challenged with LPS or pyolysin.

Table 3.2 Oxysterol concentrations in culture medium

Concentrations of oxysterols detected in serum-free culture medium.

Oxysterol	ng/ml
6 β -hydroxycholesterol	0.39
6 β -hydroxycholest-4-en-3-one	0.24
7-oxocholesterol	1.15

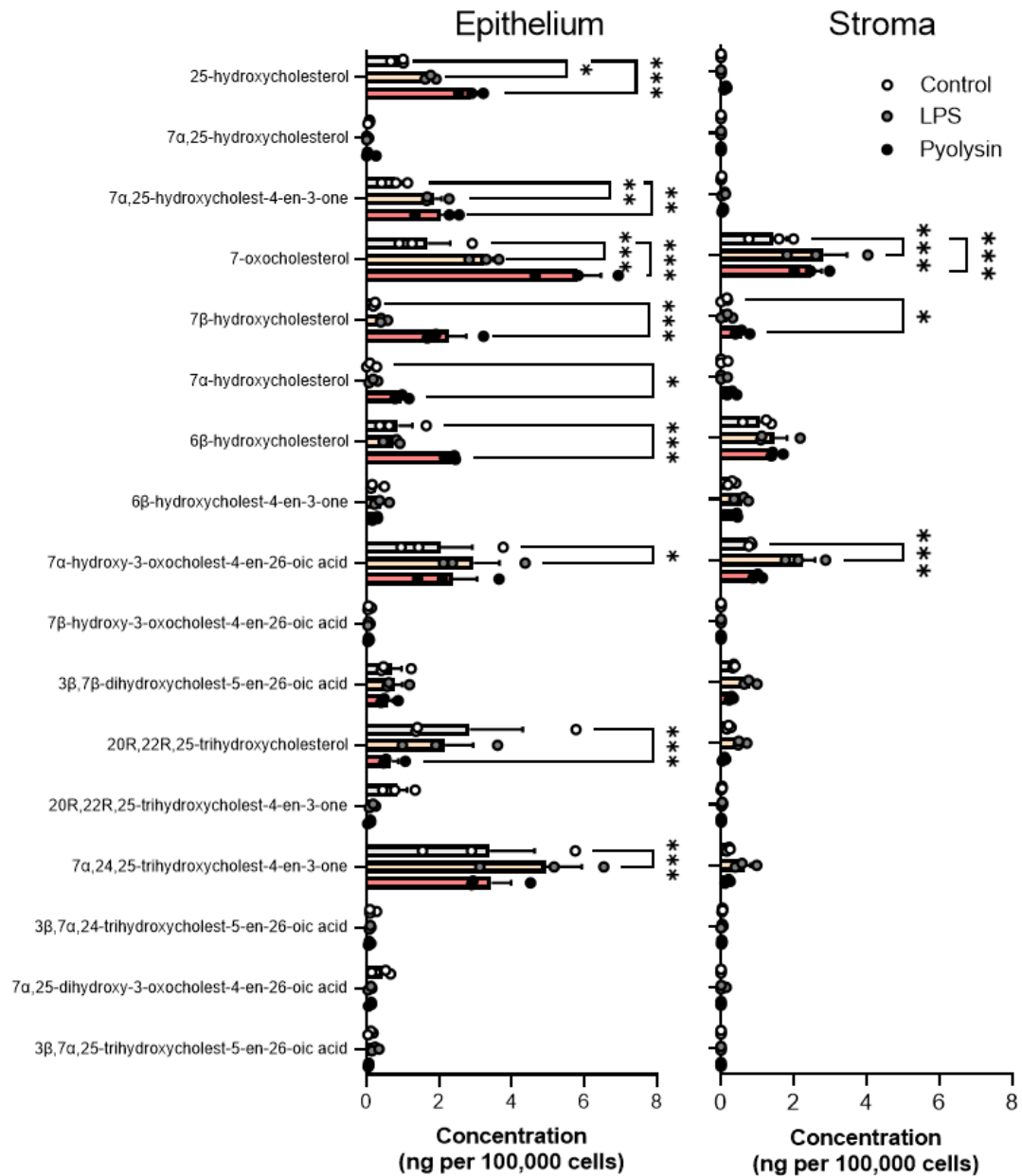


Figure 3.26 Endometrial cells release oxysterols

Concentrations of oxysterols in supernatants from epithelial and stromal cells challenged with control medium, or medium containing 1 μ g/ml LPS, or 5 HU pyolysin. Data are presented as mean (SEM) from 3 independent animals; statistical significance was determined using two-way ANOVA and Dunnett's post hoc test; *P < 0.05, **P < 0.01, ***P < 0.001.

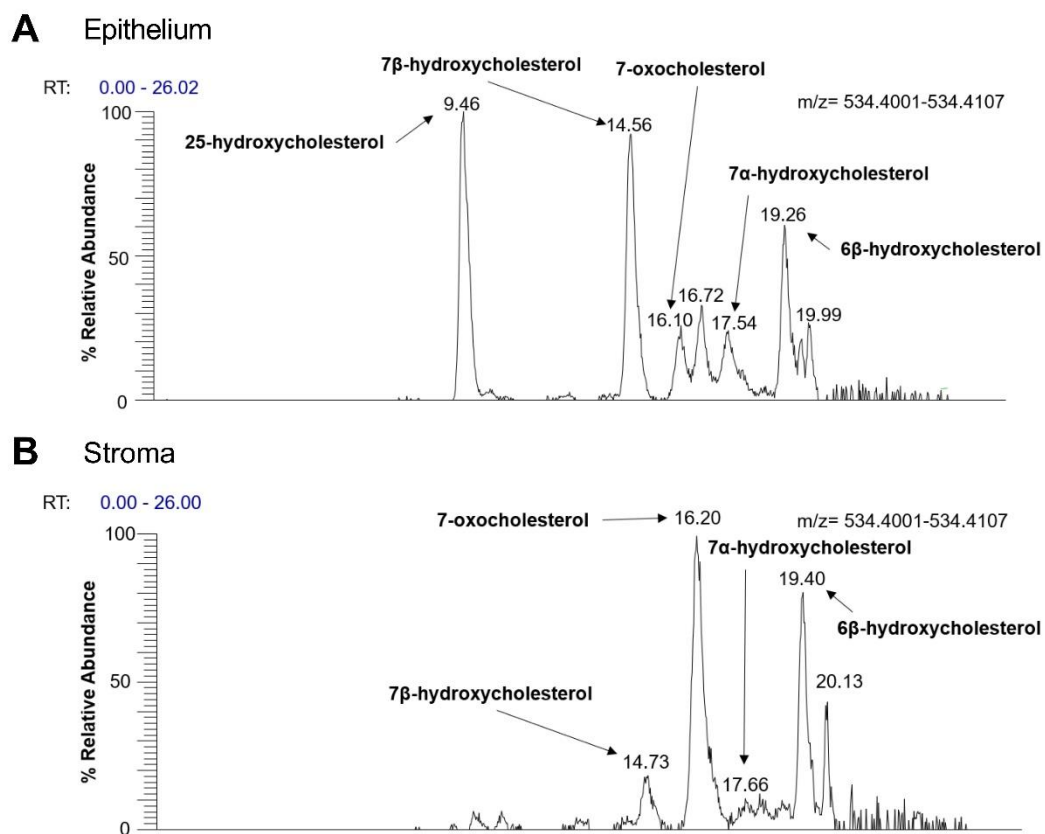


Figure 3.27 Pyolysin-induced oxysterol release in stromal and epithelial cells

Chromatographic separation (m/z 534.4054 \pm 5 ppm) of indicated oxysterols from the supernatant of (A) stroma and (B) epithelial cells challenged for 24 h with 5 HU pyolysin, derivatized with [$^2\text{H}_0$] Girard P reagent.

3.4 DISCUSSION

In this study we discovered that both 25-hydroxycholesterol and 27-hydroxycholesterol enhanced bovine endometrial cells intrinsic protection against pore-forming toxins from uterine pathogens. Whilst progesterone, oestradiol, hydrocortisone, and dexamethasone provided no significant protection against pyolysin at the concentrations and treatment duration examined in this chapter, treating epithelial or stromal cells with 25-hydroxycholesterol or 27-hydroxycholesterol, reduced the formation of pyolysin-induced plasma membrane pores and protected cells against damage. Although the side-chain oxysterols did not significantly alter cellular cholesterol abundance, there was reduced binding of pyolysin to cells, and cytoprotection was at least partly dependent on ACAT and LXRs. The side-chain oxysterol cytoprotection of endometrial cells also extended beyond a cholesterol-dependent cytolysin to *S. aureus* α -hemolysin. Interestingly, the concentrations of side-chain oxysterols we used *in vitro* were similar to the concentration of 25-hydroxycholesterol or 27-hydroxycholesterol we measured in the reproductive tract. Furthermore, pyolysin stimulated the release of more 25-hydroxycholesterol from epithelial cells. We suggest that side-chain oxysterols might be released by epithelial cells to help protect stromal cells against pore-forming toxins from pathogenic bacteria.

Challenging bovine endometrial epithelial and stromal cells with pyolysin induced the formation of membrane pores, as determined by leakage of potassium and LDH from cells. Pyolysin-induced cell damage was determined by changes in the actin cytoskeleton and cell shape, and reduced cell viability. These effects are typical of cholesterol-dependent cytolysins, which are the most common pore-forming toxins secreted by pathogenic bacteria (Peraro and van der Goot, 2016, Gurcel et al., 2006, Gonzalez et al., 2011). As previously reported, epithelial cells were more tolerant of pyolysin than stromal cells (Amos et al., 2014). This innate tolerance to pathogens is typical of epithelia (Medzhitov et al., 2012, Amos et al., 2014). However, loss of the epithelium associated with trauma during parturition, postpartum physiological regeneration of the epithelium, and damage by pore-forming toxins from invading pathogens, may explain the increased risk of developing postpartum uterine disease once underlying sensitive stromal cells are exposed to *T. pyogenes* and *S. aureus*.

It was surprising that progesterone, oestradiol or glucocorticoids, did not significantly alter pyolysin-induced cells leakage of LDH or endometrial cytolysis because the dogma is that progesterone, oestradiol and glucocorticoids modulate the risk of disease, particularly in the genital tract (Wira et al., 2015, Ogawa et al., 2005, Spann and Glass, 2013). However, these findings are similar to previous findings that ovarian steroids did not alter endometrial cell immune responses to LPS (Saut et al., 2014).

Our most striking finding was that either 27-hydroxycholesterol or 25-hydroxycholesterol protected endometrial epithelial and stromal cells against cytolysis in the face of pyolysin challenges that normally caused > 50% cytolysis. Treatment with 25 ng/ml 27-hydroxycholesterol or 5 ng/ml 25-hydroxycholesterol reduced the leakage of potassium and LDH and prevented pyolysin-induced changes in the actin cytoskeleton and cell shape. This cytoprotection was effective even when cells were treated in medium containing 10% serum, and protection against pyolysin persisted for at least 24 h. Our findings support a recent observation that mouse bone marrow-derived macrophages stimulated with interferon may protect against cholesterol-dependent cytolysins perfringolysin O, streptolysin O and anthrolysin O through an oxysterol-dependent mechanism (Zhou et al., 2020). Furthermore, injection of 25-hydroxycholesterol into the skin of mice 6 h before a 48 h challenge with anthrolysin O reduced tissue damage *in vivo* (Zhou et al., 2020). However, there is a contradictory study, where treating Chinese Hamster Ovary cells with 1 µg/ml 25-hydroxycholesterol for 1 h followed by 4 h with proaerolysin and 25-hydroxycholesterol increased cell damage (Gurcel et al., 2006).

In the present study we also examined protection against *S. aureus* α -hemolysin, which is not so dependent on the abundance of cholesterol in target cell membranes. Furthermore, the lower calcium permeability of small diameter pores impairs reparative mechanisms, emphasizing the importance of identifying methods to protect cells against these toxins (Brito et al., 2019). We found that treating endometrial cells with 27-hydroxycholesterol also reduced α -hemolysin-induced leakage of potassium and LDH and prevented cytolysis. The cells required a longer challenge with α -hemolysin than pyolysin to study cytolysis, which might reflect the ten-fold smaller diameter of the pores formed by α -hemolysin than pyolysin (Peraro and van der Goot, 2016, Song et al., 1996, Preta et al., 2016). However, taken together, our results

provide evidence for oxysterol cytoprotection of endometrial cells against pore-forming toxins.

The abundance of oxysterols in the bovine reproductive tract had not been considered previously. However, we detected the presence of 27-hydroxycholesterol and 25-hydroxycholesterol in uterine and ovarian follicular fluid. A greater abundance of oxysterols was detected in ovarian follicular fluid compared to the uterine fluid. Ovarian cells synthesize steroid hormones to regulate reproductive function (Drummond, 2006). Steroidogenesis in the ovary is augmented by tropic hormones that also increase sterol synthesis, possibly explaining the greater abundance of oxysterols in follicular fluid (Strauss et al., 1991). Interestingly, the concentrations of oxysterols observed in the uterine fluid were similar to the concentrations we used to treat endometrial cells.

Although it was known that LPS stimulation of mouse macrophages upregulates cholesterol-25-hydroxylase resulting in 25-hydroxycholesterol secretion (Diczfalusy et al., 2009, Dang et al., 2017, Reboldi et al., 2014), we unexpectedly found that epithelial cells released 25-hydroxycholesterol, and that pyolysin stimulated further release of 25-hydroxycholesterol. These findings imply that epithelial cells might release oxysterols to protect stromal cells against the damage caused by invading pathogens. Oxysterol cytoprotection may complement the defenses against pore-forming toxins that depend on immune and repair mechanisms (Gurcel et al., 2006, Amos et al., 2014, Gonzalez et al., 2011, Bromfield et al., 2015, Wira et al., 2005, Andrews and Corrotte, 2018). We suggest that oxysterols from the ovary or oxysterols released during infection of the uterus may help the endometrium tolerate the presence of pathogenic bacteria that secrete pore-forming toxins.

Side-chain oxysterol cytoprotection is likely achieved through multiple protective mechanisms. Oxysterols regulate cholesterol homeostasis, increase cholesterol esterification, modify cell membranes, and activate LXRs (Cyster et al., 2014, Schroepfer, 2000, Wang and Tontonoz, 2018, Du et al., 2004, Abrams et al., 2020). Cholesterol-dependent cytolysins require accessible cholesterol, which is independent of the essential pool and sphingomyelin-bound pools of cholesterol in plasma membranes (Das et al., 2013, Abrams et al., 2020) Synthesis, uptake, efflux and breakdown of cholesterol alters only the accessible pool of cholesterol in plasma

membranes, typically when membrane cholesterol exceeds 35 mol% of total lipids (Tweten, 2005, Das et al., 2013). Consequently, small changes in membrane cholesterol around this threshold markedly alter the binding of cholesterol-dependent cytolytic toxins to plasma membranes (Peraro and van der Goot, 2016, Das et al., 2014, Tweten, 2005, Amos et al., 2014). In the present study, 27-hydroxycholesterol reduced pyolysin binding to cells, even though oxysterols did not significantly reduce cellular cholesterol or staining with filipin III, and cytoprotection was not affected by treating cells with oxysterols in culture medium with serum containing cholesterol. These findings agree with recent observations that interferon-induced 25-hydroxycholesterol protected mouse macrophages against cytolytic toxins and reduced binding of anthrolysin O, without reducing cellular cholesterol abundance or filipin III staining (Zhou et al., 2020). Furthermore, 25-hydroxycholesterol and 27-hydroxycholesterol depleted the labile pool of cholesterol in plasma membranes accessible to anthrolysin O, without reducing total cellular cholesterol (Abrams et al., 2020). Oxysterols reduced the labile cholesterol in membranes that was accessible to cholesterol-dependent cytolytic toxins by limiting cholesterol biosynthesis and/or increasing ACAT esterification of cholesterol (Abrams et al., 2020, Zhou et al., 2020). In the present study, an ACAT inhibitor also decreased oxysterol cytoprotection against pyolysin. However, we additionally found that using siRNA to target both *NRIH3* and *NRIH2*, but not each independently, reduced the level of oxysterol cytoprotection against pyolysin. Furthermore, the synthetic LXR ligands T0901317 and GW3965 also protected stromal cells against pyolysin, reducing pyolysin-induced leakage of LDH from stromal cells by 70–75%, almost as effectively as the 82–84% reduction by the oxysterols. Collectively, these observations lead to the suggestion that oxysterol cytoprotection is partly regulated through ACAT and common targets of LXR α and LXR β .

Other mechanisms of cytoprotection to consider may not involve the binding of toxins to membranes. For example, oxysterols can stimulate increased cytosolic calcium, which could activate protective mechanisms such as endocytosis, exocytosis, caspase activity, and the unfolded protein response (Mackrill, 2011, Andrews and Corrotte, 2018, Cassidy and O'Riordan, 2013, Gonzalez et al., 2011). Therefore, the role of ion flux in oxysterol cytoprotection will be investigated in *Chapter 4*. Additionally, 25- and 27-hydroxycholesterol are known to bind to oestrogen receptors and modulate their activity in an oestrogen independent manner, so repeating experiments in an

oestrogen receptor deficient cell line might highlight any involvement (Sato et al., 2004). Another possibility is that cholesterol-dependent cytolysins may bind to the oxysterols as they only differ from cholesterol by one hydroxyl group. However, there was no evidence for this in the present study because oxysterols in treatment media were not in direct contact with the pyolysin in challenge media, levels of cytoprotection were correlated with the duration of oxysterol treatment, and oxysterols protected against α -hemolysin, which is less dependent on cholesterol than pyolysin (Peraro and van der Goot, 2016, Berube and Bubeck Wardenburg, 2013). Similarly, binding of perfringolysin O to liposomes was not detected even with concentrations of 60 mol% 25-hydroxycholesterol (Bielska et al., 2014). Finally, oxysterols might alter the expression or distribution of glycans in plasma membrane, because many cholesterol-dependent cytolysis bind membrane glycans as well as cholesterol (Shewell et al., 2020); although, this remains to be explored for pyolysin.

There are a few key limitations to the findings of the present chapter. Firstly, as we examined protection against isolated pore-forming toxins, we cannot verify that oxysterol treatment would provide bovine endometrial cells with significant protection against *T. pyogenes* infection, as the bacterium secretes other virulence factors such as neuraminidases, fimbriae, and collagen-binding proteins (Jost and Billington, 2005). Future work might address this by challenging cells with live bacterium or examining the effect of *in vivo* oxysterol treatment in cattle infected with *T. pyogenes*.

Secondly, we discount progesterone, oestradiol and glucocorticoids as cytoprotective agents in the present chapter, as they did not significantly affect pyolysin-induced LDH leakage and cytolysis in bovine endometrial cells. However, we do not provide sufficient evidence to confirm that they do not alter intrinsic cell protection against pore-forming toxins. Though glucocorticoids are explored further in *Chapter 5*, further work should examine a range of progesterone and oestradiol treatment durations, repeat experiments in a range of cell types with different toxins, use different methods to assess pore-forming toxin damage, and investigate cognate receptor activity to confirm steroid treatment is having the desired effect.

Additionally, we only examined the protection afforded by 25- and 27-hydroxycholesterol and the cytoprotective properties of other oxysterols remain to be identified. Ring modified oxysterols, such as 7 β -hydroxycholesterol, in particular

warrant investigation as they demonstrate distinctly different functions to the side-chain oxysterols used in this chapter (Lordan et al., 2009).

Finally, the limited number of animals used to collect samples for oxysterol measurement by mass spectrometry restricts the impact of this data. While we provide a novel insight into the presence of oxysterols in the bovine endometrium, without additional replicates we cannot provide a reliable estimate for typical concentrations in bovine ovarian follicular and uterine fluid. Furthermore, additional work might examine oxysterol concentrations in both healthy and diseased cattle to establish whether bacterial infection affects oxysterol abundance.

In conclusion, we found that side-chain oxysterols protected bovine endometrial cells against pore-forming toxins. It was striking that 25-hydroxycholesterol and 27-hydroxycholesterol provided near complete protection against pyolysin and α -hemolysin. The oxysterol cytoprotection against pyolysin included ACAT and LXR dependent mechanisms. Oxysterols were present in uterine and ovarian fluids, and epithelial cells released 25-hydroxycholesterol in response to pyolysin. These results provide evidence that oxysterols enhance endometrial cell-intrinsic protection against pore-forming toxins. Our findings imply that side-chain oxysterols help protect bovine endometrial cells against the damage caused by pore-forming toxins, defending the endometrium against pathogenic bacteria.

4 SIDE-CHAIN OXYSTEROLS PROTECT HUMAN EPITHELIAL CELLS AGAINST DAMAGE FROM PORE-FORMING TOXINS

4.1 INTRODUCTION

Side-chain oxysterols regulate cholesterol homeostasis through transcriptional and non-genomic mechanisms (Bielska et al., 2012, Bielska et al., 2014) and manipulate the accessibility of plasma membrane cholesterol to inhibit bacterial dissemination (Abrams et al., 2020). Additionally, 25-hydroxycholesterol inhibits the inflammatory response in macrophages (Reboldi et al., 2014, Cyster et al., 2014, Dang et al., 2017). *Chapter 3* established that 25-hydroxycholesterol and 27-hydroxycholesterol protected bovine endometrial cells against pyolysin, and the present chapter aims to expand on this finding by exploring side-chain oxysterol cytoprotection in a variety of human epithelial cells and further investigating the mechanisms involved.

Mucosal epithelial cells provide a primary defence to bacterial infection, protecting underlying sensitive cells and tissues cells. Although pathogenic bacteria can use cholesterol-dependent cytolysins to damage this epithelial barrier, pore formation is sensitive to changes in plasma membrane cholesterol (Lange et al., 1989, van Meer et al., 2008, Goluszko and Nowicki, 2005, Mazzon and Mercer, 2014). The majority of cholesterol is sequestered by proteins and lipids such as sphingomyelin (Das et al., 2014, Endapally et al., 2019). However, cholesterol becomes accessible to cholesterol-dependent cytolysins when cholesterol exceeds 35 mol% of total plasma membrane lipids, and pore formation can be prevented by depleting this cytolysin-accessible pool (Das et al., 2013). For example, inhibiting 3-hydroxy 3-methylglutaryl coenzyme A reductase (HMGCR) with statins, inhibiting farnesyl-diphosphate farnesyltransferase 1 with zaragozic acid and depleting cellular cholesterol with cyclodextrins confer resistance to cholesterol-dependent cytolysin damage (Statt et al., 2015, Griffin et al., 2018, Amos et al., 2014).

Side-chain oxysterols such as 25-hydroxycholesterol and 27-hydroxycholesterol regulate cholesterol homeostasis through several mechanisms. Both 25-hydroxycholesterol and 27-hydroxycholesterol regulate cholesterol abundance via

liver X receptor binding, with the former pore potent (Lehmann et al., 1997, Wang and Tontonoz, 2018). These side-chain oxysterols also bind to Insig-2, promoting Insig-Scap binding, and thereby inhibiting the processing of sterol regulatory element-binding proteins and suppressing cholesterol synthesis (Radhakrishnan et al., 2007). Additionally, 25-hydroxycholesterol and 27-hydroxycholesterol promote cholesterol esterification through the endoplasmic reticulum-resident protein acetyl-coenzyme A acetyltransferase (ACAT) (Bielska et al., 2014). We therefore considered whether side-chain oxysterols might increase the intrinsic protection of human epithelial cells against the damage caused by pore-forming toxins.

In this chapter, we investigated whether side-chain oxysterols could protect human epithelial cells against bacterial toxins that cause pathology through plasma membrane pore-formation. To test this hypothesis, we treated a variety of epithelial cells with side-chain oxysterols and then challenged cells with pore-forming toxins. Pyolysin was used as a model cholesterol-dependent cytolysin, as it forms pores in many types of mammalian cells and unlike other cholesterol-dependent cytolysins, it does not require thiol-activation *in vitro* (Billington et al., 1997). However, we also examined cytoprotection against α -hemolysin from *S. aureus*, a toxin that does not rely specifically on cholesterol for cytolysis. Cell protection against pore-forming toxin challenge was evaluated by measuring the leakage of potassium ions or lactate dehydrogenase (LDH), evaluating cell viability, and through microscopy. We also investigated whether oxysterol cytoprotection was mechanistically associated with mitogen-activated protein kinase (MAPK) signalling, ion flux, LXR expression, or ACAT activation.

4.2 MATERIALS AND METHODS

4.2.1 Cytoprotection experiments

To determine the amount of pyolysin required to study cytoprotection, HeLa, A549, Hep-G2, and NC1-H441 cells (4×10^4 cells/well) were cultured in serum-free medium for 24 h and then challenged for 2 h with control serum-free medium (comprising 200 μ l Dulbecco's phosphate-buffered saline (DPBS) for 15 min, then supplemented with 400 μ l serum-free medium up to 2 h) or medium containing a range of concentrations of pyolysin as specified in *Results*. HeLa and A549 cells were selected as they are often used to explore cellular responses to cholesterol-dependent cytolysins (Gonzalez et al., 2011, Turner et al., 2020, Statt et al., 2015, Ratner et al., 2006), while Hep-G2 and NC1-H441 cells were selected as they were also susceptible to toxin damage. A 2 h challenge was selected, as previous research and our experiments in *Chapter 2* demonstrated that 2 h was sufficient to cause ~75% cytolysis (Amos et al., 2014, Griffin et al., 2018); and a longer challenge might reflect repair mechanisms and replication instead of indicating tolerance. At the end of the challenge, we measured the leakage of LDH into cell supernatants and assessed cell viability using a 3-(4,5-dimethylthiazol-2-yl)-2,5-diphenyltetrazolium bromide (MTT) assay as described in *Chapter 2*. For subsequent cytoprotection experiments we selected pyolysin challenges that increased LDH leakage and caused cytolysis in HeLa (100 HU/well, Fig 4.1), A549 (25 HU/well, Fig 4.8A), Hep-G2 (100 HU/well, Fig 4.8B) and NC1-H441 (200 HU/well, Fig 4.8C) cells, see *Results* section.

To examine whether side-chain oxysterols protected cells against pyolysin, HeLa, A549, Hep-G2, and NC1-H441 cells were incubated in 1 ml/well serum-free medium (as fetal bovine serum (FBS) can cause extracellular signal-regulated kinase 1 and 2 (ERK1/2) phosphorylation (Renshaw et al., 1997), and alter cholesterol homeostasis (Brown and Goldstein, 1986), which could obscure treatment effects) containing vehicle, 25-hydroxycholesterol, or 27-hydroxycholesterol. The role of LXR agonists in cytoprotection was explored by treating HeLa and A549 cells with T0901317 (N-(2,2,2-tri-fluoro-ethyl)-N-[4-(2,2,2-trifluoro-1-hydroxy-1-trifluoro-methyl-ethyl)-phenyl]-benzenesulfonamide) and GW3965 (3-(3-(2-chloro-3-trifluoromethylbenzyl)-2,2-diphenylethylamino)propoxy)phenylacetic acid). Oxysterol concentrations, as specified in *Results*, were informed by the concentrations in human

plasma of 154 ± 43 ng/ml 27-hydroxycholesterol and 2 ± 3 ng/ml 25-hydroxycholesterol human physiology (Dzeletovic et al., 1995), alongside the 25 ng/ml 27-hydroxycholesterol and 5 ng/ml 25-hydroxycholesterol required to protect bovine endometrial cells with cytoprotection against pyolysin in *Chapter 3*. Treatments were applied for 24 h based on previous work investigating cytoprotection (Statt et al., 2015, Griffin et al., 2018, Amos et al., 2014); except for experiments exploring the duration of 27-hydroxycholesterol treatment required to protect cells against pyolysin, where HeLa cells were treated with 10 ng/ml 27-hydroxycholesterol for a range of times up to 24 h as specified in *Results*. After the treatment period, supernatants were discarded, and cells were challenged for 2 h with control serum-free medium or medium containing pyolysin in the absence of treatments. To determine whether protection extended beyond pyolysin, HeLa and A549 cells were treated for 24 h with vehicle or 10 ng/ml 27-hydroxycholesterol, and then challenged with 8 μ g α -hemolysin for 24 h (added in 200 μ l Dulbecco's phosphate-buffered saline (DPBS) for 15 min, then supplemented with 400 μ l serum-free medium up to 24 h). The concentration and duration of α -hemolysin required to challenge cells was determined by culturing cells for 24 h in serum-free medium and then challenging cells for a range of time periods from 0 to 24 h using the concentrations specified in *Results*. Experiments were informed by the concentration of α -hemolysin used to induce autophagy in HeLa cells (Mestre et al., 2010, Mestre and Colombo, 2012). At the end of the challenge period, supernatants were collected to measure LDH leakage and cell viability was evaluated using an MTT assay. Transmitted light micrographs were captured at the end of the challenge period in designated experiments using an Axiocam ERc 5s microscope camera (Zeiss). The proportion of normal, blebbing, and fragmented cells were counted using 2 independent images per treatment replicate.

To determine whether cytolysis could be prevented by pyolysin binding directly to residual treatment in wells, we tested the effect of oxysterol and pyolysin co-incubation. HeLa cells were cultured for 24 h in serum-free medium. Control and pyolysin challenge (100 HU/well) were prepared in serum-free medium containing vehicle, 10 ng/ml 25-hydroxycholesterol, 10 ng/ml 27-hydroxycholesterol, or 0.5 mM cholesterol as a positive control, vortexed for 30 s, then added to cells for 2 h. Supernatants were then collected to measure the leakage of LDH, and cell viability was measured using an MTT assay

To examine the role of ACAT in cytoprotection against pyolysin we used a selective ACAT inhibitor Sandoz 58-035 (SZ58-035) (Ross et al., 1984). HeLa cells were washed twice with phosphate-buffered saline (PBS) then treated with vehicle or 10 μ M SZ58-035 in serum-free medium for 16 h as previously described (Abrams et al., 2020). Cells were then washed twice with PBS, then incubated for 24 h in serum-free culture medium containing 10 ng/ml 25-hydroxycholesterol, or 10 ng/ml 27-hydroxycholesterol in combination with vehicle or 10 μ M SZ58-035. Cells were challenged for 2 h with control medium or medium containing 100 HU pyolysin. At the end of the challenge period, supernatants were collected to measure the leakage of LDH, and cell viability was measured using an MTT assay.

To disrupt sphingomyelin-cholesterol complexes and explore their influence on protection against pyolysin damage, we used the enzyme sphingomyelinase from *S. aureus* (Das et al., 2014). HeLa cells were treated with serum-free medium containing vehicle, or 10 ng/ml 27-hydroxycholesterol for 24 h. Supernatants were discarded, and cells were washed twice with PBS. Cells were then treated for 30 mins in serum-free medium with or without 100 mU/ml sphingomyelinase as previously described (Abrams et al., 2020). After the treatment period, cells were washed twice with PBS, and then challenged for 2 h with control medium, or medium containing 25 HU pyolysin (selected because sphingomyelinase treatment increased the susceptibility of cells to pyolysin damage). At the end of the challenge period, supernatants were collected to measure the leakage of LDH, and cell viability was measured using an MTT assay.

To explore the mechanisms involved in side-chain oxysterol cytoprotection, we focused on 27-hydroxycholesterol due to its abundance in human plasma (Dzeletovic et al., 1995). To examine the role of calcium influx on oxysterol protection against pyolysin, HeLa cells were cultured for 24 h in serum-free medium containing vehicle or 10 ng/ml 27-hydroxycholesterol. Supernatants were discarded, and cells were washed twice with calcium-free DPBS (#14190250; Thermo Fisher Scientific). Cells were challenged for 2 h with a control or pyolysin challenge (100 HU) prepared in control medium (1.8 mM CaCl₂) or calcium-free medium (#21068; Thermo Fisher Scientific) to impair calcium ion influx. After the challenge period, supernatants were collected to measure the leakage of LDH, and cell viability was measured using an MTT assay.

To examine the role of potassium efflux on oxysterol protection against pyolysin, HeLa cells were cultured for 24 h in serum-free medium containing vehicle or 10 ng/ml 27-hydroxycholesterol. Pyolysin challenge (100 HU) was prepared in control serum-free medium (5.3 mM KCl), low-potassium medium (5 mM KCl, 140 mM NaCl, 10 mM Hepes, 1.3 mM CaCl₂, 0.5 mM MgCl₂, 0.36 mM K₂HPO₄, 0.44 mM KH₂PO₄, 5.5 mM D-glucose, 4.2 mM NaHCO₃) or high-potassium medium (140 mM KCl, 5 mM NaCl, 10 mM Hepes, 1.3 mM CaCl₂, 0.5 mM MgCl₂, 0.36 mM K₂HPO₄, 0.44 mM KH₂PO₄, 5.5 mM D-glucose, 4.2 mM NaHCO₃) to prevent potassium efflux (Gurcel et al., 2006). Cells were washed twice with control, low-potassium, or high-potassium medium prior to a 2 h challenge. Supernatants were collected to measure the leakage of LDH, and cell viability was measured using an MTT assay.

To examine the role of LXR α and LXR β in oxysterol cytoprotection, we used short-interfering ribonucleic acid (siRNA) to target *NR1H3* and *NR1H2*, respectively. HeLa cells were transfected with scramble siRNA, or siRNA designed using Dharmacon siDESIGN Centre to target *NR1H3* and *NR1H2* (described in *Chapter 2*). A mixture of 20 pmol of siRNA, 100 μ l Opti-MEM 1 medium and 1.5 μ l Lipofectamine RNAiMAX Reagent were added to each well of a 24-well plate and incubated for 20 min, then 4 x 10⁴ cells HeLa cells were seeded in 900 μ l DMEM medium supplemented with 10% FBS for 48 h. Quantitative polymerase chain reaction was performed on cells to validate the effectiveness of the siRNA as described in *Chapter 2*. Supernatants were discarded and cells were treated with vehicle, 10 ng/ml 27-hydroxycholesterol, or 50 nM T0901317 for 24 h in serum-free culture medium prior to a 2 h challenge with control medium or medium containing 100 HU pyolysin. At the end of the challenge period, supernatants were collected to measure LDH leakage and cell viability was measured using an MTT assay.

4.2.2 Potassium

The leakage of potassium from cells was measured to assess whether treatments prevented toxins forming pores in the cell membrane. HeLa or A549 cells were seeded at a density of 1.5 x 10⁵ cells/well in 3 ml/well complete medium using 6-well culture plates and incubated for 24 h, before a 24 h treatment with 3 ml/well serum-free medium containing vehicle, 25-hydroxycholesterol, 27-hydroxycholesterol (concentrations specified in *Results*), 50 nM T0901317, or 1 mM methyl- β -

cyclodextrin (M β CD, #C4555; Merck) as a control known to protect HeLa cells against pyolysin by depleting cellular cholesterol (Preta et al., 2015). Supernatants were discarded, and the cells were washed three times with potassium-free buffer (129 mM choline-Cl, 0.8 mM MgCl₂, 1.5 mM CaCl₂, 5 mM citric acid, 5.6 mM glucose, 10 mM NH₄Cl, 5 mM H₃PO₄, pH 7.4; all Merck), and then incubated in potassium-free buffer with the indicated concentration of pyolysin for 5 min at 37°C. Alternatively, cells were incubated in potassium-free buffer with control medium or 8 μ g/5 \times 10⁴ cells α -hemolysin for 15 min (no potassium leakage was visible from HeLa cells after 5 min of α -hemolysin challenge). Supernatants were collected and potassium was measured using a Jenway PFP7 flame photometer as described in *Chapter 2*.

4.2.3 Cholesterol

To quantify the cellular cholesterol concentrations of HeLa cells (1.5 \times 10⁵ cells /well) were seeded in 3 ml/well complete medium using 6-well culture plates for 24 h. Cells were treated with vehicle, 10 ng/ml 25-hydroxycholesterol, 10 ng/ml 27-hydroxycholesterol, or 1 mM M β CD in 3 ml/well serum-free medium for a further 24 h. After the treatment period, cells were washed twice with DPBS then collected in 250 μ l/ well cholesterol assay 1X Reaction Buffer and stored at -20°C. Cellular cholesterol was measured using the Amplex Red Cholesterol Assay Kit as described in *Chapter 2*. Protein abundance was measured in samples using a DC protein assay (Bio-Rad), and cholesterol concentrations were normalized to protein concentrations.

4.2.4 Immunofluorescence

Staining cells with phalloidin as described previously, visualized cell damage (Turner et al., 2020). Briefly, 4 \times 10⁴ HeLa and A549 cells per well were cultured on glass cover slips in 24-well culture plates in complete-medium for 24 h, before a 24 h treatment in serum-free medium containing vehicle, 25-hydroxycholesterol, 27-hydroxycholesterol (concentrations specified in *Results*), 50 nM T0901317, 125 nM GW3965, or 1 mM M β CD as a control to deplete cellular cholesterol. The supernatants were discarded, and the cells challenged with control medium or medium containing pyolysin for 2 h, or α -hemolysin for 24 h. At the end of the challenge period cells were stained with Alexa Fluor 555-conjugated phalloidin and 4,6-diamidino-2-phenylindole (DAPI) and then imaged as described in *Chapter 2*. The proportion of cells that had cytoskeletal changes (cytoskeletal contraction, disrupted shape, or loss of actin fibre

definition) were counted using >135 cells per treatment across 3 independent images per replicate.

4.2.5 Western Blotting

First, we explored the effects of oxysterol treatment on pyolysin induced MAPK signalling. HeLa cells were seeded at a density of 1.5×10^5 cells/well in 3 ml/well complete medium using 6-well culture plates for 24 h, and then treated for 24 h in 3 ml/well serum-free medium containing vehicle, 10 ng/ml 27-hydroxycholesterol, or 50 nM T0901317, then challenge with control serum-free medium or medium containing 100 HU pyolysin for 10 min. Secondly, we investigated the effect of oxysterol treatment on the abundance of membrane bound pyolysin. HeLa cells were seeded at 1.5×10^5 cells/well on 6-well plates in complete medium for 24 h, and then treated for 24 h in serum-free medium containing vehicle, 10 ng/ml 27-hydroxycholesterol, 50 nM T0901317, before a 2 h challenge with control serum-free medium or medium containing 100 HU pyolysin. Supernatants were discarded, cells were washed with 300 μ l ice cold PBS, and lysed with 100 μ l PhosphoSafe Extraction Reagent. Protein isolation and Western blotting were performed as described in *Chapter 2*. The average peak density of bands was quantified and normalized to α -tubulin using Fiji (Schindelin et al., 2012). Phosphorylated proteins were normalized to their cognate total protein.

4.2.6 Statistical analysis

The statistical unit was each independent passage of the relevant cell line. Statistical analysis was performed using GraphPad Prism 9.0.1. Data are reported as arithmetic mean (SEM), and significance attributed when $P < 0.05$. Comparisons between treatments or challenges were made using analysis of variance (ANOVA) followed by Dunnett, Bonferroni or Tukey post hoc test for multiple comparisons, or unpaired two-tailed Student's t-test as specified in *Results*.

4.3 RESULTS

4.3.1 Side-chain oxysterol cytoprotection against pyolysin in HeLa cells

HeLa cells were challenged with a range of concentrations of pyolysin to determine the amount required to damage cells (Fig 4.1). We evaluated pyolysin-induced pore-formation in HeLa cells, identifying the concentration-dependent leakage of potassium ions into cell supernatants after 5 min (Fig 4.1A), leakage of LDH after 2 h (Fig 4.1B) and cytolysis, evaluated by the MTT cell viability assay (Fig 4.1C).

Additionally, we examined the effect of pyolysin on cell morphology. Pyolysin challenge caused cell fragmentation and induced the formation of large plasma membrane blebs (representative examples displayed in Fig 4.2). The proportion of fragmented cells following pyolysin challenge increased in a concentration dependent manner (Fig 4.3, 4.4). Interestingly the plasma membrane blebs were not always apparent in cells challenged with > 100 HU pyolysin, with cells losing all structural integrity. This suggests that pyolysin damages causes cells to progress from a normal to a blebbing and finally a fragmented phenotype. For subsequent cytoprotection experiments, we selected a 100 HU pyolysin challenge that increased potassium and LDH leakage ($P < 0.001$, ANOVA and Dunnett's post hoc test, $n=4$) and caused cytolysis, reducing cell viability by >80%.

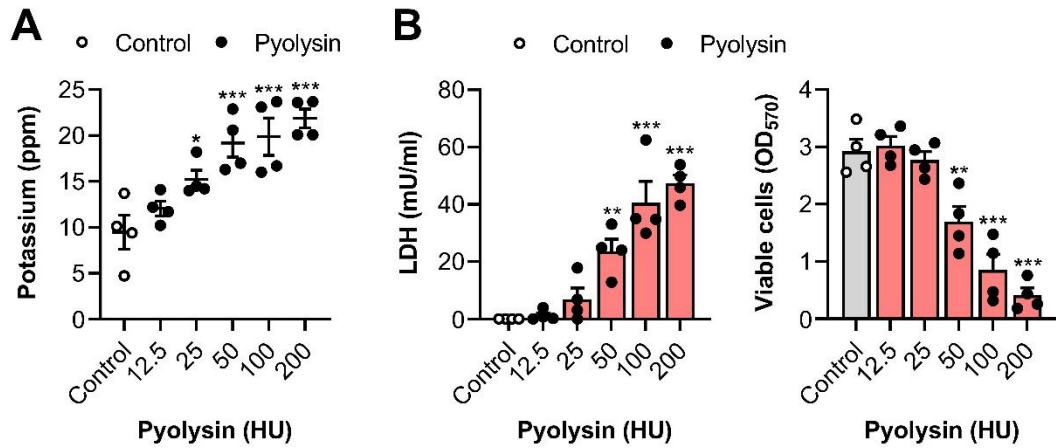


Figure 4.1 Pyolysin causes HeLa cell cytotoxicity

(A) Leakage of potassium from HeLa cells challenged for 5 min with control medium or pyolysin and (B) leakage of LDH into supernatants, and cell viability determined by MTT assay for HeLa cells challenged for 2 h with control medium or the indicated amount of pyolysin. Data are presented as mean (SEM) with dots representing the values from 4 independent experiments; statistical significance was determined using one-way ANOVA and Dunnett's post hoc test; *P < 0.05, **P < 0.01, ***P < 0.001.

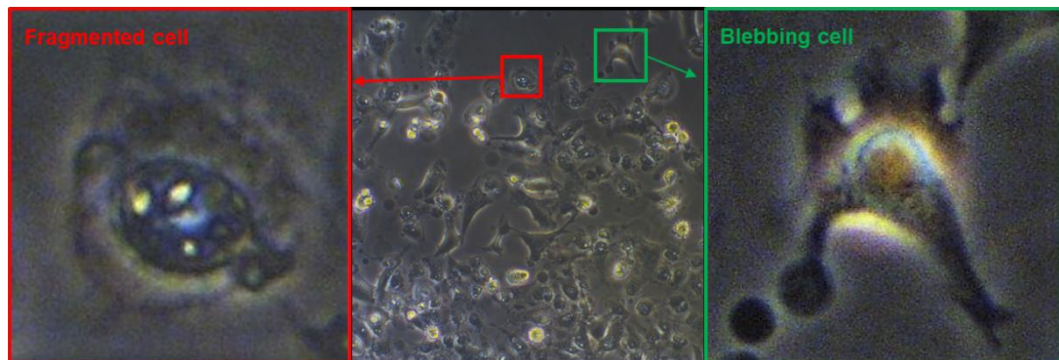


Figure 4.2 Pyolysin induces membrane blebbing and fragments HeLa cells

Phase contrast microscopy HeLa cells challenged for 2 h with control medium or 100 HU pyolysin. Images are representative of 3 independent experiments.

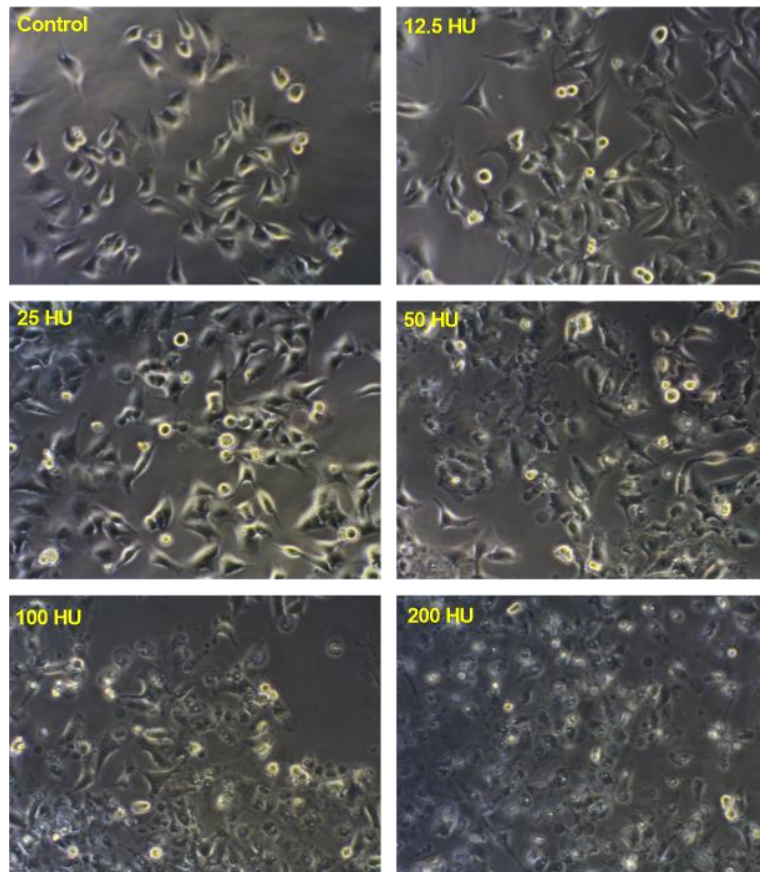


Figure 4.3 Pyolysin damages HeLa cells

Phase contrast microscopy of HeLa cells cultured for 24 h in serum-free medium, then challenged for 2 h with control medium or the indicated amount of pyolysin. Images are representative of 3 independent experiments.

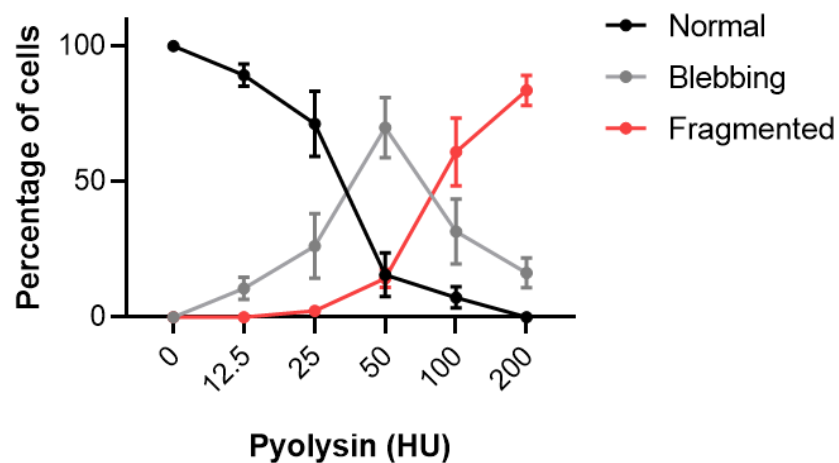


Figure 4.4 Pyolysin induces HeLa cell plasma membrane blebbing

Percentage of normal, blebbing, or fragmented HeLa cells treated for 24 h in serum-free medium, then challenged with the indicated amount of pyolysin for 2 h. Data are presented as mean (SEM) from 4 independent experiments.

To establish whether oxysterols would protect HeLa cells against pyolysin damage, cells were treated for 24 h with a range of concentrations of 25-hydroxycholesterol and 27-hydroxycholesterol. The cells were then challenged for 2 h with control medium or pyolysin in the absence of treatment. Pyolysin challenge resulted in the leakage of LDH into cell supernatants and cytolysis ($P < 0.001$, Fig 4.5A, B). However, treatment with 25-hydroxycholesterol (> 10 ng/ml) or 27-hydroxycholesterol (> 10 ng/ml) provided maximal protection against the pyolysin-induced leakage of LDH and cytolysis. The use of a control challenge showed that 27-hydroxycholesterol and 25-hydroxycholesterol did not significantly alter the leakage of LDH ($P > 0.97$) or the MTT assay ($P > 0.91$). For further experiments exploring side-chain oxysterol cytoprotection we selected 10 ng/ml 25-hydroxycholesterol and 10 ng/ml 27-hydroxycholesterol as these concentrations represented the lowest dose required to provide maximal protection.

To evaluate whether side-chain oxysterols protected against initial pyolysin pore formation, we measured the leakage of potassium into cell supernatants within 5 min of pyolysin challenge (Gonzalez et al., 2011, Turner et al., 2020). Prior to the pyolysin challenge HeLa cells were treated with 10 ng/ml 25-hydroxycholesterol, 10 ng/ml 27-hydroxycholesterol or 1 mM M β CD as a control to deplete cellular cholesterol (Preta et al., 2015). Pyolysin challenge caused potassium leakage in vehicle treated cells, but not in M β CD treated cells (Fig 4.5C). Significantly, 25-hydroxycholesterol and 27-hydroxycholesterol treatment also reduced pyolysin-induced potassium leakage. In independent experiments investigating the effect of treatment duration, cytoprotection was evident after 4 h ($P < 0.001$, ANOVA and Dunnett's post hoc test, $n = 5$, Fig 4.5D) and maximal with >12 h of treatment.

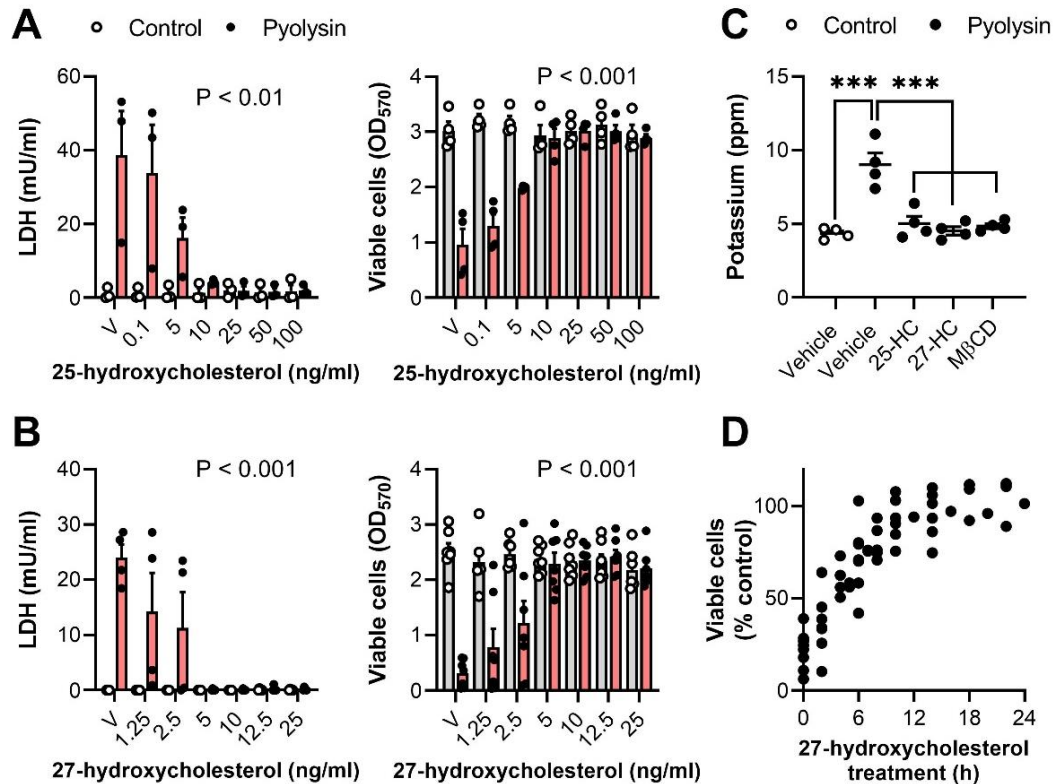


Figure 4.5 Side-chain oxysterols protect HeLa cells against pyolysin damage

(A,B) Leakage of LDH and viability of HeLa cells cultured for 24 h in serum-free medium containing vehicle (V) or the indicated concentrations of 25-hydroxycholesterol or 27-hydroxycholesterol and then challenged for 2 h with control medium or 100 HU pyolysin. Data are presented as mean (SEM) with dots representing values from cells from 4 independent experiments; statistical significance determined by two-way ANOVA and P-values are reported for the effect of treatment on pyolysin challenge. (C) Leakage of potassium from HeLa cells treated for 24 h with vehicle, 10 ng/ml 25-hydroxycholesterol (25-HC), 10 ng/ml 27-hydroxycholesterol (27-HC), or 1 mM MβCD, and then challenged for 5 min with control medium or 100 HU pyolysin. Dots represent individual values from 4 independent experiments; statistical significance was determined using one-way ANOVA with Dunnett's post hoc test; $***P < 0.001$. (D) Viability of HeLa cells treated for the indicated time periods with 10 ng/ml 27-hydroxycholesterol, and then challenged for 2 h with control medium or 100 HU pyolysin. Pyolysin data are presented as percentage viability of control challenge, with dots representing individual values across 1 to 6 independent experiments.

Staining cells with phalloidin visualized cell damage. Pyolysin challenge reduced actin fibre definition, causing the cytoskeleton to collapse around the nucleus, however, this was reduced by depleting cellular cholesterol using M β CD (16 ± 4 vs $83 \pm 5\%$ cells damaged, $P < 0.001$, ANOVA and Dunnett's post hoc test, $n = 3$, Fig 4.6). Both 25-hydroxycholesterol and 27-hydroxycholesterol treatment also reduced pyolysin-induced cytoskeletal changes in HeLa cells (20 ± 4 and 18 ± 5 vs $83 \pm 5\%$ cells damaged, $P < 0.001$, ANOVA and Dunnett's post hoc test, $n = 3$).

Large plasma membrane blebs were formed on HeLa cells challenged with pyolysin, and cells demonstrated a complete loss of shape and structure appearing fragmented. Treatment with 25-hydroxycholesterol, 27-hydroxycholesterol and M β CD reduced the formation of plasma membrane blebs ($P < 0.01$, ANOVA and Dunnett's post hoc test, Fig 4.7, Table 4.1), increasing the number of normal cells following pyolysin challenge ($P < 0.001$, ANOVA and Dunnett's post hoc test, Fig 4.7, Table 4.1), and preventing cell fragmentation ($P < 0.05$, ANOVA and Dunnett's post hoc test, Fig 4.7, Table 4.1). Together these data provide evidence for side-chain oxysterol cytoprotection of HeLa cells against pyolysin.

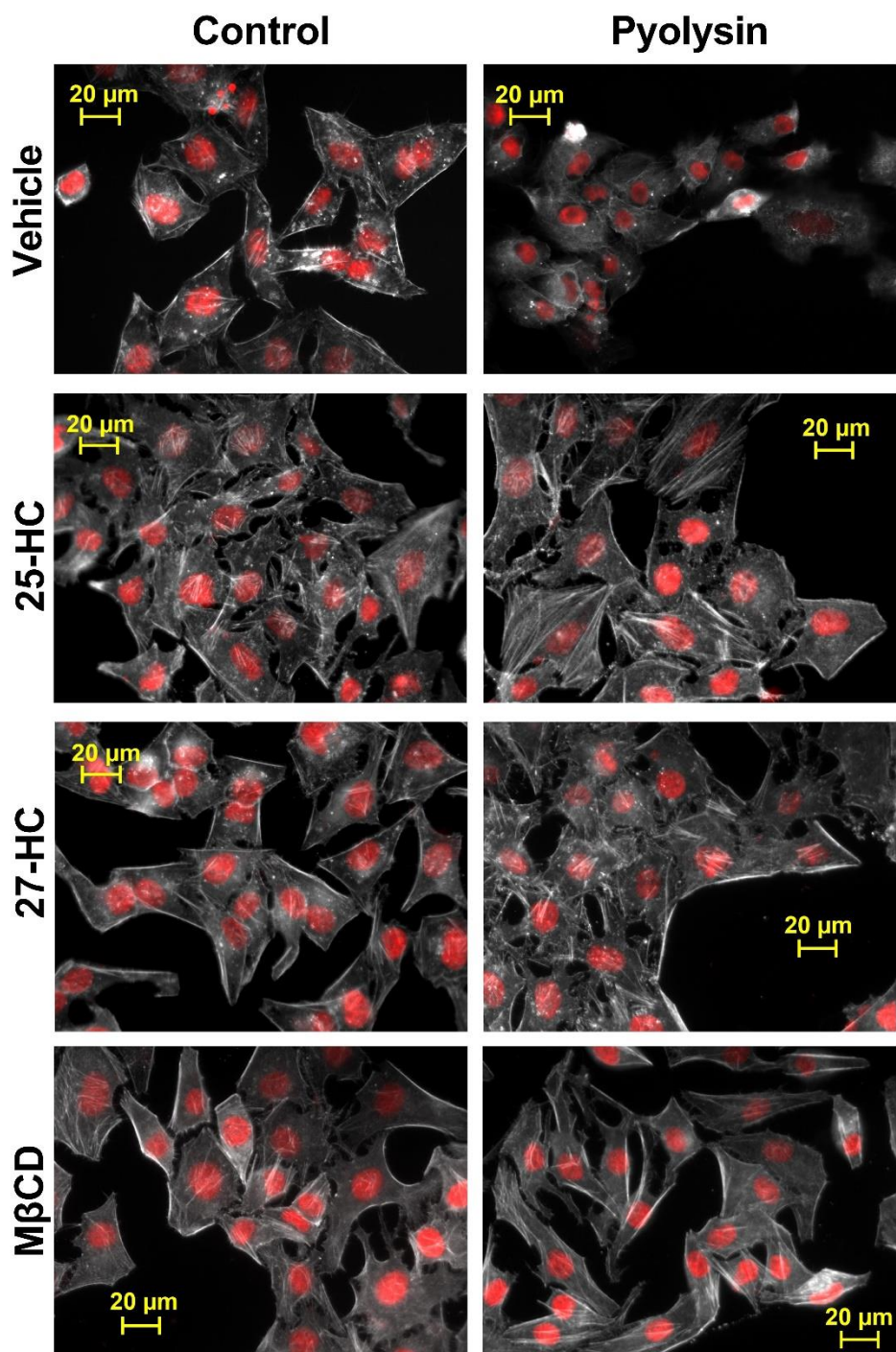


Figure 4.6 Side-chain oxysterols protect HeLa cells against pyolysin-induced actin cytoskeletal changes

Fluorescent microscope images of HeLa cells treated for 24 h with vehicle, 10 ng/ml 25-hydroxycholesterol (25-HC), 10 ng/ml 27-hydroxycholesterol (27-HC), or 1 mM M β CD, then challenged for 2 h with control medium or 100 HU pyolysin and stained with fluorescent phalloidin (white) and DAPI (red); images are representative from 4 independent experiments. Quantification of cytoskeletal changes are reported in text.

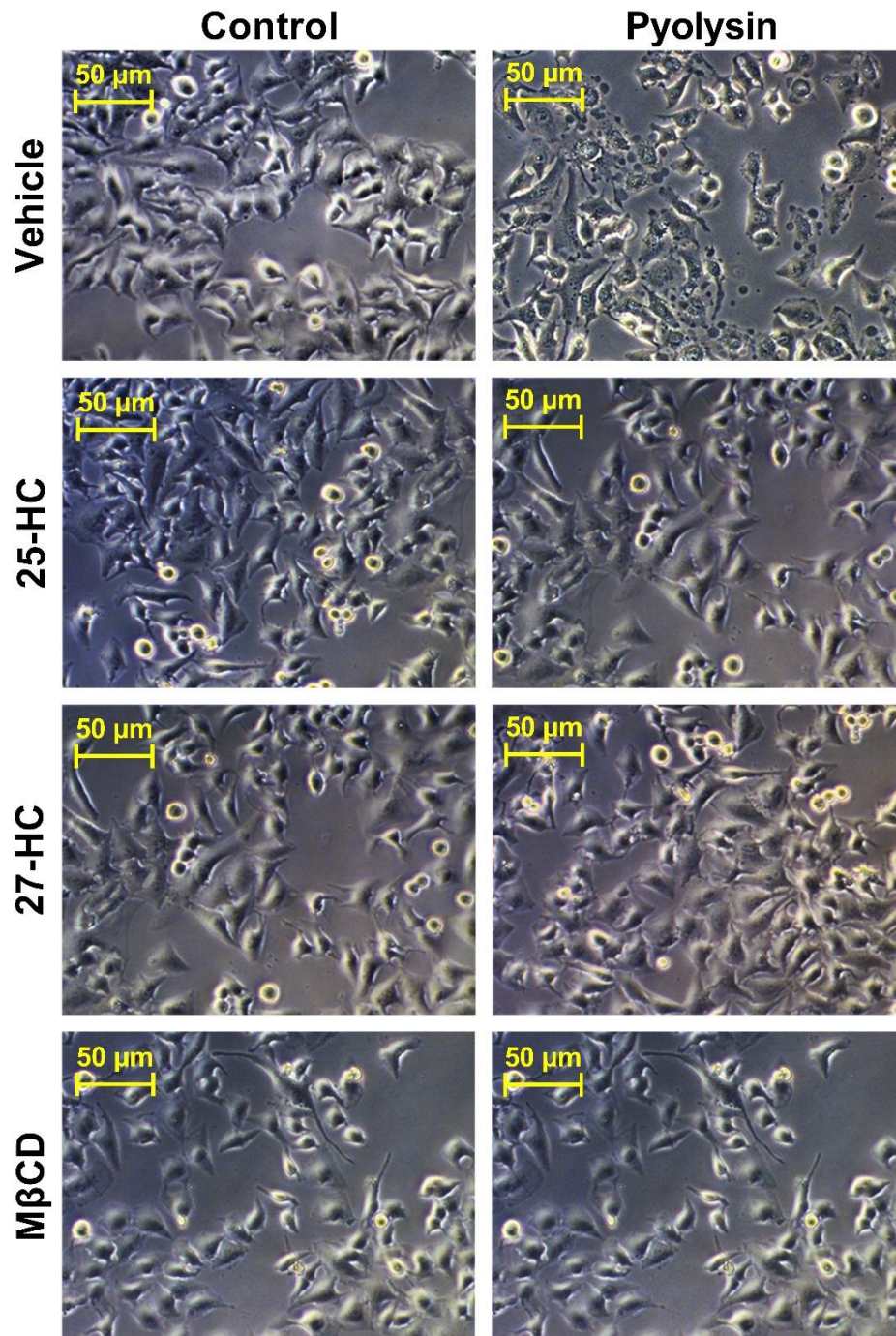


Figure 4.7 Oxysterols protect HeLa cells against pyolysin-induced blebbing

Phase contrast microscopy of HeLa cells treated for 24 h with vehicle, 10 ng/ml 25-hydroxycholesterol (25-HC), 10 ng/ml 27-hydroxycholesterol (27-HC), or 1 mM MβCD, then challenged for 2 h with control medium or 100 HU pyolysin; images are representative from 4 independent experiments, scale bars = 50 μm.

Table 4.1 Quantification of HeLa cell morphology after oxysterol treatment and pyolysin challenge

Percentage of normal, blebbing, or fragmented HeLa cells treated for 24 h with vehicle, 10 ng/ml 25-hydroxycholesterol, 10 ng/ml 27-hydroxycholesterol, or 1 mM M β CD, then challenged for 2 h with 100 HU pyolysin. Cells were imaged by phase contrast microscopy and categorized as normal, blebbed or fragmented, with >100 cells evaluated across two independent images per treatment replicate. Raw data were analyzed by ANOVA and Tukey's post hoc test with superscript indicating the differences between vehicle and treatments (*P<0.05, **P < 0.01, ***P < 0.001), and data are reported as mean \pm SEM for the pyolysin challenge as a percentage of the control challenge.

Treatment	Replicates	Percentage of cells		
		Normal	Blebbing	Fragmented
Vehicle	7	15 \pm 5	43 \pm 7	42 \pm 10
25-hydroxycholesterol	3	95 \pm 2 ***	1 \pm 1 **	4 \pm 2 *
27-hydroxycholesterol	5	91 \pm 3 ***	3 \pm 1 ***	6 \pm 2 *
M β CD	3	86 \pm 4 ***	6 \pm 1 **	8 \pm 3 *

4.3.2 Side-chain oxysterol cytoprotection against pyolysin is generalized

To establish if oxysterol cytoprotection against pyolysin was generalized beyond HeLa cervical cells, we tested A549 lung alveolar epithelial cells because they are often used to study cholesterol-dependent cytolysins (Mestre and Colombo, 2012, Statt et al., 2015). Hep-G2 liver cells and NC1-H441 lung cells were used to provide additional validation as these cells were also susceptible to pyolysin damage (Fig 4.8). We first determined the amount of pyolysin required to damage cells, selecting challenges that caused LDH leakage and cytolysis in A549 (25 HU/well; P < 0.001, ANOVA and Dunnett's post hoc test, n=4, Fig 4.8A), Hep-G2 (100 HU/well; P < 0.001, ANOVA and Dunnett's post hoc test, n=4, Fig 4.8B) and NC1-H441 (200 HU/well; P < 0.001, ANOVA and Dunnett's post hoc test, n = 4, Fig 4.8C) cells.

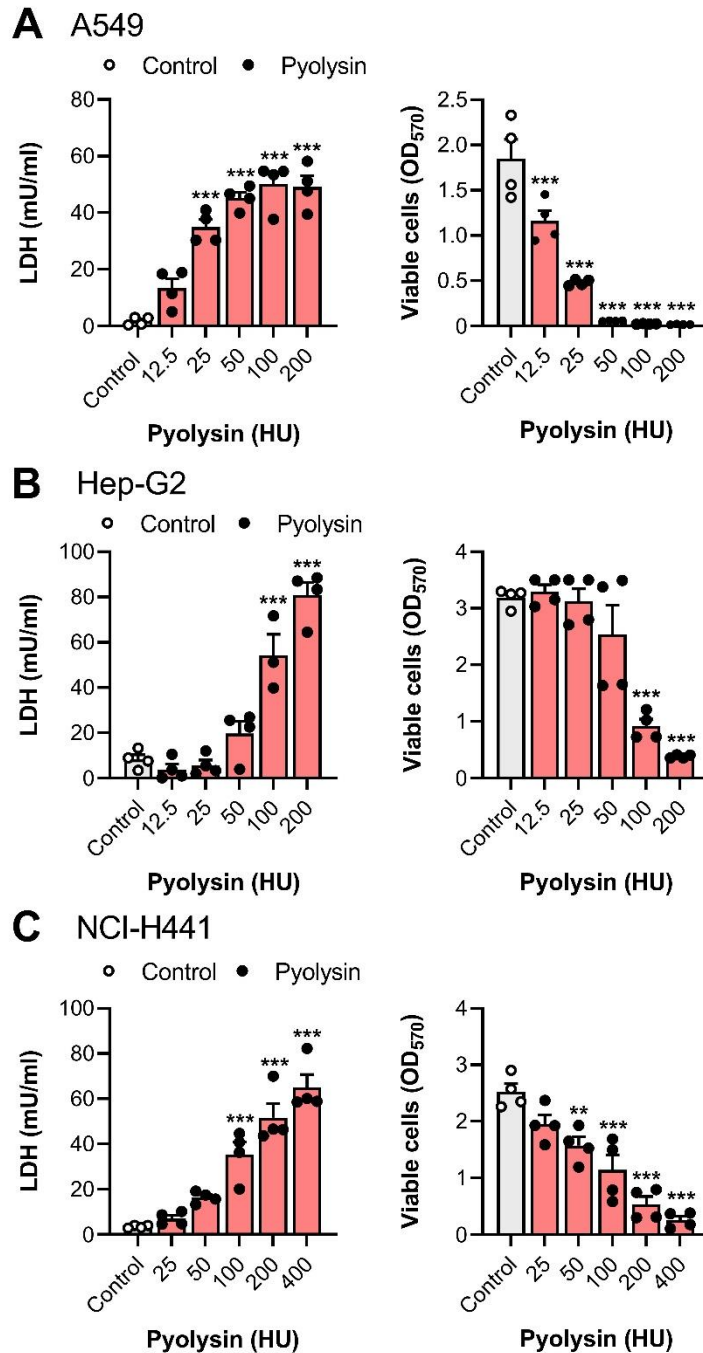


Figure 4.8 Cytolytic activity of pyolysin in A549, Hep-G2 and NC1-H441 cells
 Leakage of LDH into supernatants, and cell viability determined by MTT assay for (A) A549, (B) Hep-G2, and (C) NC1-H441 cells challenged for 2 h with control medium or pyolysin. Data are presented as mean (SEM) with dots representing the values from 4 independent experiments; statistical significance was determined using one-way ANOVA and Dunnett's post hoc test; **P < 0.01, ***P < 0.001.

Having established suitable pyolysin challenge concentrations, we treated A549 cells with 25-hydroxycholesterol or 27-hydroxycholesterol for 24 h and then challenged them with control medium or pyolysin for 2 h. Pyolysin challenge caused LDH leakage and cytolysis compared with control challenge ($P < 0.001$ Fig. 4.9A,B). Treatment with 25-hydroxycholesterol and 27-hydroxycholesterol reduced pyolysin-induced LDH leakage and cytolysis. Specifically, pyolysin induced LDH leakage was reduced by 90.5% and 80% by 50 ng/ml 25-hydroxycholesterol and 25 ng/ml 27-hydroxycholesterol respectively, therefore these concentrations were used for additional cytoprotective experiments in A549 cells. Vehicle treated A549 cells leaked potassium ions after a 5 min pyolysin challenge ($P < 0.001$, Fig. 4.9C), however, this leakage was reduced by 25-hydroxycholesterol, 27-hydroxycholesterol or M β CD treatment. A 2 h pyolysin challenge resulted in morphological and cytoskeletal changes in A549 cells (Fig 4.10). Treatment with both 25- and 27-hydroxycholesterol prevented pyolysin-induced actin changes as effectively as depleting cellular cholesterol with M β CD (15 ± 5 , 17 ± 3 , and 14 ± 2 vs $73 \pm 3\%$ cells damaged, $P < 0.001$, ANOVA and Dunnett's post hoc test, $n = 3$), with cells largely maintaining the morphology observed in control challenged cells. In addition, 27-hydroxycholesterol protected Hep-G2 and NC1-H441 cells against pyolysin challenge, reducing LDH leakage by 58% and 59% respectively, as well as reducing cytolysis (Fig 4.11). Together this data provide evidence that side-chain oxysterols protect multiple cell lines against pyolysin challenge.

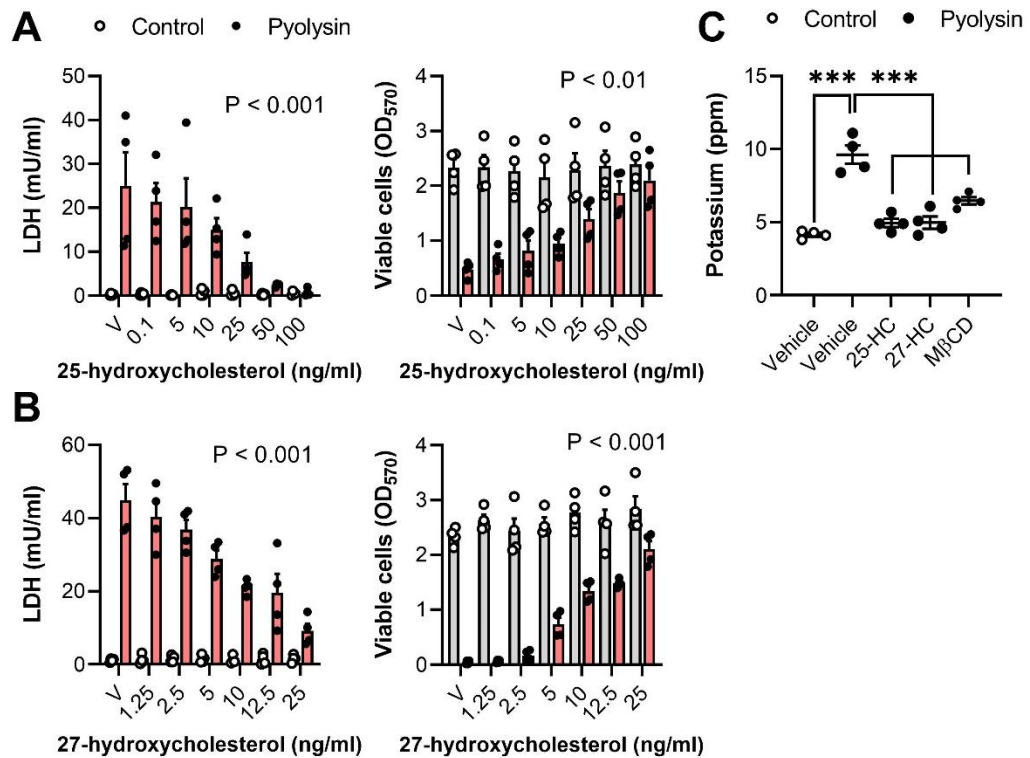


Figure 4.9 Side-chain oxysterols protect A549 cells against pyolysin damage

(A,B) Leakage of LDH and viability of A549 cells cultured for 24 h in serum-free medium containing vehicle (V) or the indicated concentrations of 25-hydroxycholesterol or 27-hydroxycholesterol and then challenged for 2 h with control medium or 25 HU pyolysin. Data are presented as mean (SEM) with dots representing values from cells from 4 independent experiments; statistical significance determined by two-way ANOVA and P-values are reported for the effect of treatment on pyolysin challenge. (C) Leakage of potassium from A549 cells treated for 24 h with vehicle, 50 ng/ml 25-hydroxycholesterol (25-HC), 25 ng/ml 27-hydroxycholesterol (27-HC), or 1 mM M β CD, and then challenged for 5 min with control medium or 25 HU pyolysin. Dots represent individual values from 4 independent experiments; statistical significance was determined using one-way ANOVA with Dunnett's post hoc test; ***P < 0.001.

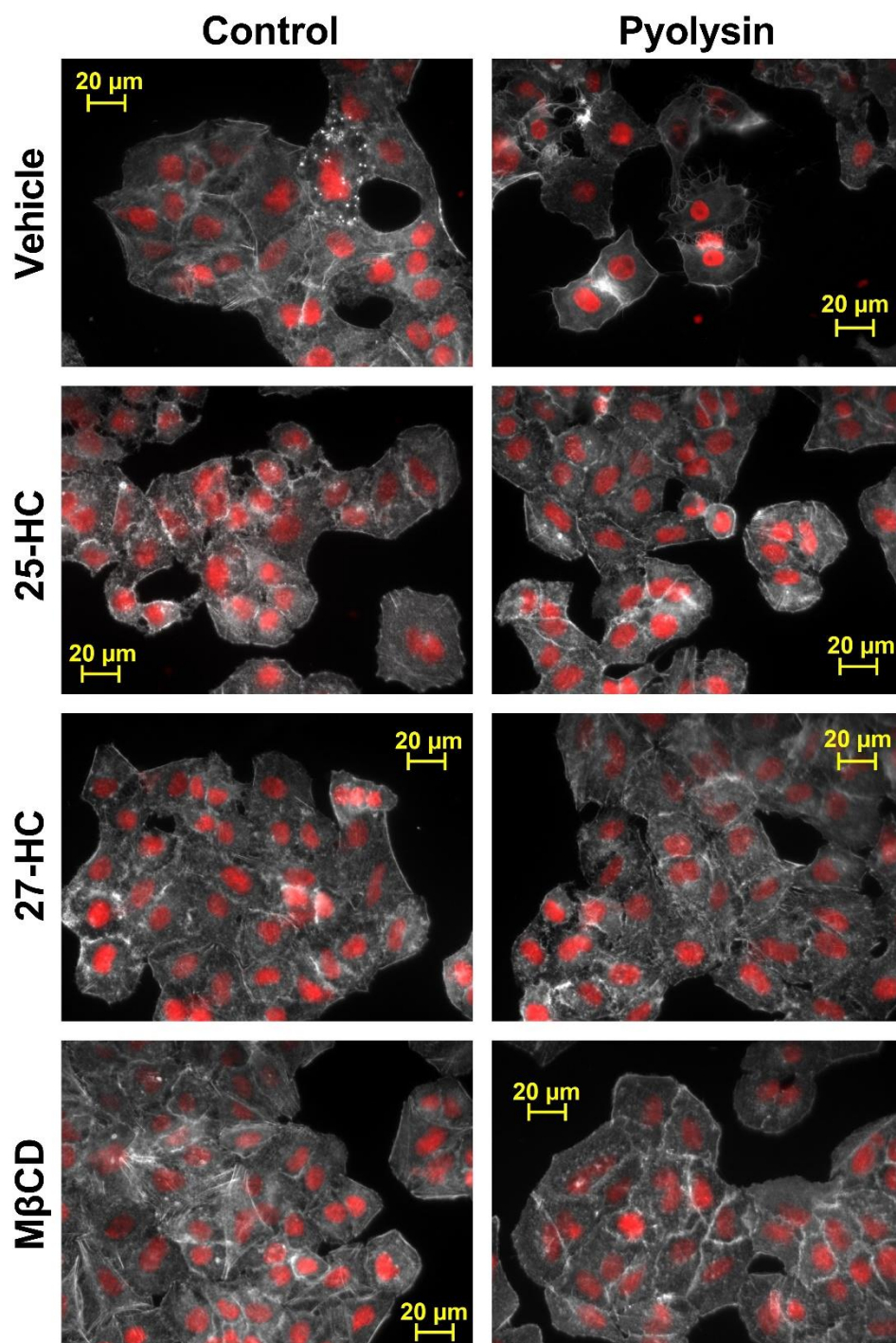


Figure 4.10 Oxysterols protect A549 cells against pyolysin-induced actin cytoskeletal changes

Fluorescent microscope images of A549 cells treated for 24 h with vehicle, 50 ng/ml 25-hydroxycholesterol (25-HC), 25 ng/ml 27-hydroxycholesterol (27-HC), or 1mM MβCD then challenged for 2 h with control medium or 25 HU pyolysin and stained with fluorescent phalloidin (white) and DAPI (red); images are representative from 4 independent experiments. Quantification of cytoskeletal changes are reported in text.

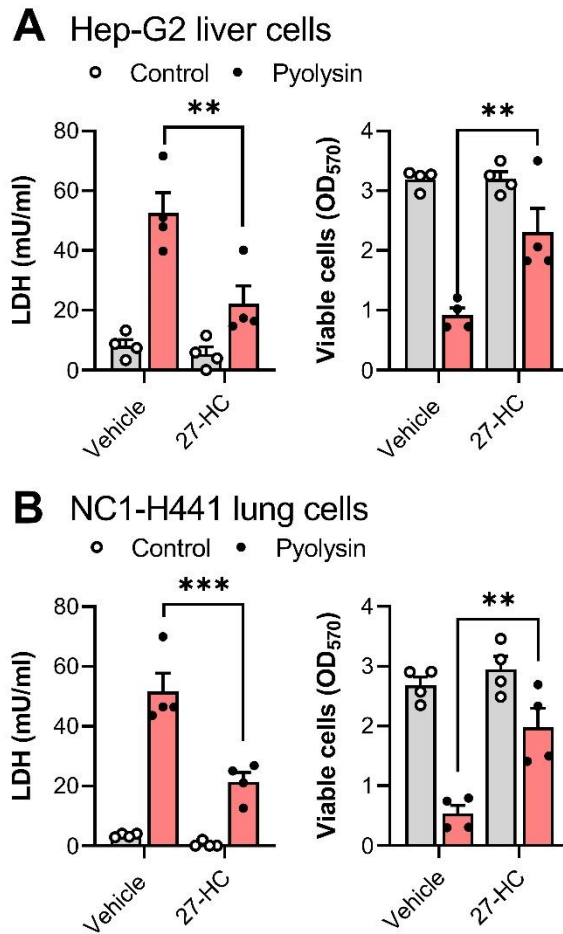


Figure 4.11 27-hydroxycholesterol cytoprotection in Hep-G2 and NC1-H44 cells. Leakage of LDH and viability of (A) Hep-G2 and (B) NCI-H441 cells treated for 24 h with vehicle or 10 ng/ml 27-hydroxycholesterol (27-HC), and then challenged for 2 h with control medium or pyolysin (Hep-G2, 100 HU; NC1-H441, 200 HU). Data are presented as mean (SEM) from 4 independent experiments; statistical significance was determined using two-way ANOVA and Bonferroni's post hoc test; ** $P < 0.01$, *** $P < 0.001$.

4.3.3 Side-chain oxysterols protect cells against α -hemolysin

To explore if side-chain oxysterol cytoprotection extended beyond cholesterol-dependent cytolysins, we also examined protection against a member of the hemolysin family of cytolysins, *S. aureus* α -hemolysin (Seilie and Bubeck Wardenburg, 2017, Song et al., 1996). α -hemolysin forms pores with an 18 nm internal diameter compared to the 1.4 nm diameter transmembrane pores formed by *S. aureus* α -hemolysin (Preta et al., 2016, Song et al., 1996). Therefore, differing cytolytic activities are expected. To determine a suitable α -hemolysin challenge a range of durations and concentrations were explored in HeLa (Fig 4.12) and A549 (Fig 4.13) cells. For cytoprotection experiments we selected a 24 h 8 μ g α -hemolysin as it caused LDH leakage and cytolysis in both HeLa and A549 cells.

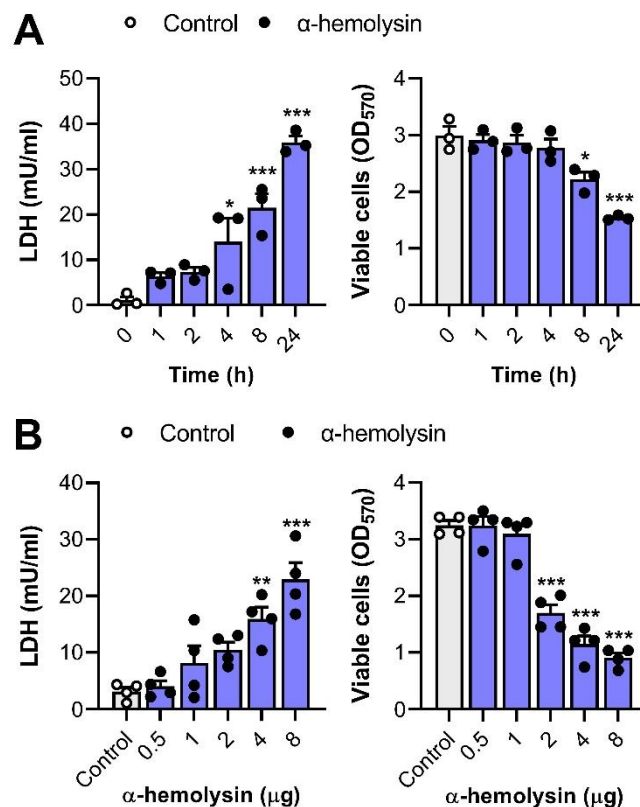


Figure 4.12 Cytolytic activity of *S. aureus* α -hemolysin in HeLa cells

HeLa cells were cultured for 24 h in serum-free medium and then (A) challenged for the indicated times with control serum-free medium or 8 μ g α -hemolysin, or (B) for the 24 h with control medium or the indicated concentration of α -hemolysin. The leakage of LDH was measured in cell supernatants and cell viability was determined by MTT. Data are presented as mean (SEM) from 4 independent experiments; statistical significance was determined using one-way ANOVA and Dunnett's post hoc test; *P < 0.05, **P < 0.01, ***P < 0.001.

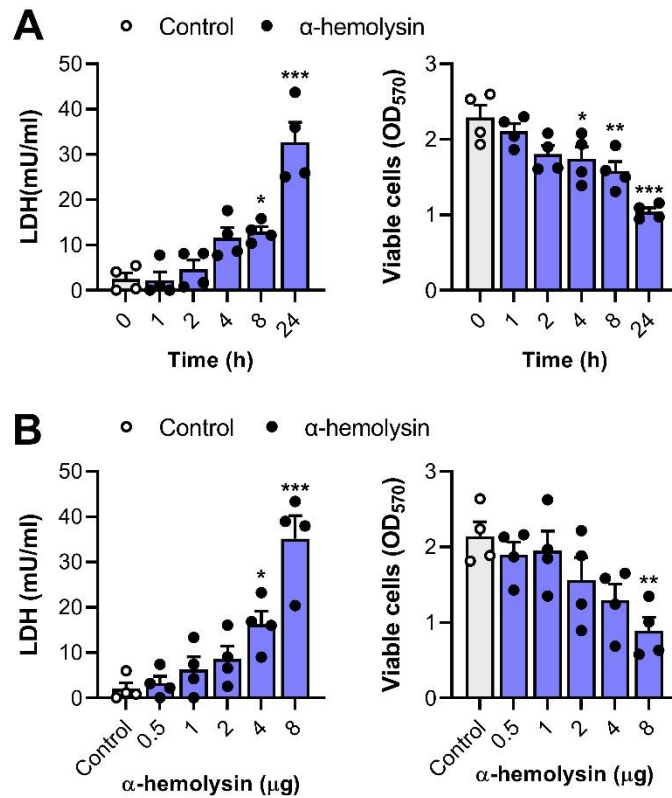


Figure 4.13 Cytolytic activity of *S. aureus* α -hemolysin in A549 cells

A549 cells were cultured for 24 h in serum-free medium and then (A) challenged for the indicated times with control serum-free medium or 8 μ g α -hemolysin, or (B) for 24 h with control medium or the indicated concentration of α -hemolysin. The leakage of LDH was measured in cell supernatants and cell viability was determined by MTT assay. Data are presented as mean (SEM) from 4 independent experiments; statistical significance was determined using one-way ANOVA and Dunnett's post hoc test; *P < 0.05, **P < 0.01, ***P < 0.001.

To examine side-chain oxysterol protection against α -hemolysin, we treated HeLa and A549 cells with 25-hydroxycholesterol or 27-hydroxycholesterol for 24 h and then challenged cells for 24 h with *S. aureus* α -hemolysin. The α -hemolysin challenge caused potassium ion leakage, LDH leakage, and cytolysis in HeLa (Fig 4.14) and A549 cells (Fig 4.14). Treatment with 27-hydroxycholesterol prevented cytolysis and reduced LDH leakage by 83% and 86% in HeLa (Fig 4.14A) and A549 (Fig 4.15A) cells respectively. Additionally, treatment with 25-hydroxycholesterol or 27-hydroxycholesterol reduced the pyolysin-induced leakage of potassium ions compared with vehicle treatment in both cell lines (Fig 4.14B. Fig 4.15B). Treatment with 27-hydroxycholesterol also reduced α -hemolysin induced cytoskeletal changes in HeLa (35 ± 1 vs $85 \pm 3\%$ cells damaged, t-test, $n = 3$, $P < 0.001$, Fig 4.14C) and A549 (18 ± 4 vs $84 \pm 6\%$ cells damaged, t-test, $n = 3$, $P < 0.01$, Fig 4.15C) cells. Together this data provide evidence that side-chain oxysterols protect cells against *S. aureus* α -hemolysin.

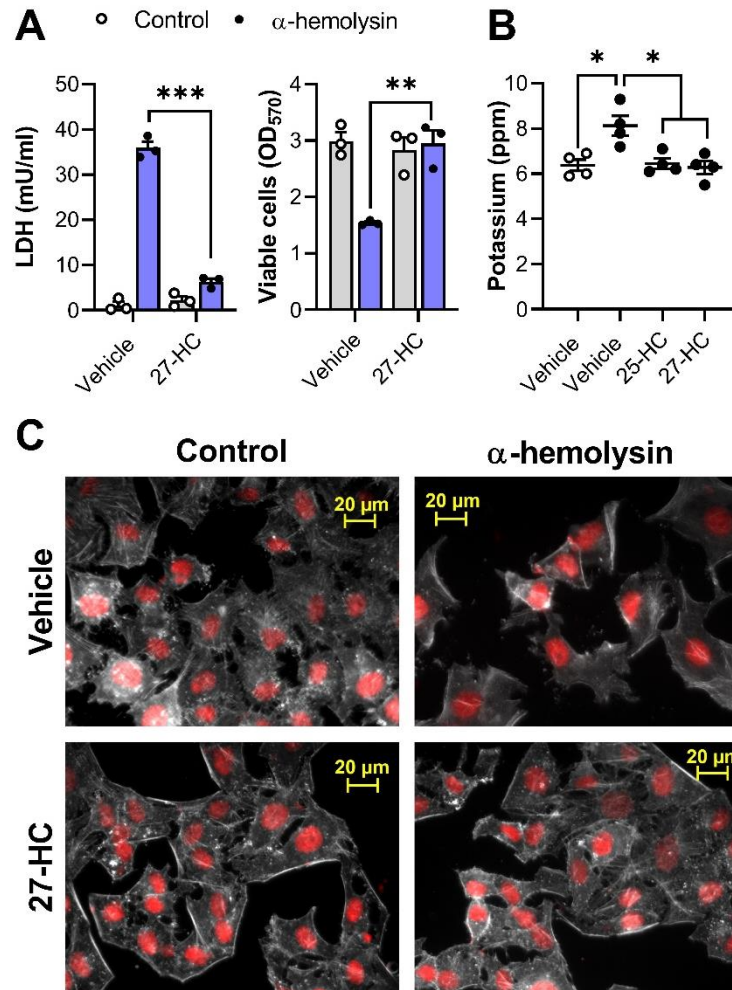


Figure 4.14 27-hydroxycholesterol protects HeLa cells against α -hemolysin

(A) Leakage of LDH and viability of HeLa cells treated for 24 h with vehicle or 10 ng/ml 27-hydroxycholesterol (27-HC), and then challenged for 24 h with 8 μ g α -hemolysin. Data are presented as mean (SEM) from 4 independent experiments; statistical significance was determined using two-way ANOVA and Bonferroni's post hoc test; ** $P < 0.01$, *** $P < 0.001$. (B) Leakage of potassium from HeLa cells treated for 24 h with vehicle, 10 ng/ml 25-hydroxycholesterol, or 10 ng/ml 27-hydroxycholesterol and then challenged for 15 min with control medium or 8 μ g α -hemolysin. Dots represent individual values from 4 independent experiments; statistical significance was determined using one-way ANOVA with Dunnett's post hoc test; * $P < 0.05$. (C) Fluorescent microscope images of HeLa cells treated for 24 h with vehicle or 10 ng/ml 27-hydroxycholesterol, then challenged for 24 h with control medium or 8 μ g α -hemolysin and stained with fluorescent phalloidin (white) and DAPI (red); images are representative from 3 independent experiments. Quantification of cytoskeletal changes are reported in text.

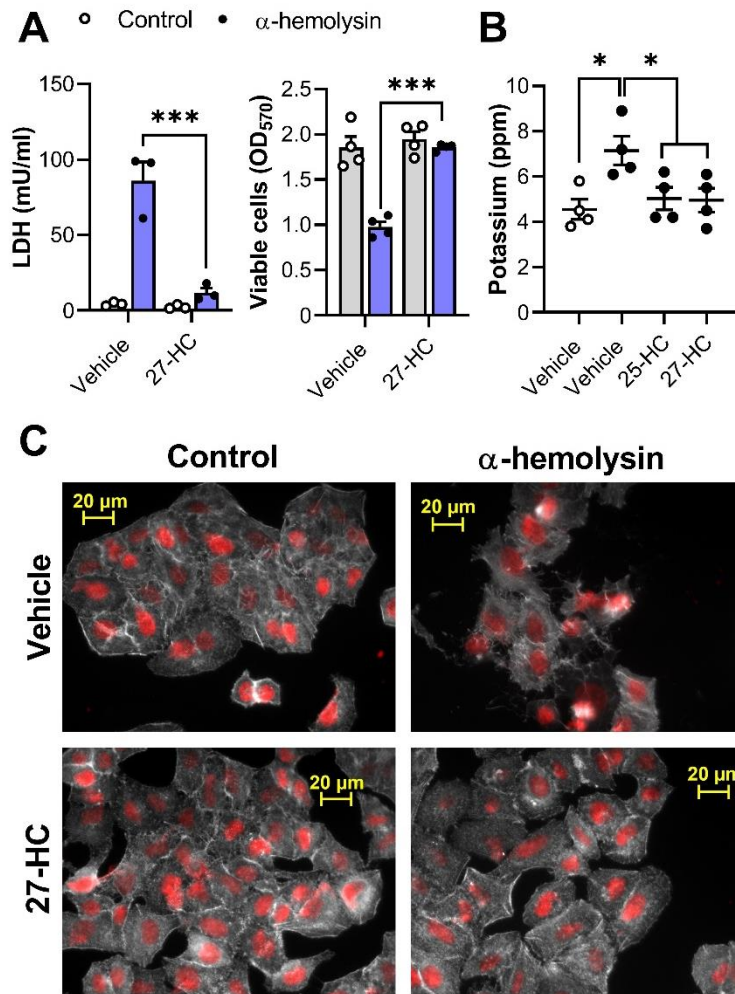


Figure 4.15: 27-hydroxycholesterol protects A549 cells against α -hemolysin.

(A) Leakage of LDH and viability of A549 cells treated for 24 h with vehicle or 25 ng/ml 27-hydroxycholesterol (27-HC), and then challenged for 24 h with 8 μ g α -hemolysin. Data are presented as mean (SEM) from 4 independent experiments; statistical significance was determined using two-way ANOVA and Bonferroni's post hoc test; *** $P < 0.001$. (B) Leakage of potassium from A549 cells treated for 24 h with vehicle, 50 ng/ml 25-hydroxycholesterol, or 25 ng/ml 27-hydroxycholesterol challenged for 15 min with control medium or 8 μ g α -hemolysin. Dots represent individual values from 4 independent experiments; statistical significance was determined using one-way ANOVA with Dunnett's post hoc test; * $P < 0.05$. (C) Fluorescent microscope images of A549 cells treated for 24 h with vehicle or 25 ng/ml 27-hydroxycholesterol, then challenged for 24 h with control medium or 8 μ g α -hemolysin and stained with fluorescent phalloidin (white) and DAPI (red); images are representative from 3 independent experiments. Quantification of cytoskeletal changes are reported in text.

4.3.4 Cellular cholesterol

Plasma membrane cholesterol is a requirement for pyolysin binding and pore-formation (Billington et al., 1997). Depleting total cellular cholesterol using cyclodextrins reduces pyolysin-induced cell damage (Amos et al., 2014). A 24 h treatment with 1 mM M β CD reduced cholesterol in HeLa cells by 49% compared with vehicle treated cells (Fig 4.16A). However, neither 25-hydroxycholesterol ($P = 0.99$) or 27-hydroxycholesterol ($P = 0.97$) significantly altered total cellular cholesterol.

Serum free medium was used for experiments exploring the effect of oxysterol treatment on cytoprotection, however, to determine whether serum affected cytoprotection, HeLa cells were treated for 24 h with 25-hydroxycholesterol in medium containing 10% fetal calf serum, before a 2 h pyolysin challenge in serum-free medium. The presence of 10% serum did not prevent 25-hydroxycholesterol protection against pyolysin induced LDH leakage or cytolysis (Fig 4.16B), however, in the presence of serum 100 ng/ml 25-hydroxycholesterol was required to provide maximal protection as opposed to 10 ng/ml in serum-free medium (Fig 4.16C).

To address a concern that side-chain oxysterols might prevent cytolysis by binding to residual treatment in wells, we prepared pyolysin challenges in medium containing 25-hydroxycholesterol, 27-hydroxycholesterol, or cholesterol, before challenging HeLa cells for 2 h. Unlike cholesterol, coincubation with side-chain oxysterols did not affect the cytolytic activity of pyolysin, providing some evidence to suggest that the oxysterols do not protect cells by binding to pyolysin (Fig 4.16D).

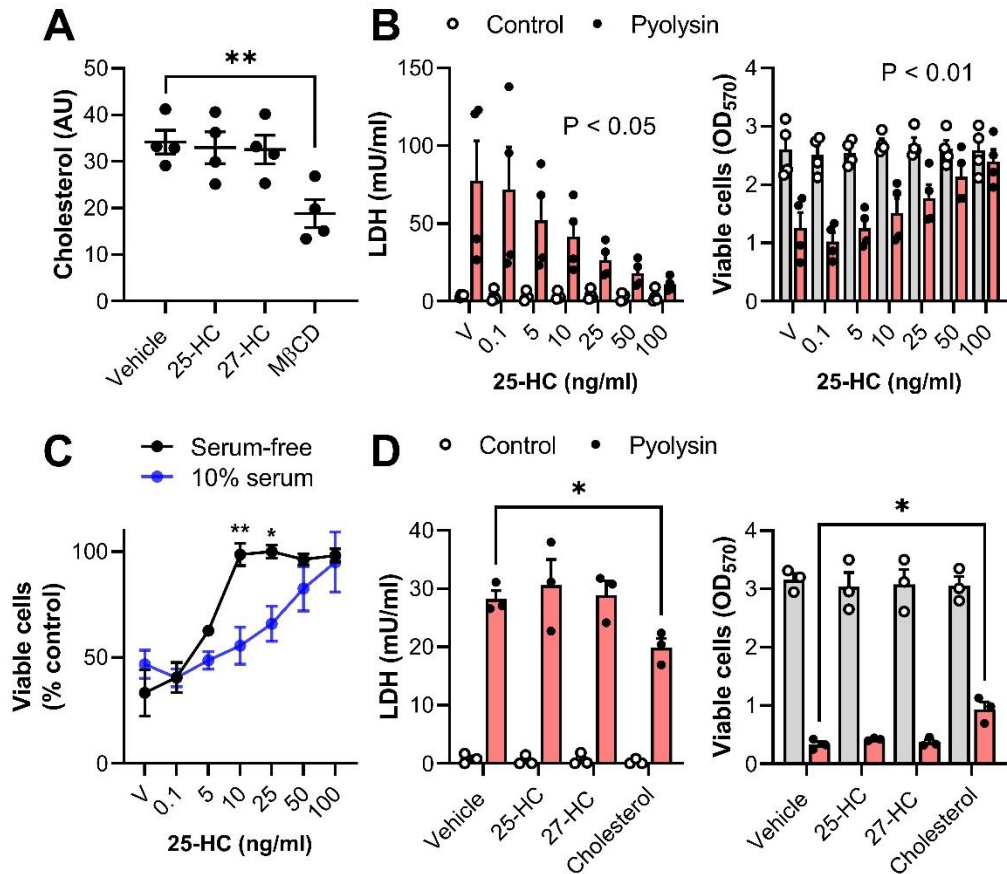


Figure 4.16 Side-chain oysterols do not reduce HeLa total cell cholesterol

(A) Cellular cholesterol in HeLa cells treated for 24 h with vehicle, 10 ng/ml 25-hydroxycholesterol (25-HC), 10 ng/ml 27-hydroxycholesterol (27-HC), or 1 mM MβCD. Data are presented as mean (SEM) from 4 independent experiments; statistical significance was determined using one-way ANOVA with Dunnett's post hoc test; ** $P < 0.01$. (B) Leakage of LDH and viability of HeLa cells treated for 24 h with vehicle, or the indicated concentrations of 25-hydroxycholesterol in complete medium containing 10% serum, and then challenged for 2 h with control medium or 100 HU pyolysin. Data are presented as mean (SEM) from 4 independent experiments; statistical significance was determined using two-way ANOVA and P-values reported for the effect of treatment on pyolysin challenge. (C) Percentage of viable HeLa cells treated for 24 h with vehicle or the indicated concentration of 25-hydroxycholesterol in serum-free or complete medium containing 10% serum, then challenged with 100 HU pyolysin. Data are presented as mean (SEM) from ≥ 3 independent experiments; statistical significance was determined by two-way ANOVA and Bonferroni's post hoc test; * $P < 0.05$, ** $P < 0.01$. (D) Leakage of LDH and viability of HeLa cells challenged for 2 h with control medium or 100 HU pyolysin, mixed with vehicle, 10 ng/ml 25-hydroxycholesterol, 10 ng/ml 27-hydroxycholesterol, or 0.5 mM cholesterol. Data are presented as mean (SEM) from 3 independent experiment; statistical significance was determined by two-way ANOVA and Dunnett's post hoc test; * $P < 0.05$.

As oxysterols did not affect total cellular cholesterol over the time required to provide cytoprotection, we aimed to investigate changes to cholesterol in the plasma membrane. There are three distinct pools of plasma membrane cholesterol: a sphingomyelin-sequestered pool, a residual pool, and a pool accessible to cholesterol-dependent cytolysin binding (Das et al., 2014). Treating HeLa cells with 27-hydroxycholesterol or T0901317 reduced pyolysin binding by 71% and 55% respectively (Fig 4.17). The membrane-bound enzyme ACAT converts cholesterol in the ER to cholesterol esters which can trigger rapid membrane remodelling reducing cholesterol accessibility (Chang et al., 2009, Abrams et al., 2020). Treatment with the ACAT inhibitor SZ58-035 partially restored pyolysin-induced LDH leakage and cytolysis in cells treated with 25-hydroxycholesterol or 27-hydroxycholesterol (Fig 4.18).

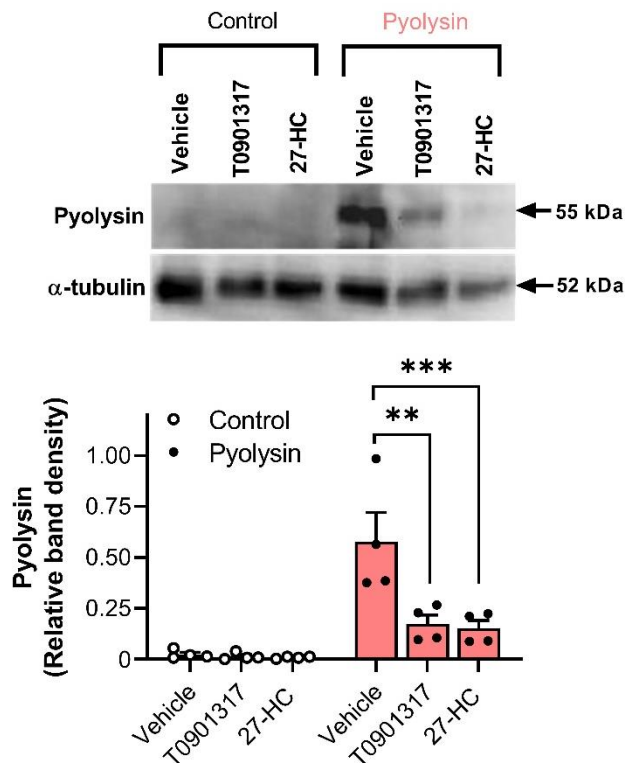


Figure 4.17 27-hydroxycholesterol reduces pyolysin binding

Representative Western blot of pyolysin binding and α -tubulin for HeLa cells treated for 24 h with vehicle, 50 nM T0901317, or 10 ng/ml 27-hydroxycholesterol (27HC), and then challenged for 2 h with control medium or 100 HU pyolysin. Densitometry data were normalized to α -tubulin and presented as mean (SEM) from 4 experiments; statistical significance was determined using ANOVA with Dunnett's post hoc test; **P < 0.01, ***P < 0.001.

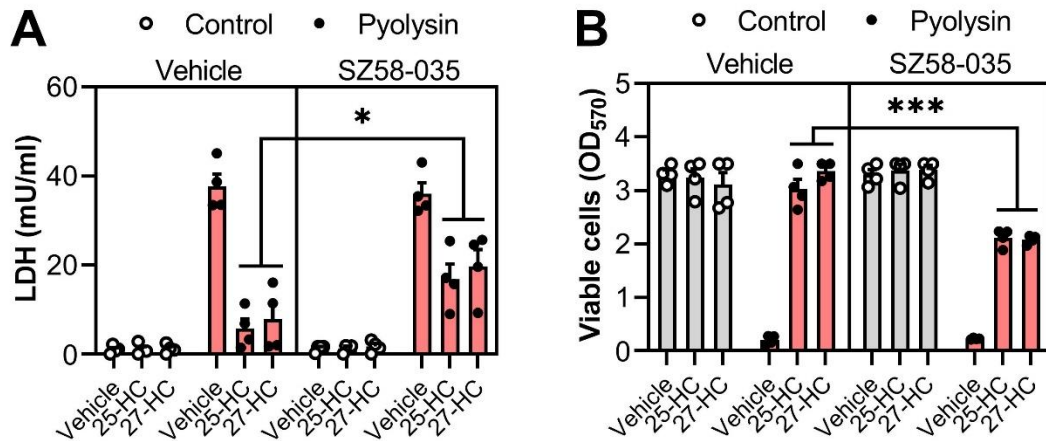


Figure 4.18 27-hydroxycholesterol cytoprotection is partially ACAT-dependent

(A) Leakage of LDH and (B) viability of HeLa cells cultured for 16 h with vehicle or 10 μ M SZ58-035, then treated for 24 h with vehicle, 10 ng/ml 25-hydroxycholesterol (25-HC), or 10 ng/ml 27-hydroxycholesterol (27-HC), in the continuing presence of vehicle or SZ58-035, and then challenged for 2 h with control medium or 100 HU pyolysin. Data are presented as mean (SEM) from 4 independent experiments; statistical significance was determined using two-way ANOVA with Tukey's post hoc test; * $P < 0.05$, *** $P < 0.001$.

If side-chain oxysterol cytoprotection is dependent on ACAT-dependent cholesterol esterification, then we reasoned that restoring the accessible pool of cholesterol should re-establish the susceptibility of cells to pyolysin. Sphingomyelinase disrupts sphingomyelin-sequestered cholesterol, generating additional pools of accessible cholesterol in the plasma membrane (Das et al., 2014, Abrams et al., 2020). Sphingomyelinase treatment increased LDH leakage and cytolysis from cells challenged with pyolysin ($P < 0.001$, Fig 4.19B). 27-hydroxycholesterol treatment still reduced LDH leakage and cytolysis, however, in the presence of sphingomyelinase 27-hydroxycholesterol protection against cytolysis was reduced from 100% to 66%. Together this data provide some evidence that oxysterols protect cells against pyolysin by reducing toxin binding through the modulation of cholesterol accessibility..

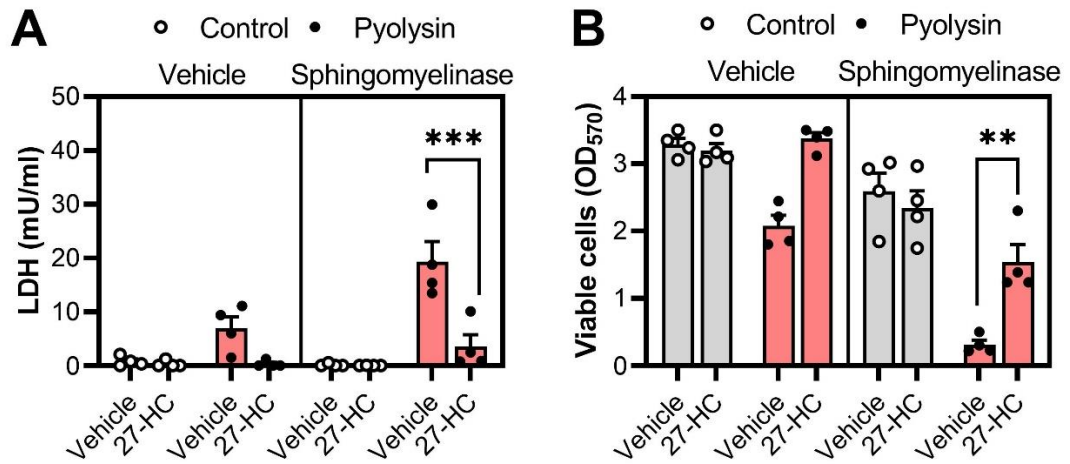


Figure 4.19 SpHINGOMYELINASE treatment doesn't prevent 27-HYDROXYCHOLESTEROL cytoprotection

(A) Leakage of LDH and (B) viability of HeLa cells were cultured for 24 h in serum-free medium containing vehicle, 10 ng/ml 27-hydroxycholesterol, treated for 30 min in serum-free medium containing vehicle or 100 mU/ml sphingomyelinase, and then challenged for 2 h with control serum-free medium or 25 HU pyolysin. Data are presented as mean (SEM) from 4 independent experiments; statistical significance was determined using two-way ANOVA and Tukey's post hoc test; ** $P < 0.01$, *** $P < 0.001$.

4.3.5 Ion flux does not contribute to oxysterol cytoprotection

Pore-forming toxins activate the MAPK cell stress response and damage repair mechanisms in response to potassium efflux and calcium influx (Kloft et al., 2009, Cassidy and O'Riordan, 2013, Gonzalez et al., 2011). The MAPKs ERK1/2, p38 and JNK are activated by pyolysin challenge (Preta et al., 2015). 27-hydroxycholesterol and T0901317 treatment did not cause MAPK phosphorylation (Fig 4.20). Furthermore, treatment with 27-hydroxycholesterol or T0901317 inhibited pyolysin induced phosphorylation of ERK1/2, p38 or JNK.

We next considered whether oxysterol cytoprotection was dependent on calcium or potassium. Depleting calcium from the challenge medium increased pyolysin-induced cell damage; shown by increased LDH leakage and cytolysis (Fig 4.21A). However, 27-hydroxycholesterol provided protection against pyolysin damage regardless of calcium concentration in the challenge medium. Furthermore, although pyolysin challenge in low-potassium medium (5 mM) resulted in increased LDH leakage and cytolysis compared with high potassium (140 mM to prevent efflux), 27-hydroxycholesterol still provided protection (Fig 4.21B). Together this data provide evidence to suggest that 27-hydroxycholesterol protection against pyolysin is not dependent on the influx of calcium ions, the efflux of potassium ions, or MAPK phosphorylation.

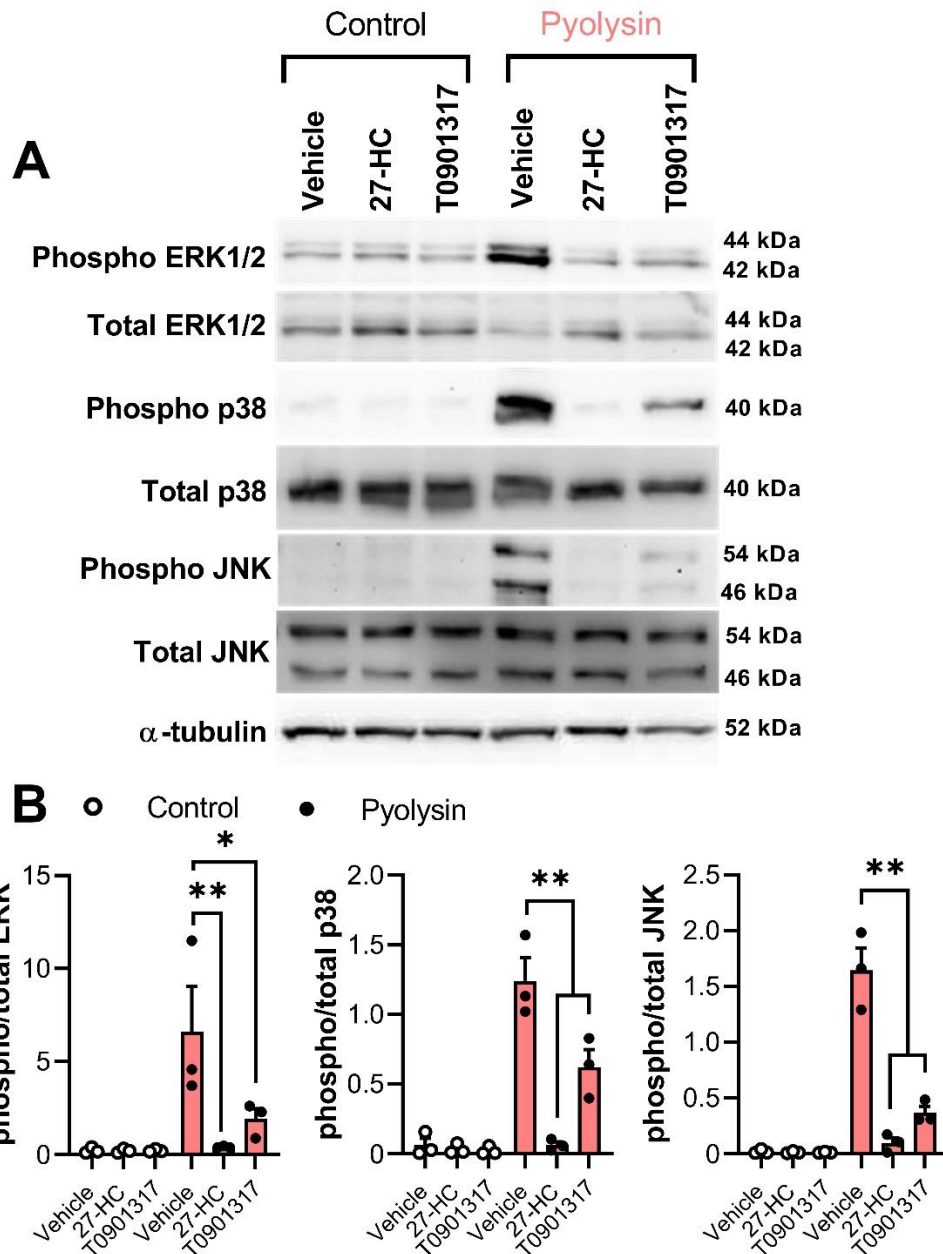


Figure 4.20 27-hydroxycholesterol and T0901317 reduces pyolysin-induced MAPK phosphorylation

Representative Western blot of phosphorylated and total ERK1/2, p38 and JNK, and α -tubulin for HeLa cells treated for 24 h with vehicle, 10 ng/ml 27-hydroxycholesterol (27-HC), or 50 nM T0901317, and challenged for 10 min with control medium or 100 HU pyolysin. Densitometry data were normalized to α -tubulin and presented as mean (SEM) from 3 independent experiments; statistical significance was determined using ANOVA and Tukey's post hoc test; * $P < 0.05$, ** $P < 0.01$.

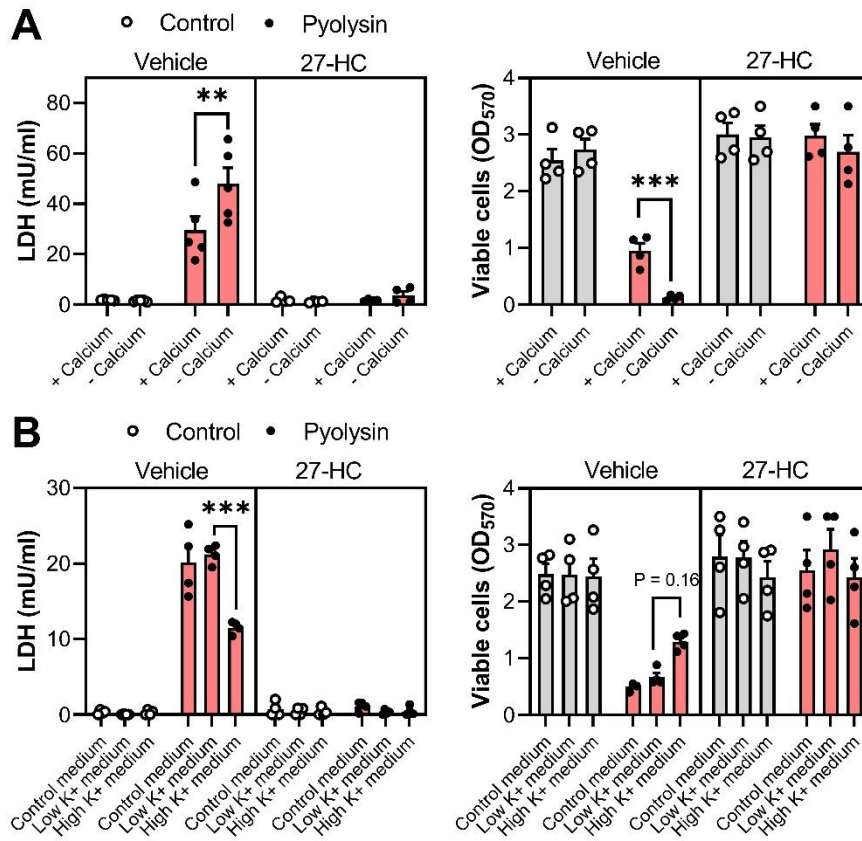


Figure 4.21 Calcium ion influx and potassium ion efflux does not affect 27-hydroxycholesterol cytoprotection

Leakage of LDH and viability of Hela cells treated for 24 h in control serum-free medium containing vehicle or 10 ng/ml 27-hydroxycholesterol (27-HC), and then challenged for 2 h with 100 HU pyolysin in (A) low/high potassium medium or (B) in medium +/- calcium. Data are presented as mean (SEM) of 4 independent experiments; statistical significance was determined using two-way ANOVA and Bonferroni's post hoc test; **P < 0.01, ***P < 0.001.

4.3.6 Liver X receptor agonists protect HeLa cells against pyolysin

As side-chain oxysterols are ligands for the liver X receptors, we explored their role in cytoprotection. Our first approach was to use siRNA to reduce the expression of both LXR α and LXR β . Transfecting HeLa cells with siRNA targeting *NR1H3* and *NR1H2* reduced the expression of LXR α and LXR β by > 80% (Fig 4.22), but had no significant effect on 27-hydroxycholesterol protection (Fig 4.23).

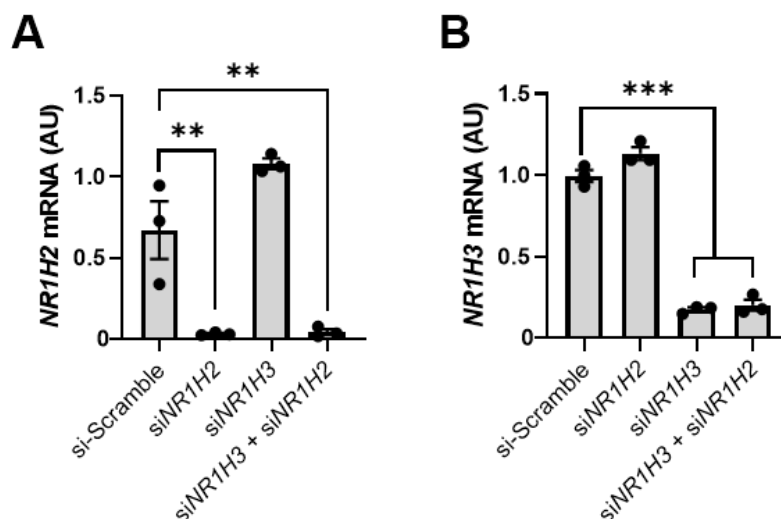


Figure 4.22 siRNA reduces the expression of *NR1H2* and *NR1H3*

HeLa cells were transfected with scramble siRNA or siRNA targeting (A) *NR1H2* and (B) *NR1H3* for 48 h. The mRNA expression of each cognate gene and the reference gene *RPL19* were measured by qPCR. Data are presented as mean with dots representing the values from 3 independent passages. Data were analysed by one-way ANOVA and Dunnett's post hoc test; **P < 0.01, ***P < 0.001.

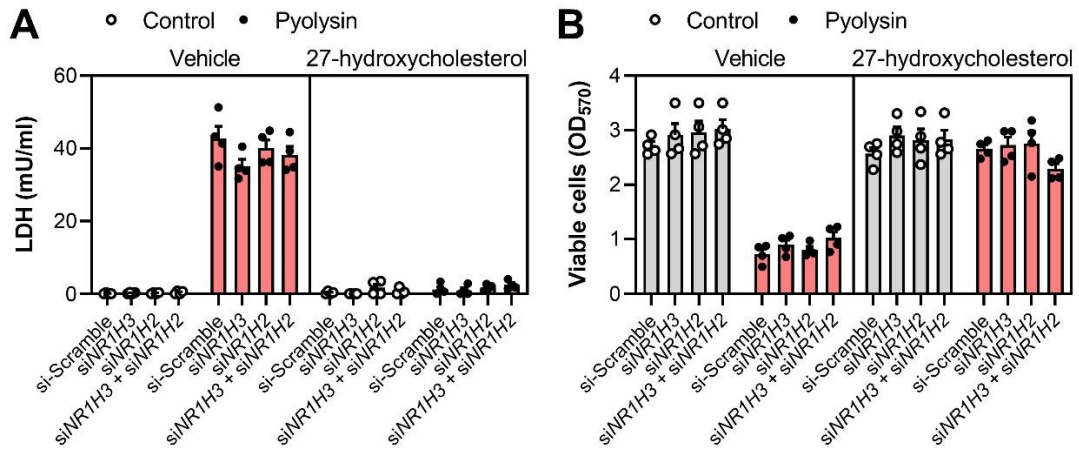


Figure 4.23 27-hydroxycholesterol cytoprotection was not LXR dependent

Leakage of LDH and viability of HeLa cells transfected for 48 h with scramble siRNA or siRNA targeting *NR1H2* and *NR1H3*, treated for 24 h with vehicle or 10 ng/ml 27-hydroxycholesterol, and then challenged for 2 h with control medium or 100 HU pyolysin. Data are presented as mean (SEM) from 4 independent experiments; statistical significance was determined using two-way ANOVA and Tukey's post hoc test.

Our second approach was to use synthetic agonists for LXR α and LXR β . Treating cells with T0901317 or GW3965, reduced the leakage of LDH and cytolysis caused by pyolysin challenge (Fig 4.24A, 4.24B). Interestingly, only GW3965 reduced the pyolysin-induced leakage of potassium ions (Fig 4.24C). In separate experiments investigating the effect of T0901317 treatment duration cytoprotection was evident after 6 h (Fig 4.24D). Additionally, pyolysin-induced actin-cytoskeletal changes were reduced by treatment with T0901317 (37 ± 9 vs $83 \pm 5\%$ cells damaged, $P < 0.01$, ANOVA and Dunnett's post hoc test, $n = 3$, Fig 4.25) and GW3965 (23 ± 11 vs $83 \pm 5\%$ cells damaged, $P < 0.001$, ANOVA and Dunnett's post hoc test, $n = 3$, Fig 4.25). Simultaneously targeting both *NR1H3* and *NR1H2* reduced the protective effects of T0901317, increasing LDH leakage and cytolysis compared with cells treated with non-targeting siRNA, providing some evidence that the agonist was providing protection through the liver X receptors (Fig 4.26).

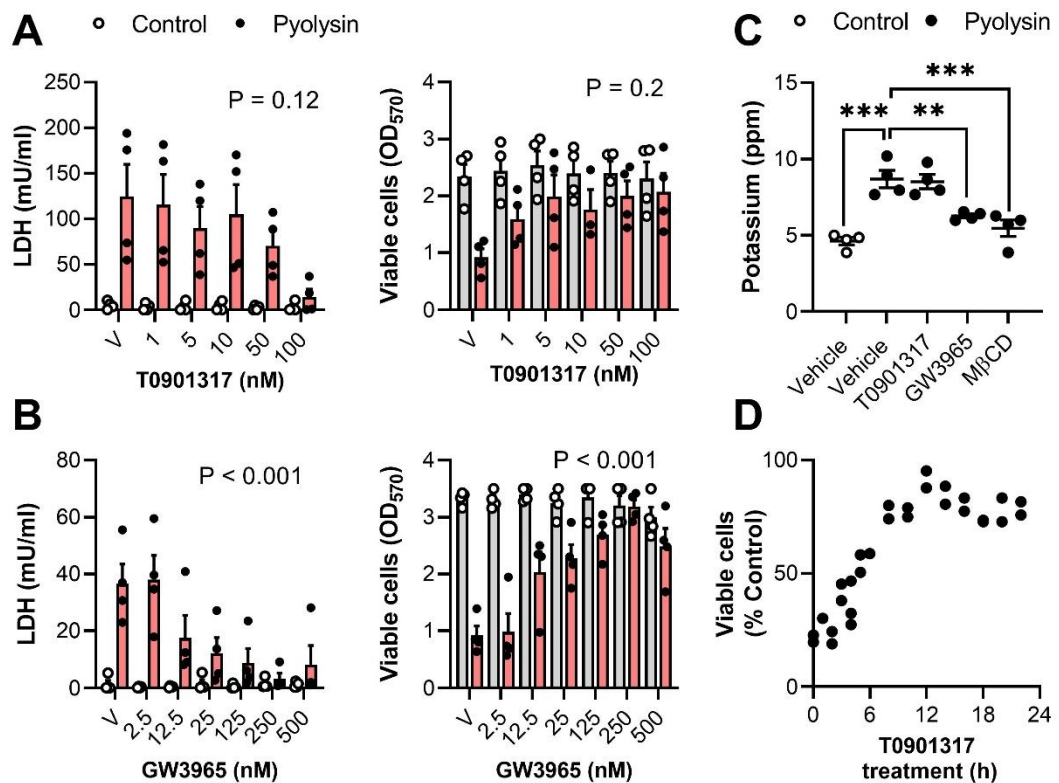


Figure 4.24 Liver X receptor agonists protect HeLa cells against pyolysin

(A,B) Leakage of LDH and viability of HeLa cells cultured for 24 h in serum-free medium containing vehicle (V) or the indicated concentrations of T0901317 or GW39665 and then challenged for 2 h with control medium or 100 HU pyolysin. Data are presented as mean (SEM) from 4 independent experiments; statistical significance determined by two-way ANOVA and P-values reported for the effect of treatment pyolysin challenge. (C) Leakage of potassium from HeLa cells treated for 24 h with vehicle, 50 nM T0901317, 125 nM GW39665, or 1 mM MβCD, and then challenged for 5 min with control medium or 100 HU pyolysin. Dots represent individual values from 4 independent experiments; statistical significance was determined using one-way ANOVA with Dunnett's post hoc test; **P < 0.01, ***P < 0.001. (D) Viability of HeLa cells treated for the indicated time periods with 50 nM T0901317, and then challenged for 2 h with control medium or 100 HU pyolysin. Pyolysin data are presented as percentage viability of control challenge, with dots representing individual values from independent experiments.

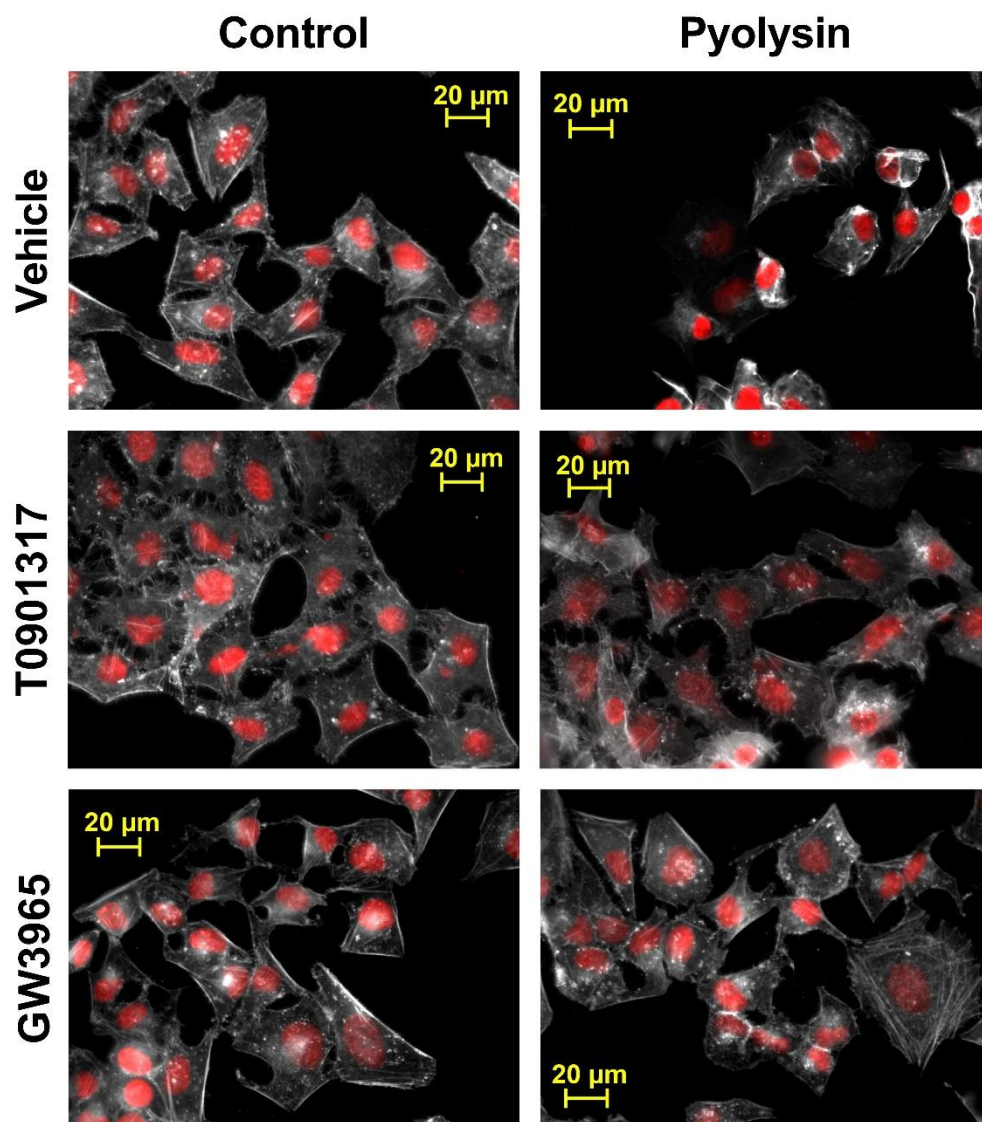


Figure 4.25 Liver X receptor agonists protect HeLa cells against pyolysin-induced actin cytoskeletal changes

Fluorescent microscope images of HeLa cells treated for 24 h with vehicle, 50 nM T0901317, or 125 nM GW3965, then challenged for 2 h with control medium or 100 HU pyolysin and stained with fluorescent phalloidin (white) and DAPI (red); images are representative from 4 independent experiments. Quantification of cytoskeletal changes are reported in text.

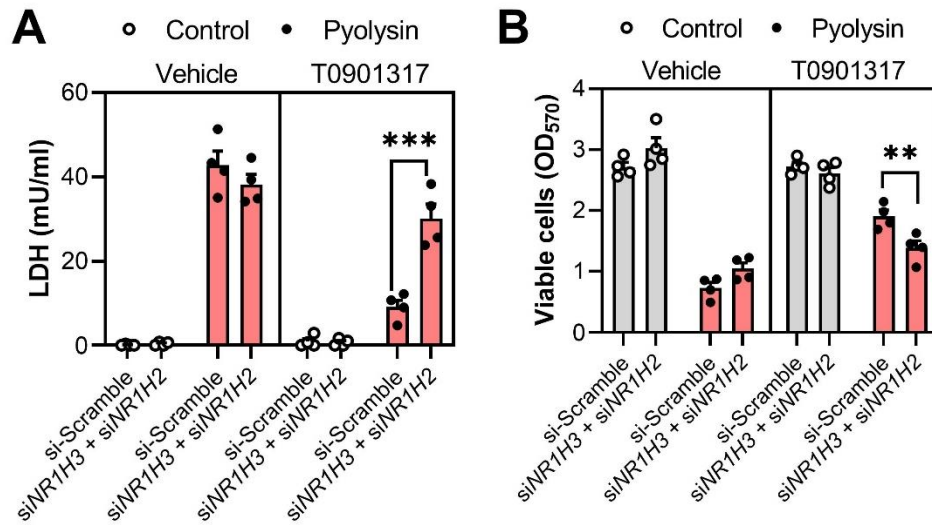


Figure 4.26 T0901317 cytoprotection against pyolysin is LXR dependent

Leakage of LDH and viability of HeLa cells transfected for 48 h with scramble siRNA or siRNA targeting *NR1H2* and *NR1H3*, treated for 24 h with vehicle or 50 nM T0901317, and then challenged for 2 h with control medium or 100 HU pyolysin. Data are presented as mean (SEM) from 4 independent experiments; statistical significance was determined using two-way ANOVA and Tukey's post hoc test; ** $P < 0.01$, *** $P < 0.001$.

Liver X receptor cytoprotection extended to A549 lung cells, reducing pyolysin-induced LDH leakage and cytolysis (Fig 4.27). Treatment with T0901317 reduced pyolysin-induced actin cytoskeletal changes (21 ± 6 vs $73 \pm 3\%$ cells damaged, $P < 0.01$, t-test, $n = 3$, Fig 4.28). Collectively, this data provides evidence that 27-hydroxycholesterol treatment does not exploit the liver X receptor in HeLa cervical cells to confer cytoprotection. However, treatment with the synthetic liver X receptor agonists can protect cells against pyolysin damage.

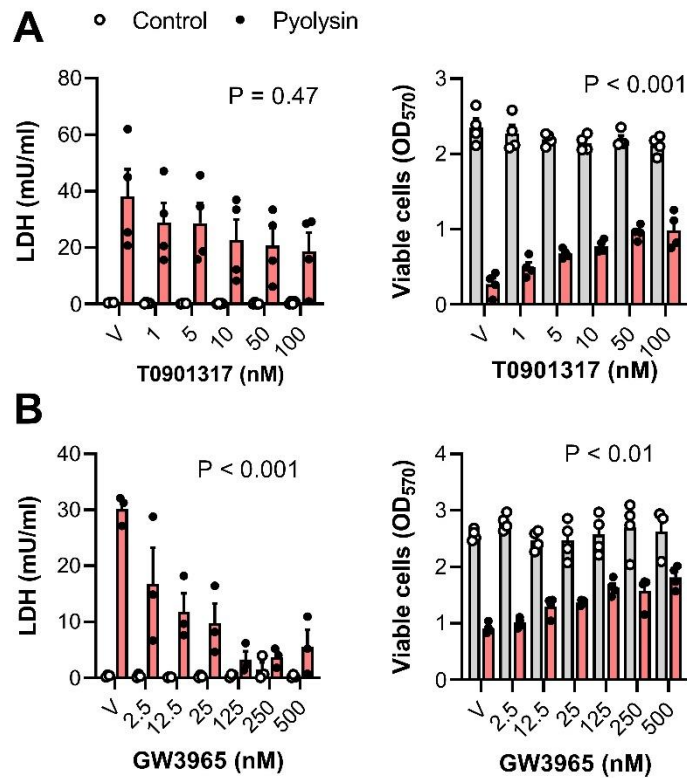


Figure 4.27 Liver X receptor agonists protect A549 cells against pyolysin
(A,B) Leakage of LDH and viability of HeLa cells cultured for 24 h in serum-free medium containing vehicle (V) or the indicated concentrations of T0901317 or GW39665 and then challenged for 2 h with control medium or 25 HU pyolysin. Data are presented as mean (SEM) with dots representing values from cells from 3 - 4 independent experiments; statistical significance determined by two-way ANOVA and P-values are reported for the effect of treatment on pyolysin challenge.

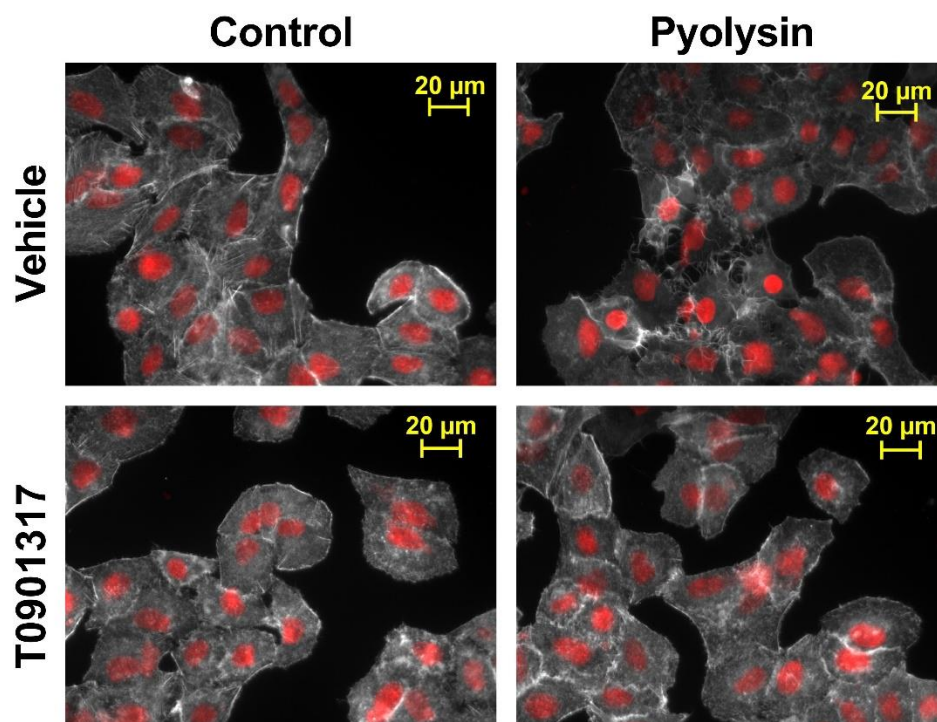


Figure 4.28 T0901317 protects A549 cells against pyolysin-induced actin cytoskeletal changes

Fluorescent microscope images of A549 cells treated for 24 h with vehicle or 50 nM T0901317, then challenged for 2 h with control medium or 25 HU pyolysin, and stained with fluorescent phalloidin (white) and DAPI (red); images are representative from 3 independent experiments. Quantification of cytoskeletal changes are reported in text.

4.4 DISCUSSION

This chapter provides evidence that side-chain oxysterols protect human epithelial cells against the damage caused by pore-forming toxins. Treatment with 25-hydroxycholesterol or 27-hydroxycholesterol protected four types of epithelial cells against pyolysin damage. The oxysterols reduced cytolysin-induced leakage of potassium ions and lactate dehydrogenase, limited cytoskeletal changes, and reduced cytolysis. This oxysterol cytoprotection did not appear to depend on potassium or calcium, MAPK phosphorylation, or the liver X receptors, but instead depended on ACAT reducing the cytolysin-accessible cholesterol in plasma membranes. The oxysterols also protected epithelial cells against damage caused by *S. aureus* α -hemolysin. Collectively, these findings imply that oxysterols can increase the intrinsic protection of epithelial cells against pore-forming toxins and may help protect tissues against pathogenic bacteria.

The key finding of this chapter was the ability of both 25-hydroxycholesterol and 27-hydroxycholesterol to reduce HeLa cell cytolysis caused by a pyolysin challenge that typically reduced cell viability by > 70%. Side-chain oxysterol treatment appeared to reduce pyolysin pore-formation, as shown by decreased potassium leakage within 5 min of challenge and decreased LDH leakage within 2 h. Furthermore, pyolysin-induced ERK1/2, p38 and JNK phosphorylation was reduced in 27-hydroxycholesterol treated cells. Cytoprotection extended to the A549, Hep-G2, and NC1-H441 epithelial cell lines and against *S. aureus* α -hemolysin. A longer challenge period was required to study α -hemolysin cytolysis compared with pyolysin, possibly due to the ten-fold smaller pore-diameter (Preta et al., 2016, Song et al., 1996). Repairing the damage caused by small toxin pores is challenging as the lower calcium permeability of small pores impairs calcium-dependent protective responses (Brito et al., 2019, Walev et al., 1993), however, 27-hydroxycholesterol completely protected both HeLa and A549 against α -hemolysin induced cytolysis. Stimulating macrophages with interferon has recently been shown to protect macrophages against perfringolysin O, streptolysin O and anthrolysin O damage, through the production of 25-hydroxycholesterol (Zhou et al., 2020). The findings of this chapter (along with the findings of *Chapter 3*) expand on these findings, highlighting the cytoprotective properties of 27-hydroxycholesterol in addition to 25-hydroxycholesterol and demonstrate that protection extends to human epithelial cells and against additional toxins.

Side-chain oxysterols regulate cholesterol homeostasis, though in the present chapter 25-hydroxycholesterol or 27-hydroxycholesterol treatment had no significant effect on the total cellular cholesterol of HeLa cells. Additionally, there was no significant effect on total cellular cholesterol in *Chapter 3* where bovine endometrial cells were treated with 25-hydroxycholesterol (5 ng/ml) or 27-hydroxycholesterol (25 ng/ml) for 24 h, and in a previous study where Chinese hamster ovary cells were treated with 25-hydroxycholesterol (2 µg/ml) for 20 h (Abrams et al., 2020). Only a small portion of plasma membrane cholesterol, is accessible to cholesterol-dependent cytolysins (Das et al., 2013), and in this chapter, 27-hydroxycholesterol treatment reduced pyolysin binding. Recent studies have discovered the ability of oxysterols to provide innate immunity to bacterial infection and antiviral immunity by remodelling plasma membrane cholesterol through the actions of the ACAT enzymes (Abrams et al., 2020, Zhou et al., 2020, Wang et al., 2020), and in the present chapter, inhibiting ACAT with SZ58-035 reduced 27-hydroxycholesterol cytoprotection against pyolysin. However, some 27-hydroxycholesterol cytoprotection against pyolysin was evident in cells treated with SZ58-035 and 27-hydroxycholesterol still provided protection in cells treated with sphingomyelinase. Furthermore, oxysterol driven ACAT-dependent cholesterol esterification is a fast-acting method of remodelling the plasma membrane lipid composition, whereas in the present chapter >12 h treatment with 27-hydroxycholesterol cytoprotection was required for maximal protection. Therefore, it seems likely that ACAT cholesterol esterification is not the sole protective mechanism involved. Side-chain oxysterols also control cholesterol homeostasis by suppressing sterol responsive element binding protein 2 (SREBP2) (Brown et al., 2018). This slower acting transcriptional mechanism might prevent the replenishment of plasma membrane accessible cholesterol over time and explain the benefit of prolonged treatment. Additionally, oxysterols can reduce cholesterol biosynthesis by increasing HMGCR degradation. Future work might target these pathways to explore their impact on oxysterol cytoprotection.

There are a multitude of cellular responses deployed by host cells to repair pore-forming toxin damage independent of membrane cholesterol (Gonzalez et al., 2011, Brito et al., 2019). Calcium ion influx activates plasma membrane repair pathways and cytoskeletal remodelling (Wippel et al., 2011, Tam et al., 2013, Babychuk et al., 2009). Depleting calcium from the pyolysin challenge medium to impair calcium

influx in the present chapter increased pyolysin-induced cytolysis but did not affect 27-hydroxycholesterol protection. Previous studies have noted calcium ion oscillations triggered within seconds of 25-hydroxycholesterol treatment in human aortic smooth muscle cells and monocytes (Ares et al., 1997, Lemaire-Ewing et al., 2009). Further research is required to establish whether side-chain oxysterols trigger calcium ion oscillations in the cells used in this chapter, and whether this could contribute to protection by activating reparative pathways in advance of pyolysin challenge. Potassium efflux also mediates cellular responses to pore-forming toxins, such as MAPK activation (Huffman et al., 2004, Munoz-Planillo et al., 2013, Cabezas et al., 2017). However, impairing efflux by increasing the concentration of potassium in the challenge medium did not affect 27-hydroxycholesterol cytoprotection. Additionally, pyolysin challenge caused less ERK1/2, p38, and JNK phosphorylation in cells treated with 27-hydroxycholesterol. This reduction in MAPK activation, alongside the reduced LDH and potassium leakage and pyolysin binding in the present study suggests that side-chain oxysterol treatment is preventing pyolysin from forming plasma membrane pores. Therefore, it seems unlikely that typical host cell reparative pathways would be activated and contribute to protection.

Side-chain oxysterols are ligands for the liver X receptors (Lehmann et al., 1997). However, in the current chapter, reducing the expression of *NR1H2* and *NR1H3*, either separately or in combination, had no effect on oxysterol cytoprotection. Interestingly, *Chapter 3* demonstrated that liver X receptors play a partial role in the 27-hydroxycholesterol cytoprotection of the bovine endometrium against pore-forming toxin damage, highlighting the diverse functions of oxysterol signalling between cell types. Although 27-hydroxycholesterol cytoprotection was independent of liver X receptors in the present chapter, activating the liver X receptors with T0901317 or GW3965 provided HeLa cells with some protection against pyolysin damage, reducing cytolysis, LDH leakage, MAPK activation, and pyolysin-induced cytoskeletal changes, as well as decreasing pyolysin binding. GW3965 also protected macrophages against cholesterol-dependent cytolysin damage (Zhou et al., 2020). The liver X receptors have also been demonstrated to play a critical role in *Mycobacterium Tuberculosis* infection. Production of IL-36 regulates cholesterol synthesis through the induction of *CH25H* and *CYP27A1* and the subsequent activation of the liver X receptors by 25-hydroxycholesterol and 27-hydroxycholesterol respectively (Ahsan et

al., 2016, Ahsan et al., 2018). Additionally, IL-36 production regulates the liver X receptor-dependent production of antimicrobial peptides such as cathelicidin, β -defensin 1, and β -defensin 2 that inhibit pathogen growth (Ahsan et al., 2018). As the production of these antimicrobial peptides can be stimulated by both oxysterols and synthetic liver X receptor agonists, future research might investigate whether they are produced in the present model system and whether they might contribute to cytoprotection.

As mentioned in *Chapter 3*, some side-chain oxysterols, such as 27-hydroxycholesterol, also demonstrate oestrogenic activity (Umetani et al., 2007, Matsubayashi et al., 2021). There is evidence to suggest that HeLa cells do not express the oestrogen receptor (DuSell et al., 2008), and cytoprotection was clearly established in this cell type, making it unlikely that the oestrogen receptor is involved in the protective mechanism. However, the absence of all oestrogen receptor isoforms in HeLa cells is inconclusive, and expression is evident in the other cell types used in this thesis. Therefore, future work might use inhibitors or siRNA to target the oestrogen receptor and verify its role in oxysterol cytoprotection.

In conclusion, we found that side-chain oxysterols protect human epithelial cells against pore-forming toxins. Treatment with 25-hydroxycholesterol or 27-hydroxycholesterol increased the intrinsic cell protection of HeLa and A549 cells against the damage caused by pyolysin and α -hemolysin. This protection was partially dependent on ACAT. Our findings demonstrate that oxysterols can increase the intrinsic protection of epithelial cells against pore-forming toxins and may help protect tissues against pathogenic bacteria.

5 GLUCOCORTICOIDS PROTECT HUMAN CELLS AGAINST PORE-FORMING TOXIN DAMAGE

5.1 INTRODUCTION

Increasing the tolerance of tissue cells to bacterial pore-forming toxins can help reduce the damage caused by bacterial infection (Medzhitov et al., 2012). *Chapters 3 and 4* highlight the ability of side-chain oxysterols to increase the intrinsic protection of eukaryotic cells against pore-forming toxins. However, there is limited research into protective mechanisms, and it is likely that more remain to be discovered. Glucocorticoid treatment reduces the mortality of bacterial infections in humans, such as pneumonia caused by *Streptococcus pneumoniae* (Stern et al., 2017). Whilst this is commonly attributed to their anti-inflammatory properties, glucocorticoids may also increase the intrinsic protection of cells against pore-forming toxins. Dexamethasone and hydrocortisone did not significantly increase the intrinsic protection of bovine endometrial cells against pyolysin in *Chapter 3*, though the pleiotropic effects of glucocorticoids are often cell type and context specific (Weikum et al., 2017). Therefore, the next obvious step was to examine the protective effect of glucocorticoids in another species and cell type.

The endogenous glucocorticoid cortisol is secreted in response to stress, inhibiting inflammation and supporting tissue repair (Kadmiel and Cidlowski, 2013, Cain and Cidlowski, 2017). Synthetic glucocorticoids such as dexamethasone and fluticasone propionate are used therapeutically in patients as anti-inflammatory drugs (Newton, 2014). Glucocorticoids induce responses by binding to the widely expressed glucocorticoid receptor (encoded by *NR3C1*), which leads to transcription factor repression, gene regulation, and non-genomic effects (Yamamoto, 1985, Bamberger et al., 1996). These effects include a diverse array of cellular functions such as the production of inflammatory mediators, suppressing innate immunity, inhibiting MAPK stress responses, and altering cell differentiation and metabolism (So et al., 2007, Wang et al., 2004, Weikum et al., 2017).

This chapter challenged the hypothesis that glucocorticoids increase the intrinsic protection of human tissue cells against pore-forming toxins. To test this hypothesis,

we treated several types of cells with glucocorticoids before challenging them with cholesterol-dependent cytolysins or α -hemolysin. We evaluated cytoprotection by measuring the leakage of lactate dehydrogenase (LDH) and potassium ions and toxin-induced changes in cell morphology and cytolysis. We also determined the role of the glucocorticoid receptor in cytoprotection and investigated potential mechanisms for glucocorticoid cytoprotection against pore-forming toxins.

5.2 MATERIALS AND METHODS

5.2.1 Cytoprotection experiments

To examine whether glucocorticoids protected cells against pyolysin, HeLa, A549, Hep-G2, NC1-H441 (4×10^4 cells/well), and NDHF cells (1.4×10^4 cells/well) were incubated in 1ml/well serum-free media containing vehicle, dexamethasone, hydrocortisone, or fluticasone propionate. Concentrations are as specified in *Results* and were initially based on the manufacturers' instructions and previous publications (Johnson, 1998, Garside et al., 2004, Croxtall et al., 2002). A 24 h treatment duration was selected based on previous work investigating tolerance and cytoprotection and on the work carried out in *Chapters 3 and 4* (Statt et al., 2015, Griffin et al., 2018, Amos et al., 2014); except for experiments exploring the duration of glucocorticoid treatment required to protect cells against pyolysin, where HeLa cells were treated with 10 μ M dexamethasone or 10 μ M hydrocortisone for a range of times up to 24 h as specified in *Results*. After the treatment period, supernatants were discarded, and cells were challenged for 2 h, or as specified in *Results*, with control serum-free medium (comprising 200 μ l Dulbecco's phosphate-buffered saline (DPBS) for 15 min, then supplemented with 400 μ l serum-free medium up to 2 h) or medium containing pyolysin (HeLa: 100 HU, A549: 25 HU, Hep-G2: 100 HU, NCI-H441: 200 HU, NDHF: 25 HU). To determine whether protection extended beyond pyolysin, after a 24 h treatment with 10 μ M dexamethasone, HeLa and A549 cells were challenged for 2 h with a range of concentrations of streptolysin O, as specified in *Results*, or for 24 h with a range of concentrations of α -hemolysin, as specified in *Results*. At the end of the challenge period LDH leakage and cell viability was evaluated as described in *Chapter 2*. Transmitted light micrographs were captured at the end of the challenge period in designated experiments using an Axiocam ERc 5s microscope camera

(Zeiss). The proportion of normal, blebbing, and fragmented cells were counted using 2 independent images per treatment replicate.

To investigate the mechanisms involved in glucocorticoid cytoprotection we used RU486, an antiglucocorticoid, cycloheximide, a translation inhibitor, and actinomycin D, a transcription inhibitor. HeLa or A549 cells were incubated in serum-free medium with vehicle, 10 μ M dexamethasone, or 10 μ M hydrocortisone, in combination with vehicle, 10 μ M RU486, or 1 μ g/ml cycloheximide as specified in *Results*. Alternatively, cells were treated with vehicle or 0.25 μ g/ml actinomycin D for 2 h, then treated for 24 h with the combinations of vehicle, 10 μ M dexamethasone, and actinomycin D, as specified in *Results*. Supernatants were discarded and the cells were challenged for 2 h with control medium or medium containing pyolysin (HeLa: 100 HU, A549: 25 HU). After the challenge period LDH leakage was evaluated from supernatants and cell viability was assessed by MTT.

To examine the role of the glucocorticoid receptor and 3-hydroxy 3-methylglutaryl coenzyme A reductase (HMGCR; a target of the glucocorticoid receptor (Cavenee and Melnykovich, 1977)) in cytoprotection, short-interfering ribonucleic acid (siRNA) was used to knockdown the expression of *NR3C1* or *HMGCR*. HeLa cells were transfected with scramble siRNA, ON-TARGETplus SMARTPool Human *NR3C1* siRNA (#L-003424-00-0005; Horizon discovery) or siRNA designed using Dharmacon siDESIGN Centre to target *HMGCR* (as described in *Chapter 2*). In 24-well culture plates, 50 pmol of siRNA was added to 100 μ l/well Opti-MEM 1 medium with 1.5 μ l Lipofectamine RNAiMAX Reagent and incubated for 20 min at room temperature. HeLa cells were then seeded at a density of 4×10^4 cells/well in 900 μ l DMEM medium supplemented with 10% serum for 48 h. Cells were then treated with vehicle, 10 μ M dexamethasone or 10 μ M hydrocortisone for 24 h in serum-free culture medium prior to a 2 h challenge with control medium or medium containing 100 HU pyolysin. At the end of the challenge period, supernatants were collected to measure LDH leakage and cell viability was measured using an MTT assay.

To determine whether cholesterol supplementation would affect glucocorticoid cytoprotection, HeLa cells were treated with vehicle, 10 μ M dexamethasone, or 10 μ M hydrocortisone in serum-free medium, or serum-free medium containing 30 μ g/ml cholesterol for 24 h (Statt et al., 2015). After the treatment period, cells were

challenged for 2 h with control serum-free medium, or medium containing 100 HU pyolysin. Supernatants were then collected to measure the leakage of LDH, and cell viability was measured using an MTT assay.

To examine the role of acetyl-coenzyme A acetyltransferase (ACAT) in glucocorticoid cytoprotection against pyolysin we used the selective ACAT inhibitor S58-035 (Ross et al., 1984, Abrams et al., 2020). HeLa cells were washed twice with PBS then treated with vehicle or 10 μ M SZ5-035 in serum-free culture medium. After a 16 h incubation, cells were washed twice with PBS, then incubated for 24 h in serum-free culture medium containing 10 ng/ml 27-hydroxycholesterol or 10 μ M dexamethasone, in combination with vehicle or 10 μ M SZ5-035. Medium was then discarded, and cells were challenged for 2 h with control medium or medium containing 100 HU pyolysin. At the end of the challenge period, supernatants were collected to measure the leakage of LDH, and cell viability was measured using an MTT assay.

To explore the effect of serum on cytoprotection, HeLa cells were treated with 10 μ M dexamethasone in medium containing 0 to 10% serum, or 10% charcoal-stripped serum for 24 h. To examine the time required for serum to reverse glucocorticoid cytoprotection against pyolysin, cells were treated with vehicle or 10 μ M dexamethasone in serum-free medium and then supplemented with 10% serum for a range of time periods from 0 to 24 h, as specified in *Results*. To investigate whether the effect of serum on cytoprotection was reversible, cells were treated with 10 μ M dexamethasone in complete medium or serum-free medium. At a range of time points, from 0 to 24 h, supernatants were discarded, cells were washed twice with PBS, and fresh serum-free medium was added for the remainder of the treatment duration. After the treatment period, cells were challenged for 2 h with control serum-free medium, or medium containing 100 HU pyolysin. At the end of the challenge period, cell viability was measured using an MTT assay.

To examine the role of calcium influx on glucocorticoid protection against pyolysin, HeLa cells were cultured for 24 h in medium containing vehicle or 10 μ M dexamethasone. Supernatants were discarded, and cells were washed twice with calcium-free DPBS. Pyolysin challenge (100 HU) was prepared in 200 μ l of calcium-free or calcium-containing DPBS. Cells were challenged for 15 min before wells were supplemented with 400 μ l of serum-free DMEM or serum-free DMEM without

calcium (as specified in *Results*) for the remaining 1 h 45 min of the challenge period. Supernatants were collected to measure the leakage of LDH, and cell viability was measured using an MTT assay.

To examine the role of potassium efflux on glucocorticoid protection against pyolysin, HeLa cells were cultured for 24 h in medium containing vehicle or 10 μ M dexamethasone. Pyolysin challenge (100 HU) was prepared in control medium (5.3 mM KCL), low-potassium medium (5 mM KCl, 140 mM NaCl, 10 mM Hepes, 1.3 mM CaCl₂, 0.5 mM MgCl₂, 0.36 mM K₂HPO₄, 0.44 mM KH₂PO₄, 5.5 mM D-glucose, 4.2 mM NaHCO₃) or high-potassium medium (5 mM NaCl, 140 mM KCl, 10 mM Hepes, 1.3 mM CaCl₂, 0.5 mM MgCl₂, 0.36 mM K₂HPO₄, 0.44 mM KH₂PO₄, 5.5 mM D-glucose, 4.2 mM NaHCO₃) to prevent potassium efflux (Gurcel et al., 2006). Cells were washed twice with control, low-potassium, or high-potassium medium prior to a 2 h challenge. Supernatants were collected to measure the leakage of LDH, and cell viability was measured using an MTT assay.

5.2.2 Potassium

The leakage of potassium from cells was measured to assess whether the treatments prevented toxins forming pores in the cell membrane. HeLa and A549 cells were seeded at a density of 1.5×10^5 cells/well in 3 ml/well complete medium using 6-well culture plates and incubated for 24 h, before a 24 h treatment with vehicle, 10 μ M dexamethasone, 10 μ M hydrocortisone, or 1 mM methyl- β -cyclodextrin (M β CD) in 3 ml/well serum-free medium. Supernatants were discarded, and the cells were washed 3 times with potassium-free choline buffer (129 mM choline-Cl, 0.8 mM MgCl₂, 1.5 mM CaCl₂, 5 mM citric acid, 5.6 mM glucose, 10 mM NH₄Cl, 5 mM H₃PO₄, pH 7.4; all Merck), and then incubated in potassium-free buffer with control medium or the indicated concentration of pyolysin or streptolysin O for 5 min at 37°C. Alternatively, cells were incubated in potassium-free buffer with control medium or 8 μ g/ 5×10^4 cells α -hemolysin for 15 min (no potassium leakage was visible from HeLa cells after 5 min of α -hemolysin challenge). Supernatants were then collected, and potassium was measured using a Jenway PFP7 flame photometer as described in *Chapter 2*.

5.2.3 Cholesterol

To quantify the cellular cholesterol concentrations of HeLa and A549 cells, 1.5×10^5 cells /well were seeded on 6-well culture plates in 3 ml/well complete medium for 24

h. Cells were treated with or without the concentrations of dexamethasone specified in *Results*, 10 μM hydrocortisone or 1 mM M β CD in 3 ml/well serum-free medium for a further 24 h. After the treatment period, cells were washed twice with DPBS then collected in 250 μl / well cholesterol assay 1X Reaction Buffer and stored at -20°C . Cellular cholesterol was measured using the Amplex Red Cholesterol Assay Kit as described in *Chapter 2*. Protein abundance was measured in samples using a DC protein assay, and cholesterol concentrations were normalized to total protein concentrations.

5.2.4 Immunofluorescence

To visualize cell damage, 4×10^4 HeLa or A549 cells/well were seeded on glass cover slips in complete medium using 24-well culture plates for 24 h, before treatment for 24 h in serum-free media with vehicle, 10 μM dexamethasone, or 10 μM hydrocortisone. The supernatants were discarded, and the cells challenged with control medium or medium containing pyolysin for 2 h, or α -hemolysin for 24 h. At the end of the challenge period cells were stained with Alexa Fluor 555-conjugated phalloidin and 4,6-diamidino-2-phenylindole (DAPI), then imaged as described in *Chapter 2*. The proportion of cells that had cytoskeletal changes (cytoskeletal contraction, disrupted shape, or loss of actin fibre definition) after pyolysin challenge were counted using >135 cells per treatment across 3 independent images per replicate.

To further investigate cell shape following pyolysin challenge, HeLa cells (4×10^4 cells/well) were cultured on glass cover slips in complete medium using 24-well culture plates for 24 h, then treated for 24 h in serum-free media containing vehicle or 10 μM dexamethasone. Supernatants were discarded, and cells were challenged for 2 h with control medium or medium containing pyolysin (100 HU). At the end of the challenge period, cells were stained with CellMask Deep Red and DAPI, then imaged as described in *Chapter 2*.

5.2.5 Western blotting

First, we explored the effects of glucocorticoid treatment on pyolysin-induced MAPK signalling. HeLa cells were seeded at a density of 1.5×10^5 cells/well in 3 ml/well complete medium using 6-well plates for 24 h, and then treated for 24 h in 3 ml/well serum-free medium containing vehicle, 10 μM dexamethasone, 10 μM hydrocortisone, or 1 mM M β CD, then challenged with control serum-free medium or

medium containing 100 HU pyolysin for 10 min. Secondly, we investigated the effect of glucocorticoid treatment on the abundance of membrane bound pyolysin. HeLa cells were seeded at 1.5×10^5 cells/well in 3 ml/well complete medium using 6-well plates for 24 h, and then treated for 24 h in 3 ml/well serum-free medium containing vehicle, 10 μ M dexamethasone, 10 μ M hydrocortisone, 50 nM T0901317, 10 ng/ml 27 hydroxycholesterol or 1 mM M β CD, before a 2 h challenge with control serum-free medium or medium containing 100 HU pyolysin. Finally, the abundance of glucocorticoid receptor and HMGCR protein was used to verify the effectiveness of siRNA targeting *NR3C1* and *HMGCR*.

At the end of all experiments, supernatants were discarded, cells were washed with 300 μ l ice-cold PBS, and lysed with 100 μ l PhosphoSafe Extraction Reagent. Protein isolation and Western blotting was performed as described in *Chapter 2*. The average peak density of bands was quantified and normalized to α -tubulin using Fiji (Schindelin et al., 2012). Phosphorylated proteins were normalized to their cognate total protein.

5.2.6 Statistical analysis

The statistical unit was each independent passage of the relevant cell line. Statistical analysis was performed using GraphPad Prism 9.0.1. Data are reported as arithmetic mean (SEM), and significance attributed when $P < 0.05$. Comparisons between treatments or challenges were made using analysis of variance (ANOVA) followed by Dunnett, Bonferroni or Tukey post hoc test for multiple comparisons, or unpaired two-tailed Student's t-test as specified in *Results*.

5.3 RESULTS

5.3.1 Glucocorticoid cytoprotection against pyolysin in HeLa cells

To investigate whether glucocorticoids were cytoprotective, HeLa cells were treated with a range of concentrations of dexamethasone or hydrocortisone and then challenged for 2 h with 100 HU pyolysin (challenge concentration and duration informed by experiments in *Chapter 4*). Cells were treated in serum-free medium, because the 1.12 mM cholesterol in the serum used throughout this thesis might confound the results by binding to cholesterol-dependent cytolysins, and serum activates signalling pathways (Iyer et al., 1999). In contrast to the experiments using bovine endometrial cells in *Chapter 3*, dexamethasone and hydrocortisone treatment protected HeLa cells as shown by the reduced the pyolysin-induced leakage of LDH and cytolysis (Fig 5.1A,B). Specifically, 10 μ M dexamethasone and 10 μ M hydrocortisone provided maximal protection, reducing pyolysin-induced LDH leakage by 84% and 70%, respectively; and reducing pyolysin-induced cytolysis of > 84% to 9% and 26%, respectively. Therefore, these concentrations were selected for further cytoprotection experiments. Treating HeLa cells with 10 μ M dexamethasone or 10 μ M hydrocortisone reduced pyolysin-induced leakage of potassium (Fig 5.1C, D), as effectively as depleting cellular cholesterol with M β CD to prevent pore formation (Amos et al., 2014). In independent experiments, dexamethasone protected HeLa cells against a range of pyolysin challenge concentrations (Fig 5.2). Additionally, glucocorticoid cytoprotection against pyolysin was evident after 6 h treatment with glucocorticoids and was maximal after 18–24 h (Fig 5.3A, B). Finally, dexamethasone cytoprotection persisted against a 24 h pyolysin challenge (Fig 5.3C).

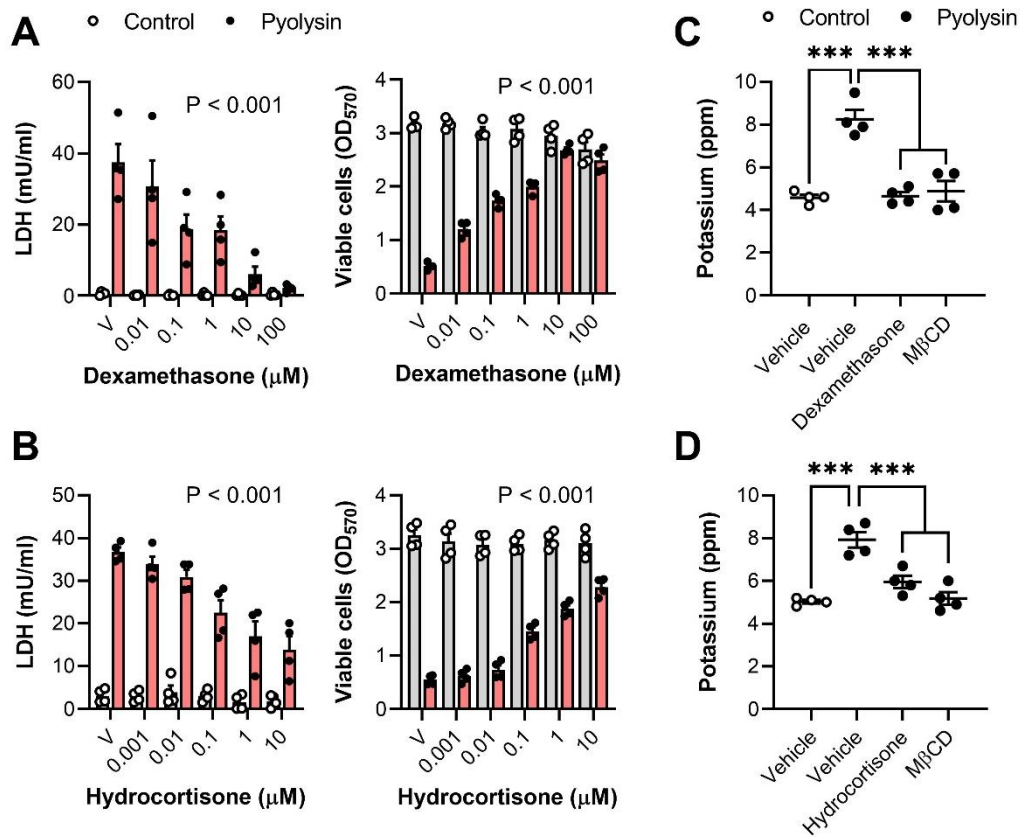


Figure 5.1 Glucocorticoids protect HeLa cells against pyolysin damage

Leakage of LDH and viability of HeLa cells following treatment for 24 h with vehicle or the indicated concentrations of (A) dexamethasone or (B) hydrocortisone, and then challenge for 2 h with control medium or 100 HU pyolysin. Data are presented as mean (SEM) from 4 independent experiments; statistical significance was determined using two-way ANOVA, and P-values reported for the effect of treatment on pyolysin challenge. (C,D) Leakage of potassium from HeLa cells treated for 24 h with vehicle, 10 μM dexamethasone, 10 μM hydrocortisone, or 1 mM M β CD, and then challenged for 5 min with control medium or 100 HU pyolysin. Dots represent individual values from 4 independent experiments; statistical significance was determined using one-way ANOVA with Dunnett's post hoc test; ***P < 0.001.

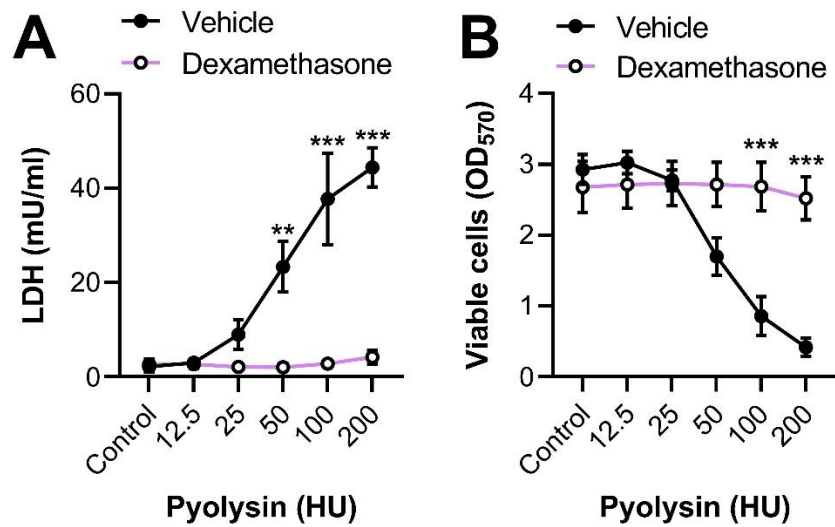


Figure 5.2 Dexamethasone protects HeLa cells against a range of pyolysin challenge concentrations

(A) Leakage of LDH and (B) viability of HeLa cells treated for 24 h with vehicle or 10 μ M dexamethasone, and then challenged for 2 h with control medium or the indicated concentrations of pyolysin. Data are presented as mean (SEM) from 4 independent experiments; statistical significance was determined using two-way ANOVA and Bonferroni's post hoc test; ** $P < 0.01$, *** $P < 0.001$.

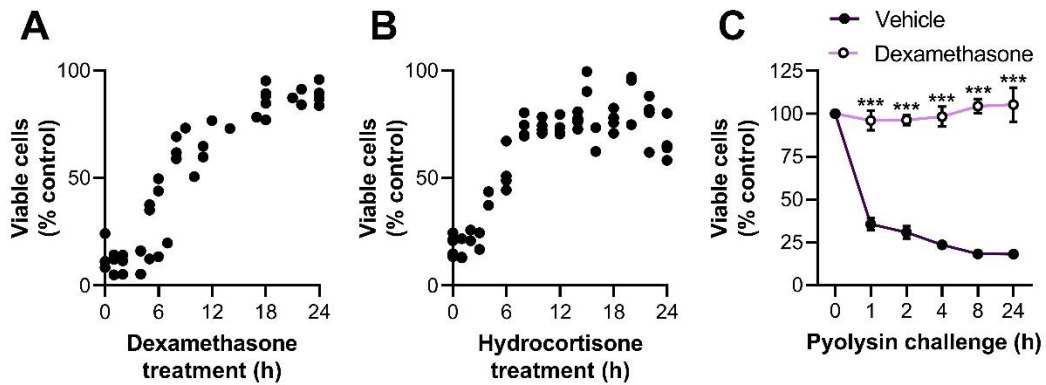


Figure 5.3 Glucocorticoid cytoprotection requires > 6 h treatment and persists against longer pyolysin challenge durations

Viability of HeLa cells treated for the indicated time periods with (A) 10 μ M dexamethasone or (B) 10 μ M hydrocortisone, and then challenged for 2 h with control medium or 100 HU pyolysin. Pyolysin data are presented as percentage viability of control challenge, with dots representing individual values from independent experiments. (C) Viability of cells treated for 24 h with vehicle or 10 μ M dexamethasone, and then challenged for the indicated time with control medium or 100 HU pyolysin. Pyolysin data are presented as mean (SEM) percentage viability of control challenge from 4 independent experiments. Statistical significance was determined using two-way ANOVA and Bonferroni's post hoc test; ***P < 0.001.

Treatment with dexamethasone and hydrocortisone also reduced pyolysin-induced cytoskeletal changes (28 ± 2 and 32 ± 9 respectively vs $88 \pm 2\%$ cells damaged, P < 0.01, ANOVA and Dunnett's post hoc test, n = 3, Fig 5.4). Additionally, glucocorticoid protection was visualized with phase-contrast microscopy and in cells stained with CellMask. A wider field of view highlighted the cell death caused by pyolysin challenge in vehicle treated cells (Fig 5.5A). Cells displayed plasma membrane blebs or a complete loss of shape and structure (Fig 5.5, 6). Dexamethasone treatment cells maintained shape, ensuring that cells maintained clearly defined edges (Fig 5.5B), and both glucocorticoids reduced pyolysin-induced plasma membrane blebbing and cell fragmentation (P < 0.001, ANOVA and Dunnett's post hoc test, Fig 5.6, Table 5.1). Together, these data provide evidence for glucocorticoid cytoprotection of HeLa cells against pyolysin.

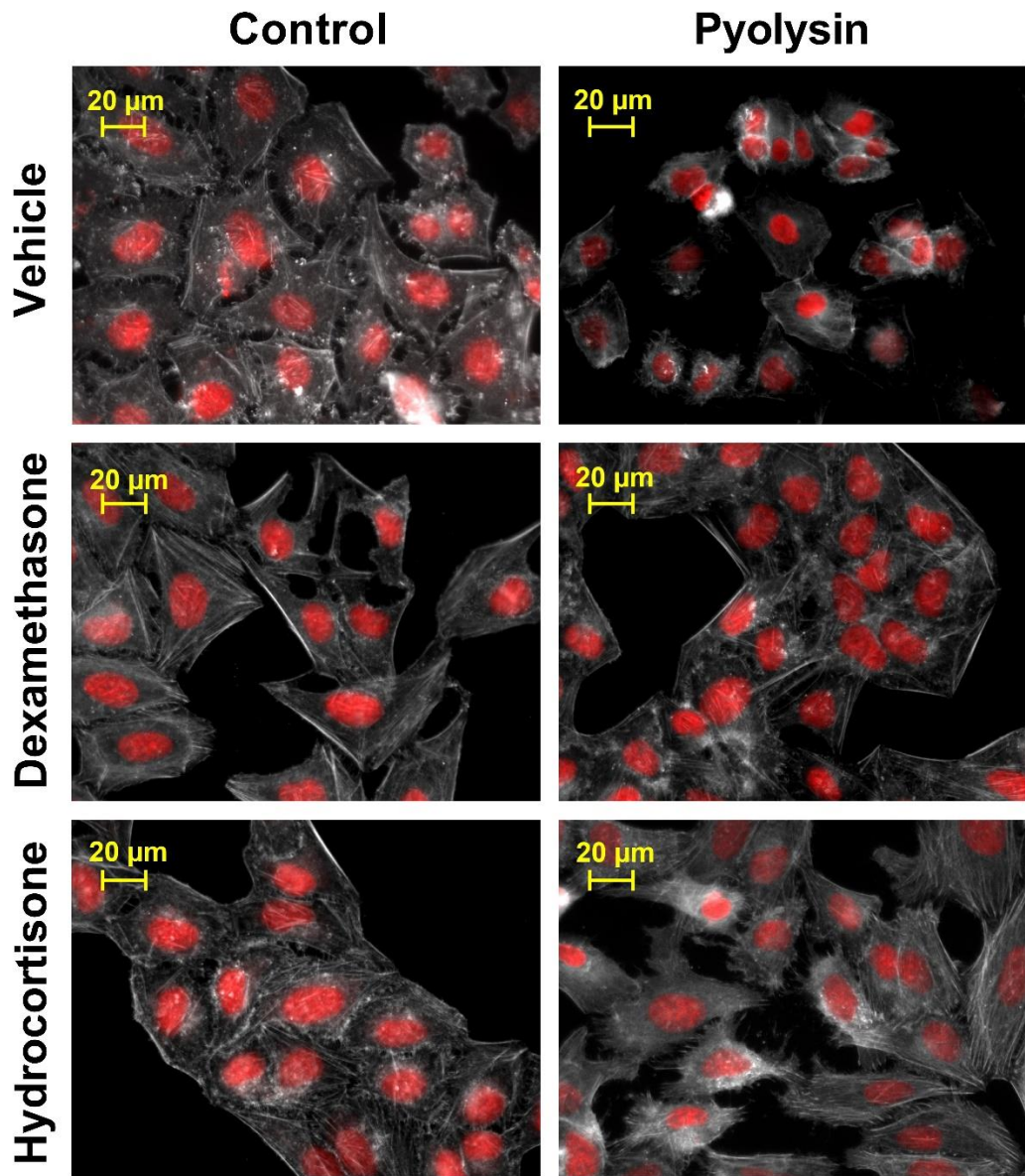


Figure 5.4 Glucocorticoids prevent pyolysin-induced HeLa cytoskeletal changes
 Fluorescent microscope images of HeLa cells treated for 24 h with vehicle, 10 μ M dexamethasone or 10 μ M hydrocortisone, then challenged for 2 h with control medium or 100 HU pyolysin and stained with fluorescent phalloidin (white) and DAPI (red); images are representative from 4 independent experiments. Quantification of cytoskeletal changes are reported in text.

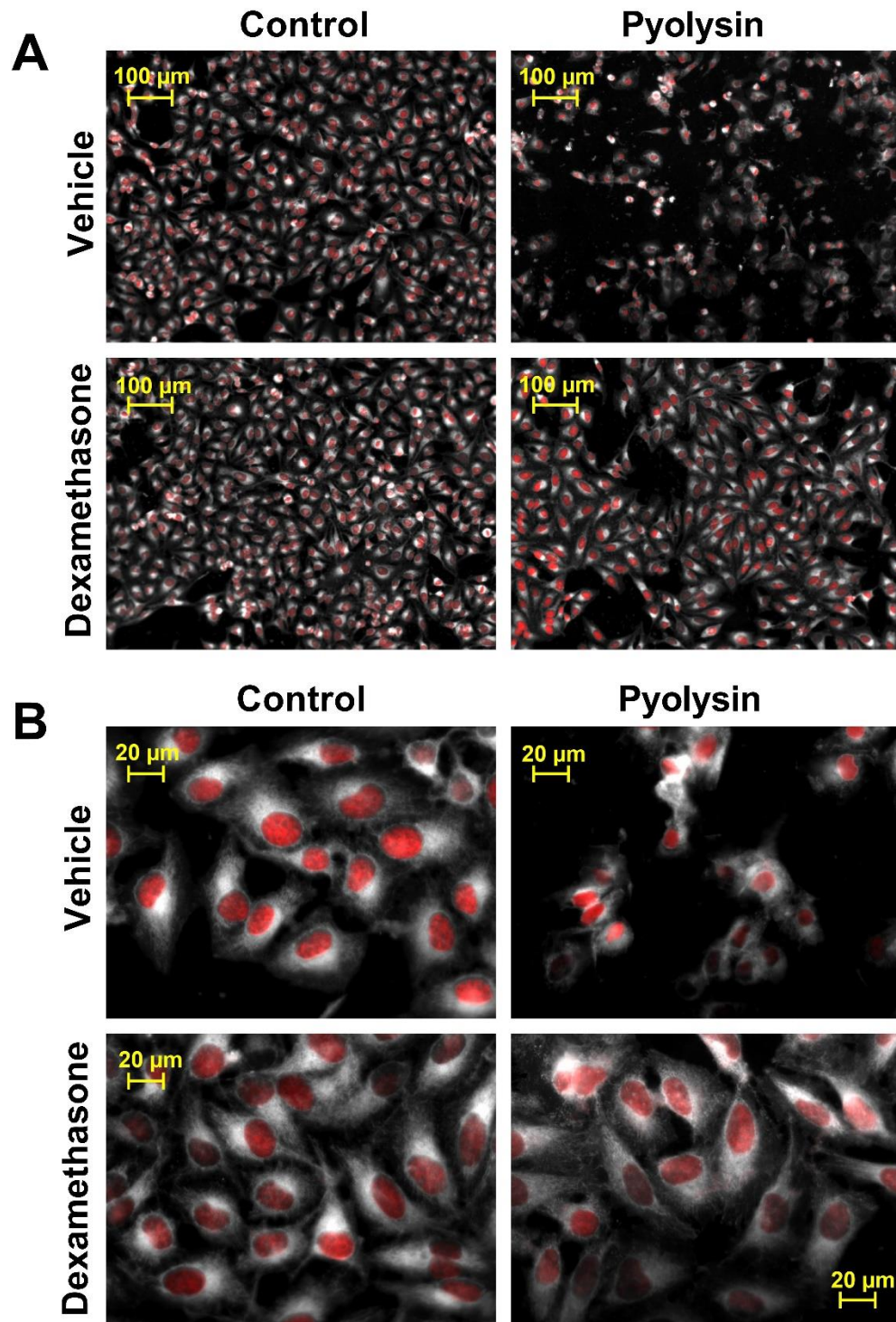


Figure 5.5 Dexamethasone protects HeLa cells against pyolysin

Fluorescent microscope images from a (A) 10X and a (B) 40X lens of HeLa cells treated for 24 h with vehicle, 10 μ M dexamethasone or 10 μ M hydrocortisone, then challenged for 2 h with control medium or 100 HU pyolysin and stained with CellMask (white) and DAPI (red); images are representative from 3 independent experiments.

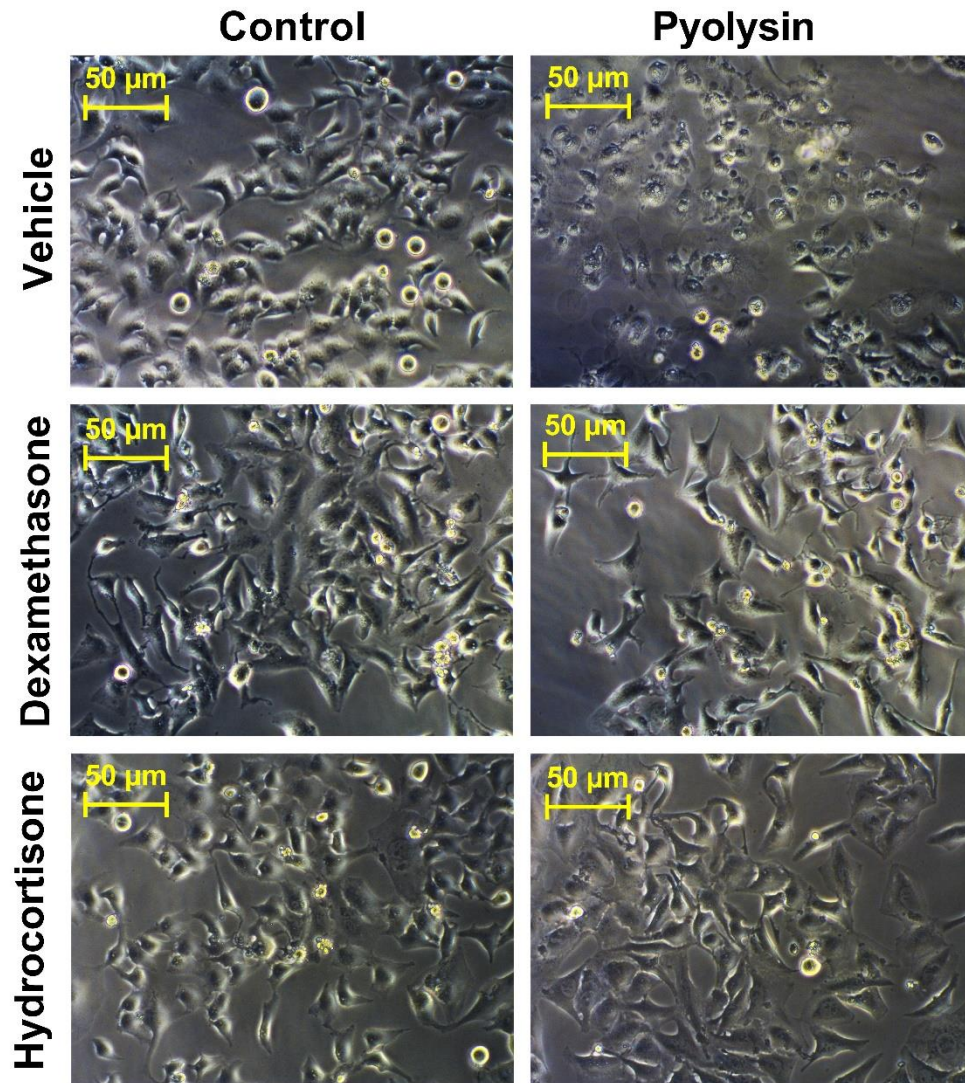


Figure 5.6 Glucocorticoids reduce pyolysin-induced HeLa cell blebbing

Phase contrast microscopy of HeLa cells treated for 24 h with vehicle, 10 μ M dexamethasone, or 10 μ M hydrocortisone, then challenged for 2 h with control medium or 100 HU pyolysin; images are representative from 4 independent experiments, scale bars = 50 μ m.

Table 5.1 Quantification of HeLa cell morphology after glucocorticoid treatment and pyolysin challenge

We quantified the percentage of normal, blebbing, or fragmented HeLa cells treated for 24 h with vehicle, 10 μ M dexamethasone, or 10 μ M hydrocortisone, then challenged for 2 h with control medium or 100 HU. Cells were imaged by phase contrast microscopy and categorized as normal, blebbed or fragmented, with >100 cells evaluated across two independent images per treatment replicate. Raw data were analyzed by ANOVA and Tukey's post hoc test with superscript indicating the differences between vehicle and treatments (**P < 0.01, ***P < 0.001), and data are reported as mean \pm SEM for the pyolysin challenge as a percentage of the control challenge.

Treatment	Replicates	Percentage of cells		
		Normal	Blebbing	Fragmented
Vehicle	10	8 \pm 2	54 \pm 6	38 \pm 6
Dexamethasone	7	87 \pm 4 ***	8 \pm 3 ***	5 \pm 2 ***
Hydrocortisone	7	67 \pm 13 ***	23 \pm 4 ***	10 \pm 3 ***

5.3.2 Glucocorticoid cytoprotection is generalized across human cells

To explore whether glucocorticoid cytoprotection is more generalized than protecting HeLa cells against pyolysin, we tested protection in A549 lung epithelial cells, because they are often used to study cholesterol-dependent cytolysins (Statt et al., 2015, Mestre et al., 2010). Pyolysin challenge, optimised in *Chapter 4*, caused LDH and potassium leakage and diminished A549 cell viability (P < 0.001, two-way ANOVA and Dunnett's multiple comparison test, Fig 5.7). However, treatment with 10 μ M dexamethasone (Fig 5.7A) or 10 μ M hydrocortisone (Fig 5.7B) reduced pyolysin-induced leakage of LDH, cytolysis, and cytoskeletal changes (7 \pm 4 and 16 \pm 4 respectively vs 71 \pm 5% cells damaged, P < 0.01, ANOVA and Dunnett's post hoc test, n = 3, Fig 5.8). Potassium ion leakage was reduced by dexamethasone treatment (P < 0.001) and tended to be reduced by hydrocortisone (P = 0.099, Fig. 5.7C). Additionally, dexamethasone protection functioned against a range of pyolysin challenge concentrations (Fig 5.9).

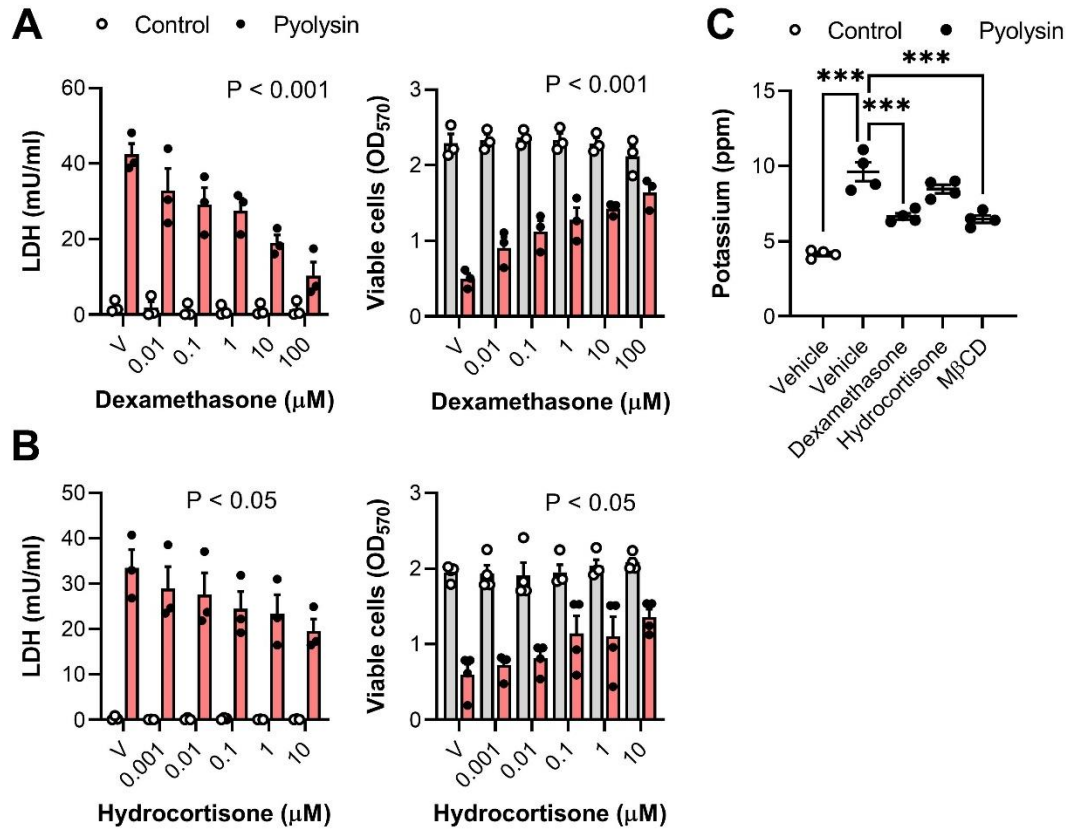


Figure 5.7 Glucocorticoids protect A549 cells against pyolysin damage

(A,B) Leakage of LDH and viability of A549 cells treated for 24 h with vehicle, or the indicated concentration of dexamethasone or hydrocortisone, and then challenged for 2 h with control medium or 25 HU pyolysin. Data are presented as mean (SEM) from 3 independent experiments; statistical significance was determined using two-way ANOVA, and P-values reported for the effect of treatment on pyolysin challenge. (C) Leakage of potassium from A549 cells treated for 24 h with vehicle, 10 μM dexamethasone, 10 μM hydrocortisone, or 1 mM M β CD, and then challenged for 5 min with control medium or 25 HU pyolysin. Dots represent individual values from 4 independent experiments; statistical significance was determined using one-way ANOVA with Dunnett's post hoc test; *** $P < 0.001$.

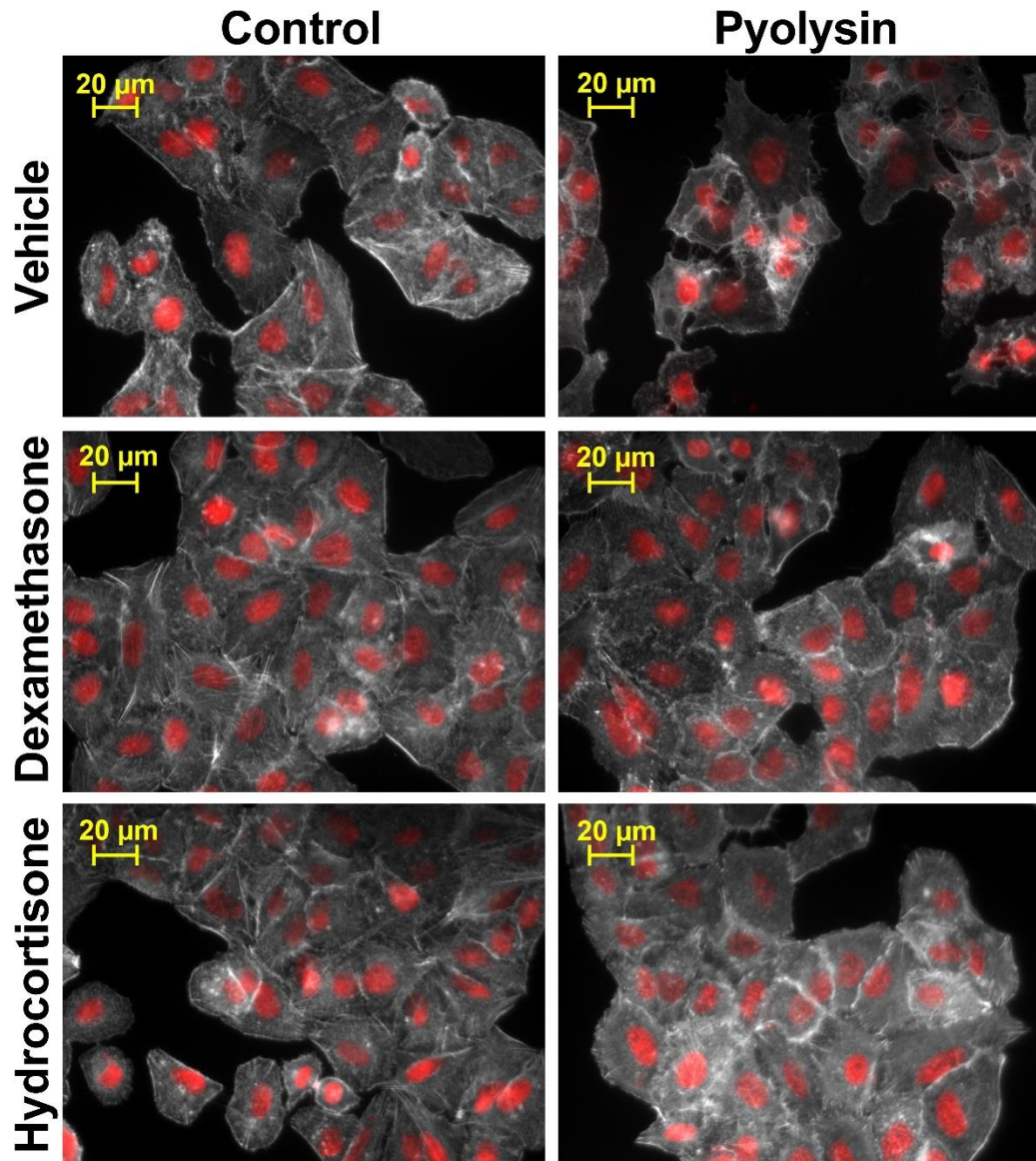


Figure 5.8 Glucocorticoids protect A549 cells against pyolysin-induced cytoskeletal changes

Fluorescent microscope images of A549 cells treated for 24 h with vehicle, 10 μ M dexamethasone or 10 μ M hydrocortisone, then challenged for 2 h with control medium or 25 HU pyolysin and stained with fluorescent phalloidin (white) and DAPI (red); images are representative from 3 independent experiments. Quantification of cytoskeletal changes are reported in text.

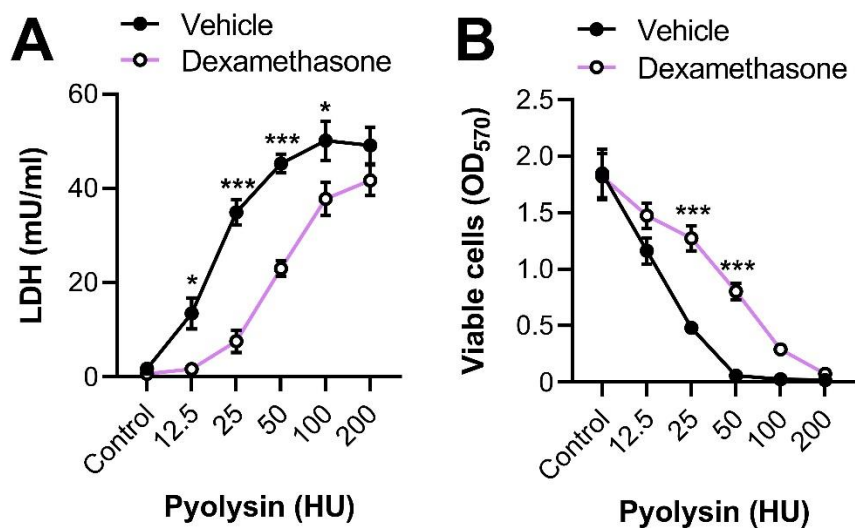


Figure 5.9 Dexamethasone protects A549 cells against a range of pyolysin challenge concentrations

(A) Leakage of LDH and (B) viability of A549 cells treated for 24 h with vehicle or 10 μ M dexamethasone, and then challenged for 2 h with control medium or the indicated concentrations of pyolysin. Data are presented as mean (SEM) from 4 independent experiments; statistical significance was determined using two-way ANOVA and Bonferroni's post hoc test; * $P < 0.05$, *** $P < 0.001$.

We used Hep-G2 liver cells, NCI-H441 lung cells, and NDHF to provide additional validation of glucocorticoid cytoprotection. The amount of pyolysin to challenge Hep-G2 and NCI-H441 cells was determined in *Chapter 4*, and we selected 25 HU pyolysin to challenge NDHF cells (Fig 5.10). Significantly, treatment with 10 μ M dexamethasone reduced pyolysin-induced leakage of LDH and cytolysis in Hep-G2, NCI-H441, and NDHF cells (Fig 5.11).

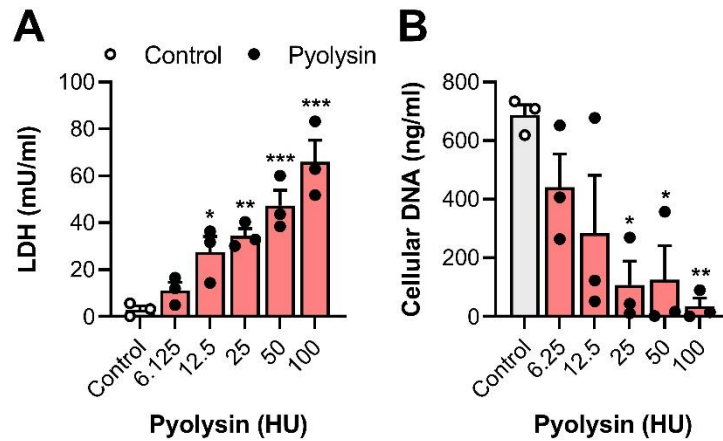


Figure 5.10 The cytolytic activity of pyolysin in dermal fibroblasts

Leakage of LDH, and cell viability determined by CyQUANT for NDHF cells challenged for 2 h with control medium or the indicated concentration of pyolysin. Data are presented as mean (SEM) with dots representing the values from 3 independent experiments; statistical significance was determined using one-way ANOVA and Dunnett's post hoc test; * $P < 0.05$, ** $P < 0.01$, *** $P < 0.001$.

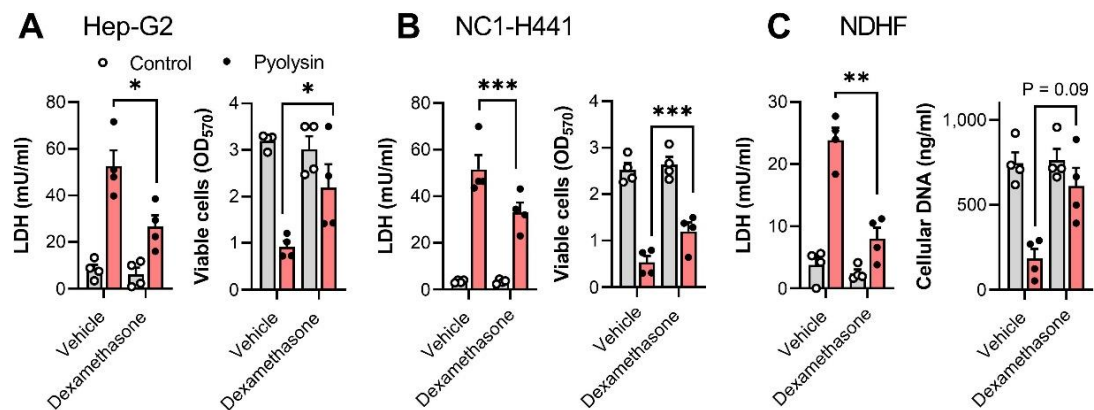


Figure 5.11 Dexamethasone protects multiple cells against pyolysin

Leakage of LDH and viability of (A) Hep-G2, (B) NCI-H441 and (C) NDHF cells treated for 24 h with vehicle or 10 μ M dexamethasone, and then challenged for 2 h with control medium or pyolysin (Hep-G2, 100 HU; NC1-H441, 200 HU; NDHF, 25 HU). Data are presented as mean (SEM) from 4 independent experiments; statistical significance was determined using two-way ANOVA, with Bonferroni's post hoc test; * $P < 0.05$, ** $P < 0.01$, *** $P < 0.001$.

To explore whether glucocorticoids protect cells against other cytolysins, we first challenged HeLa or A549 cells with another cholesterol-dependent cytolysin, streptolysin O. Dexamethasone reduced potassium and LDH leakage and cytolysis caused by streptolysin O in HeLa and A549 cells (Fig 5.12). However, interestingly hydrocortisone did not significantly reduce potassium leakage in either cell type.

We next examined cytoprotection against a member of the hemolysin family of cytolysins, *S. aureus* α -hemolysin (Peraro and van der Goot, 2016, Mestre et al., 2010). Challenging with α -hemolysin caused leakage of potassium ions within 15 min, and leakage of LDH and cytolysis after 24 h in HeLa and A549 cells (Fig 5.13, 5.14). Dexamethasone reduced α -hemolysin-induced LDH and potassium ion leakage and cytolysis in HeLa cells (Fig 5.13A,B). Additionally, dexamethasone treatment reduced the cytoskeletal changes in HeLa cells caused by the α -hemolysin challenge (17 ± 4 vs $86 \pm 3\%$ cells damaged, $P < 0.01$, t-test, $n = 3$, Fig 5.13C). Although, dexamethasone treatment did reduce the leakage of LDH from A549 cells, it did not protect against the potassium ion leakage, cytolysis, or cytoskeletal changes caused by α -hemolysin challenge (Fig 5.14). Collectively, these findings provide evidence that glucocorticoid cytoprotection extends to a range of types of cells and pore-forming toxins.

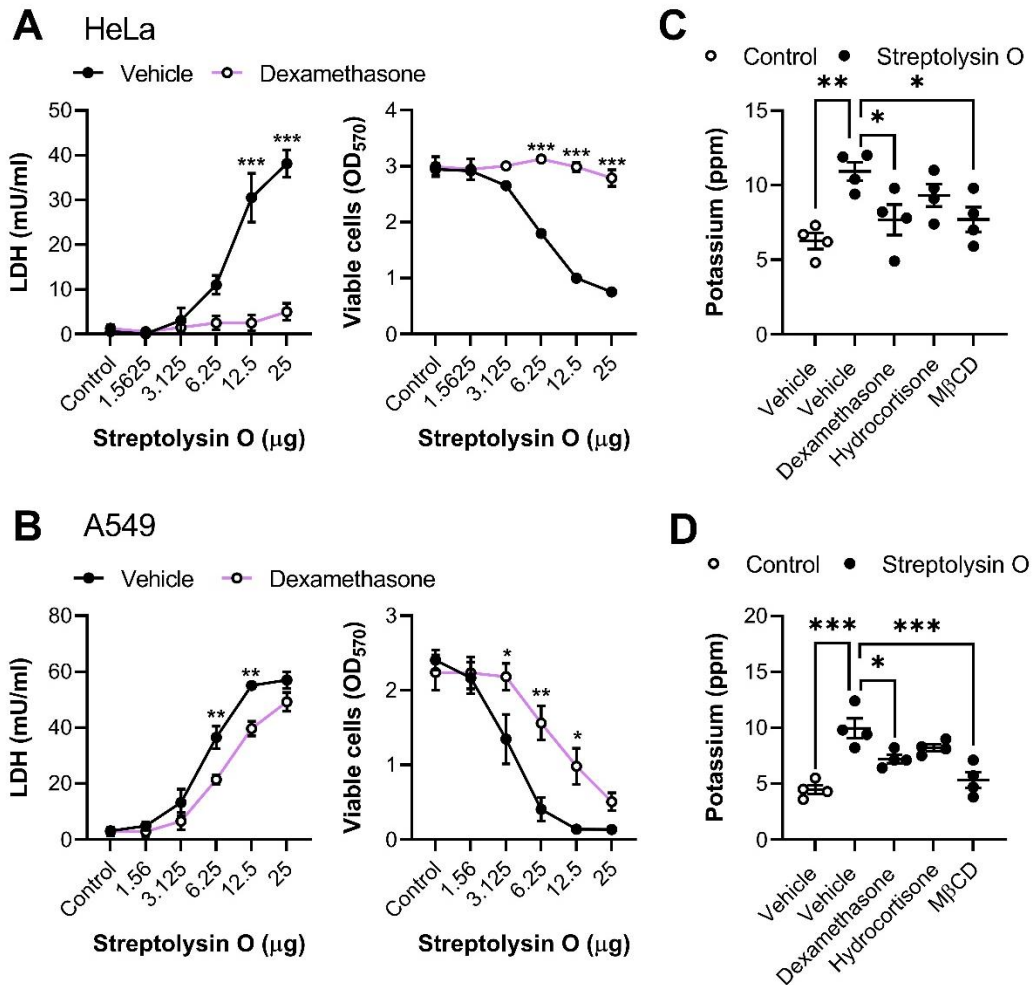


Figure 5.12 Glucocorticoids protect HeLa and A549 cells against streptolysin O
 Leakage of LDH and viability of HeLa (**A**) and A549 cells (**B**) treated for 24 h with vehicle or 10 μM dexamethasone, and then challenged for 2 h with control medium or the indicated concentrations of streptolysin O. Data are presented as mean (SEM) from 4 independent experiments; statistical significance was determined using one-way ANOVA and Bonferroni's post hoc test; * $P < 0.05$, ** $P < 0.01$, *** $P < 0.001$. Leakage of potassium from HeLa cells (**C**) and A549 cells (**D**) treated for 24 h with vehicle, 10 μM dexamethasone, 10 μM hydrocortisone or 1 mM M β CD, and then challenged for 5 min with control medium or streptolysin O (HeLa, 12.5 μg ; A549, 6.25 μg). Dots represent individual values from 4 independent experiments; statistical significance was determined using one-way ANOVA and Dunnett's post hoc test; * $P < 0.05$, *** $P < 0.001$.

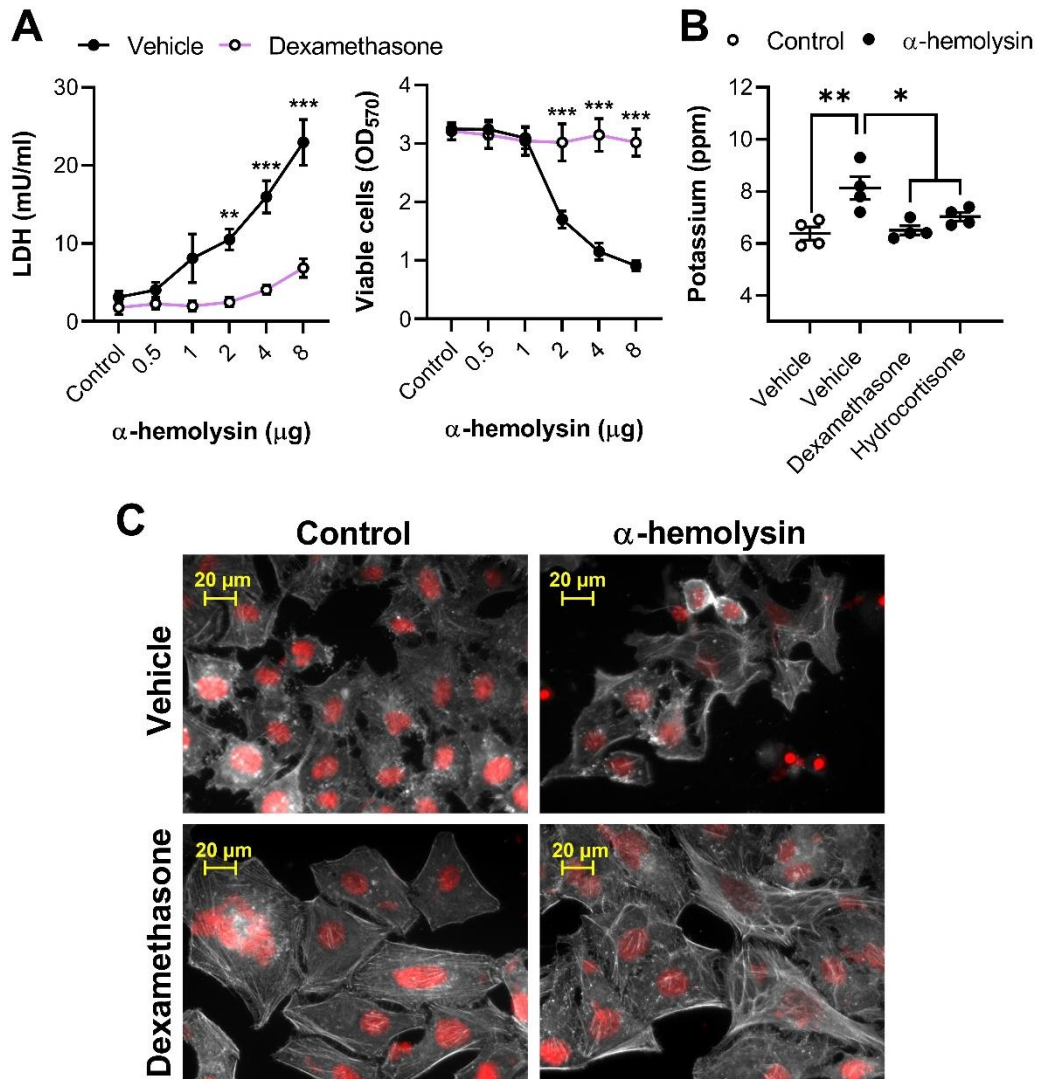


Figure 5.13 Dexamethasone protects HeLa cells against α -hemolysin damage

(A) Leakage of LDH and viability of HeLa cells treated for 24 h with vehicle or 10 μ M dexamethasone, and then challenged for 24 h with control medium or the indicated concentration of α -hemolysin. Data are presented as mean (SEM) from 4 independent experiments; statistical significance was determined using two-way ANOVA and Bonferroni's post hoc test; ** $P < 0.01$, *** $P < 0.001$. (B) Leakage of potassium from HeLa cells treated for 24 h with vehicle, 10 μ M dexamethasone, 10 μ M hydrocortisone or 1 mM M β CD, then challenged for 15 min with control medium or 8 μ g α -hemolysin. Dots represent values from 4 independent experiments; statistical significance was determined using one-way ANOVA with Dunnett's post hoc test; * $P < 0.05$, ** $P < 0.01$. (C) Fluorescent microscope images of HeLa cells treated for 24 h with vehicle or 10 μ M dexamethasone, then challenged for 24 h with control medium or 8 μ g α -hemolysin and stained with fluorescent phalloidin (white) and DAPI (red); images are representative from 3 independent experiments. Quantification of cytoskeletal changes are reported in text.

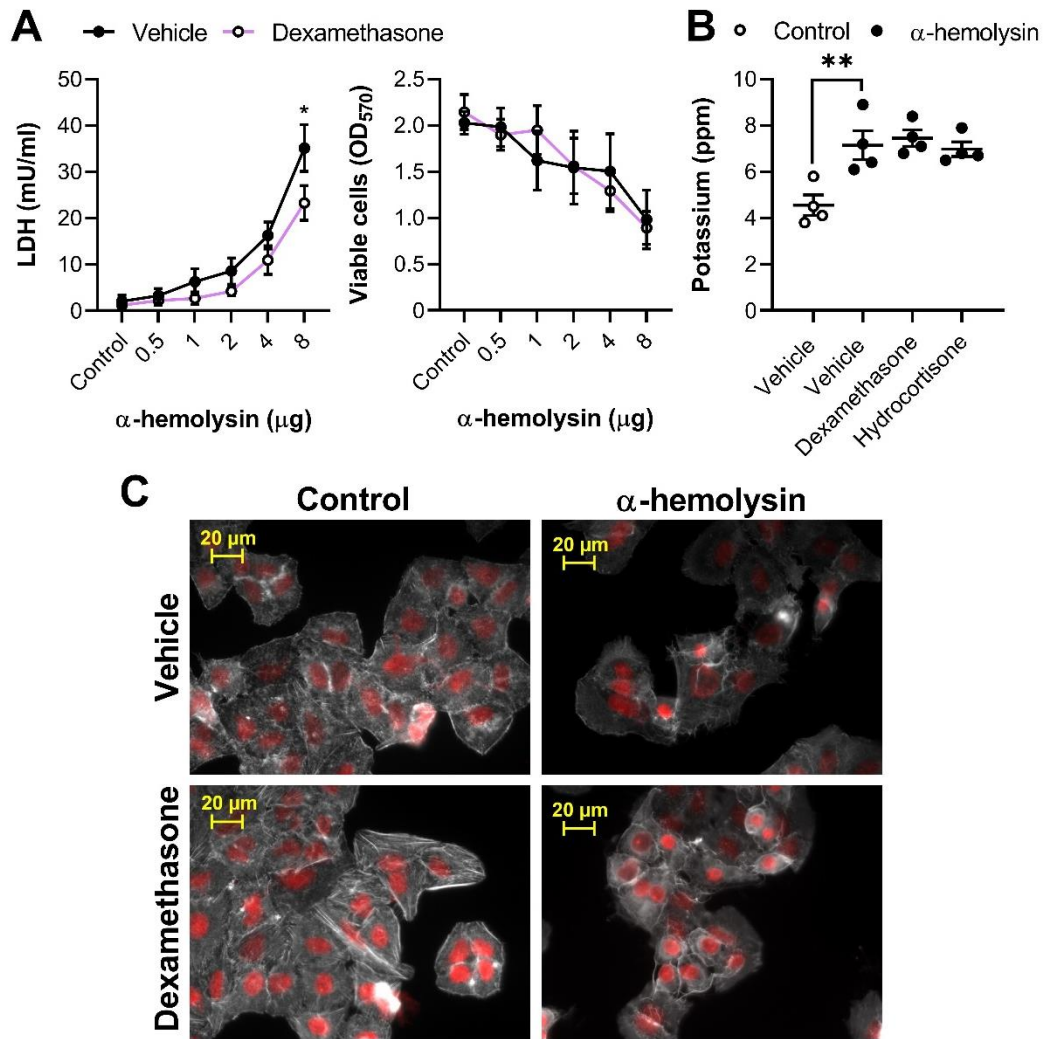


Figure 5.14 Glucocorticoids do not protect A549 cells against α -hemolysin

(A) Leakage of LDH and viability of A549 cells treated for 24 h with vehicle or 10 μM dexamethasone, and then challenged for 24 h with control medium or the indicated concentration of α -hemolysin. Data are presented as mean (SEM) from 4 independent experiments; statistical significance was determined using two-way ANOVA and Bonferroni's post hoc test; * $P < 0.05$. (B) Leakage of potassium from A549 cells treated for 24 h with vehicle, 10 μM dexamethasone, 10 μM hydrocortisone or 1 mM M β CD, and then challenged for 15 min with control medium or 8 μg α -hemolysin. Dots represent individual values from 4 independent experiments; statistical significance was determined using one-way ANOVA with Dunnett's post hoc test; ** $P < 0.01$. (C) Fluorescent microscope images of A549 cells treated for 24 h with vehicle, 10 μM dexamethasone, then challenged for 24 h with control medium or 8 μg α -hemolysin and stained with fluorescent phalloidin (white) and DAPI (red); images are representative from 3 independent experiments.

5.3.3 Cytoprotection is glucocorticoid receptor dependent

To investigate the role of the glucocorticoid receptor in cytoprotection, we first used fluticasone propionate, a glucocorticoid receptor agonist (Johnson, 1998). Fluticasone propionate is highly selective, demonstrating negligible effects on the human androgen, mineralocorticoid, or progesterone receptor (Johnson, 1998). Additionally, fluticasone is more potent than dexamethasone at activating glucocorticoid receptor target genes (Adcock and Barnes, 1996). Treatment with fluticasone propionate for 24 h reduced pyolysin-induced leakage of LDH and cytolysis in HeLa (Fig 5.15A) and A549 (Fig 5.15B) cells.

Secondly, we used the glucocorticoid receptor antagonist RU486, which binds to both the progesterone and the glucocorticoid receptor with a high affinity, (Cadepond et al., 1997). However, we focused on the anti-glucocorticoid activity as HeLa cells do not express the progesterone receptor (Mac Namara and Loughrey, 1998). Treatment with RU486 induces glucocorticoid receptor translocation, though the bound antagonist cannot induce the correct conformational change in the glucocorticoid receptor, impairing DNA interaction (Bourgeois et al., 1984, Fryer et al., 2000, Nordeen et al., 1995). Dexamethasone and hydrocortisone cytoprotection were impaired following treatment with RU486 in HeLa (Fig 5.16A,B) and in A549 (5.16C) cells, with pyolysin-induced reductions in cell viability and LDH leakage restored.

Finally, we depleted the glucocorticoid receptor in HeLa cells using siRNA to target *NR3C1* (Fig 5.17A, B). Depleting the glucocorticoid receptor impaired the cytoprotective effect of dexamethasone and hydrocortisone against pyolysin (Fig 5.17C). Together these experiments provide evidence that glucocorticoid cytoprotection against pyolysin was dependent on the glucocorticoid receptor.

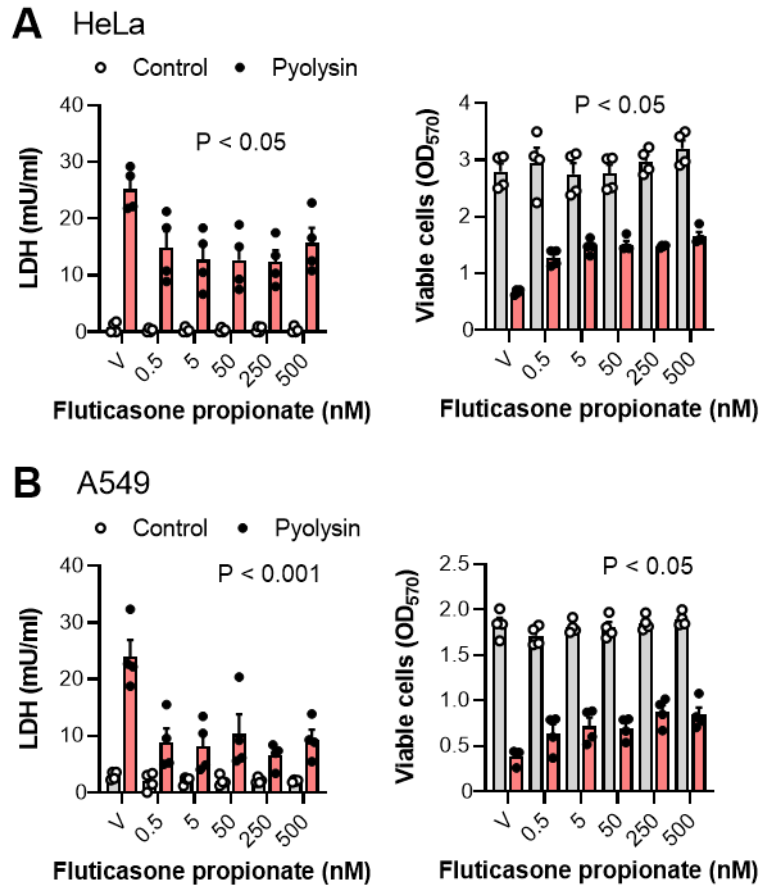


Figure 5.15 Fluticasone protects HeLa and A549 cells against pyolysin damage
 Leakage of LDH and viability of (A) HeLa and (B) A549 cells treated for 24 h with vehicle or the indicated concentrations of fluticasone propionate, and then challenged for 2 h with control medium or pyolysin (100 HU, HeLa; 25 HU, A549). Data are presented as mean (SEM) from 4 independent experiments; statistical significance was determined using two-way ANOVA, and P-values are reported for the effect of treatment on pyolysin challenge.

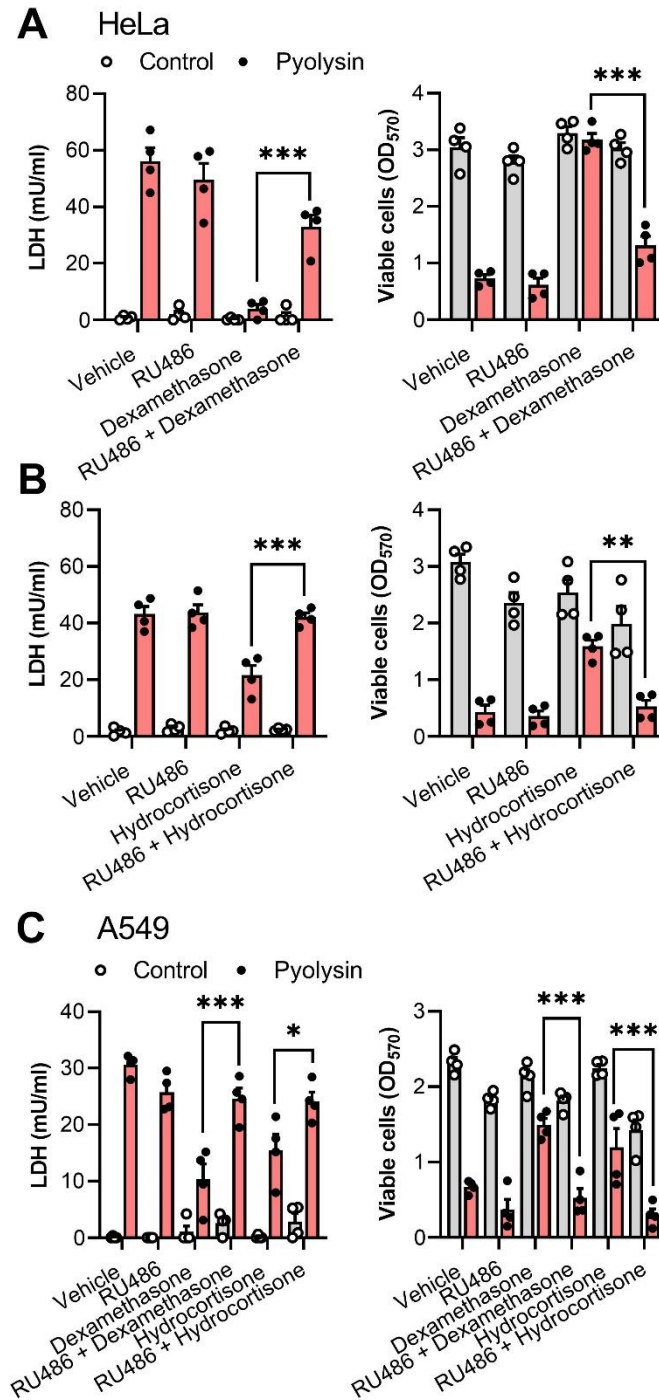


Figure 5.16 The glucocorticoid receptor contributes to cytoprotection

Leakage of LDH and viability of (A,B) HeLa and (C) A549 cells treated for 24 h with vehicle, 10 μ M dexamethasone, or 10 μ M hydrocortisone, in the presence of vehicle or 10 μ M RU486, and then challenged for 2 h with control medium or pyolysin (100 HU, HeLa; 25 HU, A549). Data are presented as mean (SEM) of 4 independent experiments; statistical significance was determined using two-way ANOVA and Bonferroni's post hoc test; * $P < 0.05$, ** $P < 0.01$, *** $P < 0.001$.

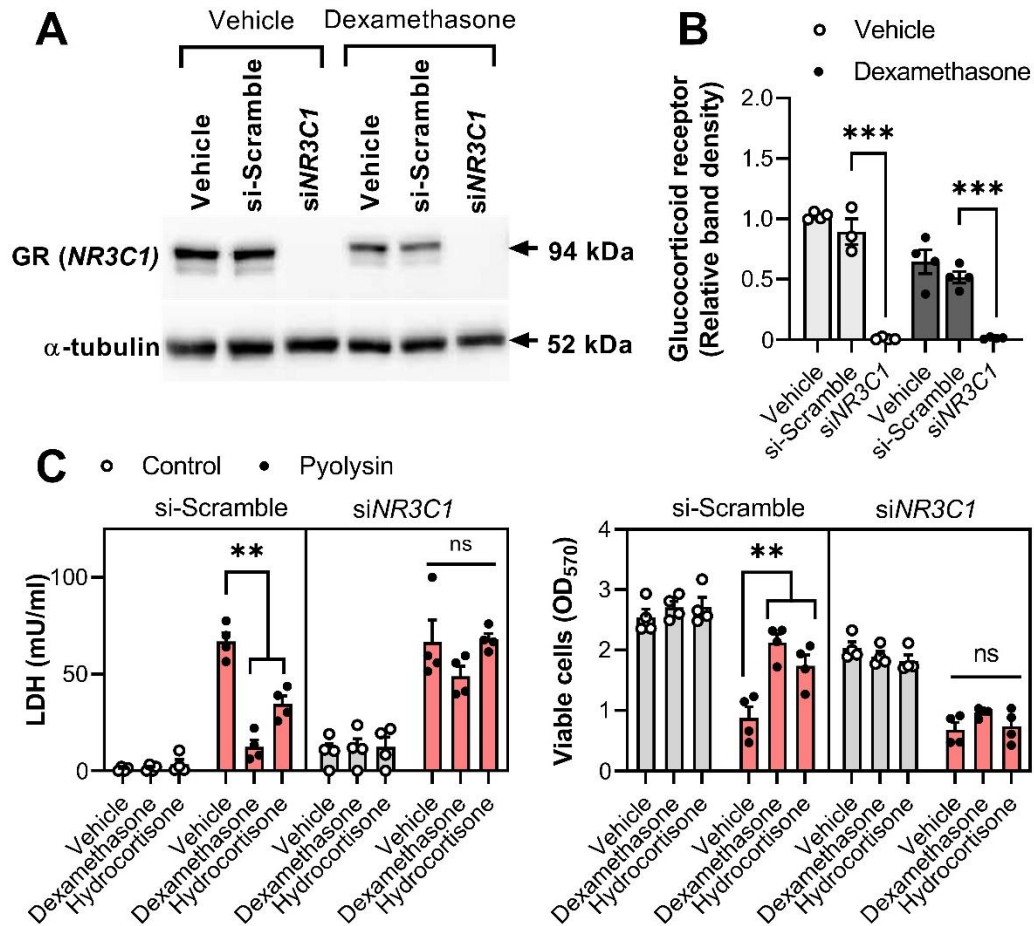


Figure 5.17 Glucocorticoid cytoprotection against pyolysin is *NR3C1* dependent
(A) Representative Western blots of glucocorticoid receptor and α -tubulin for HeLa cells transfected with scrambled siRNA or siRNA targeting *NR3C1*; image representative from 4 independent experiments. **(B)** Densitometry data for glucocorticoid receptor were normalized to α -tubulin and presented as mean (SEM); statistical significance was determined using two-way ANOVA and Dunnett's post hoc test; *** $P < 0.001$. **(C)** Leakage of LDH and viability of HeLa cells transfected for 48 h with scramble siRNA or siRNA targeting *NR3C1*, treated for 24 h with vehicle, 10 μ M dexamethasone or 10 μ M hydrocortisone, and then challenged for 2 h with control medium or 100 HU pyolysin. Data are presented as mean (SEM) from 4 independent experiments; statistical significance was determined using two-way ANOVA and Bonferroni's post hoc test; ** $P < 0.01$.

5.3.4 Cytoprotection is not dependent on changes in cellular cholesterol.

We next considered possible mechanisms for glucocorticoid cytoprotection. Cholesterol-dependent cytolysins bind to accessible cholesterol in plasma membranes (Das et al., 2013), and reducing cellular cholesterol protects against cytolysis (Statt et al., 2015, Amos et al., 2014). Although treatment with 1 mM M β CD for 24 h reduced total cellular cholesterol by 40% in HeLa (Fig 5.18A) and 52% in A549 (Fig 5.18B) cells, treatment with dexamethasone or hydrocortisone did not reduce cellular cholesterol in either cell type. In fact, dexamethasone and hydrocortisone increased the abundance of cholesterol in A549 cells ($P < 0.01$). Furthermore, even adding 30 μ g/ml cholesterol in combination with the glucocorticoid treatments did not significantly reduce cytoprotection against pyolysin (Fig 5.19).

We have shown in *Chapter 3* and *Chapter 4* that oxysterols protect cells against cholesterol-dependent cytolysins partially through ACAT esterification of cholesterol to reduce accessible labile cholesterol in plasma membranes. However, although inhibiting ACAT with SZ58-035 reduced 27-hydroxycholesterol cytoprotection against pyolysin-induced LDH leakage and cytolysis, SZ58-035 had no significant effect on dexamethasone cytoprotection (Fig 5.20). This data provides some evidence to suggest that glucocorticoids and side-chain oxysterols protect cells against pore-forming toxins through independent mechanisms.

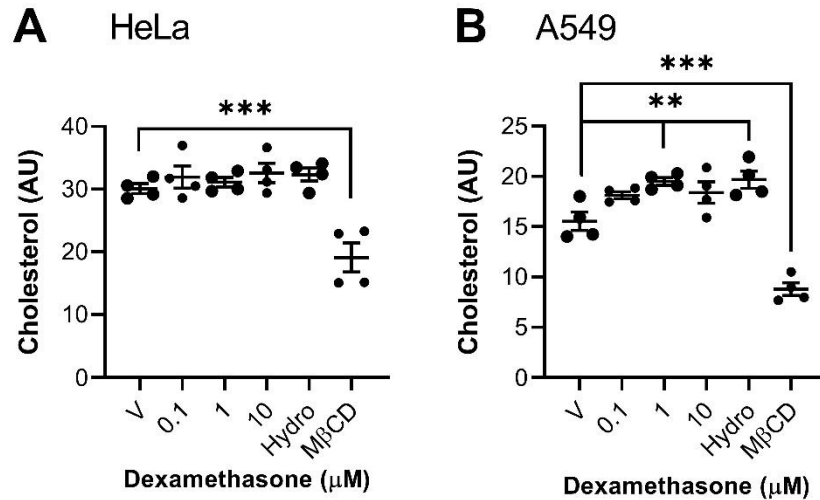


Figure 5.18 Glucocorticoids do not reduce HeLa or A549 cell cholesterol

Cellular cholesterol in (A) HeLa and (B) A549 cells treated for 24 h with vehicle (V), the indicated concentration of dexamethasone, 10 μ M hydrocortisone (Hydro) or 1 mM M β CD. Data are presented as mean (SEM) from 4 independent experiments; statistical significance was determined using one-way ANOVA with Dunnett's post hoc test; **P < 0.01, ***P < 0.001.

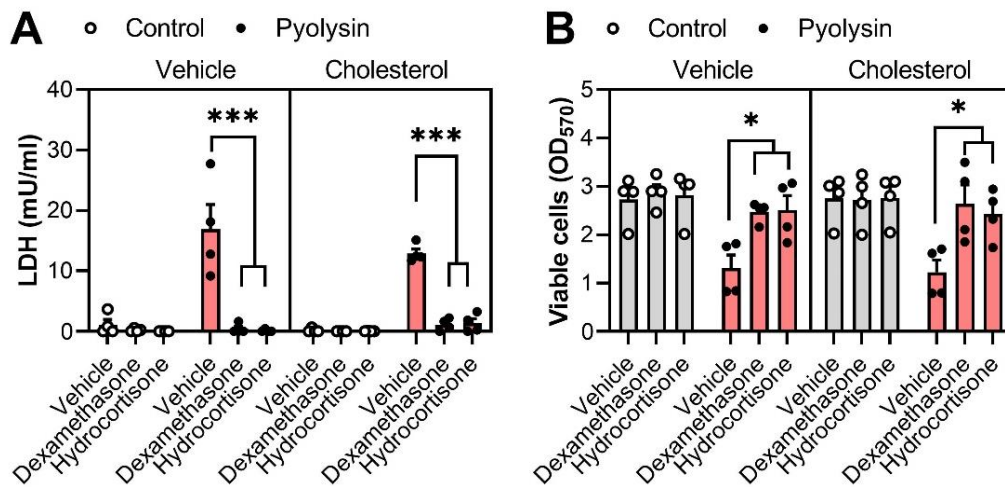


Figure 5.19 Cholesterol supplementation does not prevent glucocorticoid cytoprotection

(A) Leakage of LDH and (B) viability of HeLa cells treated for 24 h with vehicle, 10 μ M dexamethasone, or 10 μ M hydrocortisone in medium containing 30 μ g/ml cholesterol, and then challenged for 2 h with control medium or 100 HU pyolysin. Data are presented as mean (SEM) from 4 independent experiments; statistical significance was determined using two-way ANOVA with Bonferroni's multiple comparison test; *P < 0.05, ***P < 0.001.

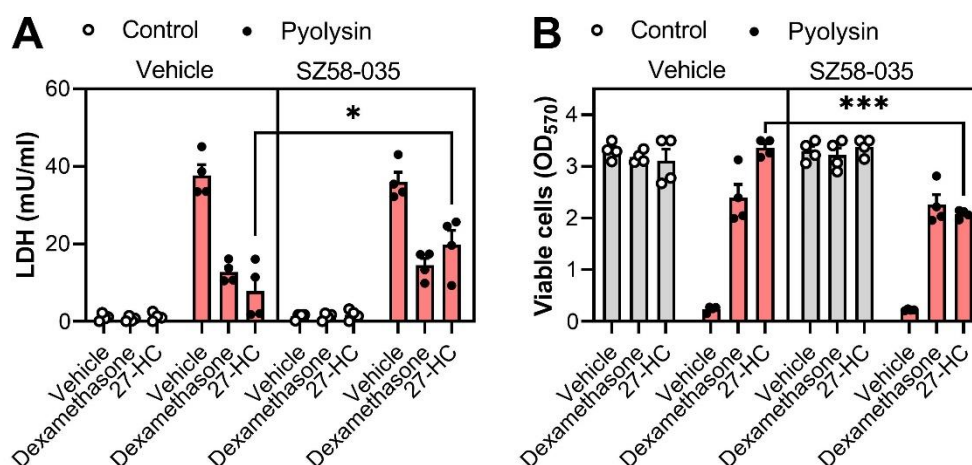


Figure 5.20 Inhibiting ACAT does not prevent glucocorticoid cytoprotection

(A) Leakage of LDH and (B) viability of HeLa cells cultured for 16 h with vehicle or 10 μ M SZ58-035, then treated for 24 h with vehicle, 10 μ M dexamethasone, or 10 ng/ml 27-hydroxycholesterol (27-HC), in the continuing presence of vehicle or SZ58-035, and then challenged for 2 h with control medium or 100 HU pyolysin. Data are presented as mean (SEM) from 4 independent experiments; statistical significance was determined using two-way ANOVA with Tukey's post hoc test; * $P < 0.05$, *** $P < 0.001$.

We also examined the binding of pyolysin to cells to evaluate if glucocorticoids altered the accessible labile cholesterol in the plasma membrane (Das et al., 2013). As expected, treating HeLa cells with, the LXR agonist T0901317, 27-hydroxycholesterol or M β CD, diminished pyolysin binding (Fig. 5.21). However, treatment with dexamethasone or hydrocortisone had no significant effect on pyolysin binding to HeLa cells, although less pyolysin bound to A549 cells (Fig 5.22). Together these results do not support the concept that glucocorticoid cytoprotection is mediated by alterations in cellular cholesterol.

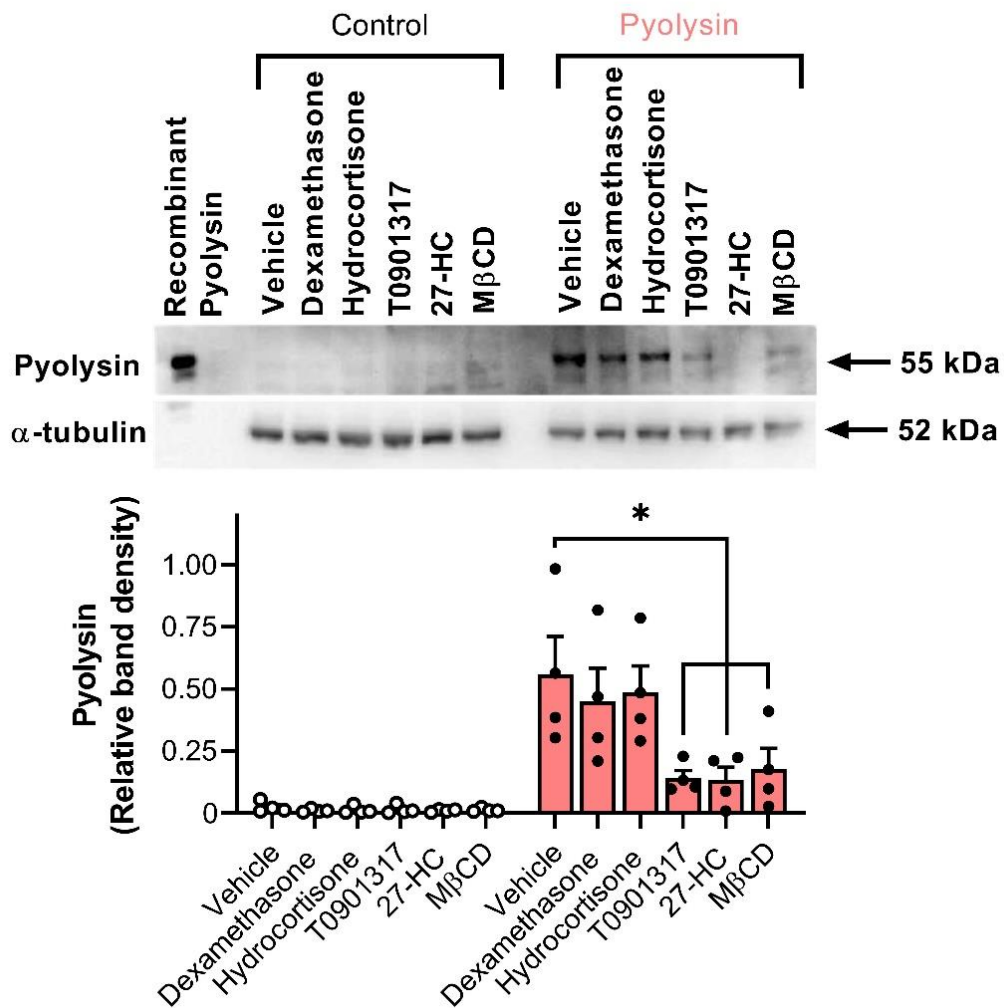


Figure 5.21 Glucocorticoids do not reduce pyolysin binding in HeLa cells

Representative Western blot of pyolysin binding and α -tubulin for HeLa cells treated for 24 h with vehicle, 10 μ M dexamethasone, 10 μ M hydrocortisone, 50 nM T0901317, 10 ng/ml 27-hydroxycholesterol (27HC), or 1 mM M β CD, and then challenged for 2 h with control medium or 100 HU pyolysin. Densitometry data were normalized to α -tubulin and presented as mean (SEM) from 4 experiments; statistical significance was determined using ANOVA and Dunnett's post hoc test; *P < 0.05.

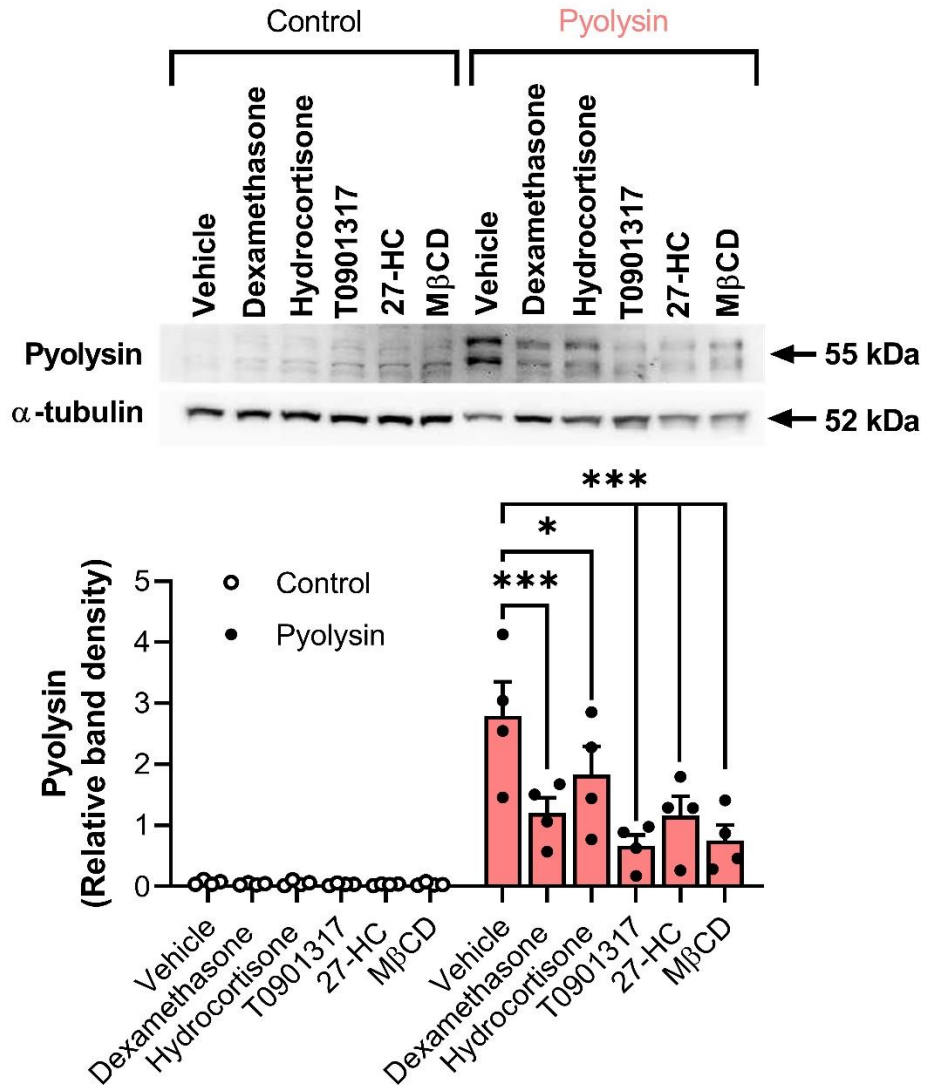


Figure 5.22 Glucocorticoids reduce pyolysin binding in A549 cells

Representative Western blot of pyolysin binding and α -tubulin for A549 cells cultured for 24 h with vehicle, 10 μ M dexamethasone, 10 μ M hydrocortisone, 50 nM T0901317, 10 ng/ml 27-hydroxycholesterol (27-HC), or 1 mM M β CD, and then challenged for 2 h with control medium or 25 HU pyolysin. Densitometry data were normalized to α -tubulin and presented as mean (SEM) from 4 independent experiments; statistical significance was determined using ANOVA and Dunnett's post hoc test, P-values are reported.

5.3.5 Serum impairs glucocorticoid cytoprotection.

Using serum-free media avoided the potentially confounding endogenous cholesterol, steroids, and LDH in serum (Thomas et al., 2015). However, to determine whether serum affected cytoprotection, HeLa cells were treated with dexamethasone, hydrocortisone or fluticasone propionate in complete medium containing 10% serum, before challenging cells for 2 h with pyolysin in serum-free medium. The presence of 10% serum impaired glucocorticoid cytoprotection in HeLa cells (Fig 5.23A). The impairment of cytoprotection by serum was concentration-dependent, but $\geq 4\%$ serum prevented cytoprotection (Fig 5.23B).

Charcoal stripping FBS can reduce the concentration of steroid hormones (such as oestrogens, androgens, and progesterone), growth factors, and vitamins that might impact glucocorticoid cytoprotection (Cao et al., 2009, Sikora et al., 2016, Tu et al., 2018). However, using 10% steroid-depleted charcoal-stripped serum did not restore cytoprotection (Fig 5.23C). Additionally, the presence of serum impaired glucocorticoid cytoprotection in A549 cells (Fig 5.24). Intriguingly, when HeLa cells were treated with dexamethasone in serum-free media for 24 h, cytoprotection was impaired if 10% serum was added for ≥ 2 h before a pyolysin challenge (Fig 5.25A). Conversely, cytoprotection was restored by replacing serum-containing medium and dexamethasone, with serum-free medium without dexamethasone for ≥ 8 h before a pyolysin challenge (Fig 5.25B). Together these data provide evidence for serum reversibly impairing glucocorticoid cytoprotection against pyolysin.

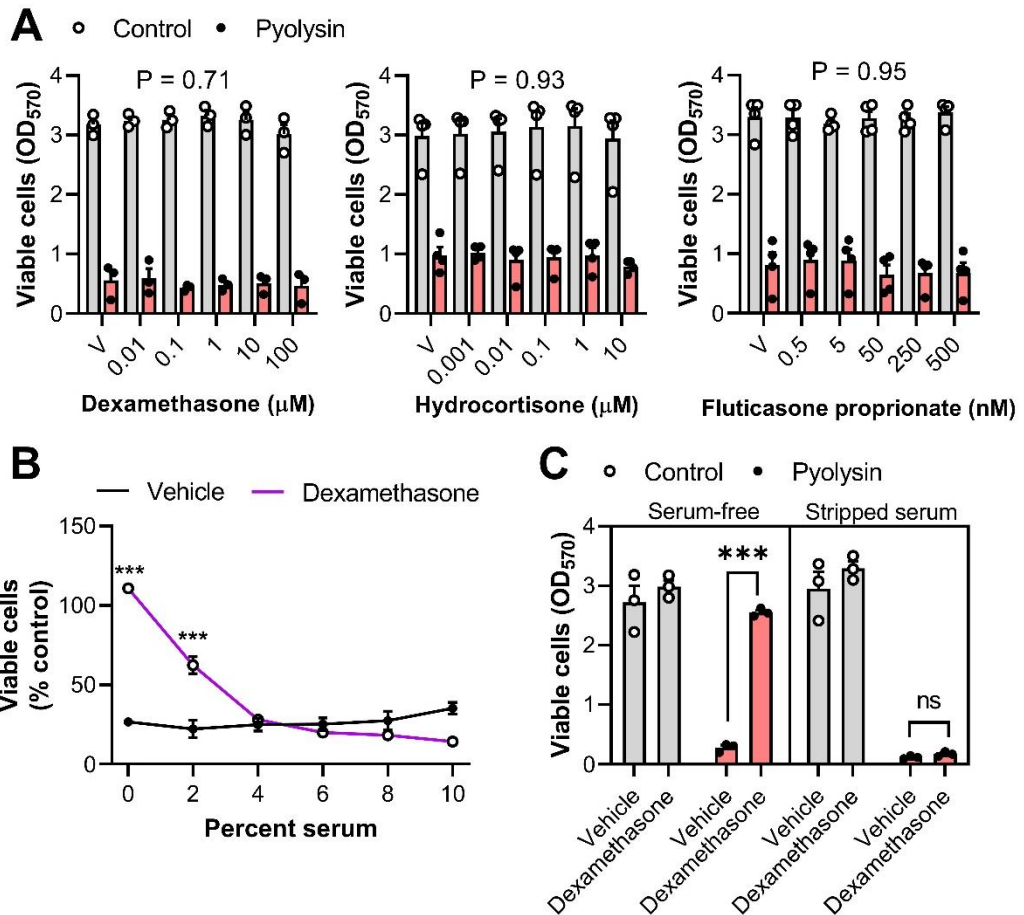


Figure 5.23 Serum prevents glucocorticoid cytoprotection in HeLa cells

(A) Viability of HeLa cells treated for 24 h with vehicle, or the indicated concentrations of dexamethasone, hydrocortisone, or fluticasone propionate in complete medium containing 10% serum, and then challenged for 2 h with control serum-free medium or 100 HU pyolysin. Data are presented as mean (SEM) from 4 independent experiments; statistical significance was determined using two-way ANOVA and P-values are reported for the effect of treatment on pyolysin challenge.

(B) Viability of HeLa cells treated with vehicle or 10 μM dexamethasone in serum-free medium or complete medium containing the indicated concentration of serum, and then challenged for 2 h with control serum-free medium or 100 HU pyolysin. Data are presented as mean (SEM) percentage viable cells compared with the control challenge from 4 independent experiments; statistical significance was determined using two-way ANOVA and Bonferroni's post hoc test; *** $P < 0.001$.

(C) Viability of HeLa cells treated with vehicle or 10 μM dexamethasone in serum-free medium or complete medium containing 10% stripped serum, and then challenged for 2 h with control serum-free medium or 100 HU pyolysin. Data are presented as mean (SEM) from 4 independent experiments; statistical significance was determined using two-way ANOVA with Bonferroni's post hoc test; *** $P < 0.001$.

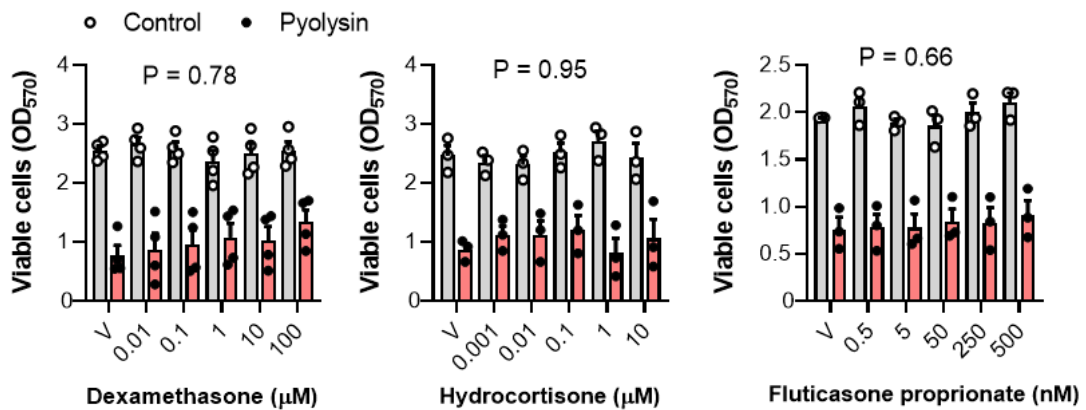


Figure 5.24 Serum prevents glucocorticoid cytoprotection in A549 cells

A549 cells were treated with vehicle or the indicated concentrations of dexamethasone, hydrocortisone, or fluticasone propionate in complete medium containing 10% serum, and then challenged for 2 h with control serum-free medium or 25 HU pyolysin. Cell viability was assessed by MTT assay. Data are presented as mean (SEM) from 4 independent experiments; statistical significance was determined using two-way ANOVA and P-values are reported for the effect of treatment on pyolysin challenge.

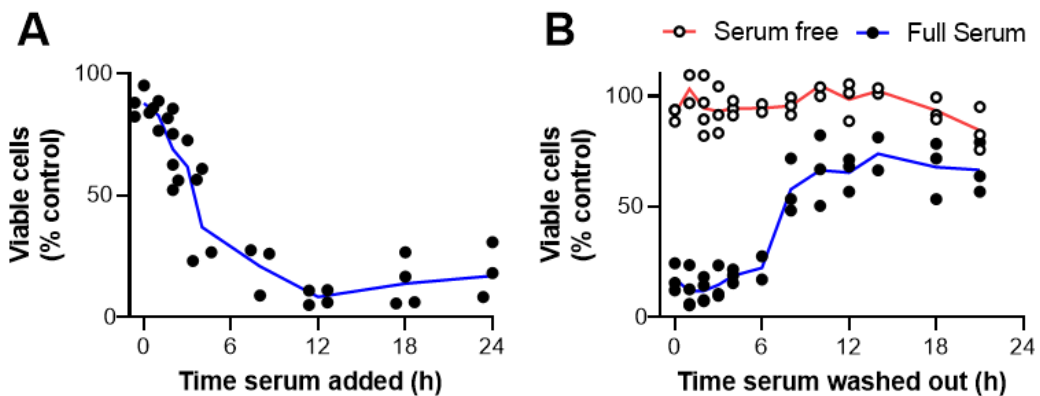


Figure 5.25 Serum reversibly inhibits glucocorticoid cytoprotection

(A) Viability of HeLa cells treated with vehicle or 10 μ M dexamethasone for 24 h in control serum-free medium, and then supplemented with 10% serum at the indicated time prior to being challenged for 2 h with control serum-free medium or 100 HU pyolysin. Data are presented as percentage viability of control challenge, and dots represent individual values from 2 to 4 cell passages at each time point. (B) Viability of HeLa cells treated for 24 h with vehicle or 10 μ M dexamethasone in serum-free or complete medium containing 10% serum, with the medium replaced with serum-free medium, without treatments, at the indicated time periods before the cells were challenged for 2 h with control serum-free medium or 100 HU pyolysin. Data are presented as percentage viable cells compared with the control challenge, and dots represent individual values from 2 to 4 cell passages at each time point.

5.3.6 Ion flux does not contribute to glucocorticoid cytoprotection

When challenged with pore-forming toxins, cells activate the MAPK cell stress response and damage repair mechanisms, principally in response to potassium efflux and calcium influx (Kloft et al., 2009, Cassidy and O'Riordan, 2013, Gonzalez et al., 2011). As expected, treatment with dexamethasone or hydrocortisone did not induce MAPK phosphorylation (Fig 5.26). Instead, dexamethasone and hydrocortisone treatment prevented pyolysin-induced phosphorylation of ERK1/2, p38 and JNK, as effectively as M β CD.

Furthermore, although cells challenged with pyolysin in low-potassium medium (5 mM KCl) leaked more LDH and were less viable than cells challenged with pyolysin in high-potassium high medium (140 mM KCl to prevent potassium efflux), dexamethasone remained cytoprotective (Fig 5.27).

To examine the impact of calcium ion flux, HeLa cells were treated with dexamethasone and challenged with pyolysin in medium with and without calcium. In *Chapter 4*, HeLa cells were significantly more susceptible to pyolysin when challenged in calcium free medium to prevent calcium ion influx. Therefore, in the present chapter we used a range of pyolysin challenge conditions to ensure that increased cell death did not mask the role of calcium ion influx on glucocorticoid cytoprotection. To cause a varying degree of LDH leakage and cytolysis, we challenge cells for 2 h with both a low and high concentration of pyolysin in medium that was calcium free for 15 min or 2 h. Limiting calcium ion influx increased pyolysin-induced LDH leakage and cytolysis in all challenge conditions (Fig 5.28). Dexamethasone treatment was consistently cytoprotective ($P < 0.01$), however, protection was significantly less effective against 100 HU pyolysin in calcium free medium for 2 h, with cells less viable and leaking more LDH than cells challenged in calcium containing medium (Fig 5.28B). Together this data provide evidence to suggest that glucocorticoid cytoprotection against pyolysin is not dependent on the influx of calcium ions, the efflux of potassium ions, or MAPK phosphorylation.

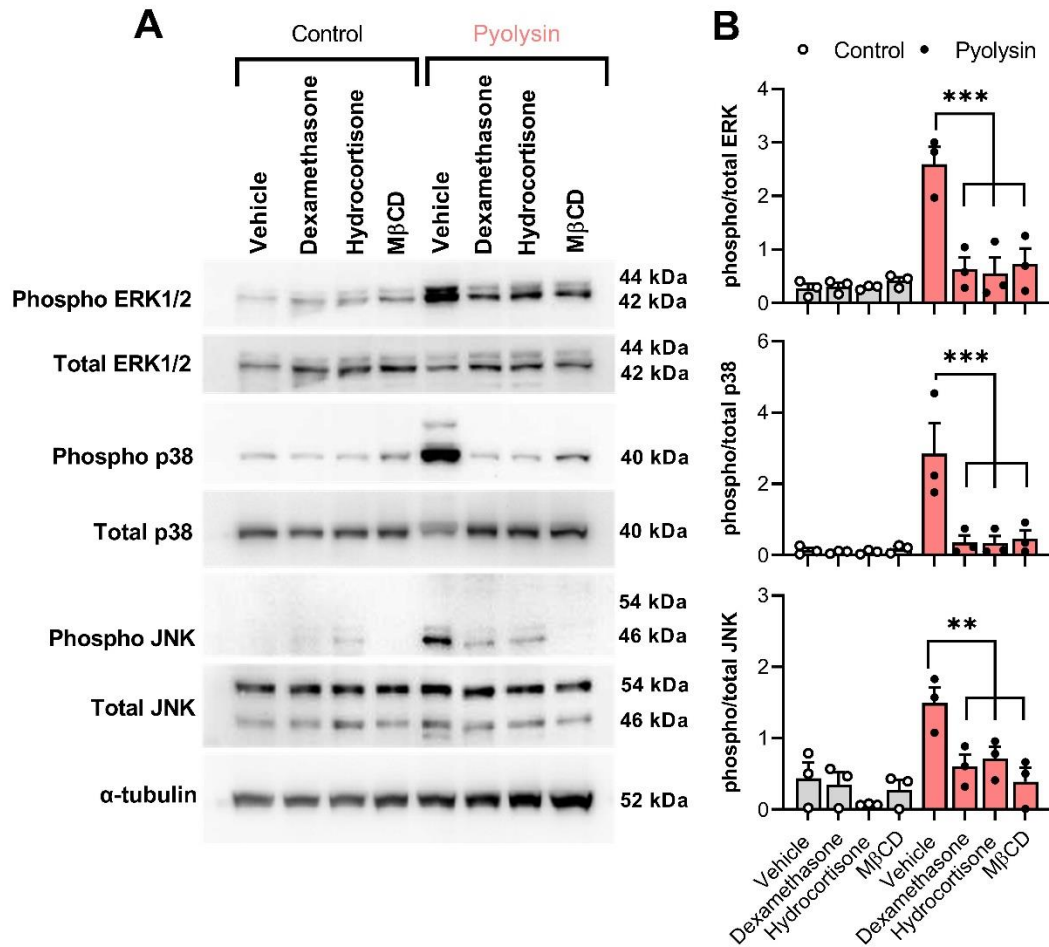


Figure 5.26 Glucocorticoids reduce pyolysin-induced MAPK phosphorylation

Representative Western blot of phosphorylated and total ERK1/2, p38 and JNK, and α -tubulin for HeLa cells treated for 24 h with vehicle, 10 μ M dexamethasone, 10 μ M hydrocortisone or 1 mM M β CD, and challenged for 10 min with control medium or 100 HU pyolysin. Densitometry data were normalized to α -tubulin and presented as mean (SEM) from 3 experiments; statistical significance was determined using ANOVA with Tukey's post hoc test; **P < 0.01, ***P < 0.001.

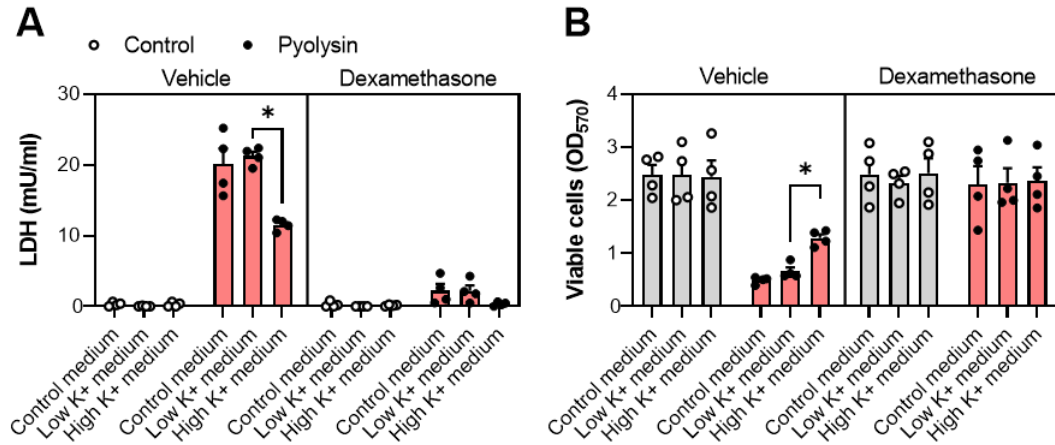


Figure 5.27 Potassium ion efflux does not affect dexamethasone cytoprotection

(A) Leakage of LDH and (B) viability of HeLa cells treated for 24 h with serum-free medium containing vehicle or 10 μ M dexamethasone and then challenged for 2 h with 100 HU pyolysin in control medium, low-potassium medium, or high-potassium medium. Data are presented as mean (SEM) from 4 independent experiments; statistical significance was determined using two-way ANOVA and Bonferroni's post hoc test; * $P < 0.05$.

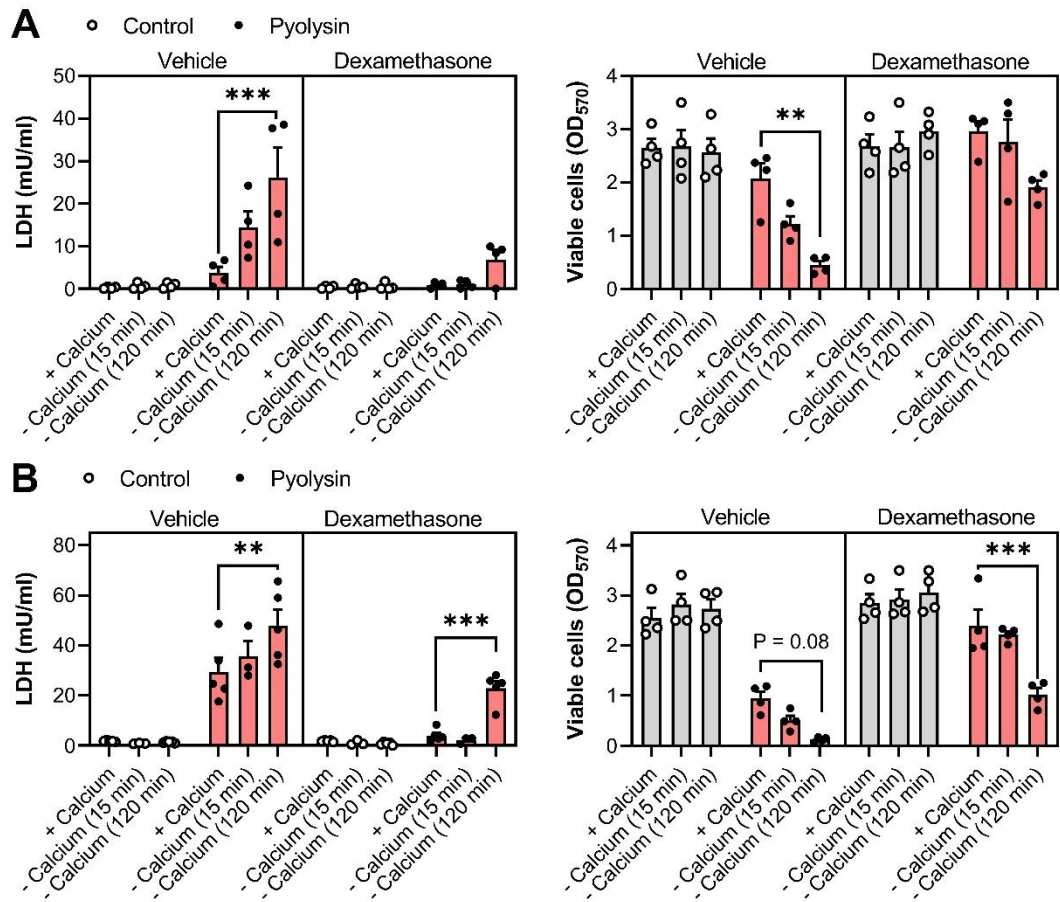


Figure 5.28 Calcium ion influx does not affect glucocorticoid cytoprotection

Hela cells were treated with control serum-free medium containing vehicle or 10 μ M dexamethasone for 24 h and challenged for 2 h with (A) 25 HU pyolysin, or (B) 100 HU pyolysin in medium containing calcium, in calcium-free medium for 15 min then supplemented with calcium for the remainder of the challenge, or in calcium-free medium for the full 2 h. The leakage of LDH was measured in cell supernatants and cell viability was assessed by MTT. Data are presented as mean (SEM) with dots representing the values of cells from 4 independent passages; and are analysed by two-way ANOVA with Bonferroni's post hoc test; ** $P < 0.01$, *** $P < 0.001$.

5.3.7 Glucocorticoid cytoprotection is partially dependent on HMGCR

We finally considered whether the cytoprotective action against pyolysin might depend on glucocorticoids activating a specific gene. Actinomycin D is a polypeptide antibiotic that intercalates into DNA, inhibiting transcription by preventing the progression of RNA polymerases (Perry and Kelley, 1970, Bensaude, 2011). Cycloheximide blocks the elongation phase of eukaryotic translation by binding to ribosomes and inhibiting enzyme II-dependent translocation (Obrig et al., 1971, Schneider-Poetsch et al., 2010). Using actinomycin to inhibit gene transcription or cycloheximide to inhibit translation in HeLa cells impaired dexamethasone cytoprotection (Fig 5.29).

Glucocorticoids and serum regulate numerous genes, though a limited number are regulated by both (Wang et al., 2004, Iyer et al., 1999). From the literature we identified 22 genes regulated by both dexamethasone and serum, of which only 15 were differentially regulated (Table 5.2A-G). This list largely contained genes that seemed unlikely to contribute to cytoprotection, however, one potential candidate was *HMGCR*, the rate-limiting enzyme in the mevalonate pathway. Dexamethasone increases and serum reduces *HMGCR* expression (Cavenee and Melnykovich, 1977, Cavenee et al., 1978, Johnston et al., 1979). Using siRNA to target *HMGCR* reduced HMGCR protein by 37% (Fig 5.30A, B), and reduced the effectiveness (but did not prevent) dexamethasone cytoprotection (Fig 5.30C). Thus, we conclude that that dexamethasone cytoprotection may be partially reliant on HMGCR.

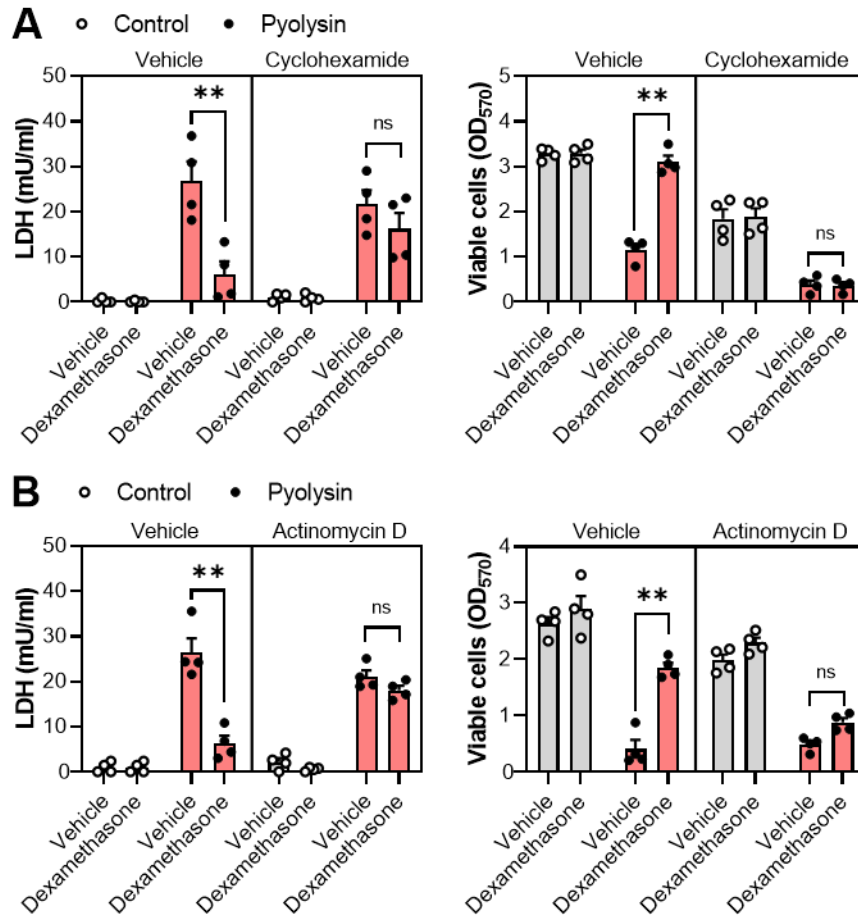


Figure 5.29 Glucocorticoid cytoprotection is dependent on transcription and translation

Leakage of LDH and viability of HeLa cells treated for 24 h with vehicle or 10 μ M dexamethasone, in medium containing vehicle, (A) 1 μ g/ml cycloheximide or (B) 0.25 μ g/ml actinomycin D (added 2 h prior to dexamethasone), and then challenged for 2 h with control medium or 100 HU pyolysin. Data are presented as mean (SEM) from 4 independent experiments; statistical significance was determined using two-way ANOVA with Bonferroni's post hoc test; **P < 0.01.

Table 5.2 Genes regulated by dexamethasone and serum

Genes grouped into sub tables **A - G** according to function. Human Gene Organisation Gene Nomenclature Committee (HGNC) ID number provided for each gene.

Key	
↑	Induced
↓	Repressed
	Differentially regulated
	Similarly regulated
References	
1. (Wang et al., 2004)	11. (Wang et al., 2007)
2. (Iyer et al., 1999)	12. (Cavenee and Melnykovych, 1977)
3. (Amano et al., 1993)	13. (Mostafa et al., 2019)
4. (Chang et al., 2001)	14. (Mayanagi et al., 2008)
5. (Kim et al., 2015)	15. (Meisinger et al., 1996)
6. (Dhawan et al., 2007)	16. (Chedid et al., 1996)
7. (Lasa et al., 2002)	17. (Yang et al., 2014)
8. (Kempainen and Behrend, 1998)	18. (Breen et al., 2012)
9. (Wang et al., 2017)	19. (van de Stolpe et al., 1993)
10. (Obradovic et al., 2019)	20. (Wang et al., 2006)

(A) Inflammation		
Gene Name (HGNC ID)	Dexamethasone	FBS
ALOX5AP (436)	↑ (1)	
CCL2 (10618)	↓ (1, 6)	↓ (2)
CCL20 (10619)	↑ (1)	
CXCL12 (10672)		↑ (2)
CXCL2 (4603)		↓ (2)
CXCL8 (6025)	↓ (4)	↓ (5)
ICAM1 (5344)	↓ (19)	↑ (2)
IL11 (5966)	↓ (1)	
IL1B (5992)	↓ (3)	↓ (2)
PDE4B (8781)	↓ (1)	
PTGS2 (9605)	↓ (1)	↑ (2)
THBD (11784)	↑ (1)	
TSC22D3 (3051)	↑ (1)	

(B) Metabolism		
Gene Name (HGNC ID)	Dexamethasone	FBS
ANGPTL4 (16039)	↑ (1)	
B3GNT5 (15684)	↑ (1)	
ETNK2 (25575)	↑ (1)	
MGAM (7043)	↑ (1)	
TXNIP (16952)	↑ (20)	↓ (2)

(C) Transport		
Gene Name (HGNC ID)	Dexamethasone	FBS
MT1A (7393)	↑ (7)	↑ (2)
MT1B (7394)		↑ (2)
MT1IP (7401)	↑ (1)	↑ (2)
SCNN1A (10599)	↑ (1)	
SLC19A2 (10938)	↑ (1)	
SLC26A2 (10994)	↑ (1)	
STOM (2282)	↑ (1)	

(D) Growth and Apoptosis		
Gene Name (HGNC ID)	Dexamethasone	FBS
BIRC3 (591)	↑ (1)	
CCNA2 (1578)		↑ (2)
CCNB1 (1579)		↑ (2)
CCND1 (1582)		↑ (2)
CDK1 (1722)		↑ (2)
CDK7 (1788)		↑ (2)
CDKN1C (1786)	↑ (1)	↓ (2)
CENPF (1857)		↑ (2)
CKS2 (2000)		↑ (2)
CTPS1 (2519)		↑ (2)
CUL1 (2551)	↓ (1)	
FGFBP1 (19695)	↓ (1)	
GADD45B (4096)	↑ (1)	
ID2 (5361)		↑ (2)
ID3 (5362)		↑ (2)
LBR (6518)		↓ (2)
MAD2L1 (6763)		↑ (2)
MFGE8 (7036)	↑ (1)	
MKI67 (7101)		↑ (2)
PCNA (8729)		↑ (2)
RRM1 (10451)		↑ (2)
RRM2 (10452)		↑ (2)
S100P (10504)	↑ (1)	
SERPINB9 (8955)	↓ (1)	
SERTAD2 (30784)	↓ (1)	
SIAH1 (10857)		↓ (2)
SNAI2 (11094)	↑ (1)	
SPRY1 (11269)	↑ (1)	
TNFAIP3 (11896)	↑ (1)	
TOP2A (11989)		↑ (2)
WEE1 (12761)		↓ (2)

(E) Cholesterol Biosynthesis		
Gene Name (HGNC ID)	Dexamethasone	FBS
CYP51A1 (2649)		↓ (2)
FDFT1 (3629)		↓ (2)
HMGCR (5006)	↑ (12)	↓ (2, 12)
IDII (5387)		↓ (2)
SQLE (11279)		↓ (2)

(F) Cell Signalling		
Gene Name (HGNC ID)	Dexamethasone	FBS
ACKR3 (23692)	↓ (1)	
AKAP13 (371)	↑ (1)	
ANKRD1 (15819)	↑ (1)	
ARL8 (25192)	↓ (1)	
BHLHE40 (1046)	↓ (1)	
CDC42EP3 (16943)	↑ (1)	
CPEB4 (21747)	↑ (1)	
DNER (24456)	↑ (1)	
DUS1 (3064)	↑ (7)	↑ (2)
EDN2 (3177)	↑ (1)	
ENC1 (3345)	↓ (1)	
EPB41L4B (19818)	↑ (1)	
FGD4 (19125)	↑ (1)	
FKBP5 (3721)	↑ (1, 17)	↓ (17)
GEM (4234)	↓ (1)	↓ (2)
IHPK3 (17269)	↑ (1)	
IRS2 (6126)	↑ (1)	
KIT (6342)		↓ (2)
PLK2 (19699)	↓ (1)	↑ (2)
POU5F1 (9221)	↑ (1)	
PPP1R14C (14952)	↑ (1)	
RASD1 (15828)	↑ (8)	↓ (9)
RGS2 (9998)	↑ (1)	
ROR1 (10256)	↑ (10)	↓ (2)
S1PR1 (3165)		↑ (2)
SEC14L1 (10698)	↑ (1)	
SGK1 (10810)	↑ (11)	↓ (2)
TGFBR3 (11774)	↑ (1)	↓ (2)
ZIC2 (12873)	↓ (1)	

(G) Other		
Gene Name (HGNC ID)	Dexamethasone	FBS
ABHD2 (18717)	↑ (1)	
ADGRF4 (19011)	↑ (1)	
AMIGO2 (24073)	↓ (1)	
ARRDC3 (29263)	↓ (1)	
CALD1 (1441)	↑ (13,14)	↓ (2)
CAVIN2 (10690)	↑ (1)	↑ (18)
CDH2 (1759)		↑ (2)
CFHR1 (4888)		↓ (2)
COL1A1 (2197)		↓ (2)
DNAJC15 (20325)	↑ (1)	
FBN2 (3604)		↓ (2)
FGF2 (3676)	↑ (15)	↑ (2)
FGF3 (3681)		↓ (2)
FGF7 (3685)	↓ (16)	↑ (2)
FHL2 (3703)		↑ (2)
FLVCR2 (20105)	↑ (1)	
FURIN (8568)		↑ (2)
GPR153 (23618)	↑ (1)	
HKDC1 (23302)	↓ (1)	
KTN1 (6467)	↓ (1)	
LAMA2 (6482)		↓ (2)
LRRC8A (19027)	↑ (1)	
MME (7154)		↓ (2)
NAV3 (15998)	↓ (1)	
OTULINL (25629)	↑ (1)	
PLEKHA7 (27049)	↑ (1)	
PLOD2 (9082)		↑ (2)
PMP2 (9117)	↓ (1)	
PNRC1 (17278)		↓ (2)
PRRG4 (30799)	↑ (1)	
SERPINB2 (8584)		↑ (2)
SERPINE1 (8583)	↑ (13)	↑ (2)
SPINK5L3 (27200)	↑ (1)	
SPTBN1 (11275)		↓ (2)
SRGN (9361)	↑ (1)	
TFPI2 (11761)	↓ (13)	↑ (2)
TNS4 (24352)	↑ (1)	

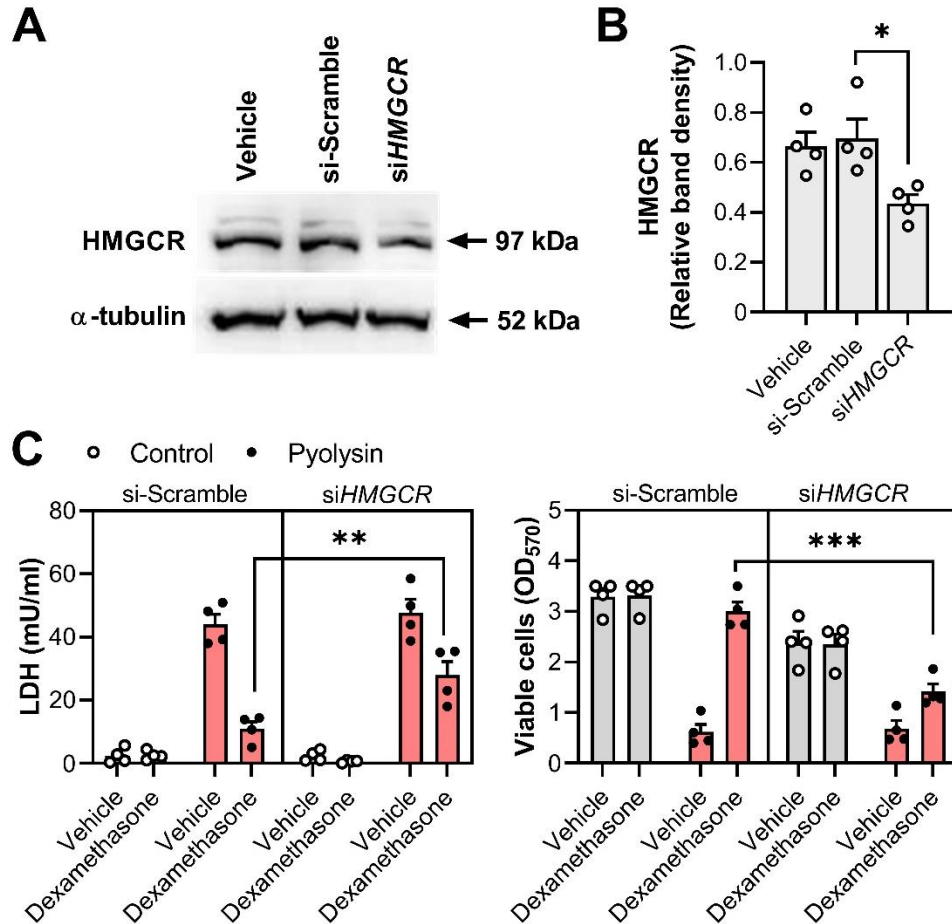


Figure 5.30 Glucocorticoid cytoprotection is partially dependent on HMGCR

(A) Representative Western blot of HMGCR and α -tubulin for HeLa cells transfected with scrambled siRNA or siRNA targeting *HMGCR*; (B) densitometry data for HMGCR were normalized to α -tubulin and presented as mean (SEM) from 4 independent experiments; statistical significance was determined using one-way ANOVA and Dunnett's post hoc test; * $P < 0.05$. (C) Leakage of LDH and viability of HeLa cells transfected for 48 h with scramble siRNA or siRNA targeting *HMGCR*, treated for 24 h with vehicle or 10 μ M dexamethasone, and then challenged for 2 h with control medium or 100 HU pyolysin. Data are presented as mean (SEM) from 4 independent experiments; statistical significance was determined using two-way ANOVA and Bonferroni's post hoc test; ** $P < 0.01$, *** $P < 0.001$.

5.4 DISCUSSION

Glucocorticoids are thought to limit the severity of disease by suppressing inflammation and immunity, however, in this chapter treatment with glucocorticoids increased the intrinsic protection of several cell types against the damage caused by pore-forming toxins. Glucocorticoids are ligands for the glucocorticoid receptor and cytoprotection was dependent on its expression, as well as being reliant on protein transcription and translation. Glucocorticoids did not significantly affect cellular cholesterol and did not appear to protect cells through cholesterol esterification or by preventing toxin binding, though protection may be mediated in part by HMGCR.

Challenging cells with pyolysin, streptolysin O and α -hemolysin led to the formation of pores in cell plasma membranes, determined by the leakage of potassium ions and LDH, activation of the MAPK stress response, changes in cytoskeleton structure, and cell cytolysis. These are typical consequences of pore-forming toxin damage that were mirrored throughout the present thesis (Kloft et al., 2009, Gonzalez et al., 2011, Dal Peraro and van der Goot, 2016).

The key and unexpected finding was that the glucocorticoids dexamethasone and hydrocortisone almost completely protected HeLa cells against cytolysis in the face of pyolysin, streptolysin O and α -hemolysin challenge that typically caused > 75% cytolysis. Treatment with 10 μ M dexamethasone and hydrocortisone, reduced potassium ion and LDH leakage, prevented the activation of the MAPKs ERK1/2, p38 and JNK, and prevented cytoskeletal changes. This protection extended to A549, Hep-G2, NC1-H441, and primary dermal fibroblasts. Collectively, these findings provide evidence for a glucocorticoid cytoprotective effect against pore-forming toxins, which contradicts their inability to significantly protect bovine endometrial cells against pyolysin in *Chapter 3*. This protection has not been previously identified, possibly due to the cell type and context specific nature of glucocorticoid responses.

Cytoprotection was dependent on the glucocorticoid receptor as the specific glucocorticoid receptor agonist fluticasone induced cytoprotection, and siRNA targeting *NR3C1* diminished glucocorticoids cytoprotection. Glucocorticoids regulate gene transcription in a cell specific manner by binding to the glucocorticoid receptor, and associating with glucocorticoid response elements (Biddie et al., 2011, So et al., 2007), though they can repress transcription factors and have immediate non-genomic

effects (Samarasinghe et al., 2012). The protective mechanism was likely genomic as preventing protein transcription and translation with the inhibitors actinomycin D and cycloheximide impaired cytoprotection, and protection required > 8 h of treatment. The transcriptional effects of glucocorticoid treatment vary extensively between cell types. This was demonstrated in a study by Franco et al. (2019) where glucocorticoid treatment caused differential expression of 9,457 unique genes across 9 different cell types, but only 25 of these were significantly differentially expressed in each cell type. Cell specific glucocorticoid responses might explain the varying degree of protection against pyolysin challenge observed across the cell types examined in this study, the limited protection of A549 cells against α -hemolysin damage, and the lack of protection in the bovine endometrium in *Chapter 3*.

Reducing cellular cholesterol is an effective method for protecting cells against cholesterol-dependent cytolytic toxins (Amos et al., 2014, Statt et al., 2015). Glucocorticoid treatment in this chapter did not decrease HeLa or A549 cellular cholesterol or prevent pyolysin binding, agreeing with previous observations that dexamethasone stimulates cholesterol synthesis and suppresses cellular cholesterol efflux (Ayaori et al., 2006). In *Chapters 3* and *4*, oxysterols protected cells against cholesterol-dependent cytolytic toxins by mobilizing cell surface accessible cholesterol through ACAT-driven cholesterol esterification and reducing toxin binding. Glucocorticoids stimulate cholesteryl ester formation in human smooth muscle cells (Petrichenko et al., 1997) and macrophages (Cheng et al., 1995). However, in the present chapter, glucocorticoids did not significantly protect HeLa cells through cholesterol esterification. We therefore reason that alterations in cellular cholesterol are unlikely to be a mechanism for glucocorticoid cytoprotection.

An unexpected finding was that the presence of serum reversibly prevented glucocorticoids from protecting cells against pyolysin. Serum contains a variety of nutritional and hormonal components and is known to have a powerful effect on transcriptional responses (Shaw et al., 1989, Treisman, 1986), however, attempting to strip some of these components away with charcoal-dextran did not restore cytoprotection. Cholesterol has been identified as a component of serum that modulates aspects of glucocorticoid action (Yang et al., 2014), but supplying exogenous cholesterol in the absence of serum in this study did not prevent protection. Lipopolysaccharide binding protein (LBP) is another important component in serum

that has a role in the innate immune response to LPS from bacteria (Heumann et al., 2003). Furthermore, A549 cells and macrophages express LBP that might be stimulated by oxysterols or glucocorticoids (Zhang et al., 2007, Sallam et al., 2014, Hu et al., 2021). Future work might consider whether serum containing, or serum stimulated proteins, such as LBP, can contribute to or interfere with cytoprotective mechanisms.

The inhibitory effect of serum inspired a search for factors that are differentially regulated by serum and glucocorticoids. Although serum and glucocorticoids regulate a wide range of genes and pathways, few are differentially regulated (Wang et al., 2004, Iyer et al., 1999). One example is that serum stimulates MAPK phosphorylation, whereas glucocorticoids suppress MAPK phosphorylation (Newton, 2014, Troppmair et al., 1994). Though the suppression of MAPK by glucocorticoids counters the expected role of MAPKs in damage repair in response to pore-forming toxins (Kloft et al., 2009, Cassidy and O'Riordan, 2013, Gonzalez et al., 2011). On the other hand, *HMGCR* is repressed by serum treatment (Iyer et al., 1999), whereas glucocorticoids increase HMGCR activity in HeLa cells in a protein synthesis-dependent manner (Cavenee and Melnykovych, 1977, Cavenee et al., 1978, Johnston et al., 1979). The increase in HMGCR activity might explain the slight increase in cellular cholesterol we noted. More striking was that siRNA targeting *HMGCR* diminished glucocorticoid cytoprotection. However, the function of HMGCR in intrinsic cell protection is unclear. Targeting HMGCR with statins or siRNA typically protects cells against cholesterol-dependent cytolysis by reducing cellular cholesterol (Statt et al., 2015, Griffin et al., 2017). In contrary to this, reducing *HMGCR* expression in the present chapter did not alter protection. Furthermore, dexamethasone treatment still provided some protection against pyolysin suggesting that HMGCR is not the sole protective mechanism. Using a gene array to verify the involvement of HMGCR or identify other potential target genes might help solve this conundrum, though this was beyond the scope of the present thesis.

Reparative mechanisms that might contribute to reducing the damage caused by pore-forming toxins include endocytosis, exocytosis, unfolded protein response, or caspase activity (Cassidy and O'Riordan, 2013, Gonzalez et al., 2011, Andrews and Corrotte, 2018). Calcium ion influx or potassium ion efflux initiate these reparative responses; however, glucocorticoid conferred protection did not depend on challenge medium ion

concentrations in the present study. Another possibility is that glucocorticoids might stimulate actin stress fiber formation and increased actin cytoskeleton stability (Mayanagi et al., 2008, Castellino et al., 1992). Dexamethasone and hydrocortisone stimulated actin stress fiber formation in HeLa and A549 cells, which might explain how glucocorticoids prevent pyolysin-induced cytoskeletal changes. However, it is unclear how this would prevent the leakage of potassium and LDH.

Glucocorticoids are used as an adjunct therapy to reduce inflammation and immunopathology caused by bacterial infection (Cain and Cidlowski, 2017, Kadmiel and Cidlowski, 2013, Newton, 2014). Our findings imply that glucocorticoids might also protect tissues against the damage caused by bacteria that secrete pore-forming toxins. A future challenge will be to untangle the anti-inflammatory and protective roles of glucocorticoids. However, prolonged high doses of glucocorticoid treatment is associated with adverse endocrine or immunosuppressive effects in patients, potentially limiting the translation of our findings (Newton, 2014). The negative connotations of glucocorticoid treatment have supported the development of selective glucocorticoid receptor agonists, such as fluticasone propionate, with a greater affinity for the glucocorticoid receptor, and an improved therapeutic index (Schacke et al., 2007, Harding, 1990, Johnson, 1998). Our findings might stimulate a search for selective glucocorticoid receptor agonists that also improve cytoprotection. Protecting cells against pore-forming toxins can help tissues better tolerate pathogens and reduce the dependence on immunity or antimicrobials to kill bacteria (Medzhitov et al., 2012).

The serum-induced suppression of glucocorticoid cytoprotection raises the question of how the findings of the present chapter translate to physiology. Unfortunately, experiments demonstrating the *in vivo* relevance of prophylactic glucocorticoid treatment to protect cells against toxin-secreting pathogenic bacteria were beyond the scope of the thesis. Additionally, we did not investigate the effect of glucocorticoid treatment on cells already exposed to pore-forming toxins. Future experiments challenging cells with pyolysin before a subsequent treatment would investigate whether glucocorticoids might also contribute to tissue recovery.

In conclusion we found that glucocorticoids protect several types of cells against pore-forming toxins. Glucocorticoids increased HeLa and A549 cell-intrinsic protection against pyolysin, streptolysin O and α -hemolysin damage. The glucocorticoid

cytoprotection was dependent on glucocorticoid receptor mediated protein synthesis and partly reliant on *HMGCR*. Our findings imply that targeting the glucocorticoid receptor could be exploited to limit the severity of disease caused by pathogens that secrete pore-forming toxins.

6 GENERAL DISCUSSION

Pore-forming toxins are secreted as virulence factors to promote bacterial invasion, releasing nutrients from lysed target cells and facilitating the delivery of additional virulence factors (Dal Peraro and van der Goot, 2016). Cholesterol-dependent cytolysins represent the largest family of pore-forming toxins (Tweten, 2005). *Trueperella pyogenes*, a common cause of uterine disease in postpartum cattle and *Streptococcus pyogenes*, a cause of pharyngitis and impetigo, represent examples of pathogens that release cholesterol-dependent cytolysins, secreting pyolysin and streptolysin O respectively (Jost and Billington, 2005, Bhakdi et al., 1985). *Staphylococcus aureus*, is an example of a bacteria that secretes another family of pore-forming toxins, causing target cell cytolysis through the release of an α -hemolysin (Seilie and Bubeck Wardenburg, 2017). Release of pyolysin, streptolysin O or α -hemolysin by their respective bacteria is associated with the severity of pathology (Amos et al., 2014, Zhu et al., 2017, Patel et al., 1987). Resilience to infection by bacteria such as *T. pyogenes*, *S. pyogenes*, and *S. aureus* is achieved through a combination of resistance and tolerance mechanisms (Schneider and Ayres, 2008). Whilst resistance mechanisms, such as innate and adaptive immunity, are well understood, research into tolerance mechanisms is ongoing (Sheldon et al., 2020). Cells can tolerate bacterial infection by repairing some of the damage caused by pore-forming toxins through the activation of pro-survival responses following the cytosolic ion and molecular flux triggered by pore-formation (Gonzalez et al., 2011, Gurcel et al., 2006, Andrews and Corrotte, 2018). Alternatively, tolerance can be achieved by protecting cells against pore-forming toxin damage. It is established that depleting cell cholesterol with methyl- β -cyclodextrin (M β CD) and statins can provide protection against the cytolysis caused by cholesterol-dependent cytolysins (Statt et al., 2015, Giddings et al., 2003), and more specifically pyolysin (Amos et al., 2014, Griffin et al., 2017, Pospiech et al., 2021), but little is known beyond this. Hence, this thesis aimed to explore other methods of protecting eukaryotic cells against the damage caused by pore-forming toxins.

Oxysterol and steroids impact the severity of disease caused by bacteria that secrete pore-forming toxins (Abrams et al., 2020, Stern et al., 2017, Lewis, 2003). Therefore, we began with the hypothesis that side-chain oxysterols and steroids alter the intrinsic

protection of eukaryotic cells against pore-forming toxins. To challenge this hypothesis, we first screened the ability of progesterone, oestradiol, glucocorticoids, or 27-hydroxycholesterol to reduce the cytolytic impact of pyolysin on the target epithelial and stromal cells of the bovine endometrium. This model represented an important biological problem, as parturition in cattle is accompanied by infection with bacteria such as *T. pyogenes* and *S. aureus* and results in the disruption of the protective epithelium in the endometrium exposing underlying sensitive stromal cells (Sheldon et al., 2019). Uterine disease is a common outcome, leading to the reduced fertility in many animals (Ribeiro et al., 2016). We found that the protection afforded by 27-hydroxycholesterol was striking. Cytoprotection was also afforded by 25-hydroxycholesterol and against α -hemolysin from *S. aureus* providing evidence to show that side-chain oxysterols can help protect bovine endometrial cells against pore-forming toxins. Furthermore, *Chapter 4* established that side-chain oxysterols also protected human epithelial cells against pore-forming toxins. Collectively these findings suggest that side-chain oxysterols may help defend tissues against pore-forming toxins from pathogenic bacteria.

Treatment with the steroids progesterone and estradiol did not protect bovine endometrial cells against pyolysin at the concentrations and treatment durations explored in this study and so were not examined further. Hydrocortisone or dexamethasone treatment did not significantly affect the pyolysin-induced cytolysis of bovine endometrial cells (though there was a trend for reduced cell death in dexamethasone treated epithelial cells); however, glucocorticoid effects vary significantly between cells and tissues. Therefore, *Chapter 5* tested the hypothesis that glucocorticoids increase the protection of human tissue cells against pore-forming toxins. Strikingly, hydrocortisone and dexamethasone protected cells against pyolysin, streptolysin O and α -hemolysin, implying that glucocorticoids could be exploited to limit the damage caused by bacteria that secrete pore-forming toxins.

Utilising a range of cell types and pore-forming toxins throughout the thesis helped to determine if protective mechanisms were generic, and the main findings are summarised in Table 6.1.

Table 6.1 Summarised cytoprotective findings

(25-HC, 25-hydroxycholesterol; 27-HC, 27-hydroxycholesterol; Dex, Dexamethasone; Hydro, Hydrocortisone; FP, Fluticasone propionate; -, not tested; ●, cytoprotective; ●, some protection noted; ●, not cytoprotective)

Cell type	Toxin	Side-chain oxysterols		LXR agonists		Glucocorticoids		
		25-HC	27-HC	T0901317	GW3965	Dex	Hydro	FP
Bovine endometrial epithelial cells	Pyolysin	●	●	●	●	●	●	-
	α-hemolysin	●	●	●	-	-	-	-
Bovine endometrial stromal cells	Pyolysin	●	●	●	●	●	●	-
	α-hemolysin	●	●	●	-	-	-	-
HeLa cervical cells	Pyolysin	●	●	●	●	●	●	●
	α-hemolysin	●	●	-	-	●	●	-
	Streptolysin O	-	-	-	-	●	●	-
A549 lung cells	Pyolysin	●	●	●	●	●	●	●
	α-hemolysin	●	●	-	-	●	●	-
	Streptolysin O	-	-	-	-	●	-	-
Hep-G2 liver cells	Pyolysin	-	●	-	-	●	-	-
NC1-H441 lung cells	Pyolysin	-	●	-	-	●	-	-
Normal human dermal fibroblasts	Pyolysin	-	-	-	-	●	-	-

6.1 SIDE-CHAIN OXYSTEROL CYTOPROTECTION

The cytoprotection afforded by side-chain oxysterols was the first notable finding of the present thesis, and reduced cytolysis in every examined cell type. Treatment with 27-hydroxycholesterol reduced pyolysin binding without decreasing total cellular cholesterol. Side-chain oxysterols remodel plasma membrane cholesterol through acetyl-coenzyme A acetyltransferase (ACAT)-dependent cholesterol esterification (Lange et al., 1999), and the ACAT inhibitor Sandoz 58-035 (SZ58-035) reduced cytoprotection in bovine endometrial and HeLa cells. Oxysterols are also ligands for the liver X receptors (LXRs) (Wang and Tontonoz, 2018). The synthetic LXRs T0901317 and GW3965 provided protection against pyolysin in bovine endometrial cells, HeLa cells, and A549 cells. Additionally, reducing the expression of the LXR genes *NR1H2* and *NR1H3* reduced cytoprotection in bovine endometrial cells. However, it is unlikely that these are the sole cytoprotective mechanisms. Inhibiting ACAT or reducing the expression of *NR1H2* and *NR1H3* only provided moderate reductions in cytoprotection, and it is unlikely that experiments combining the two would completely prevent protection. Oxysterols also inhibit cholesterol synthesis by blocking sterol responsive element binding protein (SREBP) activation and triggering 3-hydroxy 3-methylglutaryl coenzyme A reductase (HMGCR) degradation (Radhakrishnan et al., 2007, Lange et al., 2008). It is likely that these mechanisms also contribute to cytoprotection, and future *in vitro* studies might verify their involvement. We propose that oxysterol cytoprotection is derived from a combination of multiple protective pathways, stemming from their ability to regulate cholesterol homeostasis.

Side-chain oxysterol cytoprotection appeared generalized, however, a few key differences were noted when comparing protection in bovine endometrial cells to protection in human HeLa cervical cells. Firstly, the relationship between 27-hydroxycholesterol treatment duration and the degree of protection was linear up to 24 h in bovine endometrial cells, with protection evident after > 8 h treatment and maximal at ~ 24 h. However, cytoprotection was evident after 4 h in HeLa cells and maximal with > 12 h of treatment. Additionally, reducing the expression of *NR1H2* and *NR1H3* impaired 27-hydroxycholesterol cytoprotection in bovine endometrial cells but not in HeLa cells. It is possible that oxysterol cytoprotective mechanisms are tissue and cell type specific, with the involvement of individual protective pathways depending on gene expression and oxysterol sensitivity. This suggestion is supported

by the inability of oxysterols to protect bone marrow-derived macrophages against *Listeria monocytogenes* infection and the delay in 25-hydroxycholesterol driven mobilization of accessible cholesterol in Chinese hamster ovary cells that constitutively express the transcriptionally active fragment of SREBP2 (Abrams et al., 2020, Yang et al., 1994).

At the time of discovery, the ability of side-chain oxysterols to provide complete protection against pore-forming toxin damage appeared novel. However, in a recent study by Zhou et al. (2020) interferon stimulated mouse bone marrow-derived macrophages were protected against perfringolysin O, streptolysin O, and anthrolysin O in a 25-hydroxycholesterol-dependent mechanism, and the protective effects of the LXR agonist GW3965 were noted. However, the findings of the present thesis are still impactful, demonstrating protection in additional cell types and against α -hemolysin, though cytoprotection against other classes of pore-forming toxins warrants further investigation.

Prior to this study, oxysterols in the bovine uterus had not been previously examined. We found novel data demonstrating the presence of a large range of oxysterols, significantly including 25-hydroxycholesterol and 27-hydroxycholesterol, in both uterine and ovarian follicular fluid. Additionally, 25-hydroxycholesterol was released by bovine endometrial epithelial cells. Although it was known that the innate immune system triggers the secretion of 25-hydroxycholesterol from macrophages (Baumann et al., 2005, Reboldi et al., 2014), we unexpectedly found that both LPS and pyolysin stimulated the release of further 25-hydroxycholesterol. Although 27-hydroxycholesterol was detected in uterine fluid, it was not released from endometrial cells, indicating that endometrial cells were not the origin of this oxysterol in the biological fluids. Ovarian steroid hormones regulate the function of the bovine endometrium, preparing the uterus for pregnancy (Wira et al., 2005, Lewis, 2003). It is possible that the ovaries might also produce oxysterols to help protect cells against pore-forming toxins. Collectively, our data informs the proposal that oxysterols are produced in the ovaries and released from endometrial epithelial cells to contribute to uterine protection against invading pathogens (Fig 6.1). Future research might verify the significance of oxysterols in uterine disease by comparing concentrations in healthy and diseased animals and exploring cytoprotection afforded by a wider range of oxysterols, however, this was beyond the scope of the present thesis.

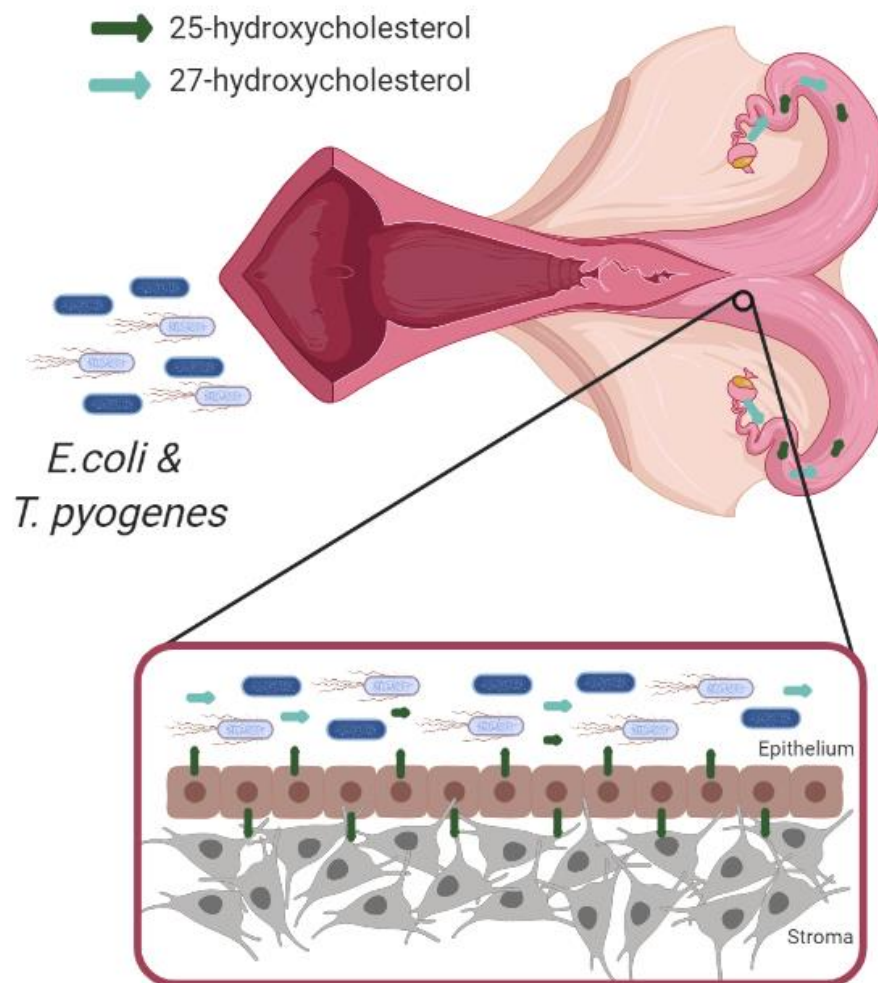


Figure 6.1 Oxysterol cytoprotection in the bovine endometrium

The oxysterols 25-hydroxycholesterol and 27-hydroxycholesterol help protect endometrial cells against damage by the cholesterol-dependent cytolysin pyolysin from *T. pyogenes* and α -hemolysin from *S. aureus*. Both oxysterols are present in uterine fluid; and endometrial epithelial, but not stromal cells, release 25-hydroxycholesterol, and this is further increased in response to pyolysin or lipopolysaccharide from Gram-negative pathogens, such as *Escherichia coli*. We propose that oxysterols from the ovary and 25-hydroxycholesterol from endometrial epithelial cells help protect the underlying sensitive stromal cells against pore-forming toxins. Created with BioRender.com.

6.2 GLUCOCORTICOID CYTOPROTECTION

Another novel finding in the present thesis was that glucocorticoids increase the intrinsic protection of cells against the damage caused by pore-forming toxins. Glucocorticoids are thought to limit the severity of disease by suppressing inflammation and immunity (Kadmiel and Cidlowski, 2013), however, our findings suggest that glucocorticoids may also increase the tolerance of tissues to pathogenic bacteria by protect cells against pore-forming toxins. Dexamethasone and hydrocortisone protected HeLa cells against the damage caused by pyolysin, streptolysin O and α -hemolysin, preventing the leakage of cytosolic molecules, cell cytolysis, cytoskeletal changes, and mitogen-activated protein kinase (MAPK) activation. Protection extended to A549, Hep-G2, NC1-H441 cells and to dermal fibroblasts. Unsurprisingly, cytoprotection was dependent on the glucocorticoid receptor. Although the glucocorticoid receptor can mediate fast-acting non-genomic effects (Buttgereit and Scheffold, 2002), cytoprotection is likely a genomic mechanism as protection requires > 8 h treatment and inhibiting transcription and translation diminished cytoprotection.

The resulting transcriptional response following glucocorticoid treatment depends on a range of elements including cell type and glucocorticoid target gene expression, chromatin accessibility, interactions with other transcription factors, and the presence of other cells and extracellular molecules (Quatrini and Ugolini, 2021, John et al., 2011). Collectively, these factors contribute to the cell and context specific nature of glucocorticoid responses. Therefore, it is not surprising that the cytoprotection afforded by glucocorticoids varied across the cell types examined in this study. Specifically, this might explain the inability of hydrocortisone or dexamethasone to significantly protect bovine endometrial cells against pyolysin and the limited protection of A549 cells against α -hemolysin.

The mechanisms contributing to glucocorticoid cytoprotection appear unrelated to those utilised by oxysterols. Glucocorticoid treatment increases the accumulation of cholesterol esters in human macrophages and smooth muscle cells cultured without serum (Petrichenko et al., 1997, Cheng et al., 1995). However, glucocorticoids did not appear to protect HeLa cells through cholesterol esterification as the ACAT inhibitor SZ58-035 did not diminish glucocorticoid cytoprotection despite reducing the effectiveness of 27-hydroxycholesterol cytoprotection. Additionally, glucocorticoids

did not prevent HeLa cell pyolysin binding, suggesting that accessible cholesterol is not reduced. However, evaluating pyolysin binding in A549 cells did not provide such clear-cut results and further experiments might explore the involvement of ACAT in glucocorticoid cytoprotection in additional cell types.

Uncovering the precise mechanisms involved in glucocorticoid cytoprotection proved elusive. Glucocorticoids stimulate actin stress fibre formation which might help stabilize the cytoskeleton (Mayanagi et al., 2008, Castellino et al., 1992), but it is unlikely that this would prevent LDH and potassium leakage. Experiments targeting *HMGCR* with short-interfering ribonucleic acid (siRNA), impaired glucocorticoid protection. Statins can also be used to inhibit HMGCR activity, however, as they also provide protection against cholesterol-dependent cytolysins it was not possible to use them to explore the role of HMGCR in glucocorticoid cytoprotection. Dexamethasone increases HMGCR activity in HeLa cells (Cavenee and Melnykovich, 1977), and this might explain the slight increase in cellular cholesterol, but it is not clear how this would contribute to protection. Perhaps this excess cholesterol is continually compartmentalized and/or removed from the cell via efflux, providing a dynamic pool of accessible cholesterol that makes pyolysin oligomerization and pore formation challenging. It is also important to consider whether the involvement of HMGCR in HeLa cell glucocorticoid cytoprotection is part of the generalized glucocorticoid cytoprotective mechanism or is a product of the cell type specific nature of glucocorticoid responses. Future experiments might use siRNA to verify the involvement of HMGCR in glucocorticoid cytoprotection in the other cell types used in the present thesis.

6.3 SERUM AND CYTOPROTECTION

An unexpected finding was the fact that serum, reversibly diminished glucocorticoid cytoprotection. Serum contains a variety of nutritional and signalling components and has powerful effects on transcriptional responses (Treisman, 1986). A bioassay has previously identified the ability of serum to impair glucocorticoid activity (Perogamvros et al., 2011). Corticosteroid-binding globulins in serum bind to endogenous glucocorticoids, controlling their transport and bioavailability (Hammond, 1990). However, it is unlikely that corticosteroid-binding globulins are responsible for the inhibitory effect, as the synthetic glucocorticoids dexamethasone

and fluticasone propionate demonstrate negligible corticosteroid-binding globulin binding affinity (Maitra et al., 1993, Bodor et al., 2016).

Yang et al. (2014) aimed to uncover the components of serum that control glucocorticoid sensitivity using HeLa cells and synthetic reporter assays. The serum effect on glucocorticoid signalling required c-Jun (N)-terminal kinase (JNK)/activating protein-1 activation and was modulated by serum cholesterol content. However, experiments examined the inhibitory effect of 50% serum compared to 10% serum and so the findings do not necessarily translate to the present thesis. Furthermore, charcoal stripping serum restored some glucocorticoid sensitivity and supplementing cholesterol impaired glucocorticoid action (Yang et al., 2014), whereas in the present study charcoal stripping serum did not restore glucocorticoid cytoprotection and glucocorticoid treatment in serum-free medium containing 30 µg/ml cholesterol still protected cells against pyolysin. Future experiments using lipoprotein deficient serum might provide more insight into the role of lipids in the inhibitory effect of serum on glucocorticoid cytoprotection.

Serum and glucocorticoids both regulate a wide range of genes and pathways (Iyer et al., 1999, Wang et al., 2004). Ideally a gene array would be used to thoroughly screen genes differentially regulated by serum and glucocorticoids to help uncover specific protective pathways activated in the cell types used in the present thesis. However, as this was beyond the scope of our project, we examined existing data available in the literature to identify possible targets. This helped identify the involvement of HMGR as described above (section 6.2). Mitogen-activated protein kinase phosphorylation is also differentially regulated by glucocorticoids and serum. Glucocorticoids suppress MAPK activation whereas serum stimulates MAPK phosphorylation (Troppmair et al., 1994, Newton, 2014). Suppressing MAPK phosphorylation is at odds with the protective role of MAPK against damage by pore-forming toxins and so we did not consider its involvement in cytoprotection (Gonzalez et al., 2011, Kloft et al., 2009, Cassidy and O'Riordan, 2013). However, glucocorticoid receptor transcriptional activation can be selectively impaired by JNK and extracellular signal-regulated kinase 1 and 2 (ERK1/2) activation (Newton, 2014, Yang et al., 2014, Rogatsky et al., 1998). Therefore, future experiments might use inhibitors to explore whether serum-induced MAPK phosphorylation impairs glucocorticoid cytoprotection.

Additionally, incubating cells in serum-free medium for 24 h is likely to cause a wide-range of starvation-related phenotypes. It is unclear if glucocorticoid treatment just alters starvation responses, instead of serum activating transcriptional pathways that counteract the function of the glucocorticoid cytoprotective mechanism. Animal studies would be required to determine whether glucocorticoid cytoprotection would be relevant to non-starved cells *in vivo*.

Although the presence of serum did not prevent side-chain oxysterol cytoprotection, it increased the concentration of 25-hydroxycholesterol required to completely protect bovine endometrial and HeLa cells against pyolysin. Furthermore, in a separate study the effective concentration of 25-hydroxycholesterol required to mobilize cellular cholesterol in CHO-7 was approximately 40-fold higher in the presence of serum (Abrams et al., 2020). Culturing cells in the presence of serum alters cholesterol homeostasis and is likely to interfere with the ability of treatments to adjust cholesterol accessibility (Brown and Goldstein, 1986). However, as oxysterol treatment still provided protection in the presence of serum it seems likely that this protection would translate to *in vivo* studies. Indeed, in the recent study by Zhou et al. (2020), pre-injecting the dermis of mice with 25-hydroxycholesterol reduced the tissue damage induced by anthrolysin.

6.4 CELL REPAIR AND CYTOPROTECTION

Little is known about the intrinsic protection of cells against pore-forming toxins; however, cell repair is well documented. Several reparative processes were outlined in *Chapter 1*, such as membrane remodelling, MAPK activation and inflammasome activation (Andrews and Corrotte, 2018, Gurcel et al., 2006, Gonzalez et al., 2011), and these pathways are largely triggered by the changes to cytosolic ion concentrations caused by pore formation (Gekara et al., 2007, Kloft et al., 2009, Cabezas et al., 2017).

Manipulating the concentration of calcium and potassium ions in the challenge medium effected the susceptibility of HeLa cells to pyolysin challenge. Cells were more susceptible to pyolysin when challenged in calcium free medium, possibly because a lack of calcium ion influx prevented the activation of repair pathways. On the other hand, impairing potassium ion efflux by challenging cells with pyolysin in high potassium medium appeared to reduce the susceptibility of cells to damage. This contradicts the belief that potassium efflux activates reparative pathways to reduce cell

damage (Kloft et al., 2009, Gonzalez et al., 2011). However, cholesterol-dependent cytolysins form large diameter pores and the high concentrations of pyolysin used in our experiments facilitate the rapid and excessive loss of cytosolic contents. Perhaps increasing extracellular potassium concentrations mediates the loss of intracellular ion concentrations. Nevertheless, side-chain oxysterols and glucocorticoid cytoprotection against pyolysin in HeLa cells was not dependent on ion concentrations in the challenge medium.

Side-chain oxysterol and glucocorticoid treatment also appeared to prevent pyolysin pore formation, as demonstrated by reduced LDH and potassium ion leakage, suggesting that the cellular cytosolic contents remain stable. Additionally, both side-chain oxysterols and glucocorticoids prevented MAPK phosphorylation, highlighting an absence of cell stress. Collectively, these findings suggest that the mechanisms of side-chain oxysterol and glucocorticoid cytoprotection are likely to be independent from cell repair mechanisms that are triggered by toxin-induced changes to cytosolic ion concentrations. However, it is possible that treatments could alter cytosolic ion concentrations and activate pro-survival pathways in advance of the pore-forming toxin challenge. Indeed, oxysterol treatment can trigger immediate calcium ion oscillations and this might help prepare the cell for the upcoming membrane perforation and increase the chance of survival (Mackrill, 2011).

Cells can recover from pore-forming toxin damage by repairing damaged membrane. Plasma membrane blebs are typically generated by plasma membrane damage (Bischofberger et al., 2009). Blebbing human embryonic kidney cells are more likely to recover from streptolysin O damage (Babiychuk et al., 2011, Babiychuk et al., 2009), however, their contribution to repair is contentious (Andrews and Corrotte, 2018). It was assumed that pore-containing blebs are released from the injured membrane, allowing cells to reseal the plasma membrane, though they might just reflect reversible membrane remodelling. In the present thesis we quantified plasma membrane blebs to assess cell damage and examine whether blebbing contribute to side-chain oxysterol and glucocorticoid cytoprotection. Unfortunately, blebbing was not consistently visible in bovine endometrial epithelial and stromal cells. Pyolysin challenge induced the formation of large plasma membrane blebs in HeLa cells. Challenges containing higher concentrations of pyolysin fragmented cells, and blebbing was no longer visible. The fact that dead cells do not produce blebs suggests

that it is an active process that might contribute repairing the membrane damage caused by lower pyolysin concentrations. However, treatment with side-chain oxysterols and glucocorticoids reduced blebbing and protected against cell fragmentation, indicating an absence of membrane damage, and suggesting that blebbing does not contribute to cytoprotection.

6.5 LIMITATIONS

Though the present thesis provided clear evidence that demonstrated the ability of side-chain oxysterols and glucocorticoids to protect cells against pore-forming toxins, there were several key limitations to our findings. Firstly, we only examined protection against isolated pore-forming toxins, but this does not accurately represent bacterial infection. Bacteria secrete several additional virulence factors that also contribute to pathology (Jost and Billington, 2005, Chen et al., 2005). Experiments challenging cells with bacteria should be used to confirm whether side-chain oxysterol or glucocorticoid treatment can increase the tolerance of tissues to pathogenic bacteria. Examples of isolates that could be used to complement the bovine endometrial cell model include live *T. pyogenes* (MS249) and a *plo*-inactivated *T. pyogenes* mutant of the same strain. Alternatively, should cytoprotection extend to pneumolysin, *Streptococcus pneumoniae* (D39) could be utilised in a model alongside the lung cells from the present thesis. Furthermore, resilience to infection is achieved by resisting as well as tolerating pathogenic bacteria (Medzhitov et al., 2012, Schneider and Ayres, 2008). Although it seems likely that protection against toxins will increase tissue tolerance and reduce pathology, *in vivo* studies are required to determine how cellular protection interacts with other tolerance and resistance mechanisms to contribute to infection resilience.

Secondly, although our experiments utilised two families of pore-forming toxins, protection remains to be explored against many other families (listed in Table 1.1). Critically, α -pore-forming toxins perforate plasma membranes in a different manner to β -pore-forming toxins (Cosentino et al., 2016). Future experiments challenging cells with a broader range of toxins would uncover the true extent of side-chain oxysterol and glucocorticoid cytoprotection.

Although using mass spectrometry provided a novel insight into the presence of oxysterols in the bovine endometrium, we were limited by the number of replicates we

could analyse. Unfortunately, without additional replicates, our data is not sufficient to provide a reliable estimate for typical bovine ovarian follicular and uterine fluid oxysterol concentrations and simply highlights their presence. It is also possible that ovarian cycle stage and the presence of infection might alter oxysterol abundance, and both present possible avenues of future research.

Additionally, Western blot is not the optimal method for measuring pyolysin binding. Though side-chain oxysterol treatment demonstrates a clear reduction in binding, experiments using glucocorticoids do not provide such clear results. The variability of the assay impairs the detection of more sensitive changes in binding. Furthermore, it does not provide any information with regards to the state and location of bound toxin. Perhaps glucocorticoid treatments cause the rapid internalization of pyolysin or prevent bound monomers from permeabilizing the membrane. Surface labelling cells with mutant pyolysin would allow more detailed observations and might be a focus of future studies.

Finally, the concentrations of dexamethasone and hydrocortisone used throughout this thesis are unusually high and might limit their therapeutic potential. The EC_{50} of dexamethasone and hydrocortisone to the glucocorticoid receptor is typically as ~5 nM and ~70 nM respectively (Novotna et al., 2012, Sedlak et al., 2011), but 10 μ M dexamethasone or hydrocortisone was required to provide maximal protection in our studies. However, protection was still afforded by 0.1 μ M dexamethasone or hydrocortisone in HeLa cells. Additionally, fluticasone propionate was protective at much lower concentrations (≥ 0.5 nM). Furthermore, throughout infection cells many cells are exposed to lower concentrations of toxin than those used to challenge cells in our *in vitro* experiments and lower concentrations of glucocorticoid treatment might still provide protection against these lower toxin concentrations. This variation in toxin concentrations during infection, along with other confounding factors located in the biological fluids that surround infected tissues, limits the relevance of the effective treatment concentrations determined in the present thesis of side-chain oxysterols as well as glucocorticoids. Therapeutic concentrations must be informed from future *in vivo* studies.

6.6 FUTURE APPLICATIONS

The increased consumption and improper prescription of antimicrobials results in selective pressure that drives drug resistance in exposed bacteria (Fair and Tor, 2014). This drug resistance is an increasing global concern that compromises our ability to treat common infections, resulting in enduring illness and increased mortality (O'Neill, 2016). Antimicrobial therapy is the recommended course of treatment for most *Staphylococcus* and *Streptococcus* skin and soft tissue infections (Stevens et al., 2014). Horizontal gene transfer of antimicrobial genes between organisms has driven the development of *S. aureus* strains that are resistant to multiple antimicrobial compounds (Jensen and Lyon, 2009). Though *S. pyogenes* has remained susceptible to almost all classes of antibiotics (Blondeau et al., 1999, Alves-Barroco et al., 2020), there are reports of increased resistance to macrolides (Richter et al., 2005, Abraham and Sistla, 2018). Very few novel classes of antibiotics have been introduced in recent years, highlighting the requirement for alternative therapeutic options (Silver, 2011). Future research might examine the therapeutic potential of side-chain oxysterols, LXR agonists, and glucocorticoids. By protecting cells against streptolysin O and α -hemolysin, side-chain oxysterols, LXR agonists, and glucocorticoids might increase the tolerance of tissues to *S. aureus* and *S. pyogenes* (and potentially other pathogenic bacteria that secrete pore-forming toxins), reduce disease severity, and decrease the reliance on antimicrobials.

Glucocorticoids are regularly administered therapeutically to suppress inflammation; however, treatment is associated with complex adverse endocrine and immunosuppressive side-effects, spurring the development of selective glucocorticoid receptor agonists (Newton, 2014). As glucocorticoid cytoprotection was dependent on the glucocorticoid receptor, our work might guide drug design through the development of novel selective glucocorticoid receptor agonists that would also protect cells against pore-forming toxins, possibly providing another alternative to antimicrobials.

Uterine disease remains a concern in cattle, causing pain, decreased milk yields, reduced fertility, and an annual global cost of over \$2 billion (Fourichon et al., 2000, Haimerl and Heuwieser, 2014, Sheldon et al., 2009). The current use of antibiotics needs re-thinking as it does not resolve fertility issues (Haimerl and Heuwieser, 2014). Furthermore, several governments advise against the use of antibiotics in food

producing animals because of the threat of antimicrobial resistance (Rochford et al., 2018). Uterine infections can be treated with the topical application of pharmaceutical molecules via an intrauterine infusion (Sheldon et al., 2009). Intrauterine infusion of side-chain oxysterols or synthetic LXR agonists could be used to limit the severity of uterine disease in postpartum animals by increasing the tolerance of the compromised endometrium to pathogenic bacteria that secrete pore-forming toxins. Alternatively, an attempt could be made to target the pre-existing abundance of oxysterols in the bovine endometrium. Alongside the enzymatic and nonenzymatic transformation of endogenous sterols, oxysterols can be derived from diet (Brzeska et al., 2016). Oxysterol concentrations are particularly high in processed or thermal treated food products. The most common dietary oxysterols are oxidative ring modifications (7-hydroxycholesterol and 7-ketocholesterol), though side-chain oxidation products (19-hydroxycholesterol, 20-hydroxycholesterol, 24-hydroxycholesterol, and 25-hydroxycholesterol) are present in a smaller amount (Linseisen and Wolfram, 1998, Otaegui-Arrazola et al., 2010). Controlling the diet of cattle to adjust oxysterol concentrations *in vivo* might present a straightforward and economical method of reducing the severity of uterine disease. However, it is not clear whether manipulating dietary oxysterols would affect the concentration of oxysterols in the endometrium, or whether this might have other negative side-effects that compromise the health of the animal. Should targeting oxysterols to reduce the severity of uterine disease in cattle prove successful, then there is a potential for these principles to be applied to reduce the severity of disease caused by bacteria that secrete pore-forming toxins in other areas of the agricultural sector.

6.7 CONCLUSION

In summary, the present thesis aimed to explore methods of protecting eukaryotic cells against the damage caused by pore-forming toxins. The side-chain oxysterols 25-hydroxycholesterol and 27-hydroxycholesterol protected bovine endometrial and human epithelial cells against pyolysin damage through a partially ACAT-dependent mechanism. Protection also extended to *S. aureus* α -hemolysin. Interestingly, the protective concentrations of 25-hydroxycholesterol and 27-hydroxycholesterol were similar to concentrations in the bovine uterus and ovary. Though the involvement of the liver X receptors in oxysterol cytoprotection was inconsistent, the synthetic LXR agonists T0901317 and GW3965 provided both bovine and human tissue cells with

moderate protection against pyolysin damage. Despite the fact that progesterone, oestradiol, and glucocorticoids did provide bovine endometrial cells with significant protection against pyolysin damage, glucocorticoids did increase the protection of human cells against pyolysin, streptolysin O and *S. aureus* α -hemolysin. This protection was dependent on the glucocorticoid receptor, *de novo* protein synthesis, and partially reliant on the expression of *HMGCR*. In conclusion, side-chain oxysterols and glucocorticoids increase the intrinsic protection of eukaryotic cells against pore-forming toxins. These findings might be exploited to limit the severity of disease caused by pathogenic bacteria that secrete pore-forming toxins.

REFERENCES

- ABDEL-KHALIK, J., YUTUC, E., CRICK, P. J., GUSTAFSSON, J. A., WARNER, M., ROMAN, G., TALBOT, K., GRAY, E., GRIFFITHS, W. J., TURNER, M. R. & WANG, Y. 2017. Defective cholesterol metabolism in amyotrophic lateral sclerosis. *Journal of Lipid Research*, 58, 267-278.
- ABRAHAM, T. & SISTLA, S. 2018. Trends in antimicrobial resistance patterns of Group A streptococci, molecular basis and implications. *Indian Journal of Medical Microbiology*, 36, 186-191.
- ABRAMS, M. E., JOHNSON, K. A., PERELMAN, S. S., ZHANG, L. S., ENDAPALLY, S., MAR, K. B., THOMPSON, B. M., MCDONALD, J. G., SCHOGGINS, J. W., RADHAKRISHNAN, A. & ALTO, N. M. 2020. Oxysterols provide innate immunity to bacterial infection by mobilizing cell surface accessible cholesterol. *Nature Microbiology*, 5, 929-942.
- ADCOCK, I. M. & BARNES, P. J. 1996. Ligand-induced differentiation of glucocorticoid receptor (GR) trans-repression and transactivation. *Biochemical Society Transactions*, 24, 267S.
- AGUILAR, J. L., KULKARNI, R., RANDIS, T. M., SOMAN, S., KIKUCHI, A., YIN, Y. & RATNER, A. J. 2009. Phosphatase-dependent regulation of epithelial mitogen-activated protein kinase responses to toxin-induced membrane pores. *PLoS One*, 4, e8076.
- AHSAN, F., MAERTZDORF, J., GUHLICH-BORNHOF, U., KAUFMANN, S. H. E. & MOURA-ALVES, P. 2018. IL-36/LXR axis modulates cholesterol metabolism and immune defense to *Mycobacterium tuberculosis*. *Scientific Reports*, 8, 1520.
- AHSAN, F., MOURA-ALVES, P., GUHLICH-BORNHOF, U., KLEMM, M., KAUFMANN, S. H. & MAERTZDORF, J. 2016. Role of interleukin 36 γ in host defense against tuberculosis. *The Journal of Infectious Diseases*, 214, 464-474.
- ALONZO III, F., KOZHAYA, L., RAWLINGS, S. A., REYES-ROBLES, T., DUMONT, A. L., MYSZKA, D. G., LANDAU, N. R., UNUTMAZ, D. & TORRES, V. J. 2013. CCR5 is a receptor for *Staphylococcus aureus* leukotoxin ED. *Nature*, 493, 51-55.
- ALOUF, J. E. 1980. Streptococcal toxins (streptolysin O, streptolysin S, erythrogenic toxin). *Pharmacology and Therapeutics*, 11, 661-717.
- ALVAREZ, M. B. & JOHNSON, H. D. 1973. Environmental heat exposure on cattle plasma catecholamine and glucocorticoids. *Journal of Dairy Science*, 56, 189-194.
- ALVES-BARROCO, C., RIVAS-GARCIA, L., FERNANDES, A. R. & BAPTISTA, P. V. 2020. Tackling multidrug resistance in streptococci - From novel biotherapeutic strategies to nanomedicines. *Frontiers in Microbiology*, 11, 2487.

- AMANO, Y., LEE, S. W. & ALLISON, A. C. 1993. Inhibition by glucocorticoids of the formation of interleukin-1 α , interleukin-1 β , and interleukin-6: mediation by decreased mRNA stability. *Molecular Pharmacology*, 43, 176-182.
- AMOS, M. R., HEALEY, G. D., GOLDSTONE, R. J., MAHAN, S. M., DUVEL, A., SCHUBERTH, H. J., SANDRA, O., ZIEGER, P., DIEUZY-LABAYE, I., SMITH, D. G. & SHELDON, I. M. 2014. Differential endometrial cell sensitivity to a cholesterol-dependent cytolysin links *Trueperella pyogenes* to uterine disease in cattle. *Biology of Reproduction*, 90, 54-61.
- ANDREWS, N. W. & CORROTTE, M. 2018. Plasma membrane repair. *Current Biology*, 28, R392-R397.
- ARAFAH, B. M. 2006. Hypothalamic pituitary adrenal function during critical illness: limitations of current assessment methods. *Journal of Clinical Endocrinology and Metabolism*, 91, 3725-3745.
- ARES, M. P., PORN-ARES, M. I., THYBERG, J., JUNTTI-BERGGREN, L., BERGGREN, P. O., DICZFALUSY, U., KALLIN, B., BJORKHEM, I., ORRENIUS, S. & NILSSON, J. 1997. Ca²⁺ channel blockers verapamil and nifedipine inhibit apoptosis induced by 25-hydroxycholesterol in human aortic smooth muscle cells. *Journal of Lipid Research*, 38, 2049-2061.
- ARZANLOU, M. & BOHLOOLI, S. 2010. Inhibition of streptolysin O by allicin - an active component of garlic. *Journal of Medical Microbiology*, 59, 1044-1049.
- AYAORI, M., SAWADA, S., YONEMURA, A., IWAMOTO, N., OGURA, M., TANAKA, N., NAKAYA, K., KUSUHARA, M., NAKAMURA, H. & OHSUZU, F. 2006. Glucocorticoid receptor regulates ATP-binding cassette transporter-A1 expression and apolipoprotein-mediated cholesterol efflux from macrophages. *Arteriosclerosis, Thrombosis, and Vascular Biology*, 26, 163-168.
- AYROLDI, E., CANNARILE, L., MIGLIORATI, G., NOCENTINI, G., DELFINO, D. V. & RICCARDI, C. 2012. Mechanisms of the anti-inflammatory effects of glucocorticoids: genomic and nongenomic interference with MAPK signaling pathways. *The FASEB Journal*, 26, 4805-4820.
- AYROLDI, E. & RICCARDI, C. 2009. Glucocorticoid-induced leucine zipper (GILZ): a new important mediator of glucocorticoid action. *The FASEB Journal*, 23, 3649-3658.
- BABIYCHUK, E. B., MONASTYRSKAYA, K., POTEZ, S. & DRAEGER, A. 2009. Intracellular Ca²⁺ operates a switch between repair and lysis of streptolysin O-perforated cells. *Cell Death and Differentiation*, 16, 1126-1134.
- BABIYCHUK, E. B., MONASTYRSKAYA, K., POTEZ, S. & DRAEGER, A. 2011. Blebbing confers resistance against cell lysis. *Cell Death and Differentiation*, 18, 80-89.
- BAMBERGER, C. M., BAMBERGER, A.-M., DE CASTRO, M. & CHROUSOS, G. P. 1995. Glucocorticoid receptor β , a potential endogenous inhibitor of glucocorticoid action in humans. *The Journal of Clinical Investigation*, 95, 2435-2441.

- BAMBERGER, C. M., SCHULTE, H. M. & CHROUSOS, G. P. 1996. Molecular determinants of glucocorticoid receptor function and tissue sensitivity to glucocorticoids. *Endocrine Reviews*, 17, 245-261.
- BANTEL, H., SINHA, B., DOMSCHKE, W., PETERS, G., SCHULZE-OSTHOFF, K. & JANICKE, R. U. 2001. alpha-Toxin is a mediator of *Staphylococcus aureus*-induced cell death and activates caspases via the intrinsic death pathway independently of death receptor signaling. *The Journal of Cell Biology*, 155, 637-648.
- BARENHOLZ, Y. & THOMPSON, T. E. 1980. Sphingomyelins in bilayers and biological membranes. *Biochimica et Biophysica Acta*, 604, 129-158.
- BARNARD, W. & TODD, E. 1940. Lesions in the mouse produced by streptolysins O and S. *Journal of Pathology and Bacteriology*, 51, 43-47.
- BARNES, P. J. & ADCOCK, I. M. 2009. Glucocorticoid resistance in inflammatory diseases. *Lancet*, 373, 1905-1917.
- BAUMAN, D. R., BITMANSOUR, A. D., MCDONALD, J. G., THOMPSON, B. M., LIANG, G. & RUSSELL, D. W. 2009. 25-Hydroxycholesterol secreted by macrophages in response to Toll-like receptor activation suppresses immunoglobulin A production. *Proceedings of the National Academy of Sciences of the United States of America*, 106, 16764-16769.
- BAUMANN, N. A., SULLIVAN, D. P., OHVO-REKILA, H., SIMONOT, C., POTTEKAT, A., KLAASSEN, Z., BEH, C. T. & MENON, A. K. 2005. Transport of newly synthesized sterol to the sterol-enriched plasma membrane occurs via nonvesicular equilibration. *Biochemistry*, 44, 5816-5826.
- BEAULIEU, E. & MORAND, E. F. 2011. Role of GILZ in immune regulation, glucocorticoid actions and rheumatoid arthritis. *Nature Reviews. Rheumatology*, 7, 340-348.
- BEGER, C., GERDES, K., LAUTEN, M., TISSING, W. J., FERNANDEZ-MUNOZ, I., SCHRAPPE, M. & WELTE, K. 2003. Expression and structural analysis of glucocorticoid receptor isoform gamma in human leukaemia cells using an isoform-specific real-time polymerase chain reaction approach. *British Journal of Haematology*, 122, 245-252.
- BENSAUDE, O. 2011. Inhibiting eukaryotic transcription: Which compound to choose? How to evaluate its activity? *Transcription*, 2, 103-108.
- BERUBE, B. J. & BUBECK WARDENBURG, J. 2013. *Staphylococcus aureus* alpha-toxin: nearly a century of intrigue. *Toxins*, 5, 1140-1166.
- BEZANILLA, M., GLADFELTER, A. S., KOVAR, D. R. & LEE, W. L. 2015. Cytoskeletal dynamics: a view from the membrane. *The Journal of Cell Biology*, 209, 329-337.
- BHAKDI, S., TRANUM-JENSEN, J. & SZIEGOLEIT, A. 1985. Mechanism of membrane damage by streptolysin-O. *Infection and Immunity*, 47, 52-60.

- BIDDIE, S. C., JOHN, S., SABO, P. J., THURMAN, R. E., JOHNSON, T. A., SCHILTZ, R. L., MIRANDA, T. B., SUNG, M. H., TRUMP, S., LIGHTMAN, S. L., VINSON, C., STAMATOYANNOPOULOS, J. A. & HAGER, G. L. 2011. Transcription factor API potentiates chromatin accessibility and glucocorticoid receptor binding. *Molecular Cell*, 43, 145-155.
- BIELSKA, A. A., OLSEN, B. N., GALE, S. E., MYDOCK-MCGRANE, L., KRISHNAN, K., BAKER, N. A., SCHLESINGER, P. H., COVEY, D. F. & ORY, D. S. 2014. Side-chain oxysterols modulate cholesterol accessibility through membrane remodeling. *Biochemistry*, 53, 3042-3051.
- BIELSKA, A. A., SCHLESINGER, P., COVEY, D. F. & ORY, D. S. 2012. Oxysterols as non-genomic regulators of cholesterol homeostasis. *Trends in Endocrinology and Metabolism*, 23, 99-106.
- BILLINGTON, S. J., JOST, B. H., CUEVAS, W. A., BRIGHT, K. R. & SONGER, J. G. 1997. The *Arcanobacterium* (Actinomyces) *pyogenes* hemolysin, pyolysin, is a novel member of the thiol-activated cytolysin family. *Journal of Bacteriology*, 179, 6100-6106.
- BILLINGTON, S. J., JOST, B. H. & SONGER, J. G. 2000. Thiol-activated cytolysins: structure, function and role in pathogenesis. *FEMS Microbiology Letters*, 182, 197-205.
- BISCHOF, L. J., KAO, C. Y., LOS, F. C., GONZALEZ, M. R., SHEN, Z., BRIGGS, S. P., VAN DER GOOT, F. G. & AROIAN, R. V. 2008. Activation of the unfolded protein response is required for defenses against bacterial pore-forming toxin in vivo. *PLoS Pathogens*, 4, e1000176.
- BISCHOFBERGER, M., GONZALEZ, M. R. & VAN DER GOOT, F. G. 2009. Membrane injury by pore-forming proteins. *Current Opinion in Cell Biology*, 21, 589-595.
- BISCHOFBERGER, M., IACOVACHE, I. & VAN DER GOOT, F. G. 2012. Pathogenic pore-forming proteins: function and host response. *Cell Host and Microbe*, 12, 266-275.
- BJORKHEM, I. & EGGERTSEN, G. 2001. Genes involved in initial steps of bile acid synthesis. *Current Opinion in Lipidology*, 12, 97-103.
- BJORKHEM, I., LEONI, V. & SVENNINGSSON, P. 2019. On the fluxes of side-chain oxidized oxysterols across blood-brain and blood-CSF barriers and origin of these steroids in CSF (Review). *The Journal of Steroid Biochemistry and Molecular Biology*, 188, 86-89.
- BLOCH, K. 1965. The biological synthesis of cholesterol. *Science*, 150, 19-28.
- BLOCH, K. 1992. Sterol molecule: structure, biosynthesis, and function. *Steroids*, 57, 378-383.
- BLONDEAU, J. M., CHURCH, D., YASCHUK, Y. & BJARNASON, J. 1999. In vitro activity of several antimicrobial agents against 1003 isolates of *Streptococcus pyogenes* collected from Western Canada. *International Journal of Antimicrobial Agents*, 12, 67-70.

- BODIN, K., ANDERSSON, U., RYSTEDT, E., ELLIS, E., NORLIN, M., PIKULEVA, I., EGGERTSEN, G., BJORKHEM, I. & DICZFALUSY, U. 2002. Metabolism of 4 β -hydroxycholesterol in humans. *The Journal of Biological Chemistry*, 277, 31534-31540.
- BODOR, E. T., WU, W. M., CHANDRAN, V. R. & BODOR, N. 2016. Enhanced activity of topical hydrocortisone by competitive binding of corticosteroid-binding globulin. *Journal of Pharmaceutical Sciences*, 105, 2873-2878.
- BONFINI, A. & BUCHON, N. 2016. Pore-forming toxins trigger the purge. *Cell Host and Microbe*, 20, 693-694.
- BONILLA, F. A. & OETTGEN, H. C. 2010. Adaptive immunity. *Journal of Allergy and Clinical Immunology*, 125, S33-S40.
- BONNETT, B. N., MARTIN, S. W., GANNON, V. P., MILLER, R. B. & ETHERINGTON, W. G. 1991. Endometrial biopsy in Holstein-Friesian dairy cows. III. Bacteriological analysis and correlations with histological findings. *Canadian Journal of Veterinary Research*, 55, 168-173.
- BOURGEOIS, S., PFAHL, M. & BAULIEU, E. E. 1984. DNA binding properties of glucocorticosteroid receptors bound to the steroid antagonist RU-486. *The EMBO Journal*, 3, 751-755.
- BREEN, M. R., CAMPS, M., CARVALHO-SIMÕES, F., ZORZANO, A. & PILCH, P. F. 2012. Cholesterol depletion in adipocytes causes caveolae collapse concomitant with proteosomal degradation of cavin-2 in a switch-like fashion. *PLoS One*, 7, e34516.
- BRITO, C., CABANES, D., SARMENTO MESQUITA, F. & SOUSA, S. 2019. Mechanisms protecting host cells against bacterial pore-forming toxins. *Cellular and Molecular Life Sciences*, 76, 1319-1339.
- BROMFIELD, J. J., SANTOS, J. E., BLOCK, J., WILLIAMS, R. S. & SHELDON, I. M. 2015. PHYSIOLOGY AND ENDOCRINOLOGY SYMPOSIUM: Uterine infection: linking infection and innate immunity with infertility in the high-producing dairy cow. *Journal of Animal Science*, 93, 2021-2033.
- BROMFIELD, J. J. & SHELDON, I. M. 2011. Lipopolysaccharide initiates inflammation in bovine granulosa cells via the TLR4 pathway and perturbs oocyte meiotic progression in vitro. *Endocrinology*, 152, 5029-5040.
- BROWN, M. S. & GOLDSTEIN, J. L. 1976. Receptor-mediated control of cholesterol metabolism. *Science*, 191, 150-154.
- BROWN, M. S. & GOLDSTEIN, J. L. 1986. A receptor-mediated pathway for cholesterol homeostasis. *Science*, 232, 34-47.
- BROWN, M. S. & GOLDSTEIN, J. L. 1997. The SREBP pathway: regulation of cholesterol metabolism by proteolysis of a membrane-bound transcription factor. *Cell*, 89, 331-340.

- BROWN, M. S. & GOLDSTEIN, J. L. 1999. A proteolytic pathway that controls the cholesterol content of membranes, cells, and blood. *Proceedings of the National Academy of Sciences of the United States of America*, 96, 11041-11048.
- BROWN, M. S., RADHAKRISHNAN, A. & GOLDSTEIN, J. L. 2018. Retrospective on Cholesterol Homeostasis: The Central Role of Scap. *Annual Review of Biochemistry*, 87, 783-807.
- BRZESKA, M., SZYMCZYK, K. & SZTERK, A. 2016. Current knowledge about oxysterols: A review. *Journal of Food Science*, 81, R2299-R2308.
- BUBECK WARDENBURG, J. & SCHNEEWIND, O. 2008. Vaccine protection against *Staphylococcus aureus* pneumonia. *The Journal of Experimental Medicine*, 205, 287-294.
- BUFFINGTON, D., COLLIER, R. J. & CANTON, G. 1983. Shade management systems to reduce heat stress for dairy cows in hot, humid climates. *Transactions of the ASAE*, 26, 1798-1802.
- BUTTGEREIT, F. & SCHEFFOLD, A. 2002. Rapid glucocorticoid effects on immune cells. *Steroids*, 67, 529-534.
- CABEZAS, S., HO, S., ROS, U., LANIO, M. E., ALVAREZ, C. & VANDER GOOT, F. G. 2017. Damage of eukaryotic cells by the pore-forming toxin sticholysin II: Consequences of the potassium efflux. *Biochimica et Biophysica Acta. Biomembranes*, 1859, 982-992.
- CADEPOND, P., F, ULMANN, M., PHD, A & BAULIEU, M., PHD, E-E 1997. RU486 (mifepristone): mechanisms of action and clinical uses. *Annual Review of Medicine*, 48, 129-156.
- CAIN, D. W. & CIDLOWSKI, J. A. 2017. Immune regulation by glucocorticoids. *Nature Reviews. Immunology*, 17, 233-247.
- CAO, Z., WEST, C., NORTON-WENZEL, C. S., REJ, R., DAVIS, F. B., DAVIS, P. J. & REJ, R. 2009. Effects of resin or charcoal treatment on fetal bovine serum and bovine calf serum. *Endocrine Research*, 34, 101-108.
- CARAPETIS, J. R., STEER, A. C., MULHOLLAND, E. K. & WEBER, M. 2005. The global burden of group A streptococcal diseases. *The Lancet. Infectious Diseases*, 5, 685-694.
- CARGNELLO, M. & ROUX, P. P. 2011. Activation and function of the MAPKs and their substrates, the MAPK-activated protein kinases. *Microbiology and Molecular Biology Reviews*, 75, 50-83.
- CASSIDY, S. K. & O'RIORDAN, M. X. 2013. More than a pore: the cellular response to cholesterol-dependent cytolysins. *Toxins*, 5, 618-636.
- CASTELLINO, F., HEUSER, J., MARCHETTI, S., BRUNO, B. & LUINI, A. 1992. Glucocorticoid stabilization of actin filaments: a possible mechanism for inhibition of corticotropin release. *Proceedings of the National Academy of Sciences of the United States of America*, 89, 3775-3779.

- CAVENEY, W. K., JOHNSTON, D. & MELNYKOVYCH, G. 1978. Regulation of cholesterol biosynthesis in HeLa S3G cells by serum lipoproteins: dexamethasone-mediated interference with suppression of 3-hydroxy-3-methylglutaryl coenzyme A reductase. *Proceedings of the National Academy of Sciences of the United States of America*, 75, 2103-2107.
- CAVENEY, W. K. & MELNYKOVYCH, G. 1977. Induction of 3-hydroxy-3-methylglutaryl coenzyme A reductase in HeLa cells by glucocorticoids. *The Journal of Biological Chemistry*, 252, 3272-3276.
- CHAKRABARTI, S., KOBAYASHI, K. S., FLAVELL, R. A., MARKS, C. B., MIYAKE, K., LISTON, D. R., FOWLER, K. T., GORELICK, F. S. & ANDREWS, N. W. 2003. Impaired membrane resealing and autoimmune myositis in synaptotagmin VII-deficient mice. *The Journal of Cell Biology*, 162, 543-549.
- CHANG, M. M., JUAREZ, M., HYDE, D. M. & WU, R. 2001. Mechanism of dexamethasone-mediated interleukin-8 gene suppression in cultured airway epithelial cells. *American Journal of Physiology. Lung Cellular and Molecular Physiology*, 280, L107-L115.
- CHANG, T. Y., LI, B. L., CHANG, C. C. & URANO, Y. 2009. Acyl-coenzyme A:cholesterol acyltransferases. *American Journal of Physiology. Endocrinology and Metabolism*, 297, E1-E9.
- CHEDID, M., HOYLE, J. R., CSAKY, K. G. & RUBIN, J. S. 1996. Glucocorticoids inhibit keratinocyte growth factor production in primary dermal fibroblasts. *Endocrinology*, 137, 2232-2237.
- CHEN, L., YANG, J., YU, J., YAO, Z., SUN, L., SHEN, Y. & JIN, Q. 2005. VFDB: a reference database for bacterial virulence factors. *Nucleic Acids Research*, 33, D325-D328.
- CHENG, W., KVILEKVAL, K. V. & ABUMRAD, N. A. 1995. Dexamethasone enhances accumulation of cholesteryl esters by human macrophages. *The American Journal of Physiology*, 269, E642-E648.
- CHIRASE, N. K., GREENE, L. W., PURDY, C. W., LOAN, R. W., AUVERMANN, B. W., PARKER, D. B., WALBORG, E. F., JR., STEVENSON, D. E., XU, Y. & KLAUNIG, J. E. 2004. Effect of transport stress on respiratory disease, serum antioxidant status, and serum concentrations of lipid peroxidation biomarkers in beef cattle. *American Journal of Veterinary Research*, 65, 860-864.
- CHRISTISON, G. I. & JOHNSON, H. D. 1972. Cortisol turnover in heat-stressed cow. *Journal of Animal Science*, 35, 1005-1010.
- CHROUSOS, G. P. 2009. Stress and disorders of the stress system. *Nature Reviews. Endocrinology*, 5, 374-381.
- COOPER, G. M. 2000. Structure of the Plasma Membrane. *The Cell: A Molecular Approach. 2nd edition*. Sunderland (MA): Sinauer Associates.

- CORROTTE, M., ALMEIDA, P. E., TAM, C., CASTRO-GOMES, T., FERNANDES, M. C., MILLIS, B. A., CORTEZ, M., MILLER, H., SONG, W., MAUGEL, T. K. & ANDREWS, N. W. 2013. Caveolae internalization repairs wounded cells and muscle fibers. *eLife*, 2, e00926.
- CORROTTE, M., FERNANDES, M. C., TAM, C. & ANDREWS, N. W. 2012. Toxin pores endocytosed during plasma membrane repair traffic into the lumen of MVBs for degradation. *Traffic*, 13, 483-494.
- COSENTINO, K., ROS, U. & GARCIA-SAEZ, A. J. 2016. Assembling the puzzle: Oligomerization of alpha-pore forming proteins in membranes. *Biochimica et Biophysica Acta*, 1858, 457-466.
- CRICK, P. J., WILLIAM BENTLEY, T., ABDEL-KHALIK, J., MATTHEWS, I., CLAYTON, P. T., MORRIS, A. A., BIGGER, B. W., ZERBINATI, C., TRITAPEPE, L., IULIANO, L., WANG, Y. & GRIFFITHS, W. J. 2015. Quantitative charge-tags for sterol and oxysterol analysis. *Clinical Chemistry*, 61, 400-411.
- CRONIN, J., HEALEY, G. D., MACKINTOSH, S. B. P., TURNER, M. L., HEALY, L. L. & SHELDON, I. M. 2014. Bovine endometrial epithelial and stromal cells - Standard operating procedures for isolation and culture of primary bovine endometrial epithelial and stromal cells. *Swansea: ResearchGate*, 1-15.
- CRONIN, J. G., TURNER, M. L., GOETZE, L., BRYANT, C. E. & SHELDON, I. M. 2012. Toll-like receptor 4 and MYD88-dependent signaling mechanisms of the innate immune system are essential for the response to lipopolysaccharide by epithelial and stromal cells of the bovine endometrium. *Biology of Reproduction*, 86, 51, 1-9.
- CROWE, M. A. & WILLIAMS, E. J. 2012. Triennial Lactation Symposium: Effects of stress on postpartum reproduction in dairy cows. *Journal of Animal Science*, 90, 1722-1727.
- CROXTALL, J. D., VAN HAL, P. T., CHOUDHURY, Q., GILROY, D. W. & FLOWER, R. J. 2002. Different glucocorticoids vary in their genomic and non-genomic mechanism of action in A549 cells. *British Journal of Pharmacology*, 135, 511-519.
- CUNNINGHAM, M. W. 2000. Pathogenesis of group A streptococcal infections. *Clinical Microbiology Reviews*, 13, 470-511.
- CURATOLO, W. 1987. The physical properties of glycolipids. *Biochimica et Biophysica Acta*, 906, 111-136.
- CURTIS, V. A. 2007. A natural history of hygiene. *The Canadian Journal of Infectious Diseases and Medical Microbiology*, 18, 11-14.
- CURTIS, V. A. 2014. Infection-avoidance behaviour in humans and other animals. *Trends in Immunology*, 35, 457-464.
- CYSTER, J. G., DANG, E. V., REBOLDI, A. & YI, T. 2014. 25-Hydroxycholesterols in innate and adaptive immunity. *Nature Reviews. Immunology*, 14, 731-743.

- DAL PERARO, M. & VAN DER GOOT, F. G. 2016. Pore-forming toxins: ancient, but never really out of fashion. *Nature Reviews. Microbiology*, 14, 77-92.
- DANG, E. V., MCDONALD, J. G., RUSSELL, D. W. & CYSTER, J. G. 2017. Oxysterol restraint of cholesterol synthesis prevents AIM2 inflammasome activation. *Cell*, 171, 1057-1071.
- DAS, A., BROWN, M. S., ANDERSON, D. D., GOLDSTEIN, J. L. & RADHAKRISHNAN, A. 2014. Three pools of plasma membrane cholesterol and their relation to cholesterol homeostasis. *eLife*, 3, e02882.
- DAS, A., GOLDSTEIN, J. L., ANDERSON, D. D., BROWN, M. S. & RADHAKRISHNAN, A. 2013. Use of mutant 125I-perfringolysin O to probe transport and organization of cholesterol in membranes of animal cells. *Proceedings of the National Academy of Sciences of the United States of America*, 110, 10580-10585.
- DE GANS, J., VAN DE BEEK, D. & EUROPEAN DEXAMETHASONE IN ADULTHOOD BACTERIAL MENINGITIS STUDY, I. 2002. Dexamethasone in adults with bacterial meningitis. *The New England Journal of Medicine*, 347, 1549-1556.
- DECKER, T. & LOHMANN-MATTHES, M. L. 1988. A quick and simple method for the quantitation of lactate dehydrogenase release in measurements of cellular cytotoxicity and tumor necrosis factor (TNF) activity. *Journal of Immunological Methods*, 115, 61-69.
- DEFOUR, A., VAN DER MEULEN, J. H., BHAT, R., BIGOT, A., BASHIR, R., NAGARAJU, K. & JAISWAL, J. K. 2014. Dysferlin regulates cell membrane repair by facilitating injury-triggered acid sphingomyelinase secretion. *Cell Death and Disease*, 5, e1306.
- DHAWAN, L., LIU, B., BLAXALL, B. C. & TAUBMAN, M. B. 2007. A novel role for the glucocorticoid receptor in the regulation of monocyte chemoattractant protein-1 mRNA stability. *The Journal of Biological Chemistry*, 282, 10146-10152.
- DI RENZO, G. C., GIARDINA, I., CLERICI, G., BRILLO, E. & GERLI, S. 2016. Progesterone in normal and pathological pregnancy. *Hormone Molecular Biology and Clinical Investigation*, 27, 35-48.
- DICZFALUSY, U., OLOFSSON, K. E., CARLSSON, A. M., GONG, M., GOLENBOCK, D. T., ROOYACKERS, O., FLARING, U. & BJORKBACKA, H. 2009. Marked upregulation of cholesterol 25-hydroxylase expression by lipopolysaccharide. *Journal of Lipid Research*, 50, 2258-2264.
- DINARELLO, C. A. 1998. Interleukin-1 β , interleukin-18, and the interleukin-1 β converting enzyme. *Annals of the New York Academy of Sciences*, 856, 1-11.
- DISEASES, G. B. D. & INJURIES, C. 2020. Global burden of 369 diseases and injuries in 204 countries and territories, 1990-2019: a systematic analysis for the Global Burden of Disease Study 2019. *Lancet*, 396, 1204-1222.

- DITTMAR, K. D. & PRATT, W. B. 1997. Folding of the glucocorticoid receptor by the reconstituted Hsp90-based chaperone machinery. The initial hsp90.p60.hsp70-dependent step is sufficient for creating the steroid binding conformation. *The Journal of Biological Chemistry*, 272, 13047-13054.
- DOWD, K. J., FARRAND, A. J. & TWETEN, R. K. 2012. The cholesterol-dependent cytolysin signature motif: a critical element in the allosteric pathway that couples membrane binding to pore assembly. *PLoS Pathogens*, 8, e1002787.
- DRUMMOND, A. E. 2006. The role of steroids in follicular growth. *Reproduction Biology and Endocrinology*, 4, 1-11.
- DU, X., PHAM, Y. H. & BROWN, A. J. 2004. Effects of 25-hydroxycholesterol on cholesterol esterification and sterol regulatory element-binding protein processing are dissociable: implications for cholesterol movement to the regulatory pool in the endoplasmic reticulum. *The Journal of Biological Chemistry*, 279, 47010-47016.
- DUMA, D., JEWELL, C. M. & CIDLOWSKI, J. A. 2006. Multiple glucocorticoid receptor isoforms and mechanisms of post-translational modification. *The Journal of Steroid Biochemistry and Molecular Biology*, 102, 11-21.
- DUNNE, A., ROSS, P. J., POSPISILOVA, E., MASIN, J., MEANEY, A., SUTTON, C. E., IWAKURA, Y., TSCHOPP, J., SEBO, P. & MILLS, K. H. 2010. Inflammasome activation by adenylate cyclase toxin directs Th17 responses and protection against *Bordetella pertussis*. *Journal of Immunology*, 185, 1711-1719.
- DUSELL, C. D., UMETANI, M., SHAUL, P. W., MANGELSDORF, D. J. & MCDONNELL, D. P. 2008. 27-hydroxycholesterol is an endogenous selective estrogen receptor modulator. *Molecular Endocrinology*, 22, 65-77.
- DYKMAN, T. R., GLUCK, O. S., MURPHY, W. A., HAHN, T. J. & HAHN, B. H. 1985. Evaluation of factors associated with glucocorticoid-induced osteopenia in patients with rheumatic diseases. *Arthritis and Rheuma*, 28, 361-368.
- DZELETOVIC, S., BREUER, O., LUND, E. & DICZFALUSY, U. 1995. Determination of cholesterol oxidation products in human plasma by isotope dilution-mass spectrometry. *Analytical Biochemistry*, 225, 73-80.
- EDWARDS, P. A., KENNEDY, M. A. & MAK, P. A. 2002. LXRs; oxysterol-activated nuclear receptors that regulate genes controlling lipid homeostasis. *Vascul Pharmacology*, 38, 249-256.
- ENCARNACAO, M., ESPADA, L., ESCREVENTE, C., MATEUS, D., RAMALHO, J., MICHELET, X., SANTARINO, I., HSU, V. W., BRENNER, M. B., BARRAL, D. C. & VIEIRA, O. V. 2016. A Rab3a-dependent complex essential for lysosome positioning and plasma membrane repair. *The Journal of Cell Biology*, 213, 631-640.
- ENDAPALLY, S., FRIAS, D., GRZEMSKA, M., GAY, A., TOMCHICK, D. R. & RADHAKRISHNAN, A. 2019. Molecular discrimination between two conformations of sphingomyelin in plasma membranes. *Cell*, 176, 1040-1053.

- EPAND, R. M. & VOGEL, H. J. 1999. Diversity of antimicrobial peptides and their mechanisms of action. *Biochimica et Biophysica Acta*, 1462, 11-28.
- ESCOLL, P. & BUCHRIESER, C. 2018. Metabolic reprogramming of host cells upon bacterial infection: Why shift to a Warburg-like metabolism? *The FEBS Journal*, 285, 2146-2160.
- FACKLER, O. T. & GROSSE, R. 2008. Cell motility through plasma membrane blebbing. *The Journal of Cell Biology*, 181, 879-884.
- FAIR, R. J. & TOR, Y. 2014. Antibiotics and bacterial resistance in the 21st century. *Perspectives in Medicinal Chemistry*, 6, 25-64.
- FANCHIN, R., AYOUBI, J. M., OLIVENNES, F., RIGHINI, C., DE ZIEGLER, D. & FRYDMAN, R. 2000. Hormonal influence on the uterine contractility during ovarian stimulation. *Human Reproduction*, 15 Suppl 1, 90-100.
- FARNEGARDH, M., BONN, T., SUN, S., LJUNGGREN, J., AHOLA, H., WILHELMSSON, A., GUSTAFSSON, J. A. & CARLQUIST, M. 2003. The three-dimensional structure of the liver X receptor β reveals a flexible ligand-binding pocket that can accommodate fundamentally different ligands. *The Journal of Biological Chemistry*, 278, 38821-38828.
- FARRAND, A. J., LACHAPELLE, S., HOTZE, E. M., JOHNSON, A. E. & TWETEN, R. K. 2010. Only two amino acids are essential for cytolytic toxin recognition of cholesterol at the membrane surface. *Proceedings of the National Academy of Sciences of the United States of America*, 107, 4341-4346.
- FINDLAY, J. K., LIEW, S. H., SIMPSON, E. R. & KORACH, K. S. 2010. Estrogen signaling in the regulation of female reproductive functions. *Handbook of Experimental Pharmacology*, 29-35.
- FISCHER, C., DRILLICH, M., ODAU, S., HEUWIESER, W., EINSPANIER, R. & GABLER, C. 2010. Selected pro-inflammatory factor transcripts in bovine endometrial epithelial cells are regulated during the oestrous cycle and elevated in case of subclinical or clinical endometritis. *Reproduction, Fertility, and Development*, 22, 818-829.
- FIVAZ, M., ABRAMI, L. & VAN DER GOOT, F. G. 1999. Landing on lipid rafts. *Trends in Cell Biology*, 9, 212-213.
- FIVAZ, M., ABRAMI, L. & VAN DER GOOT, F. G. 2000. Pathogens, toxins, and lipid rafts. *Protoplasma*, 212, 8-14.
- FLANAGAN, J. J., TWETEN, R. K., JOHNSON, A. E. & HEUCK, A. P. 2009. Cholesterol exposure at the membrane surface is necessary and sufficient to trigger perfringolysin O binding. *Biochemistry*, 48, 3977-3987.
- FORTIER, M. A., GUILBAULT, L. A. & GRASSO, F. 1988. Specific properties of epithelial and stromal cells from the endometrium of cows. *Journal of Reproduction and Fertility*, 83, 239-248.

- FOURICHON, C., SEEGER, H. & MALHER, X. 2000. Effect of disease on reproduction in the dairy cow: a meta-analysis. *Theriogenology*, 53, 1729-1759.
- FRANCO, L. M., GADKARI, M., HOWE, K. N., SUN, J., KARDAVA, L., KUMAR, P., KUMARI, S., HU, Z., FRASER, I. D. C., MOIR, S., TSANG, J. S. & GERMAIN, R. N. 2019. Immune regulation by glucocorticoids can be linked to cell type-dependent transcriptional responses. *The Journal of Experimental Medicine*, 216, 384-406.
- FRYER, C. J., KINYAMU, H. K., ROGATSKY, I., GARABEDIAN, M. J. & ARCHER, T. K. 2000. Selective activation of the glucocorticoid receptor by steroid antagonists in human breast cancer and osteosarcoma cells. *The Journal of Biological Chemistry*, 275, 17771-17777.
- GALVÃO, K., FLAMINIO, M., BRITTIN, S., SPER, R., FRAGA, M., CAIXETA, L., RICCI, A., GUARD, C., BUTLER, W. & GILBERT, R. 2010. Association between uterine disease and indicators of neutrophil and systemic energy status in lactating Holstein cows. *Journal of Dairy Science*, 93, 2926-2937.
- GARSIDE, H., STEVENS, A., FARROW, S., NORMAND, C., HOULE, B., BERRY, A., MASCHERA, B. & RAY, D. 2004. Glucocorticoid ligands specify different interactions with NF- κ B by allosteric effects on the glucocorticoid receptor DNA binding domain. *The Journal of Biological Chemistry*, 279, 50050-50059.
- GEERAERTS, M. D., RONVEAUX-DUPAL, M. F., LEMASTERS, J. J. & HERMAN, B. 1991. Cytosolic free Ca²⁺ and proteolysis in lethal oxidative injury in endothelial cells. *The American Journal of Physiology*, 261, C889-C896.
- GEKARA, N. O., WESTPHAL, K., MA, B., ROHDE, M., GROEBE, L. & WEISS, S. 2007. The multiple mechanisms of Ca²⁺ signalling by listeriolysin O, the cholesterol-dependent cytolysin of *Listeria monocytogenes*. *Cell Microbiology*, 9, 2008-2021.
- GENY, B. & POPOFF, M. R. 2006. Bacterial protein toxins and lipids: pore formation or toxin entry into cells. *Biology of the Cell*, 98, 667-678.
- GIDDINGS, K. S., JOHNSON, A. E. & TWETEN, R. K. 2003. Redefining cholesterol's role in the mechanism of the cholesterol-dependent cytolysins. *Proceedings of the National Academy of Sciences of the United States of America*, 100, 11315-11320.
- GIGUERE, V., TREMBLAY, A. & TREMBLAY, G. B. 1998. Estrogen receptor β : re-evaluation of estrogen and antiestrogen signaling. *Steroids*, 63, 335-339.
- GILL, S., CHOW, R. & BROWN, A. J. 2008. Sterol regulators of cholesterol homeostasis and beyond: the oxysterol hypothesis revisited and revised. *Progress in Lipid Research*, 47, 391-404.
- GOLDSTEIN, J. L. & BROWN, M. S. 1990. Regulation of the mevalonate pathway. *Nature*, 343, 425-430.

- GOLDSTEIN, J. L., DEBOSE-BOYD, R. A. & BROWN, M. S. 2006. Protein sensors for membrane sterols. *Cell*, 124, 35-46.
- GOLUSZKO, P. & NOWICKI, B. 2005. Membrane cholesterol: a crucial molecule affecting interactions of microbial pathogens with mammalian cells. *Infection and Immunity*, 73, 7791-7996.
- GONZALEZ, M. R., BISCHOFBERGER, M., FRECHE, B., HO, S., PARTON, R. G. & VAN DER GOOT, F. G. 2011. Pore-forming toxins induce multiple cellular responses promoting survival. *Cell Microbiology*, 13, 1026-1043.
- GOUAUX, E. 1997. Channel-forming toxins: tales of transformation. *Current Opinion in Structural Biology*, 7, 566-573.
- GRIFFIN, J. F., HARTIGAN, P. J. & NUNN, W. R. 1974. Non-specific uterine infection and bovine fertility. I. Infection patterns and endometritis during the first seven weeks post-partum. *Theriogenology*, 1, 91-106.
- GRIFFIN, S., HEALEY, G. D. & SHELDON, I. M. 2018. Isoprenoids increase bovine endometrial stromal cell tolerance to the cholesterol-dependent cytolysin from *Trueperella pyogenes*. *Biology of Reproduction*, 99, 749-760.
- GRIFFIN, S., PRETA, G. & SHELDON, I. M. 2017. Inhibiting mevalonate pathway enzymes increases stromal cell resilience to a cholesterol-dependent cytolysin. *Scientific Reports*, 7, 1-13.
- GRIFFITHS, W. J., CRICK, P. J., WANG, Y., OGUNDARE, M., TUSCHL, K., MORRIS, A. A., BIGGER, B. W., CLAYTON, P. T. & WANG, Y. 2013. Analytical strategies for characterization of oxysterol lipidomes: liver X receptor ligands in plasma. *Free Radical Biology and Medicine*, 59, 69-84.
- GRUYS, E., TOUSSAINT, M. J., NIEWOLD, T. A. & KOOPMANS, S. J. 2005. Acute phase reaction and acute phase proteins. *Journal of Zhejiang University Science. B*, 6, 1045-1056.
- GURCEL, L., ABRAMI, L., GIRARDIN, S., TSCHOPP, J. & VAN DER GOOT, F. G. 2006. Caspase-1 activation of lipid metabolic pathways in response to bacterial pore-forming toxins promotes cell survival. *Cell*, 126, 1135-1145.
- GUTIERREZ, M. G., SAKA, H. A., CHINEN, I., ZOPPINO, F. C., YOSHIMORI, T., BOCCO, J. L. & COLOMBO, M. I. 2007. Protective role of autophagy against *Vibrio cholerae* cytolysin, a pore-forming toxin from *V. cholerae*. *Proceedings of the National Academy of Sciences of the United States of America*, 104, 1829-1834.
- HAIMERL, P. & HEUWIESER, W. 2014. Invited review: Antibiotic treatment of metritis in dairy cows: a systematic approach. *Journal of Dairy Science*, 97, 6649-6661.
- HALL, J. M., COUSE, J. F. & KORACH, K. S. 2001. The multifaceted mechanisms of estradiol and estrogen receptor signaling. *The Journal of Biological Chemistry*, 276, 36869-36872.

- HAMMOND, G. L. 1990. Molecular properties of corticosteroid binding globulin and the sex-steroid binding proteins. *Endocrine Reviews*, 11, 65-79.
- HANUKOGLU, I. 1992. Steroidogenic enzymes: structure, function, and role in regulation of steroid hormone biosynthesis. *The Journal of Steroid Biochemistry and Molecular Biology*, 43, 779-804.
- HARDING, S. 1990. The human pharmacology of fluticasone propionate. *Respiratory Medicine*, 84, 25-29.
- HAYWARD, G., THOMPSON, M. J., PERERA, R., GLASZIOU, P. P., DEL MAR, C. B. & HENEGHAN, C. J. 2012. Corticosteroids as standalone or add-on treatment for sore throat. *The Cochrane Database of Systematic Reviews*, 10, CD008268.
- HECK, S., BENDER, K., KULLMANN, M., GÖTTLICHER, M., HERRLICH, P. & CATO, A. C. 1997. I κ B α -independent downregulation of NF- κ B activity by glucocorticoid receptor. *The EMBO Journal*, 16, 4698-4707.
- HEIN, M., VALORE, E. V., HELMIG, R. B., ULDBJERG, N. & GANZ, T. 2002. Antimicrobial factors in the cervical mucus plug. *American Journal of Obstetrics and Gynecology*, 187, 137-144.
- HENRY, B. D., NEILL, D. R., BECKER, K. A., GORE, S., BRICIO-MORENO, L., ZIOBRO, R., EDWARDS, M. J., MUHLEMANN, K., STEINMANN, J., KLEUSER, B., JAPTOK, L., LUGINBUHL, M., WOLFMEIER, H., SCHERAG, A., GULBINS, E., KADIOGLU, A., DRAEGER, A. & BABIYCHUK, E. B. 2015. Engineered liposomes sequester bacterial exotoxins and protect from severe invasive infections in mice. *Nature Biotechnology*, 33, 81-88.
- HEUCK, A. P., MOE, P. C. & JOHNSON, B. B. 2010. The cholesterol-dependent cytolysin family of gram-positive bacterial toxins. *Sub-cellular Biochemistry*, 51, 551-577.
- HEUMANN, D., LAUENER, R. & RYFFEL, B. 2003. The dual role of LBP and CD14 in response to Gram-negative bacteria or Gram-negative compounds. *Journal of Endotoxin Research*, 9, 381-384.
- HEWITT, L. & TODD, E. 1939. The effect of cholesterol and of sera contaminated with bacteria on the haemolysins produced by haemolytic streptococci. *Journal of Pathology and Bacteriology*, 49, 45-51.
- HILDEBRAND, A., POHL, M. & BHAKDI, S. 1991. *Staphylococcus aureus* alpha-toxin. Dual mechanism of binding to target cells. *The Journal of Biological Chemistry*, 266, 17195-17200.
- HO, J. T., AL-MUSALHI, H., CHAPMAN, M. J., QUACH, T., THOMAS, P. D., BAGLEY, C. J., LEWIS, J. G. & TORPY, D. J. 2006. Septic shock and sepsis: a comparison of total and free plasma cortisol levels. *Journal of Clinical Endocrinology and Metabolism*, 91, 105-114.

- HOES, J. N., VAN DER GOES, M. C., VAN RAALTE, D. H., VAN DER ZIJL, N. J., DEN UYL, D., LEMS, W. F., LAFEBER, F. P., JACOBS, J. W., WELSING, P. M., DIAMANT, M. & BIJLSMA, J. W. 2011. Glucose tolerance, insulin sensitivity and β -cell function in patients with rheumatoid arthritis treated with or without low-to-medium dose glucocorticoids. *Annals of the Rheumatic Diseases*, 70, 1887-1894.
- HOLLENBERG, S. M., WEINBERGER, C., ONG, E. S., CERELLI, G., ORO, A., LEBO, R., THOMPSON, E. B., ROSENFELD, M. G. & EVANS, R. M. 1985. Primary structure and expression of a functional human glucocorticoid receptor cDNA. *Nature*, 318, 635-641.
- HOTZE, E. M. & TWETEN, R. K. 2012. Membrane assembly of the cholesterol-dependent cytolysin pore complex. *Biochimica et Biophysica Acta*, 1818, 1028-1038.
- HOWARD, J. G. & WALLACE, K. R. 1953. The comparative resistances of rabbits, guinea pigs and mice to the lethal actions of streptolysin O and saponin. *British Journal of Experimental Pathology*, 34, 185-190.
- HU, J., ZHANG, Z., SHEN, W. J. & AZHAR, S. 2010. Cellular cholesterol delivery, intracellular processing and utilization for biosynthesis of steroid hormones. *Nutrition and Metabolism*, 7, 1-25.
- HU, W., JIANG, C., KIM, M., YANG, W., ZHU, K., GUAN, D., LV, W., XIAO, Y., WILSON, J. R., RADER, D. J., PUI, C. H., RELLING, M. V. & LAZAR, M. A. 2021. Individual-specific functional epigenomics reveals genetic determinants of adverse metabolic effects of glucocorticoids. *Cell Metabolism*, 33, 1592-1609 e7.
- HUDSON, S., MULLFORD, M., WHITTLESTONE, W. G. & PAYNE, E. 1976. Bovine plasma corticoids during parturition. *Journal of Dairy Science*, 59, 744-746.
- HUFFMAN, D. L., ABRAMI, L., SASIK, R., CORBEIL, J., VAN DER GOOT, F. G. & AROIAN, R. V. 2004. Mitogen-activated protein kinase pathways defend against bacterial pore-forming toxins. *Proceedings of the National Academy of Sciences of the United States of America*, 101, 10995-11000.
- HUGHES, T. R., ROSS, K. S., COWAN, G. J., SIVASANKAR, B., HARRIS, C. L., MITCHELL, T. J. & MORGAN, B. P. 2009. Identification of the high affinity binding site in the *Streptococcus intermedius* toxin intermedilysin for its membrane receptor, the human complement regulator CD59. *Molecular Immunology*, 46, 1561-1567.
- HUSMANN, M., DERSCH, K., BOBKIEWICZ, W., BECKMANN, E., VEERACHATO, G. & BHAKDI, S. 2006. Differential role of p38 mitogen activated protein kinase for cellular recovery from attack by pore-forming *S. aureus* alpha-toxin or streptolysin O. *Biochemical and Biophysical Research Communications*, 344, 1128-1134.

- IDONE, V., TAM, C., GOSS, J. W., TOOMRE, D., PYPAERT, M. & ANDREWS, N. W. 2008. Repair of injured plasma membrane by rapid Ca²⁺-dependent endocytosis. *The Journal of Cell Biology*, 180, 905-914.
- ILIEV, A. I., DJANNATIAN, J. R., NAU, R., MITCHELL, T. J. & WOUTERS, F. S. 2007. Cholesterol-dependent actin remodeling via RhoA and Rac1 activation by the *Streptococcus pneumoniae* toxin pneumolysin. *Proceedings of the National Academy of Sciences of the United States of America*, 104, 2897-2902.
- IMMORDINO, M. L., DOSIO, F. & CATTEL, L. 2006. Stealth liposomes: review of the basic science, rationale, and clinical applications, existing and potential. *International Journal of Nanomedicine*, 1, 297-315.
- ISOHASHI, F. & OKAMOTO, K. 1993. ATP-stimulated translocation promoter that enhances the nuclear binding of activated glucocorticoid receptor complex. Biochemical properties and its function (mini-review). *Receptor*, 3, 113-124.
- ITO, A., HONG, C., RONG, X., ZHU, X., TARLING, E. J., HEDDE, P. N., GRATTON, E., PARKS, J. & TONTONOZ, P. 2015. LXRs link metabolism to inflammation through Abca1-dependent regulation of membrane composition and TLR signaling. *eLife*, 4, e08009.
- IWAMOTO, M., OHNO-IWASHITA, Y. & ANDO, S. 1987. Role of the essential thiol group in the thiol-activated cytolysin from *Clostridium perfringens*. *European Journal of Biochemistry*, 167, 425-430.
- IYER, V. R., EISEN, M. B., ROSS, D. T., SCHULER, G., MOORE, T., LEE, J. C., TRENT, J. M., STAUDT, L. M., HUDSON, J., JR., BOGUSKI, M. S., LASHKARI, D., SHALON, D., BOTSTEIN, D. & BROWN, P. O. 1999. The transcriptional program in the response of human fibroblasts to serum. *Science*, 283, 83-87.
- JAMIESON, A. M., YU, S., ANNICELLI, C. H. & MEDZHITOV, R. 2010. Influenza virus-induced glucocorticoids compromise innate host defense against a secondary bacterial infection. *Cell Host and Microbe*, 7, 103-114.
- JANOWSKI, B. A., WILLY, P. J., DEVI, T. R., FALCK, J. R. & MANGELSDORF, D. J. 1996. An oxysterol signalling pathway mediated by the nuclear receptor LXR α . *Nature*, 383, 728-731.
- JENSEN, S. O. & LYON, B. R. 2009. Genetics of antimicrobial resistance in *Staphylococcus aureus*. *Future Microbiology*, 4, 565-582.
- JIMENEZ, A. J., MAIURI, P., LAFAURIE-JANVORE, J., DIVOUX, S., PIEL, M. & PEREZ, F. 2014. ESCRT machinery is required for plasma membrane repair. *Science*, 343, 1247136.
- JIMENEZ, A. J. & PEREZ, F. 2017. Plasma membrane repair: the adaptable cell life-insurance. *Current Opinion in Cell Biology*, 47, 99-107.
- JIN, L., MARTYNOWSKI, D., ZHENG, S., WADA, T., XIE, W. & LI, Y. 2010. Structural basis for hydroxycholesterols as natural ligands of orphan nuclear receptor ROR γ . *Molecular Endocrinology*, 24, 923-929.

- JO, Y. & DEBOSE-BOYD, R. A. 2010. Control of cholesterol synthesis through regulated ER-associated degradation of HMG CoA reductase. *Critical Reviews in Biochemistry and Molecular Biology*, 45, 185-198.
- JOHN, S., SABO, P. J., THURMAN, R. E., SUNG, M. H., BIDDIE, S. C., JOHNSON, T. A., HAGER, G. L. & STAMATOYANNOPOULOS, J. A. 2011. Chromatin accessibility pre-determines glucocorticoid receptor binding patterns. *Nature Genetics*, 43, 264-268.
- JOHNSON, M. 1998. Development of fluticasone propionate and comparison with other inhaled corticosteroids. *The Journal of Allergy and Clinical Immunology*, 101, S434-S439.
- JOHNSTON, D., CAVENEE, W. K., RAMACHANDRAN, C. K. & MELNYKOVYCH, G. 1979. Cholesterol biosynthesis in a variety of cultured cells. Lack of correlation between synthesis and activity of 3-hydroxy-3-methylglutaryl coenzyme A reductase caused by dexamethasone. *Biochimica et Biophysica Acta. Lipids and lipid metabolism*, 572, 188-192.
- JONAT, C., RAHMSDORF, H. J., PARK, K.-K., CATO, A. C., GEBEL, S., PONTA, H. & HERRLICH, P. 1990. Antitumor promotion and antiinflammation: down-modulation of AP-1 (Fos/Jun) activity by glucocorticoid hormone. *Cell*, 62, 1189-1204.
- JOSEPH, S. B., CASTRILLO, A., LAFFITTE, B. A., MANGELSDORF, D. J. & TONTONOZ, P. 2003. Reciprocal regulation of inflammation and lipid metabolism by liver X receptors. *Nature Medicine*, 9, 213-219.
- JOST, B. H. & BILLINGTON, S. J. 2005. *Arcanobacterium pyogenes*: molecular pathogenesis of an animal opportunist. *Antonie Van Leeuwenhoek*, 88, 87-102.
- KADIYALA, V., SASSE, S. K., ALTONSY, M. O., BERMAN, R., CHU, H. W., PHANG, T. L. & GERBER, A. N. 2016. Cistrome-based cooperation between airway epithelial glucocorticoid receptor and NF- κ B orchestrates anti-inflammatory effects. *The Journal of Biological Chemistry*, 291, 12673-12687.
- KADMIEL, M. & CIDLOWSKI, J. A. 2013. Glucocorticoid receptor signaling in health and disease. *Trends in Pharmacological Sciences*, 34, 518-530.
- KADZERE, C. T., MURPHY, M., SILANIKOVE, N. & MALTZ, E. 2002. Heat stress in lactating dairy cows: a review. *Livestock Production Science*, 77, 59-91.
- KAO, C. Y., LOS, F. C., HUFFMAN, D. L., WACHI, S., KLOFT, N., HUSMANN, M., KARABRAHIMI, V., SCHWARTZ, J. L., BELLIER, A., HA, C., SAGONG, Y., FAN, H., GHOSH, P., HSIEH, M., HSU, C. S., CHEN, L. & AROIAN, R. V. 2011. Global functional analyses of cellular responses to pore-forming toxins. *PLoS Pathogens*, 7, e1001314.
- KAUFFMAN, J. M., WESTERMAN, P. W. & CAREY, M. C. 2000. Fluorocholesterols, in contrast to hydroxycholesterols, exhibit interfacial properties similar to cholesterol. *Journal of Lipid Research*, 41, 991-1003.

- KEMPPAINEN, R. J. & BEHREND, E. N. 1998. Dexamethasone rapidly induces a novel ras superfamily member-related gene in AtT-20 cells. *The Journal of Biological Chemistry*, 273, 3129-3131.
- KENNEDY, A. D., BUBECK WARDENBURG, J., GARDNER, D. J., LONG, D., WHITNEY, A. R., BRAUGHTON, K. R., SCHNEEWIND, O. & DELEO, F. R. 2010. Targeting of alpha-hemolysin by active or passive immunization decreases severity of USA300 skin infection in a mouse model. *The Journal of Infectious Diseases*, 202, 1050-1058.
- KENNEDY, C. L., SMITH, D. J., LYRAS, D., CHAKRAVORTY, A. & ROOD, J. I. 2009. Programmed cellular necrosis mediated by the pore-forming alpha-toxin from *Clostridium septicum*. *PLoS Pathogens*, 5, e1000516.
- KEYEL, P. A., LOULTCHEVA, L., ROTH, R., SALTER, R. D., WATKINS, S. C., YOKOYAMA, W. M. & HEUSER, J. E. 2011. Streptolysin O clearance through sequestration into blebs that bud passively from the plasma membrane. *Journal of Cell Science*, 124, 2414-2423.
- KHANG, Y.-H. & COLLABORATORS, G. L. R. I. 2018. Estimates of the global, regional, and national morbidity, mortality, and aetiologies of lower respiratory infections in 195 countries, 1990-2016: a systematic analysis for the Global Burden of Disease Study 2016. *The Lancet. Infectious Diseases*, 18, 1191-1210.
- KHO, M. F., BELLIER, A., BALASUBRAMANI, V., HU, Y., HSU, W., NIELSEN-LEROUX, C., MCGILLIVRAY, S. M., NIZET, V. & AROIAN, R. V. 2011. The pore-forming protein Cry5B elicits the pathogenicity of *Bacillus sp.* against *Caenorhabditis elegans*. *PLoS One*, 6, e29122.
- KIM, S. W., KIM, S. J., LANGLEY, R. R. & FIDLER, I. J. 2015. Modulation of the cancer cell transcriptome by culture media formulations and cell density. *International Journal of Oncology*, 46, 2067-2075.
- KIMMINS, S. & MACLAREN, L. A. 2001. Oestrous cycle and pregnancy effects on the distribution of oestrogen and progesterone receptors in bovine endometrium. *Placenta*, 22, 742-8.
- KLOFT, N., BUSCH, T., NEUKIRCH, C., WEIS, S., BOUKHALLOUK, F., BOBKIEWICZ, W., CIBIS, I., BHAKDI, S. & HUSMANN, M. 2009. Pore-forming toxins activate MAPK p38 by causing loss of cellular potassium. *Biochemical and Biophysical Research Communications*, 385, 503-506.
- KNAPP, O., MAIER, E., MKADDEM, S. B., BENZ, R., BENS, M., CHENAL, A., GENY, B., VANDEWALLE, A. & POPOFF, M. R. 2010. *Clostridium septicum* alpha-toxin forms pores and induces rapid cell necrosis. *Toxicon*, 55, 61-72.
- KONTULA, K., PAAVONEN, T., LUUKKAINEN, T. & ANDERSSON, L. C. 1983. Binding of progestins to the glucocorticoid receptor. Correlation to their glucocorticoid-like effects on in vitro functions of human mononuclear leukocytes. *Biochemical Pharmacology*, 32, 1511-1518.

- KOSTER, D. V. & MAYOR, S. 2016. Cortical actin and the plasma membrane: inextricably intertwined. *Current Opinion in Cell Biology*, 38, 81-89.
- KRETT, N. L., PILLAY, S., MOALLI, P. A., GREIPP, P. R. & ROSEN, S. T. 1995. A variant glucocorticoid receptor messenger RNA is expressed in multiple myeloma patients. *Cancer Research*, 55, 2727-2729.
- LANGE, Y., ORY, D. S., YE, J., LANIER, M. H., HSU, F. F. & STECK, T. L. 2008. Effectors of rapid homeostatic responses of endoplasmic reticulum cholesterol and 3-hydroxy-3-methylglutaryl-CoA reductase. *The Journal of Biological Chemistry*, 283, 1445-1455.
- LANGE, Y. & STECK, T. L. 1997. Quantitation of the pool of cholesterol associated with acyl-CoA:cholesterol acyltransferase in human fibroblasts. *The Journal of Biological Chemistry*, 272, 13103-13108.
- LANGE, Y., SWAISGOOD, M. H., RAMOS, B. V. & STECK, T. L. 1989. Plasma membranes contain half the phospholipid and 90% of the cholesterol and sphingomyelin in cultured human fibroblasts. *The Journal of Biological Chemistry*, 264, 3786-3793.
- LANGE, Y., YE, J., RIGNEY, M. & STECK, T. L. 1999. Regulation of endoplasmic reticulum cholesterol by plasma membrane cholesterol. *Journal of Lipid Research*, 40, 2264-2270.
- LASA, M., ABRAHAM, S. M., BOUCHERON, C., SAKLATVALA, J. & CLARK, A. R. 2002. Dexamethasone causes sustained expression of mitogen-activated protein kinase (MAPK) phosphatase 1 and phosphatase-mediated inhibition of MAPK p38. *Molecular Biology of the Cell*, 22, 7802-7811.
- LEHMANN, J. M., KLIEWER, S. A., MOORE, L. B., SMITH-OLIVER, T. A., OLIVER, B. B., SU, J. L., SUNDSETH, S. S., WINEGAR, D. A., BLANCHARD, D. E., SPENCER, T. A. & WILLSON, T. M. 1997. Activation of the nuclear receptor LXR by oxysterols defines a new hormone response pathway. *The Journal of Biological Chemistry*, 272, 3137-3140.
- LEMAIRE-EWING, S., BERTHIER, A., ROYER, M. C., LOGETTE, E., CORCOS, L., BOUCHOT, A., MONIER, S., PRUNET, C., RAVENEAU, M., REBE, C., DESRUMAUX, C., LIZARD, G. & NEEL, D. 2009. 7 β -Hydroxycholesterol and 25-hydroxycholesterol-induced interleukin-8 secretion involves a calcium-dependent activation of c-fos via the ERK1/2 signaling pathway in THP-1 cells: oxysterols-induced IL-8 secretion is calcium-dependent. *Cell Biology Toxicology*, 25, 127-139.
- LEUNG, C., DUDKINA, N. V., LUKOYANOVA, N., HODEL, A. W., FARABELLA, I., PANDURANGAN, A. P., JAHAN, N., PIRES DAMASO, M., OSMANOVIC, D., REBOUL, C. F., DUNSTONE, M. A., ANDREW, P. W., LONNEN, R., TOPF, M., SAIBIL, H. R. & HOOGENBOOM, B. W. 2014. Stepwise visualization of membrane pore formation by sullysin, a bacterial cholesterol-dependent cytolysin. *eLife*, 3, e04247.

- LEWIS, G. S. 2003. Role of ovarian progesterone and potential role of prostaglandin F₂ α and prostaglandin E₂ in modulating the uterine response to infectious bacteria in postpartum ewes. *Journal of Animal Science*, 81, 285-293.
- LEWIS, G. S. 2004. Steroidal regulation of uterine immune defenses. *Animal Reproduction Science*, 82-83, 281-294.
- LI, H., ZHAO, X., WANG, J., DONG, Y., MENG, S., LI, R., NIU, X. & DENG, X. 2015. β -sitosterol interacts with pneumolysin to prevent *Streptococcus pneumoniae* infection. *Scientific Reports*, 5, 1-9.
- LIMBAGO, B., PENUMALLI, V., WEINRICK, B. & SCOTT, J. R. 2000. Role of streptolysin O in a mouse model of invasive group A streptococcal disease. *Infection and Immunity*, 68, 6384-6390.
- LIN, C. F., CHEN, C. L., HUANG, W. C., CHENG, Y. L., HSIEH, C. Y., WANG, C. Y. & HONG, M. Y. 2010. Different types of cell death induced by enterotoxins. *Toxins*, 2, 2158-2176.
- LINDEN, S. K., SUTTON, P., KARLSSON, N. G., KOROLIK, V. & MCGUCKIN, M. A. 2008. Mucins in the mucosal barrier to infection. *Mucosal Immunology*, 1, 183-197.
- LINSEISEN, J. & WOLFRAM, G. 1998. Absorption of cholesterol oxidation products from ordinary foodstuff in humans. *Annals of Nutrition and Metabolism*, 42, 221-230.
- LOCHMILLER, R. L. & DEERENBERG, C. 2000. Trade-offs in evolutionary immunology: just what is the cost of immunity? *Oikos*, 88, 87-98.
- LORDAN, S., MACKRILL, J. J. & O'BRIEN, N. M. 2009. Oxysterols and mechanisms of apoptotic signaling: implications in the pathology of degenerative diseases. *The Journal of Nutritional Biochemistry*, 20, 321-336.
- LOS, F. C., RANDIS, T. M., AROIAN, R. V. & RATNER, A. J. 2013. Role of pore-forming toxins in bacterial infectious diseases. *Microbiology and Molecular Biology Reviews*, 77, 173-207.
- LOWY, F. D. 1998. *Staphylococcus aureus* infections. *The New England Journal of Medicine*, 339, 520-532.
- LUND, E. G., KERR, T. A., SAKAI, J., LI, W. P. & RUSSELL, D. W. 1998. cDNA cloning of mouse and human cholesterol 25-hydroxylases, polytopic membrane proteins that synthesize a potent oxysterol regulator of lipid metabolism. *The Journal of Biological Chemistry*, 273, 34316-34327.
- MA, L. & NELSON, E. R. 2019. Oxysterols and nuclear receptors. *Molecular and Cellular Endocrinology*, 484, 42-51.
- MAC NAMARA, P. & LOUGHREY, H. C. 1998. Progesterone receptor A and B isoform expression in human osteoblasts. *Calcified Tissue International*, 63, 39-46.

- MACKRILL, J. J. 2011. Oxysterols and calcium signal transduction. *Chemistry and Physics of Lipids*, 164, 488-495.
- MAITRA, U. S., KHAN, M. S. & ROSNER, W. 1993. Corticosteroid-binding globulin receptor of the rat hepatic membrane: solubilization, partial characterization, and the effect of steroids on binding. *Endocrinology*, 133, 1817-1822.
- MARIK, P. E., PASTORES, S. M., ANNANE, D., MEDURI, G. U., SPRUNG, C. L., ARLT, W., KEH, D., BRIEGEL, J., BEISHUIZEN, A. & DIMOPOULOU, I. 2008. Recommendations for the diagnosis and management of corticosteroid insufficiency in critically ill adult patients: consensus statements from an international task force by the American College of Critical Care Medicine. *Critical Care Medicine*, 36, 1937-1949.
- MARON, D. J., FAZIO, S. & LINTON, M. F. 2000. Current perspectives on statins. *Circulation*, 101, 207-213.
- MATSUBAYASHI, M., SAKAGUCHI, Y. M., SAHARA, Y., NANAURA, H., KIKUCHI, S., ASGHARI, A., BUI, L., KOBASHIGAWA, S., NAKANISHI, M., NAGATA, R., MATSUI, T. K., KASHINO, G., HASEGAWA, M., TAKASAWA, S., ERIGUCHI, M., TSURUYA, K., NAGAMORI, S., SUGIE, K., NAKAGAWA, T., TAKASATO, M., UMETANI, M. & MORI, E. 2021. 27-Hydroxycholesterol regulates human SLC22A12 gene expression through estrogen receptor action. *The FASEB Journal*, 35, e21262.
- MAXFIELD, F. R. & WUSTNER, D. 2012. Analysis of cholesterol trafficking with fluorescent probes. *Methods in Cell Biology*, 108, 367-393.
- MAYANAGI, T., MORITA, T., HAYASHI, K., FUKUMOTO, K. & SOBUE, K. 2008. Glucocorticoid receptor-mediated expression of caldesmon regulates cell migration via the reorganization of the actin cytoskeleton. *The Journal of Biological Chemistry*, 283, 31183-31196.
- MAZZON, M. & MERCER, J. 2014. Lipid interactions during virus entry and infection. *Cell Microbiology*, 16, 1493-1502.
- MCCAIN, J. 2013. The MAPK (ERK) pathway: Investigational combinations for the treatment of BRAF-mutated metastatic melanoma. *Pharmacy and Therapeutics*, 38, 96-108.
- MCCARVILLE, J. L. & AYRES, J. S. 2018. Disease tolerance: concept and mechanisms. *Current Opinion in Immunology*, 50, 88-93.
- MCCONNELL, H. M. & RADHAKRISHNAN, A. 2003. Condensed complexes of cholesterol and phospholipids. *Biochimica et Biophysica Acta*, 1610, 159-173.
- MCDONNELL, D. P. & NORRIS, J. D. 2002. Connections and regulation of the human estrogen receptor. *Science*, 296, 1642-1644.

- MCNEELA, E. A., BURKE, A., NEILL, D. R., BAXTER, C., FERNANDES, V. E., FERREIRA, D., SMEATON, S., EL-RACHKIDY, R., MCLOUGHLIN, R. M., MORI, A., MORAN, B., FITZGERALD, K. A., TSCHOPP, J., PETRILLI, V., ANDREW, P. W., KADIOGLU, A. & LAVELLE, E. C. 2010. Pneumolysin activates the NLRP3 inflammasome and promotes proinflammatory cytokines independently of TLR4. *PLoS Pathogens*, 6, e1001191.
- MCNEIL, A. K., RESCHER, U., GERKE, V. & MCNEIL, P. L. 2006. Requirement for annexin A1 in plasma membrane repair. *The Journal of Biological Chemistry*, 281, 35202-35207.
- MCNEIL, P. L. & KIRCHHAUSEN, T. 2005. An emergency response team for membrane repair. *Nature Reviews. Molecular Cell Biology*, 6, 499-505.
- MCNEIL, P. L. & STEINHARDT, R. A. 1997. Loss, restoration, and maintenance of plasma membrane integrity. *The Journal of Cell Biology*, 137, 1-4.
- MEDZHITOV, R. & JANEWAY JR, C. 2000. Innate immunity. *New England Journal of Medicine*, 343, 338-344.
- MEDZHITOV, R., SCHNEIDER, D. S. & SOARES, M. P. 2012. Disease tolerance as a defense strategy. *Science*, 335, 936-941.
- MEIJVIS, S. C., HARDEMAN, H., REMMELTS, H. H., HEIJLIGENBERG, R., RIJKERS, G. T., VAN VELZEN-BLAD, H., VOORN, G. P., VAN DE GARDE, E. M., ENDEMAN, H., GRUTTERS, J. C., BOS, W. J. & BIESMA, D. H. 2011. Dexamethasone and length of hospital stay in patients with community-acquired pneumonia: a randomised, double-blind, placebo-controlled trial. *Lancet*, 377, 2023-2030.
- MEISINGER, C., ZESCHNIGK, C. & GROTHE, C. 1996. In vivo and in vitro effect of glucocorticoids on fibroblast growth factor (FGF)-2 and FGF receptor 1 expression. *The Journal of Biological Chemistry*, 271, 16520-16525.
- MEIXENBERGER, K., PACHE, F., EITEL, J., SCHMECK, B., HIPPENSTIEL, S., SLEVOGT, H., N'GUESSAN, P., WITZENRATH, M., NETEA, M. G., CHAKRABORTY, T., SUTTORP, N. & OPITZ, B. 2010. *Listeria monocytogenes*-infected human peripheral blood mononuclear cells produce IL-1 β , depending on listeriolysin O and NLRP3. *Journal of Immunology*, 184, 922-930.
- MENESTRINA, G., SERRA, M. D. & PREVOST, G. 2001. Mode of action of β -barrel pore-forming toxins of the staphylococcal alpha-hemolysin family. *Toxicon*, 39, 1661-1672.
- MESQUITA, F. S., BRITO, C., MAZON MOYA, M. J., PINHEIRO, J. C., MOSTOWY, S., CABANES, D. & SOUSA, S. 2017. Endoplasmic reticulum chaperone Gp96 controls actomyosin dynamics and protects against pore-forming toxins. *EMBO Reports*, 18, 303-318.
- MESTRE, M. B. & COLOMBO, M. I. 2012. cAMP and EPAC are key players in the regulation of the signal transduction pathway involved in the alpha-hemolysin autophagic response. *PLoS Pathogens*, 8, e1002664.

- MESTRE, M. B., FADER, C. M., SOLA, C. & COLOMBO, M. I. 2010. Alpha-hemolysin is required for the activation of the autophagic pathway in *Staphylococcus aureus*-infected cells. *Autophagy*, 6, 110-125.
- MILLER, W. L. 1988. Molecular biology of steroid hormone synthesis. *Endocrine Reviews*, 9, 295-318.
- MIZIORKO, H. M. 2011. Enzymes of the mevalonate pathway of isoprenoid biosynthesis. *Archives of Biochemistry and Biophysics*, 505, 131-143.
- MOSMANN, T. 1983. Rapid colorimetric assay for cellular growth and survival: application to proliferation and cytotoxicity assays. *Journal of Immunological Methods*, 65, 55-63.
- MOSTAFA, M. M., RIDER, C. F., SHAH, S., TRAVES, S. L., GORDON, P. M. K., MILLER-LARSSON, A., LEIGH, R. & NEWTON, R. 2019. Glucocorticoid-driven transcriptomes in human airway epithelial cells: commonalities, differences and functional insight from cell lines and primary cells. *BMC Medical Genomics*, 12, 1-21.
- MOUZAT, K., BARON, S., MARCEAU, G., CAIRA, F., SAPIN, V., VOLLE, D. H., LUMBROSO, S. & LOBACCARO, J.-M. 2013. Emerging roles for LXRs and LRH-1 in female reproduction. *Molecular and Cellular Endocrinology*, 368, 47-58.
- MUNCK, A., GUYRE, P. M. & HOLBROOK, N. J. 1984. Physiological functions of glucocorticoids in stress and their relation to pharmacological actions. *Endocrine Reviews*, 5, 25-44.
- MUNOZ-PLANILLO, R., KUFFA, P., MARTINEZ-COLON, G., SMITH, B. L., RAJENDIRAN, T. M. & NUNEZ, G. 2013. K(+) efflux is the common trigger of NLRP3 inflammasome activation by bacterial toxins and particulate matter. *Immunity*, 38, 1142-1153.
- MUTEMBEREZI, V., GUILLEMOT-LEGRIS, O. & MUCCIOLI, G. G. 2016. Oxysterols: From cholesterol metabolites to key mediators. *Progress in Lipid Research*, 64, 152-169.
- NANDA, A., DOBSON, H. & WARD, W. 1990. Relationship between an increase in plasma cortisol during transport-induced stress and failure of oestradiol to induce a luteinising hormone surge in dairy cows. *Research in Veterinary Science*, 49, 25-28.
- NELSON, E. R., WARDELL, S. E., JASPER, J. S., PARK, S., SUCHINDRAN, S., HOWE, M. K., CARVER, N. J., PILLAI, R. V., SULLIVAN, P. M., SONDHI, V., UMETANI, M., GERADTS, J. & MCDONNELL, D. P. 2013. 27-Hydroxycholesterol links hypercholesterolemia and breast cancer pathophysiology. *Science*, 342, 1094-1098.
- NEWTON, R. 2014. Anti-inflammatory glucocorticoids: changing concepts. *European Journal of Pharmacology*, 724, 231-236.

- NICHOLSON, A. M. & FERREIRA, A. 2009. Increased membrane cholesterol might render mature hippocampal neurons more susceptible to beta-amyloid-induced calpain activation and tau toxicity. *The Journal of Neuroscience*, 29, 4640-4651.
- NISSEN, R. M. & YAMAMOTO, K. R. 2000. The glucocorticoid receptor inhibits NFkappaB by interfering with serine-2 phosphorylation of the RNA polymerase II carboxy-terminal domain. *Genes and Development*, 14, 2314-2329.
- NORDEEN, S. K., BONA, B. J., BECK, C. A., EDWARDS, D. P., BORROR, K. C. & DEFRANCO, D. B. 1995. The two faces of a steroid antagonist: when an antagonist isn't. *Steroids*, 60, 97-104.
- NOVOTNA, A., PAVEK, P. & DVORAK, Z. 2012. Construction and characterization of a reporter gene cell line for assessment of human glucocorticoid receptor activation. *European Journal of Pharmaceutical Sciences*, 47, 842-847.
- O'CALLAGHAN, Y. C., WOODS, J. A. & O'BRIEN, N. M. 2001. Comparative study of the cytotoxicity and apoptosis-inducing potential of commonly occurring oxysterols. *Cell Biology Toxicology*, 17, 127-137.
- O'NEILL, J. 2016. Review on antimicrobial resistance: tackling drug-resistant infections globally: final report and recommendations. *Review on antimicrobial resistance: tackling drug-resistant infections globally: final report and recommendations*.
- OAKLEY, R. H. & CIDLOWSKI, J. A. 2011. Cellular processing of the glucocorticoid receptor gene and protein: new mechanisms for generating tissue-specific actions of glucocorticoids. *The Journal of Biological Chemistry*, 286, 3177-3184.
- OAKLEY, R. H., SAR, M. & CIDLOWSKI, J. A. 1996. The human glucocorticoid receptor β isoform: expression, biochemical properties, and putative function. *The Journal of Biological Chemistry*, 271, 9550-9559.
- OBRADOVIC, M. M. S., HAMELIN, B., MANEVSKI, N., COUTO, J. P., SETHI, A., COISSIEUX, M. M., MUNST, S., OKAMOTO, R., KOHLER, H., SCHMIDT, A. & BENTIREN-ALJ, M. 2019. Glucocorticoids promote breast cancer metastasis. *Nature*, 567, 540-544.
- OBRIG, T. G., CULP, W. J., MCKEEHAN, W. L. & HARDESTY, B. 1971. The mechanism by which cycloheximide and related glutarimide antibiotics inhibit peptide synthesis on reticulocyte ribosomes. *The Journal of Biological Chemistry*, 246, 174-181.
- OGAWA, S., LOZACH, J., BENNER, C., PASCUAL, G., TANGIRALA, R. K., WESTIN, S., HOFFMANN, A., SUBRAMANIAM, S., DAVID, M., ROSENFELD, M. G. & GLASS, C. K. 2005. Molecular determinants of crosstalk between nuclear receptors and toll-like receptors. *Cell*, 122, 707-721.
- OIKARINEN, A. & AUTIO, P. 1991. New aspects of the mechanism of corticosteroid-induced dermal atrophy. *Clinical and Experimental Dermatology*, 16, 416-419.

- OIKARINEN, A., HAAPASAARI, K. M., SUTINEN, M. & TASANEN, K. 1998. The molecular basis of glucocorticoid-induced skin atrophy: topical glucocorticoid apparently decreases both collagen synthesis and the corresponding collagen mRNA level in human skin in vivo. *The British Journal of Dermatology*, 139, 1106-1110.
- OLIVER, W. R., JR., SHENK, J. L., SNAITH, M. R., RUSSELL, C. S., PLUNKET, K. D., BODKIN, N. L., LEWIS, M. C., WINEGAR, D. A., SZNAIDMAN, M. L., LAMBERT, M. H., XU, H. E., STERNBACH, D. D., KLEWER, S. A., HANSEN, B. C. & WILLSON, T. M. 2001. A selective peroxisome proliferator-activated receptor delta agonist promotes reverse cholesterol transport. *Proceedings of the National Academy of Sciences of the United States of America*, 98, 5306-5311.
- OLKKONEN, V. M., BEASLAS, O. & NISSILA, E. 2012. Oxysterols and their cellular effectors. *Biomolecules*, 2, 76-103.
- OLKKONEN, V. M. & HYNYNEN, R. 2009. Interactions of oxysterols with membranes and proteins. *Molecular Aspects of Medicine*, 30, 123-133.
- OMERSA, N., PODOBNIK, M. & ANDERLUH, G. 2019. Inhibition of pore-forming proteins. *Toxins*, 11, 545.
- ONO, Y. & SORIMACHI, H. 2012. Calpains: an elaborate proteolytic system. *Biochimica et Biophysica Acta*, 1824, 224-236.
- OTAEGUI-ARRAZOLA, A., MENENDEZ-CARRENO, M., ANSORENA, D. & ASTIASARAN, I. 2010. Oxysterols: A world to explore. *Food and Chemical Toxicology*, 48, 3289-3303.
- PARKER, K. L. & SCHIMMER, B. P. 1995. Transcriptional regulation of the genes encoding the cytochrome P-450 steroid hydroxylases. *Vitamins and Hormones*, 51, 339-370.
- PARKER, M. W. & FEIL, S. C. 2005. Pore-forming protein toxins: from structure to function. *Progress in Biophysics and Molecular Biology*, 88, 91-142.
- PATEL, A. H., NOWLAN, P., WEAVERS, E. D. & FOSTER, T. 1987. Virulence of protein A-deficient and alpha-toxin-deficient mutants of *Staphylococcus aureus* isolated by allele replacement. *Infection and Immunity*, 55, 3103-3110.
- PERARO, M. D. & VAN DER GOOT, F. G. 2016. Pore-forming toxins: ancient, but never really out of fashion. *Nature Reviews. Microbiology*, 14, 77-92.
- PEROGAMVROS, I., KAYAHARA, M., TRAINER, P. J. & RAY, D. W. 2011. Serum regulates cortisol bioactivity by corticosteroid-binding globulin-dependent and independent mechanisms, as revealed by combined bioassay and physicochemical assay approaches. *Clinical Endocrinology*, 75, 31-38.
- PERRY, R. P. & KELLEY, D. E. 1970. Inhibition of RNA synthesis by actinomycin D: characteristic dose-response of different RNA species. *Journal of Cellular Physiology*, 76, 127-139.

- PETRICHENKO, I. E., DARET, D., KOLPAKOVA, G. V., SHAKHOV, Y. A. & LARRUE, J. 1997. Glucocorticoids stimulate cholesteryl ester formation in human smooth muscle cells. *Arteriosclerosis, Thrombosis, and Vascular Biology*, 17, 1143-1151.
- PIKE, L. J. 2006. Rafts defined: a report on the Keystone Symposium on Lipid Rafts and Cell Function. *Journal of Lipid Research*, 47, 1597-1598.
- POKRAJAC, L., BAIK, C., HARRIS, J. R., SARRAF, N. S. & PALMER, M. 2012. Partial oligomerization of pyolysin induced by a disulfide-tethered mutant. *Biochemistry and Cell Biology*, 90, 709-717.
- POKRAJAC, L., HARRIS, J. R., SARRAF, N. & PALMER, M. 2013. Oligomerization and hemolytic properties of the C-terminal domain of pyolysin, a cholesterol-dependent cytolysin. *Biochemistry and Cell Biology*, 91, 59-66.
- PORTA, H., CANCINO-RODEZNO, A., SOBERON, M. & BRAVO, A. 2011. Role of MAPK p38 in the cellular responses to pore-forming toxins. *Peptides*, 32, 601-606.
- POSPIECH, M., OWENS, S. E., MILLER, D. J., AUSTIN-MUTTITT, K., MULLINS, J. G. L., CRONIN, J. G., ALLEMANN, R. K. & SHELDON, I. M. 2021. Bisphosphonate inhibitors of squalene synthase protect cells against cholesterol-dependent cytolysins. *The FASEB Journal*, 35, e21640.
- PRETA, G., JANKUNEC, M., HEINRICH, F., GRIFFIN, S., SHELDON, I. M. & VALINCIUS, G. 2016. Tethered bilayer membranes as a complementary tool for functional and structural studies: The pyolysin case. *Biochimica et Biophysica Acta*, 1858, 2070-2080.
- PRETA, G., LOTTI, V., CRONIN, J. G. & SHELDON, I. M. 2015. Protective role of the dynamin inhibitor Dynasore against the cholesterol-dependent cytolysin of *Trueperella pyogenes*. *The FASEB Journal*, 29, 1516-1528.
- PRIGENT, D. & ALOUF, J. E. 1976. Interaction of streptolysin O with sterols. *Biochimica et Biophysica Acta*, 443, 288-300.
- QUATRINI, L. & UGOLINI, S. 2021. New insights into the cell- and tissue-specificity of glucocorticoid actions. *Cellular and Molecular Immunology*, 18, 269-278.
- RADHAKRISHNAN, A., IKEDA, Y., KWON, H. J., BROWN, M. S. & GOLDSTEIN, J. L. 2007. Sterol-regulated transport of SREBPs from endoplasmic reticulum to Golgi: oxysterols block transport by binding to Insig. *Proceedings of the National Academy of Sciences of the United States of America*, 104, 6511-6518.
- RADHAKRISHNAN, A., SUN, L. P., KWON, H. J., BROWN, M. S. & GOLDSTEIN, J. L. 2004. Direct binding of cholesterol to the purified membrane region of SCAP: mechanism for a sterol-sensing domain. *Molecular Cell*, 15, 259-268.

- RAMACHANDRAN, R., HEUCK, A. P., TWETEN, R. K. & JOHNSON, A. E. 2002. Structural insights into the membrane-anchoring mechanism of a cholesterol-dependent cytolysin. *Nature Structural Biology*, 9, 823-827.
- RAMAMOORTHY, S. & CIDLOWSKI, J. A. 2013. Exploring the molecular mechanisms of glucocorticoid receptor action from sensitivity to resistance. *Endocrine Development*, 24, 41-56.
- RATMAN, D., VANDEN BERGHE, W., DEJAGER, L., LIBERT, C., TAVERNIER, J., BECK, I. M. & DE BOSSCHER, K. 2013. How glucocorticoid receptors modulate the activity of other transcription factors: a scope beyond tethering. *Molecular and Cellular Endocrinology*, 380, 41-54.
- RATNER, A. J., HIPPE, K. R., AGUILAR, J. L., BENDER, M. H., NELSON, A. L. & WEISER, J. N. 2006. Epithelial cells are sensitive detectors of bacterial pore-forming toxins. *The Journal of Biological Chemistry*, 281, 12994-12998.
- RAY, A., JATANA, N. & THUKRAL, L. 2017. Lipidated proteins: Spotlight on protein-membrane binding interfaces. *Progress in Biophysics and Molecular Biology*, 128, 74-84.
- READ, A. F., GRAHAM, A. L. & RABERG, L. 2008. Animal defenses against infectious agents: is damage control more important than pathogen control. *PLoS Biology*, 6, e1000004.
- REBOLDI, A., DANG, E. V., MCDONALD, J. G., LIANG, G., RUSSELL, D. W. & CYSTER, J. G. 2014. Inflammation. 25-Hydroxycholesterol suppresses interleukin-1-driven inflammation downstream of type I interferon. *Science*, 345, 679-684.
- REBOUL, C. F., WHISSTOCK, J. C. & DUNSTONE, M. A. 2014. A new model for pore formation by cholesterol-dependent cytolysins. *PLoS Computational Biology*, 10, e1003791.
- REDPATH, G. M., WOOLGER, N., PIPER, A. K., LEMCKERT, F. A., LEK, A., GREER, P. A., NORTH, K. N. & COOPER, S. T. 2014. Calpain cleavage within dysferlin exon 40a releases a synaptotagmin-like module for membrane repair. *Molecular Biology of the Cell*, 25, 3037-3048.
- REID, I. R. 2000. Glucocorticoid-induced osteoporosis. *Best Practice and Research. Clinical Endocrinology and Metabolism*, 14, 279-298.
- RENSHAW, M. W., REN, X. D. & SCHWARTZ, M. A. 1997. Growth factor activation of MAP kinase requires cell adhesion. *The EMBO Journal* 16, 5592-5599.
- RESH, M. D. 2006. Trafficking and signaling by fatty-acylated and prenylated proteins. *Nature Chemical Biology*, 2, 584-590.
- RHEN, T. & CIDLOWSKI, J. A. 2005. Antiinflammatory action of glucocorticoids—new mechanisms for old drugs. *The New England Journal of Medicine*, 353, 1711-1723.

- RIBEIRO, E. S., GOMES, G., GRECO, L. F., CERRI, R. L. A., VIEIRA-NETO, A., MONTEIRO, P. L. J., LIMA, F. S., BISINOTTO, R. S., THATCHER, W. W. & SANTOS, J. E. P. 2016. Carryover effect of postpartum inflammatory diseases on developmental biology and fertility in lactating dairy cows. *Journal of Dairy Science*, 99, 2201-2220.
- RIBEIRO, M. G., RISSETI, R. M., BOLANOS, C. A., CAFFARO, K. A., DE MORAIS, A. C., LARA, G. H., ZAMPROGNA, T. O., PAES, A. C., LISTONI, F. J. & FRANCO, M. M. 2015. *Trueperella pyogenes* multispecies infections in domestic animals: a retrospective study of 144 cases (2002 to 2012). *The Veterinary Quarterly*, 35, 82-87.
- RICHTER, S. S., HEILMANN, K. P., BEEKMANN, S. E., MILLER, N. J., MILLER, A. L., RICE, C. L., DOERN, C. D., REID, S. D. & DOERN, G. V. 2005. Macrolide-resistant *Streptococcus pyogenes* in the United States, 2002-2003. *Clinical Infectious Diseases*, 41, 599-608.
- ROCHFORD, C., SRIDHAR, D., WOODS, N., SALEH, Z., HARTENSTEIN, L., AHLAWAT, H., WHITING, E., DYBUL, M., CARS, O., GOOSBY, E., CASSELS, A., VELASQUEZ, G., HOFFMAN, S., BARIS, E., WADSWORTH, J., GYANSA-LUTTERODT, M. & DAVIES, S. 2018. Global governance of antimicrobial resistance. *Lancet*, 391, 1976-1978.
- RODRIGUEZ, A., WEBSTER, P., ORTEGO, J. & ANDREWS, N. W. 1997. Lysosomes behave as Ca²⁺-regulated exocytic vesicles in fibroblasts and epithelial cells. *The Journal of Cell Biology*, 137, 93-104.
- RODRIGUEZ, J. M., MONSALVES-ALVAREZ, M., HENRIQUEZ, S., LLANOS, M. N. & TRONCOSO, R. 2016. Glucocorticoid resistance in chronic diseases. *Steroids*, 115, 182-192.
- ROGATSKY, I., LOGAN, S. K. & GARABEDIAN, M. J. 1998. Antagonism of glucocorticoid receptor transcriptional activation by the c-Jun N-terminal kinase. *Proceedings of the National Academy of Sciences of the United States of America*, 95, 2050-2055.
- ROMERO, M., KEYEL, M., SHI, G., BHATTACHARJEE, P., ROTH, R., HEUSER, J. E. & KEYEL, P. A. 2017. Intrinsic repair protects cells from pore-forming toxins by microvesicle shedding. *Cell Death and Differentiation*, 24, 798-808.
- ROSADO, C. J., KONDOS, S., BULL, T. E., KUIPER, M. J., LAW, R. H., BUCKLE, A. M., VOSKOBOINIK, I., BIRD, P. I., TRAPANI, J. A., WHISSTOCK, J. C. & DUNSTONE, M. A. 2008. The MACPF/CDC family of pore-forming toxins. *Cell Microbiology*, 10, 1765-1774.
- ROSS, A. C., GO, K. J., HEIDER, J. G. & ROTHBLAT, G. H. 1984. Selective inhibition of acyl coenzyme A:cholesterol acyltransferase by compound 58-035. *The Journal of Biological Chemistry*, 259, 815-819.
- ROWSON, L. E., LAMMING, G. E. & FRY, R. M. 1953. Influence of ovarian hormones on uterine infection. *Nature*, 171, 749-750.
- RUSSELL, D. W. 2000. Oxysterol biosynthetic enzymes. *Biochimica et Biophysica Acta*, 1529, 126-135.

- SAKA, H. A., GUTIERREZ, M. G., BOCCO, J. L. & COLOMBO, M. I. 2007. The autophagic pathway: a cell survival strategy against the bacterial pore-forming toxin *Vibrio cholerae* cytolysin. *Autophagy*, 3, 363-365.
- SAKAKURA, Y., SHIMANO, H., SONE, H., TAKAHASHI, A., INOUE, N., TOYOSHIMA, H., SUZUKI, S. & YAMADA, N. 2001. Sterol regulatory element-binding proteins induce an entire pathway of cholesterol synthesis. *Biochemical and Biophysical Research Communications*, 286, 176-183.
- SALLAM, T., ITO, A., RONG, X., KIM, J., VAN STIJN, C., CHAMBERLAIN, B. T., JUNG, M. E., CHAO, L. C., JONES, M., GILLILAND, T., WU, X., SU, G. L., TANGIRALA, R. K., TONTONOZ, P. & HONG, C. 2014. The macrophage LBP gene is an LXR target that promotes macrophage survival and atherosclerosis. *Journal of Lipid Research*, 55, 1120-1130.
- SAM, S., CORBRIDGE, T. C., MOKHLESI, B., COMELLAS, A. P. & MOLITCH, M. E. 2004. Cortisol levels and mortality in severe sepsis. *Clinical Endocrinology*, 60, 29-35.
- SAMARASINGHE, R. A., WITCHELL, S. F. & DEFRANCO, D. B. 2012. Cooperativity and complementarity: synergies in non-classical and classical glucocorticoid signaling. *Cell Cycle*, 11, 2819-2827.
- SATO, H., NISHIDA, S., TOMOYORI, H., SATO, M., IKEDA, I. & IMAIZUMI, K. 2004. Oxysterol regulation of estrogen receptor alpha-mediated gene expression in a transcriptional activation assay system using HeLa cells. *Bioscience, Biotechnology, and Biochemistry*, 68, 1790-1793.
- SAUT, J. P., HEALEY, G. D., BORGES, A. M. & SHELDON, I. M. 2014. Ovarian steroids do not affect bovine endometrial cytokine or chemokine responses to *Escherichia coli* or LPS in vitro. *Reproduction*, 148, 593-606.
- SAVIO, J. D., THATCHER, W. W., MORRIS, G. R., ENTWISTLE, K., DROST, M. & MATTIACCI, M. R. 1993. Effects of induction of low plasma progesterone concentrations with a progesterone-releasing intravaginal device on follicular turnover and fertility in cattle. *Journal of Reproduction and Fertility*, 98, 77-84.
- SCHACKE, H., BERGER, M., REHWINKEL, H. & ASADULLAH, K. 2007. Selective glucocorticoid receptor agonists (SEGRAs): novel ligands with an improved therapeutic index. *Molecular and Cellular Endocrinology*, 275, 109-117.
- SCHACKE, H., DOCKE, W. D. & ASADULLAH, K. 2002. Mechanisms involved in the side effects of glucocorticoids. *Pharmacology and Therapeutics*, 96, 23-43.
- SCHINDELIN, J., ARGANDA-CARRERAS, I., FRISE, E., KAYNIG, V., LONGAIR, M., PIETZSCH, T., PREIBISCH, S., RUEDEN, C., SAALFELD, S., SCHMID, B., TINEVEZ, J. Y., WHITE, D. J., HARTENSTEIN, V., ELICEIRI, K., TOMANCAK, P. & CARDONA, A. 2012. Fiji: an open-source platform for biological-image analysis. *Nature Methods*, 9, 676-682.

- SCHNEIDER-POETSCH, T., JU, J., EYLER, D. E., DANG, Y., BHAT, S., MERRICK, W. C., GREEN, R., SHEN, B. & LIU, J. O. 2010. Inhibition of eukaryotic translation elongation by cycloheximide and lactimidomycin. *Nature Chemical Biology*, 6, 209-217.
- SCHNEIDER, D. S. & AYRES, J. S. 2008. Two ways to survive infection: what resistance and tolerance can teach us about treating infectious diseases. *Nature Reviews. Immunology*, 8, 889-895.
- SCHNEIKERT, J., HUBNER, S., MARTIN, E. & CATO, A. C. 1999. A nuclear action of the eukaryotic cochaperone RAP46 in downregulation of glucocorticoid receptor activity. *The Journal of Cell Biology*, 146, 929-940.
- SCHOENLE, L. A., MOORE, I. T., DUDEK, A. M., GARCIA, E. B., MAYS, M., HAUSSMANN, M. F., CIMINI, D. & BONIER, F. 2019. Exogenous glucocorticoids amplify the costs of infection by reducing resistance and tolerance, but effects are mitigated by co-infection. *Proceedings. Biological Sciences*, 286, 20182913.
- SCHOENLE, L. A., SCHOEPF, I., WEINSTEIN, N. M., MOORE, I. T. & BONIER, F. 2018. Higher plasma corticosterone is associated with reduced costs of infection in red-winged blackbirds. *General and Comparative Endocrinology*, 256, 89-98.
- SCHROEPFER, G. J., JR. 2000. Oxysterols: modulators of cholesterol metabolism and other processes. *Physiological Reviews*, 80, 361-554.
- SCHULTZ, J. R., TU, H., LUK, A., REPA, J. J., MEDINA, J. C., LI, L., SCHWENDNER, S., WANG, S., THOOLEN, M., MANGELSDORF, D. J., LUSTIG, K. D. & SHAN, B. 2000. Role of LXRs in control of lipogenesis. *Genes and Development*, 14, 2831-2838.
- SCHWARTZ, N., XUE, X., ELOVITZ, M. A., DOWLING, O. & METZ, C. N. 2009. Progesterone suppresses the fetal inflammatory response ex vivo. *American Journal of Obstetrics and Gynecology*, 201, 211 e1-9.
- SEDLAK, D., PAGUIO, A. & BARTUNEK, P. 2011. Two panels of steroid receptor luciferase reporter cell lines for compound profiling. *Combinational Chemistry and High Throughput Screening*, 14, 248-266.
- SEILIE, E. S. & BUBECK WARDENBURG, J. 2017. *Staphylococcus aureus* pore-forming toxins: The interface of pathogen and host complexity. *Seminars in Cell and Developmental Biology*, 72, 101-116.
- SEZGIN, E., LEVENTAL, I., MAYOR, S. & EGGELING, C. 2017. The mystery of membrane organization: composition, regulation and roles of lipid rafts. *Nature Reviews. Molecular Cell Biology*, 18, 361-374.
- SHAW, P. E., SCHROTER, H. & NORDHEIM, A. 1989. The ability of a ternary complex to form over the serum response element correlates with serum inducibility of the human c-fos promoter. *Cell*, 56, 563-572.

- SHELDON, I. M., CRONIN, J., GOETZE, L., DONOFRIO, G. & SCHUBERTH, H. J. 2009. Defining postpartum uterine disease and the mechanisms of infection and immunity in the female reproductive tract in cattle. *Biology of Reproduction*, 81, 1025-1032.
- SHELDON, I. M., CRONIN, J. G. & BROMFIELD, J. J. 2019. Tolerance and innate immunity shape the development of postpartum uterine disease and the impact of endometritis in dairy cattle. *Annual Review of Animal Biosciences*, 7, 361-384.
- SHELDON, I. M., LEWIS, G. S., LEBLANC, S. & GILBERT, R. O. 2006. Defining postpartum uterine disease in cattle. *Theriogenology*, 65, 1516-1530.
- SHELDON, I. M., MOLINARI, P. C. C., ORMSBY, T. J. R. & BROMFIELD, J. J. 2020. Preventing postpartum uterine disease in dairy cattle depends on avoiding, tolerating and resisting pathogenic bacteria. *Theriogenology*, 150, 158-165.
- SHELDON, I. M., NOAKES, D. E., RYCROFT, A. N., PFEIFFER, D. U. & DOBSON, H. 2002. Influence of uterine bacterial contamination after parturition on ovarian dominant follicle selection and follicle growth and function in cattle. *Reproduction*, 123, 837-845.
- SHELDON, I. M., RYCROFT, A. N., DOGAN, B., CRAVEN, M., BROMFIELD, J. J., CHANDLER, A., ROBERTS, M. H., PRICE, S. B., GILBERT, R. O. & SIMPSON, K. W. 2010. Specific strains of *Escherichia coli* are pathogenic for the endometrium of cattle and cause pelvic inflammatory disease in cattle and mice. *PLoS One*, 5, e9192.
- SHEWELL, L. K., DAY, C. J., JEN, F. E.-C., HASELHORST, T., ATACK, J. M., REIJNEVELD, J. F., EVEREST-DASS, A., JAMES, D. B. A., BOGUSLAWSKI, K. M., BROUWER, S., GILLEN, C. M., LUO, Z., KOBE, B., NIZET, V., VON ITZSTEIN, M., WALKER, M. J., PATON, A. W., PATON, J. C., TORRES, V. J. & JENNINGS, M. P. 2020. All major cholesterol-dependent cytolysins use glycans as cellular receptors. *Science Advances*, 6, eaaz4926.
- SIERIG, G., CYWES, C., WESSELS, M. R. & ASHBAUGH, C. D. 2003. Cytotoxic effects of streptolysin o and streptolysin s enhance the virulence of poorly encapsulated group a streptococci. *Infection and Immunity*, 71, 446-455.
- SIKORA, M. J., JOHNSON, M. D., LEE, A. V. & OESTERREICH, S. 2016. Endocrine response phenotypes are altered by charcoal-stripped serum variability. *Endocrinology*, 157, 3760-3766.
- SILVER, L. L. 2011. Challenges of antibacterial discovery. *Clinical Microbiology Reviews*, 24, 71-109.
- SIMONS, K. & VAZ, W. L. 2004. Model systems, lipid rafts, and cell membranes. *Annual Review of Biophysics and Biomolecular Structure*, 33, 269-295.
- SINGER, S. J. & NICOLSON, G. L. 1972. The fluid mosaic model of the structure of cell membranes. *Science*, 175, 720-731.

- SKONER, D. P., RACHELEFSKY, G. S., MELTZER, E. O., CHERVINSKY, P., MORRIS, R. M., SELTZER, J. M., STORMS, W. W. & WOOD, R. A. 2000. Detection of growth suppression in children during treatment with intranasal beclomethasone dipropionate. *Pediatrics*, 105, E23.
- SLOTTE, J. P. 1999. Sphingomyelin-cholesterol interactions in biological and model membranes. *Chemistry and Physics of Lipids*, 102, 13-27.
- SO, A. Y., CHAIVORAPOL, C., BOLTON, E. C., LI, H. & YAMAMOTO, K. R. 2007. Determinants of cell- and gene-specific transcriptional regulation by the glucocorticoid receptor. *PLoS Genetics*, 3, e94.
- SOLTANI, C. E., HOTZE, E. M., JOHNSON, A. E. & TWETEN, R. K. 2007. Structural elements of the cholesterol-dependent cytolysins that are responsible for their cholesterol-sensitive membrane interactions. *Proceedings of the National Academy of Sciences of the United States of America*, 104, 20226-20231.
- SONG, B. L., JAVITT, N. B. & DEBOSE-BOYD, R. A. 2005. Insig-mediated degradation of HMG CoA reductase stimulated by lanosterol, an intermediate in the synthesis of cholesterol. *Cell Metabolism*, 1, 179-189.
- SONG, L., HOBAUGH, M. R., SHUSTAK, C., CHELEY, S., BAYLEY, H. & GOUAUX, J. E. 1996. Structure of staphylococcal alpha-hemolysin, a heptameric transmembrane pore. *Science*, 274, 1859-1866.
- SONNEN, A. F., PLITZKO, J. M. & GILBERT, R. J. 2014. Incomplete pneumolysin oligomers form membrane pores. *Open Biology*, 4, 140044.
- SOONG, G., CHUN, J., PARKER, D. & PRINCE, A. 2012. *Staphylococcus aureus* activation of caspase 1/calpain signaling mediates invasion through human keratinocytes. *The Journal of Infectious Diseases*, 205, 1571-1579.
- SOROOSH, P., WU, J., XUE, X., SONG, J., SUTTON, S. W., SABLAD, M., YU, J., NELEN, M. I., LIU, X., CASTRO, G., LUNA, R., CRAWFORD, S., BANIE, H., DANDRIDGE, R. A., DENG, X., BITTNER, A., KUEI, C., TOOTOONCHI, M., ROZENKRANTS, N., HERMAN, K., GAO, J., YANG, X. V., SACHEN, K., NGO, K., FUNG-LEUNG, W. P., NGUYEN, S., DE LEON-TABALDO, A., BLEVITT, J., ZHANG, Y., CUMMINGS, M. D., RAO, T., MANI, N. S., LIU, C., MCKINNON, M., MILLA, M. E., FOURIE, A. M. & SUN, S. 2014. Oxysterols are agonist ligands of ROR γ t and drive Th17 cell differentiation. *Proceedings of the National Academy of Sciences of the United States of America*, 111, 12163-12168.
- SPANN, N. J. & GLASS, C. K. 2013. Sterols and oxysterols in immune cell function. *Nature Immunology*, 14, 893-900.
- SPENCER, T. E. & BAZER, F. W. 2002. Biology of progesterone action during pregnancy recognition and maintenance of pregnancy. *Frontiers in Bioscience*, 7, d1879-d1898.
- STANFEL, M. N., SHAMIEH, L. S., KAEBERLEIN, M. & KENNEDY, B. K. 2009. The TOR pathway comes of age. *Biochimica et Biophysica Acta*, 1790, 1067-1074.

- STASSEN, M., MULLER, C., RICHTER, C., NEUDORFL, C., HULTNER, L., BHAKDI, S., WALEV, I. & SCHMITT, E. 2003. The streptococcal exotoxin streptolysin O activates mast cells to produce tumor necrosis factor alpha by p38 mitogen-activated protein kinase- and protein kinase C-dependent pathways. *Infection and Immunity*, 71, 6171-6177.
- STATT, S., RUAN, J. W., HUNG, L. Y., CHANG, C. Y., HUANG, C. T., LIM, J. H., LI, J. D., WU, R. & KAO, C. Y. 2015. Statin-conferred enhanced cellular resistance against bacterial pore-forming toxins in airway epithelial cells. *American Journal of Respiratory Cell and Molecular Biology*, 53, 689-702.
- STERN, A., SKALSKY, K., AVNI, T., CARRARA, E., LEIBOVICI, L. & PAUL, M. 2017. Corticosteroids for pneumonia. *The Cochrane Database of Systematic Reviews*, 12, CD007720.
- STEVENS, D. L., BISNO, A. L., CHAMBERS, H. F., DELLINGER, E. P., GOLDSTEIN, E. J., GORBACH, S. L., HIRSCHMANN, J. V., KAPLAN, S. L., MONTOYA, J. G., WADE, J. C. & INFECTIOUS DISEASES SOCIETY OF, A. 2014. Practice guidelines for the diagnosis and management of skin and soft tissue infections: 2014 update by the Infectious Diseases Society of America. *Clinical Infectious Diseases*, 59, e10-e52.
- STRAUSS, J. F., RENNERT, H., YAMAMOTO, R., KAO, L.-C. & ALVAREZ, J. G. 1991. Oxysterols: Regulation of biosynthesis and role in controlling cellular cholesterol homeostasis in ovarian cells. *Signaling Mechanisms and Gene Expression in the Ovary*. New York: Springer.
- STREHL, C., GABER, T., LOWENBERG, M., HOMMES, D. W., VERHAAR, A. P., SCHELLMANN, S., HAHNE, M., FANGRADT, M., WAGEGG, M., HOFF, P., SCHEFFOLD, A., SPIES, C. M., BURMESTER, G. R. & BUTTGEREIT, F. 2011. Origin and functional activity of the membrane-bound glucocorticoid receptor. *Arthritis and Rheuma*, 63, 3779-3788.
- TABAS, I. 2002. Consequences of cellular cholesterol accumulation: basic concepts and physiological implications. *The Journal of Clinical Investigation* 110, 905-911.
- TAKEUCHI, O. & AKIRA, S. 2010. Pattern recognition receptors and inflammation. *Cell*, 140, 805-820.
- TAM, C., FLANNERY, A. R. & ANDREWS, N. 2013. Live imaging assay for assessing the roles of Ca²⁺ and sphingomyelinase in the repair of pore-forming toxin wounds. *Journal of Visualized Experiments*, e50531.
- TARABORRELLI, S. 2015. Physiology, production and action of progesterone. *Acta Obstetrica et Gynecologica Scandinavica*, 94, 8-16.
- THEUNISSEN, J. J., JACKSON, R. L., KEMPEN, H. J. & DEMEL, R. A. 1986. Membrane properties of oxysterols. Interfacial orientation, influence on membrane permeability and redistribution between membranes. *Biochimica et Biophysica Acta*, 860, 66-74.

- THOMAS, M. G., MARWOOD, R. M., PARSONS, A. E. & PARSONS, R. B. 2015. The effect of foetal bovine serum supplementation upon the lactate dehydrogenase cytotoxicity assay: Important considerations for in vitro toxicity analysis. *Toxicology in Vitro*, 30, 300-308.
- THOMAS, M. P. & POTTER, B. V. 2013. The structural biology of oestrogen metabolism. *The Journal of Steroid Biochemistry and Molecular Biology*, 137, 27-49.
- TREISMAN, R. 1986. Identification of a protein-binding site that mediates transcriptional response of the c-fos gene to serum factors. *Cell*, 46, 567-574.
- TROPMAIR, J., BRUDER, J. T., MUNOZ, H., LLOYD, P. A., KYRIAKIS, J., BANERJEE, P., AVRUCH, J. & RAPP, U. R. 1994. Mitogen-activated protein kinase/extracellular signal-regulated protein kinase activation by oncogenes, serum, and 12-O-tetradecanoylphorbol-13-acetate requires Raf and is necessary for transformation. *The Journal of Biological Chemistry*, 269, 7030-7035.
- TRUMAN, J. P., AL GADBAN, M. M., SMITH, K. J. & HAMMAD, S. M. 2011. Acid sphingomyelinase in macrophage biology. *Cellular and Molecular Life Sciences*, 68, 3293-3305.
- TU, C., FIANDALO, M. V., POP, E., STOCKING, J. J., AZABDAFTARI, G., LI, J., WEI, H., MA, D., QU, J., MOHLER, J. L., TANG, L. & WU, Y. 2018. Proteomic analysis of charcoal-stripped fetal bovine serum reveals changes in the insulin-like growth factor signaling pathway. *Journal of Proteome Research*, 17, 2963-2977.
- TURNER, M. L., CRONIN, J. G., HEALEY, G. D. & SHELDON, I. M. 2014. Epithelial and stromal cells of bovine endometrium have roles in innate immunity and initiate inflammatory responses to bacterial lipopeptides in vitro via Toll-like receptors TLR2, TLR1, and TLR6. *Endocrinology*, 155, 1453-1465.
- TURNER, M. L., OWENS, S. E. & SHELDON, I. M. 2020. Glutamine supports the protection of tissue cells against the damage caused by cholesterol-dependent cytolysins from pathogenic bacteria. *PLoS One*, 15, e0219275.
- TWETEN, R. K. 2005. Cholesterol-dependent cytolysins, a family of versatile pore-forming toxins. *Infection and Immunity*, 73, 6199-6209.
- UMETANI, M., DOMOTO, H., GORMLEY, A. K., YUHANNA, I. S., CUMMINS, C. L., JAVITT, N. B., KORACH, K. S., SHAUL, P. W. & MANGELSDORF, D. J. 2007. 27-Hydroxycholesterol is an endogenous SERM that inhibits the cardiovascular effects of estrogen. *Nature Medicine*, 13, 1185-1192.
- VAN DE BEEK, D. 2009. Corticosteroids for acute adult bacterial meningitis. *Médecine et Maladies Infectieuses*, 39, 531-8.

- VAN DE STOLPE, A., CALDENHOVEN, E., RAAIJMAKERS, J. A., VAN DER SAAG, P. T. & KOENDERMAN, L. 1993. Glucocorticoid-mediated repression of intercellular adhesion molecule-1 expression in human monocytic and bronchial epithelial cell lines. *American Journal of Respiratory Cell and Molecular Biology*, 8, 340-347.
- VAN MEER, G., VOELKER, D. R. & FEIGENSON, G. W. 2008. Membrane lipids: where they are and how they behave. *Nature Reviews. Molecular Cell Biology*, 9, 112-124.
- VON LANGEN, J., FRITZEMEIER, K. H., DIEKMANN, S. & HILLISCH, A. 2005. Molecular basis of the interaction specificity between the human glucocorticoid receptor and its endogenous steroid ligand cortisol. *ChemBioChem: A European Journal of Chemical Biology*, 6, 1110-1118.
- WADA, T., KANG, H. S., JETTEN, A. M. & XIE, W. 2008. The emerging role of nuclear receptor ROR α and its crosstalk with LXR in xeno- and endobiotic gene regulation. *Experimental Biology and Medicine*, 233, 1191-1201.
- WALEV, I., BHAKDI, S. C., HOFMANN, F., DJONDER, N., VALEVA, A., AKTORIES, K. & BHAKDI, S. 2001. Delivery of proteins into living cells by reversible membrane permeabilization with streptolysin-O. *Proceedings of the National Academy of Sciences of the United States of America*, 98, 3185-3190.
- WALEV, I., MARTIN, E., JONAS, D., MOHAMADZADEH, M., MULLER-KLIESER, W., KUNZ, L. & BHAKDI, S. 1993. Staphylococcal alpha-toxin kills human keratinocytes by permeabilizing the plasma membrane for monovalent ions. *Infection and Immunity*, 61, 4972-4979.
- WALEV, I., RESKE, K., PALMER, M., VALEVA, A. & BHAKDI, S. 1995. Potassium-inhibited processing of IL-1 β in human monocytes. *The EMBO Journal* 14, 1607-1614.
- WANG, B. & TONTONOZ, P. 2018. Liver X receptors in lipid signalling and membrane homeostasis. *Nature Reviews. Endocrinology*, 14, 452-463.
- WANG, D., ZHANG, H., LANG, F. & YUN, C. C. 2007. Acute activation of NHE3 by dexamethasone correlates with activation of SGK1 and requires a functional glucocorticoid receptor. *American Journal of Physiology. Cell Physiology*, 292, C396-404.
- WANG, J. C., DERYNCK, M. K., NONAKA, D. F., KHODABAKHSH, D. B., HAQQ, C. & YAMAMOTO, K. R. 2004. Chromatin immunoprecipitation (ChIP) scanning identifies primary glucocorticoid receptor target genes. *Proceedings of the National Academy of Sciences of the United States of America*, 101, 15603-15608.
- WANG, L., MITSUI, T., ISHIDA, M., IZAWA, M. & ARITA, J. 2017. Rasd1 is an estrogen-responsive immediate early gene and modulates expression of late genes in rat anterior pituitary cells. *Endocrine Journal*, 64, 1063-1071.

- WANG, S., LI, W., HUI, H., TIWARI, S. K., ZHANG, Q., CROKER, B. A., RAWLINGS, S., SMITH, D., CARLIN, A. F. & RANA, T. M. 2020. Cholesterol 25-Hydroxylase inhibits SARS-CoV-2 and other coronaviruses by depleting membrane cholesterol. *The EMBO Journal*, 39, e106057.
- WANG, Y., KUMAR, N., CRUMBLEY, C., GRIFFIN, P. R. & BURRIS, T. P. 2010. A second class of nuclear receptors for oxysterols: Regulation of ROR α and ROR γ activity by 24S-hydroxycholesterol (cerebrosterol). *Biochimica et Biophysica Acta*, 1801, 917-923.
- WANG, Z., RONG, Y. P., MALONE, M. H., DAVIS, M. C., ZHONG, F. & DISTELHORST, C. W. 2006. Thioredoxin-interacting protein (txnip) is a glucocorticoid-regulated primary response gene involved in mediating glucocorticoid-induced apoptosis. *Oncogene*, 25, 1903-1913.
- WANNAMAKER, L. 1970. Medical progress: Differences between streptococcal infections of the throat and of the skin. *The New England Journal of Medicine*, 282, 23-31.
- WEI, P., INAMDAR, N. & VEDECKIS, W. V. 1998. Transrepression of c-jun gene expression by the glucocorticoid receptor requires both AP-1 sites in the c-jun promoter. *Molecular Endocrinology*, 12, 1322-1333.
- WEIKUM, E. R., KNUESEL, M. T., ORTLUND, E. A. & YAMAMOTO, K. R. 2017. Glucocorticoid receptor control of transcription: precision and plasticity via allosteric. *Nature Reviews. Molecular Cell Biology*, 18, 159-174.
- WESTERMANN, S., DRILLICH, M., KAUFMANN, T. B., MADOZ, L. V. & HEUWIESER, W. 2010. A clinical approach to determine false positive findings of clinical endometritis by vaginoscopy by the use of uterine bacteriology and cytology in dairy cows. *Theriogenology*, 74, 1248-1255.
- WILKE, G. A. & BUBECK WARDENBURG, J. 2010. Role of a disintegrin and metalloprotease 10 in *Staphylococcus aureus* alpha-hemolysin-mediated cellular injury. *Proceedings of the National Academy of Sciences of the United States of America*, 107, 13473-13478.
- WILLY, P. J., UMESONO, K., ONG, E. S., EVANS, R. M., HEYMAN, R. A. & MANGELSDORF, D. J. 1995. LXR, a nuclear receptor that defines a distinct retinoid response pathway. *Genes and Development*, 9, 1033-1045.
- WIPPEL, C., FORTSCH, C., HUPP, S., MAIER, E., BENZ, R., MA, J., MITCHELL, T. J. & ILIEV, A. I. 2011. Extracellular calcium reduction strongly increases the lytic capacity of pneumolysin from *Streptococcus pneumoniae* in brain tissue. *The Journal of Infectious Diseases*, 204, 930-936.
- WIRA, C. R., FAHEY, J. V., SENTMAN, C. L., PIOLI, P. A. & SHEN, L. 2005. Innate and adaptive immunity in female genital tract: cellular responses and interactions. *Immunological Reviews*, 206, 306-335.
- WIRA, C. R., RODRIGUEZ-GARCIA, M. & PATEL, M. V. 2015. The role of sex hormones in immune protection of the female reproductive tract. *Nature Reviews. Immunology*, 15, 217-230.

- WITZENRATH, M., PACHE, F., LORENZ, D., KOPPE, U., GUTBIER, B., TABELING, C., REPPE, K., MEIXENBERGER, K., DORHOI, A., MA, J., HOLMES, A., TRENDELENBURG, G., HEIMESAAT, M. M., BERESWILL, S., VAN DER LINDEN, M., TSCHOPP, J., MITCHELL, T. J., SUTTORP, N. & OPITZ, B. 2011. The NLRP3 inflammasome is differentially activated by pneumolysin variants and contributes to host defense in pneumococcal pneumonia. *Journal of Immunology*, 187, 434-440.
- WOLFMEIER, H., RADECKE, J., SCHOENAUER, R., KOEFFEL, R., BABIYCHUK, V. S., DRUCKER, P., HATHAWAY, L. J., MITCHELL, T. J., ZUBER, B., DRAEGER, A. & BABIYCHUK, E. B. 2016. Active release of pneumolysin prepores and pores by mammalian cells undergoing a *Streptococcus pneumoniae* attack. *Biochimica et Biophysica Acta*, 1860, 2498-2509.
- WU, Q., ISHIKAWA, T., SIRIANNI, R., TANG, H., MCDONALD, J. G., YUHANNA, I. S., THOMPSON, B., GIRARD, L., MINEO, C., BREKKEN, R. A., UMETANI, M., EUHUS, D. M., XIE, Y. & SHAUL, P. W. 2013. 27-Hydroxycholesterol promotes cell-autonomous, ER-positive breast cancer growth. *Cell Reports*, 5, 637-645.
- WULF, M. & VOSS, A. 2008. MRSA in livestock animals-an epidemic waiting to happen? *Clinical Microbiology and Infection*, 14, 519-521.
- YAMAKAWA, T. & NAGAI, Y. 1978. Glycolipids at the cell surface and their biological functions. *Trends in Biochemical Sciences*, 3, 128-131.
- YAMAMOTO, K. R. 1985. Steroid receptor regulated transcription of specific genes and gene networks. *Annual Review of Genetics*, 19, 209-252.
- YANG-YEN, H. F., CHAMBARD, J. C., SUN, Y. L., SMEAL, T., SCHMIDT, T. J., DROUIN, J. & KARIN, M. 1990. Transcriptional interference between c-Jun and the glucocorticoid receptor: mutual inhibition of DNA binding due to direct protein-protein interaction. *Cell*, 62, 1205-1215.
- YANG, J., SATO, R., GOLDSTEIN, J. L. & BROWN, M. S. 1994. Sterol-resistant transcription in CHO cells caused by gene rearrangement that truncates SREBP-2. *Genes and Development*, 8, 1910-1919.
- YANG, N., CARATTI, G., INCE, L. M., POOLMAN, T. M., TREBBLE, P. J., HOLT, C. M., RAY, D. W. & MATTHEWS, L. C. 2014. Serum cholesterol selectively regulates glucocorticoid sensitivity through activation of JNK. *The Journal of Endocrinology*, 223, 155-166.
- YASIR, M., GOYAL, A., BANSAL, P. & SONTHALIA, S. 2018. *Corticosteroid adverse effects*, StatPearls Publishing, Treasure Island (FL).
- YEAGLE, P. L. 1985. Cholesterol and the cell membrane. *Biochimica et Biophysica Acta*, 822, 267-287.
- ZELCER, N., HONG, C., BOYADJIAN, R. & TONTONOZ, P. 2009. LXR regulates cholesterol uptake through Idol-dependent ubiquitination of the LDL receptor. *Science*, 325, 100-104.

- ZERBINATI, C. & IULIANO, L. 2017. Cholesterol and related sterols autoxidation. *Free Radical Biology and Medicine*, 111, 151-155.
- ZHANG, N., TRUONG-TRAN, Q. A., TANCOWNY, B., HARRIS, K. E. & SCHLEIMER, R. P. 2007. Glucocorticoids enhance or spare innate immunity: effects in airway epithelium are mediated by CCAAT/enhancer binding proteins. *Journal of Immunology*, 179, 578-589.
- ZHAO, X., LI, H., WANG, J., GUO, Y., LIU, B., DENG, X. & NIU, X. 2016. Verbascoside alleviates pneumococcal pneumonia by reducing pneumolysin oligomers. *Molecular Pharmacology*, 89, 376-387.
- ZHAO, X., LIU, B., LIU, S., WANG, L. & WANG, J. 2017. Anticytotoxin effects of amentoflavone to pneumolysin. *Biological and Pharmaceutical Bulletin*, 40, 61-67.
- ZHOU, Q. D., CHI, X., LEE, M. S., HSIEH, W. Y., MKRTCHYAN, J. J., FENG, A. C., HE, C., YORK, A. G., BUI, V. L., KRONENBERGER, E. B., FERRARI, A., XIAO, X., DALY, A. E., TARLING, E. J., DAMOISEAUX, R., SCUMPIA, P. O., SMALE, S. T., WILLIAMS, K. J., TONTONOZ, P. & BENSINGER, S. J. 2020. Interferon-mediated reprogramming of membrane cholesterol to evade bacterial toxins. *Nature Immunology*, 21, 746-755.
- ZHU, L., OLSEN, R. J., LEE, J. D., PORTER, A. R., DELEO, F. R. & MUSSER, J. M. 2017. Contribution of secreted NADase and streptolysin O to the pathogenesis of epidemic serotype M1 *Streptococcus pyogenes* infections. *The American Journal of Pathology*, 187, 605-613.